DEVELOPMENT OF A MODEL FOR EVALUATING HYDROELECTRIC POWER POTENTIALS OF SOME SELECTED RIVERS IN EDO NORTH

BY

AUDU, Luqman Muhammed

PhD/SEET/2017/927

DEPARTMENT OF MECHANICAL ENGINEERING

FEDERAL UNIVERSITY OF TECHNOLOGY,

MINNA.

MARCH 2023

DEVELOPMENT OF A MODEL FOR EVALU[illegible]HYDROELECTRIC POWER POTENTIALS OF SOME SELECTED RIVERS IN EDO NORTH

BY

AUDU, Luqman Muhammed

PhD/SEET/2017/927

THESIS SUBMITTED TO THE POSTGRADUATE SCHOOL

FEDERAL UNIVERSITY OF TECHNOLOGY, MINNA, NIGERIA IN PARTIAL FULFILLMENT OF THE REQUIREMENTS FOR THE AWARD OF DOCTOR OF PHILOSOPHY(PhD) DEGREE IN MECHANICAL ENGINEERING (THERMOFLUID AND POWER PLANT

ENGINEERING, OPTION)

MARCH 2023

ABSTRACT

Nigeria's power generation capacity is now far insufficient to satisfy the needs of the country's socioeconomic development. 82 % of the country's electricity is produced by thermal power plants, which have low capacity utilization and high greenhouse gas emissions. This has projected the necessity for the growth of hydropower. In underdeveloped nations, achieving this goal still presents some challenges due to inadequate meteorological and hydrological databases, which are mostly caused by the absence of functional gauging channels. The aim of the study is to develop a model for evaluating hydroelectric power potentials of River Orle, Edion and Orbeh in Edo North of Edo State. Measurements were carried out on River Orle, Edion and Orbeh with the determination of channel geometry, average monthly velocity, flow rate, hydro power and associated uncertainty. A 60 years data extension was effected from the observed two years discharged data using the Gauss Newton Regression Algorithm. The mass curve method was used to determine the storage capacity of the reservoir on the basis of the cumulative inflow process for a uniform discharge throughout the year. An optimal design approach was adopted for the penstock with Solid Works 2021 simulation used to determine penstock flow dynamics and characteristics. The developed, automated and validated flow model has an accuracy of 99.99%, 99.54% and 99.98% for cross sectional area, velocity and flow rate measurement respectively compare to the analytical process while being faster and more user friendly. The study established similar discharge characteristics for the three rivers with a uniform power output from R. Orle of 10.00 MW, 4.477 MW for Edion and 5.718 MW for R. Orbe with uncertainty of discharge measurement of ±10 %. The rivers are capable of yielding power throughout the year. A levelized cost of energy of $0.044/kWh was established for the hydropower plants. The EIA on the rivers indicated low level risk and impact by the reservoirs construction and operation to human and assets in the study area. The study concluded that the developed model is reliable and accurate in the evaluation of the hydroelectric generation potentials of rivers and recommend its implementation in the exploration of Nigeria hydropower resources that will provide the required electrical power generation to sustain the Nigerian economy.

TABLE OF CONTENTS

CHAPTER ONE

CHAPTER TWO

CHAPTER FIVE

LIST OF TABLES

LIST OF FIGURES

LIST OF APPENDICES

ABBREVIATIONS, GLOSSARIES AND SYMBOLS

ANOVA:	Analysis of Variance
CERFACS:	Centre Européen de Recherche et de Formation Avancée en Calcul Scientifique (European Center for Research and Advanced Training in Scientific Computing)
ExternE:	External Cost of Energy
FEA:	Finite Element Analysis
LOWESS:	Locally Weighted Scatterplot Smoothing
K:	Kelvin
kW:	Kilo Watt
MW:	Mega Watt
Pa:	*Pascal*
PWh:	Peca Watt Hour
^{0}C:	Degree Celsius

R:	*Correlation Coefficient*
Sig:	*Significant*
Std:	*Standard*
SE:	*Standard Error*

CHAPTER ONE

1.0 INTRODUCTION

1.1 Background to the Study

Electricity as a secondary source of energy is essential to meet society's basic needs, improve living standards, and boost socio-economic development. Electricity is an integral part of modern life. The Electricity generation of any nation serves the tool that powers the economy of such nations. Adequate power generation is fundamental to the industrial development and economic growth of any nation. Electricity availability and consumption are directly related to the per capita consumption of nations, which serves as a pointer to the level of development of the nations (Dai *et al*., 2022).

For decades, the Nigerian economy has struggled with unsolvable issues with the quality of its energy supply, which has had a significant impact on the economic growth of the country (Olaoye *et al.,* 2016). The main power generating base of thermal power plants has not produced enough sustainably generated electricity to support the Nigerian economy (Etukudor *et al*., 2015).

Nigeria's population growth necessitates more electricity production and availability in order for the country to prosper economically (Cepin, 2011). The assessment and development of potential hydroelectric power sources is essential to diversifying Nigeria's electrical power generation base for increased and sustainable electricity supply in line with environmental friendliness (Akinlo, 2009; Olaoye et al., 2016). Due to its ability to quickly and effectively change generation rates, hydroelectric power (HP) is well suited to deliver peak power. Additionally, HP is an important source of renewable energy because of its almost negligible pollution emissions and capacity to react swiftly to peak loads.

Nigeria has many prospective hydropower resources; a total of 76 micro dams, 126 mini dams, and 86 small hydroelectric power sites along numerous river systems have been identified as possible sources of electricity (Abdulkadir *et al.*, 2013).

Hydropower plants harness energy from flowing water to produce electricity. A body of water moving down a height difference contains kinetic energy which can be harvested with a turbine. The rotational energy is used to produce electricity through a generator. The turbine converts the kinetic energy of the water into mechanical energy while the generator converts the mechanical energy into electrical energy (Spilsbury *et al.*, 2008).

One-fifth of electricity worldwide is generated using hydropower. The cost of hydroelectricity from hydropower is relatively low, making it a competitive source of renewable energy. Hydropower stations do not require fuel inputs to operate, unlike some other power plants. The average cost of electricity from a hydropower plants is $0.05 per/kWh which is relatively competitive compared to other power sources.

Nigeria currently has three Hydropower producing Stations, namely Shiror, Jebba and Kaniji hydro power plants. The installed power ratings of 600 MW, 560 MW, and 700 MW respectively (Ladokun *et al.*, 2018).

Their available capacity fluctuates according to the availability of water for power generation. In other to make provision for future power demands in Nigeria, the Federal Government of Nigeria has initiated action in the construction of hydro power plants in the Mambila Plateau with a capacity of 3050 MW, Zungeru of 700 MW, Gurara of 30 MW, Dadin Kowa of 35 MW, Kashimbila of 40 MW (International Hydropower Association, 2018).

The main focus of research and development efforts in hydropower generation is currently on the development of small hydro technology because of the low

environmental impact (Vasiliev *et al*., 2013). The exploitation of hydroelectric power generation potentials of hydro sites is done with the evaluation of the flow characteristics of the river channel to determine the profile and maximum power that can be obtained from the site. Some popular methods include the area – rainfall and area – velocity methods. The area - rainfall method is suitable for territories with good metreological data base with reliable and documented data of close to 30 years (Bailey and Bass, 2009). The area - velocity method utilizes the direct measurement of the river flow characteristics with current velocity meter or floats. The discharge is determined form the measurement of the mean velocity of the stream and the cross- sectional area of the channel. The current velocity meter and other related equipments are used in areas with standard gauging stations that are adapted to the instruments characteristics for the area – velocity method. The current velocity meter has severe limitations in the measurement of flow data in case of low velocity of flow, shallow depths, excessive velocity, presence of materials in suspension and access problems which are prevalent in developing countries river channels due to the general absence of functional gauging stations along most stream channels in these countries (Ezemonye and Emeribe, 2013). In Edo State in particular there is the general absence of gauging station along the length of river channels. In such situation, a float is the alternative instrument for measurement.

Feasibility projects in hydroelectric power generation capacity evaluation involves complex methods that are tedious, costly and requiring the accumulation of large amount of data up to about 30 years documented in a reliable data management process acquired from gauging and meteorological stations. In Nigeria there is general hydrological data sparsity due to poor financial support, low technical and institutional capacity and outdated infrastructures in the nation gauging stations. A large number of

the institutions have been decommissioned or inactive. Edo North is at least about 57 km from the nearest reliable meteorological data station of Benin and Okene.

Uncertainties are present in the measurement of physical quantities. These uncertainties which constitute the error is the difference between the actual and measured value, and is expressed quantitatively as a parameter. The International Organization for Standardization (ISO) requires that the uncertainty present in the flow characteristics of rivers should be established for the determination of the true value of the measurements (ISO, 2021). The uncertainty is determined from the measured flow characteristics by the identification of the defining features and components of errors in the data, evaluation of the quantity of uncertainty and summation of the components of uncertainty applied to the channel flow. The uncertainty is composed into one standard deviation and is stated as a percentage of the measured value (ISO, 2021).

While uncertainty associated with the use of current velocity meter is well documented and established, not much work has been done in the study of uncertainty using floats (ISO, 2021). In this respect the ISO 748:2007 regulation provides little guidance and reliable research information for the effective determination of uncertainty using floats. Further, due to the possible difference in the flow characteristics of rivers in different climates and regions, the specific determination of the uncertainty of discharge of floats in different locations is an imperative.

This study presents a developed model for the fast, accurate, reliable and easy evaluation of the hydroelectric power generation capacity of rivers with poorly gauged channels using floats to overcome the challenges impose by the present methods, which include the area – rainfall, area-velocity, interpolation of rainfall-discharge methods, etc. There is a significant reduction in cost, amount of data and time requirement

compare to present methods. Components of the study includes the accurate determination of the flow characteristics of rivers and associated uncertainty, data extension from short term to longer term, determination of the specifications and characteristics of the penstock with Solid Works software (fluid) FEA simulations, and turbine selection for the developed power generation phase of the plants and prediction of the future power generation capacity of the three rivers using empirical rainfall - runoff model with nonlinear regression algorithm.

Climate data for the study was obtained from the Department of Meteorology, Federal University of Technology, Akure using metrological data sourced from the archives of National Centre for Metrological Research (CNRM).

1.2 Statement of the Research Problem

The Nigeria economy currently requires 30,000 MW of electricity generation for sustainable development (Izura, 2022). The electrical power availability peaks at 6056 MW as at January 2020 (Nigeria Electricity Regulatory Commission (NERC), 2018). Hydro electric power generation availability is 1060 MW of the total power output (NERC, 2018). The thermal plants that contribute about 82% of the nation electricity suffer from low capacity utilization factor due to aging and irregularity in gas supply (Emovon *et al.,* 2018). Therefore, the imperative of offsetting the balance in power generation has projected the essential need to focus research on hydroelectric power systems especially small hydropower.

Most development projects in hydroelectric power plants installations are initiated with tedious, extensive time ranging between 20 – 30 years and expensive feasibility studies requiring large amount of data to ascertain the viability of the projects. In Nigeria and Edo North in particular, there is data sparsity and general absence of functional gauging

stations where reliable extensive data could be obtained at low cost. It is therefore necessary to develop a model that is easy, fast and reliable with minimum time and data requirement to facilitate Nigeria hydro resources exploration using floats. The model also incorporates the capacity to determine the uncertainty associated with the flow characteristic and hydroelectric power evaluation and predicting the future power output of the selected rivers using empirical rainfall runoff model with nonlinear regression algorithm.

The model generates the value of associated uncertainty and is a quicker, more affordable, and more practical process for evaluating the viability of hydro projects.

1.3 Aim and Objectives of the Study

The aim of the study is to determine the hydroelectric power generation potentials of River Orle, Edion and Orbeh in Edo North of Edo State.

The study specific objectives are to:

i. Develop a reliable model to measure the flow characteristics of the selected river, determine suitable hydraulic head for the hydro power projects and establish the uncertainty associated with the flow characteristic measurement for rivers in Edo North using floats.
ii. Carry out the rivers flow data extrapolation to 30 years using empirical rainfall – runoff nonlinear regression model and predict the future generation capacity of the selected rivers.
iii. Determine the reservoirs capacity, penstock specification through Solid Works software modeling and appropriate turbine selection for the power generation scenario of the plants.

iv. Conduct an Environmental Impact Assessment (EIA) to determine the impact of the hydropower projects in the immediate and extended environment.

1.4 Justification for the Study

Currently, the power generation base of Nigeria is highly inadequate to meet the nation socio-economic development requirements. In the current generation scenario, the thermal power plants with large output of greenhouse gasses and low capacity utilization generate 82 % of the nation electricity. The balance of 18 % is generated by large hydro technology with associated social and ecological impact. The growing awareness to protect the environment has directed attention to small hydroelectric plants as important technology for electricity generation. Conventional feasibility studies on hydro power projects require large amount of data generation between 20 – 30 years in a highly energy consuming, tedious and expensive process. This study is aimed at the development of a model that is fast and accurate with capability of reducing hydro feasibility studies time and large hydrological data requirement from a minimum of 20 years to two years for the evaluation of small hydro plants hydrological potentials and determination of the uncertainty associated with the flow characteristics measurement.

1.7 Scope of the Study

The study covered only three major Rivers in Edo North senatorial District, namely river Orle, Obeh and Edion with good hydroelectric generation features along their flow courses.

Flow characteristic measurement and evaluation were carried out on the three river channels each month from January to December for 2018 and 2019 respectively to determine the rivers hydroelectric power generation characteristics. The uncertainty of measurement associated with the flow characteristics measurements according to the types of floats were established. Discharge data extension and prediction of the future

hydroelectric power generation potentials of the rivers with the Gauss – Newton nonlinear algorithm was carried out.

Determination of the basic system components sizes, specifications and power generation scenario for optimal performance of the plants. Both technical and economic feasibility of the selected rivers projects for power generation were carried out.

The study also accessed the effects on the environmental of the construction of the plants and determined mitigation measures to be adopted in the reservoirs design, construction and operation to minimize the impact of the plants on the environment.

1.8 Significance of the Research

This study provides significant savings of resources spent on tedious, expensive, and time consuming feasibility studies and facilitates the estimation of the viability of hydro power plants. It will provide and establish a model that integrate and automate the evaluation of the hydroelectric generation potentials of hydro sites and characterization of uncertainty associated with the measurement process using floats, and also provides a basis that develops insights into the future power generation capacity of hydro plants.

By offering a methodology to make it easier to use Nigeria's hydroelectric power potential with few resources, it would lay the foundation for a sustainable power supply for the country's economy. The study provided a feasibility study, extensive discharge data extension, system components design and optimal operation of hydropower plants.

CHAPTER TWO

2.0 LITERATURE REVIEW

The chapter covers the review of related literature in hydroelectric power generation and utilization through the methods of assessing the hydroelectric generation potentials of sites, hydro system modeling, simulation and configuration, equipment sizing and selection. The review process was directly correlated with the objectives of the present study alongside other emerging essential issues and challenges in environmentally-friendly and water management hydro power generation.

2.1 Hydroelectric Power Generation

Waterfall energy is harnessed by hydropower facilities to produce electricity. A mass of water going down a height difference contains energy that can be captured by a turbine to create electricity. The amount of electricity produced depends on the hydropower system's speed, number of generator windings, head, and flow rate. The plant's head directly influences how much electricity is produced.

The kinetic energy of the water is transformed into mechanical energy via a turbine. The mechanical energy from the turbine is then transformed into electrical energy by a generator attached to it. The water's direct kinetic energy is used to turn the blades, which are attached to power generators (Spilsbury *et al.,* 2008). Water energy, primarily hydropower, is used to produce around one fifth of the world's electricity. Hydroelectricity is a competitive source of renewable energy because of its affordable cost. In contrast to other types of power generation, the hydro plant uses no fuel.

2.1.1 Hydroelectric power generation potentials

The total amount of power that might theoretically be produced if all available water resources were used to produce electricity is known as the gross theoretical potential.

The hydroelectric power content that is appealing and is easily tapped using current technology is represented by the technically potential. The amount of hydroelectric power generation capacity that is estimated after a feasibility study of a project at current pricing past the breakeven threshold is known as the economically feasible potential.

2.1.2 Classification of hydropower systems

According to the US Directorate of Energy (DOE), Hydropower plants are categorized according to size of power output. Large hydropower is generally classified between installation capacity of 100 MW and above. Medium hydro plant capacity rating is between 15 – 100 MW, while small hydro is between 1 MW – 15 MW (Crettenand, 2012). Mini, micro, and pico hydro power systems are additional subcategories of small hydropower plants.

i. Mini hydro power system

A mini hydropower system is the production of hydroelectric power on a scale adequate for local community and industries consumption. It could also contribute to the grid power network in a country (Crettenand, 2012). It has generation capacity of 100 kW to 1 MW (Crettenand, 2012).

ii. Micro hydropower systems

Micro hydro is a term used for hydroelectric power installations that typically produce up to 100 kW of power (Crettenand, 2012). These installations can provide power to an isolated home or small community, or are sometimes connected to electric power networks. Micro hydro systems can complement solar energy systems because available hydro power is highest in the winter when solar energy is at a minimum (Clack *et al.*, 2017). A Micro hydropower plant is shown in Figure 2.1.

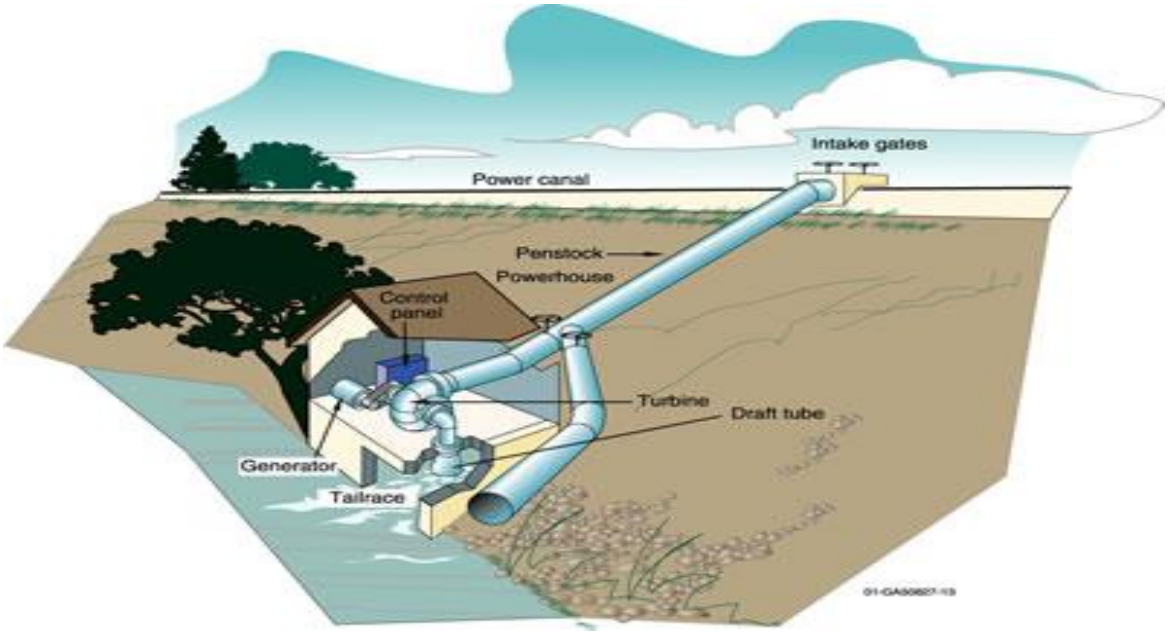

Figure 2.1: Micro Hydro Power Scheme (Directorate of Energy, 2018)

iii. Pico hydropower systems

Pico hydro is hydro power with a maximum electrical output of 5 kW (Clack *et al.*, 2017). It is useful in small, remote communities that require only a small amount of electricity. Pico-hydro setup is typically run-of-the-river scheme, meaning that dams are not used, but rather pipes divert some of the flow, drop this down a gradient, and through the turbine before returning it to the stream. Hydropower systems of this size benefit in terms of cost and simplicity from different approaches in the design, planning and installation than those which are applied to larger hydro power. A summary of hydro power scheme is presented in Table 2.1.

Table 2.1: Classification of Hydro Power Scheme (Clack *et al.*, 2017).

Type of hydropower plant	Capacity
Large	100 MW and above
Medium	Between 15 MW to 100 MW
Small	Between 1 MW to 15 MW
Mini	Between 100 kW to 1 MW
Micro	Between 6 kW to 100 kW
Pico	Up to 5 kW

2.2 Hydropower Generation Methods

2.2.1 Conventional method (dams)

Using conventional method water is stored in large reservoirs to build up the head and quantity of water. The water acquires a high potential energy which is converted into kinetic energy in the turbine blades. A large penstock delivers water from the reservoir to the turbine (Clack *et al.*, 2017). A conventional hydropower plant is shown in Figure 2.2.

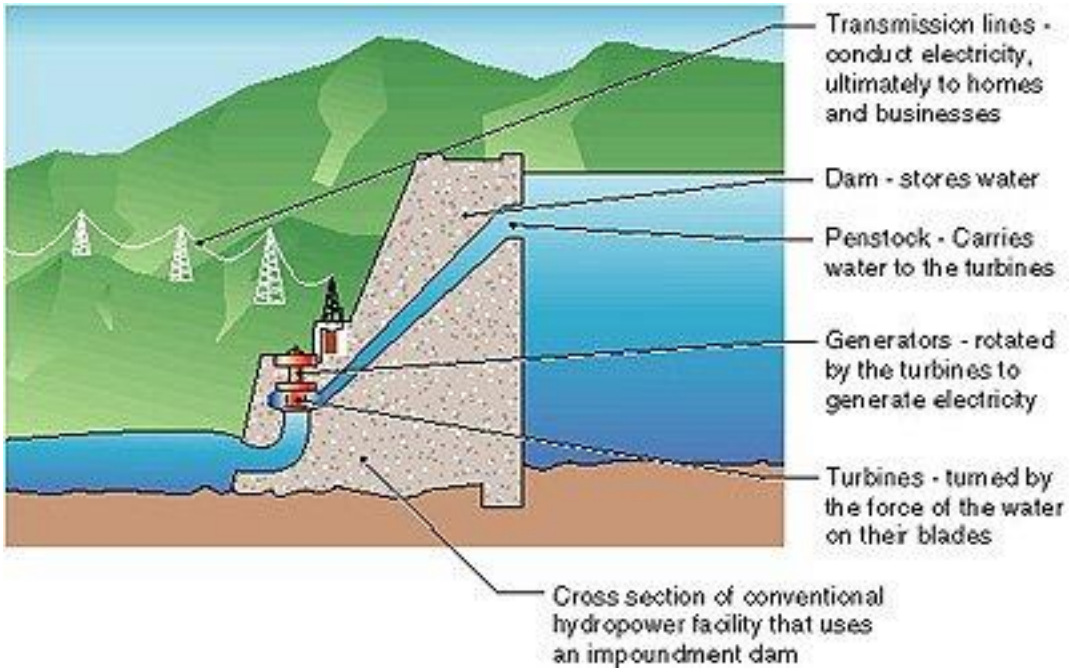

Figure 2.2: Conventional Hydropower Setup (Directorate of Energy, 2018)

2.2.2 Pump storage method

This method produces electricity to supply high peak demands by moving water between reservoirs at different elevations. At times of low electrical demand, the excess generation capacity is used to pump water into the higher reservoir. When the demand becomes greater, water is released back into the lower reservoir through a turbine. Pumped-storage schemes currently provide the most commercially important means of large-scale grid energy storage and improve the daily capacity factor of the generation system (Energy Storage Association, 2018). A pumped storage power is depicted in Figure 2.3.

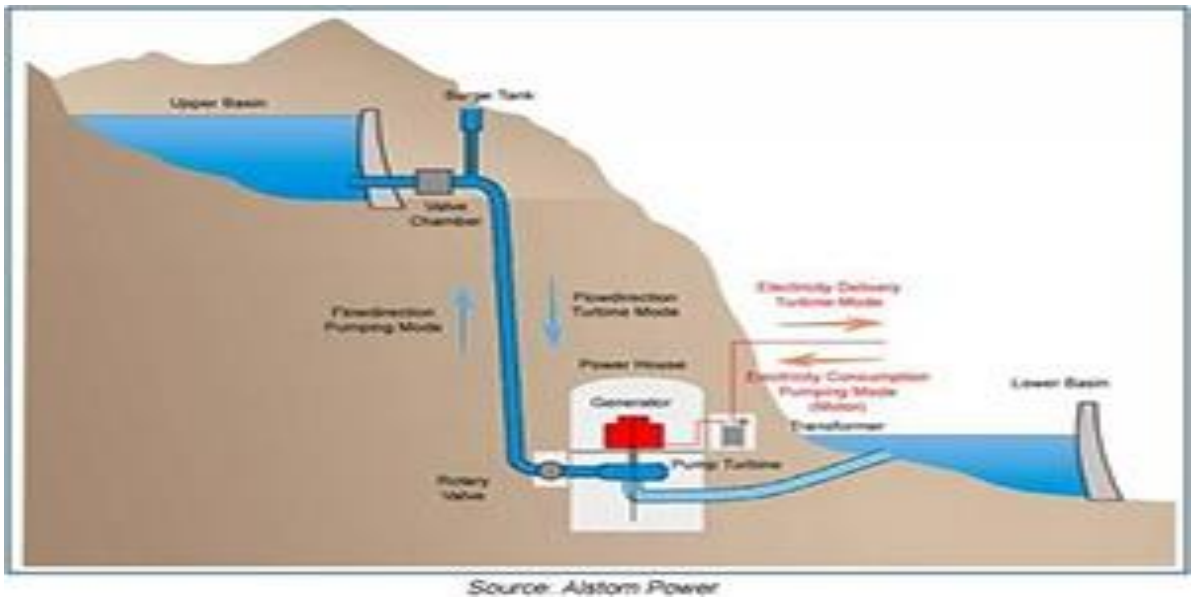

Figure 2.3: Pumped Storage Hydro Scheme (Energy Storage Association, 2018)

2.2.3 Run-of-the-river scheme

Run-of-the-river (ROR) hydroelectric stations are ones that have little to no reservoir storage space, allowing just the water from the upstream stream to be utilised for generation at any given time and forcing any excess water to flow by unused. When selecting locations for run-of-the-river systems, having a steady supply of water from a lake or existing reservoir upstream is quite advantageous (Mbakaa and Mwanikibi, 2016). A ROR is shown in Figure 2.4.

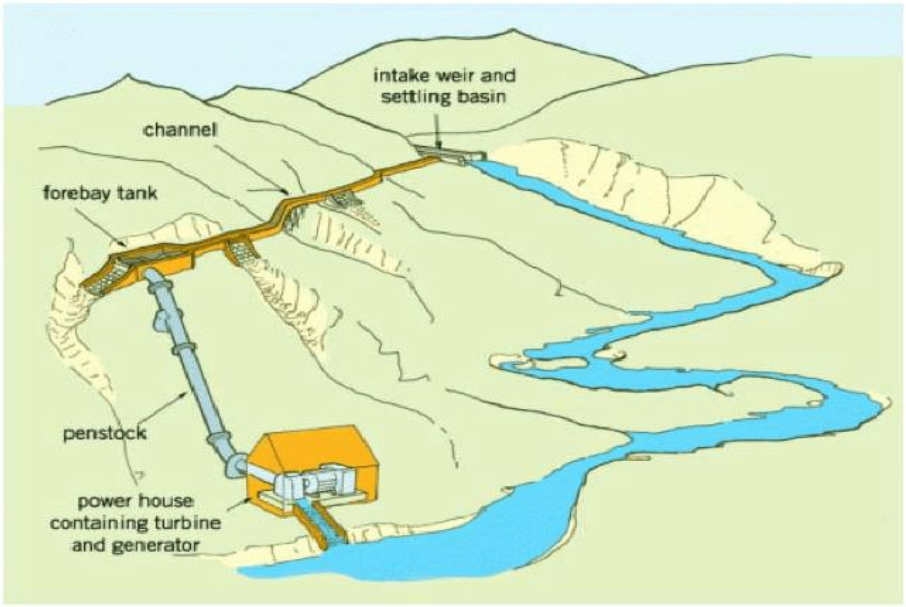

Figure 2.4: Run-of- the-river Hydro Power Arrangement (Mbakaa and Mwanikibi, 2016)

2.3 Technology of Hydroelectric Power

A dam serves two purposes at a hydro plant. First, a dam increases the head of a waterfall and controls the flow of water. Dams release water when it is needed for electricity production. Special gates called spillway gates release excess water from the reservoir during heavy rain falls.

Both dams and run-of-river systems use turbines. Inside each turbine there is a shaft, which is attached to a generator. Water turns the rotor of the turbine. There are wire coils made of copper that move inside a circular stratum of magnets when the rotor turns. This creates electrons when the wire coils pass the magnets, and the flow of these electrons is electricity (Spilsbury *et al*. 2008). The generator is attached to transformers so that the electricity can be transmitted through cables over distances. The generator is attached to transformers so that the electricity can be transmitted through cables over distances.

2.3.1 Head and flow rate

Whenever water flows from a higher elevation to a lower elevation there is the potential to harness that energy to do useful work. The energy available in the water is a function of two variables: the head and the flow-rate. The head is the vertical distance through which the water can be made to fall. The flow-rate is the quantity of water moving past a fixed point in a given time. Both head and flow-rate contribute equally to the energy of a stream. The greater the volume of water and the higher up it is, the more energy it contains. In general, less water flow is required in high-head plants than at low-head plants to generate the same quantity of energy. The relationship between head and flow rate impacts power output. In general, less water flow is required in high-head plants than at low-head plants to generate the same quantity of energy. The relationship between head and flow rate impacts power output.

2.3.2 Losses in penstock

Losses exist in the penstock and turbine due to friction and turbulence. The gross head which obtained when there is no flow through the penstock does not take into account these losses. The effective head, which is the head manifest at the turbine inlet in the form of hydraulic pressure, is the gross head less the head losses. Head losses depend on the pipe length, diameter, surface texture, flow-rate, and the number and type of fittings between the intake and the turbine. Typically pipe losses are broken out into two parts: the losses due to the pipe itself and the losses due to the fittings. Friction in a straight pipe is directly related to the water's speed and to the pipe's length to diameter ratio. The building material and flow conditions have an impact on the friction factor.

Minor losses refer to turbulence-induced pipe losses from fittings and valves. As their total losses might be substantial, it is best to reduce the length of the pipe as well as the

quantity of elbows, valves, and other fittings in the flow route. Any decrease in the effective head will result in a proportional decrease in power output.

2.3.3 Hydropower system flow estimation methods

The flow-rate of hydropower scheme can be estimated using analytical techniques, such as the area-rainfall method, or measured directly. In each case, a hydrology study should be based on many years of daily records (Harvey, 2006). Typically, for short duration studies, the area-rainfall method is preferable were historic precipitation data is relatively easy to obtain. It is recommended to take periodic site measurements, to verify that the results of the analysis are reasonable.

2.3.4 Head measurement methodology

The gross head can be determined by surveying the land using GIS equipment or by counting the contours from a good-quality topographical map. Either method is considered adequate for site assessment calculations.

2.4 Hydropower System Intake Components

This allows a constant stream of water to enter the penstock without any air. Gravels and floating debris are restrained from entry the penstock. Healthy intake is self-cleaning and doesn't clog easily.

2.4.1 The penstock

Most hydro schemes use a penstock to deliver water under pressure to the turbine. The vertical distance that the water drops as it travels through the penstock is what generates the head. The length of the penstock has no bearing on the gross head, but it does influence the effective head because of fluid friction. The penstock should be of sufficiently large diameter to supply the needed flow without excessive losses. For any

given diameter of pipe, there is an optimum flow-rate, above which the power will begin to decrease with increasing flow. Therefore, care must be given to selecting the proper size pipe for a given application (Bailey and Bass, 2009). Although it is true that bigger pipes always have less losses, doing so might not always be cost-effective. Large diameter pipes are pricey, and the penstock is sometimes the system's most expensive individual component. More than just choosing the proper pipe size and material is involved in penstock design. PVC pipe stretches and shrinks around five times more than steel. The expansion and contraction that takes place as a function of temperature must be taken into account. The phenomenon known as "water hammer" and the surge pressures that result from valves closing quickly can both cause pipe breakage.

Although it is true that bigger pipes always have less losses, doing so might not always be cost-effective. Large diameter pipes are pricey, and the penstock is sometimes the system's most expensive individual component. More than just choosing the proper pipe size and material is involved in penstock design. PVC pipe stretches and shrinks around five times more than steel. The expansion and contraction that takes place as a function of temperature must be taken into account. The phenomenon known as water hammer and the surge pressures that result from valves closing quickly can both cause pipe breakage.

The penstock has a power valve and an adjustable nozzle that may be used to regulate the water pressure and flow rate, respectively, to maximize the turbine speed. It also has a pressure gauge, which is required to monitor the water pressure level so that the user may determine the ideal pressure level for power generation, to measure the water pressure that corresponds to the net head (Bailey and Bass, 2009).

2.4.2 Turbine system

The turbine converts the kinetic energy of the water into torque for the generation of electricity. Turbines can be broadly categorized as either impulse turbines or reaction turbines. Impulse turbines convert the kinetic energy of a jet of water in air into movement by striking buckets or blades. The blades of a reaction turbine are totally immersed in the flow of water, and the angular as well as linear momentum of water is converted into shaft power. Reaction turbines typically require large flows and moderate heads.

The generator's function is the transformation of mechanical energy into electrical energy. Generators can be either direct current or alternating current versions, and their sizes must match the available shaft power. With very small size devices, permanent magnet DC generators are typical. Alternating current is almost often used in larger systems.

2.4.3 Flow control system

Sites with variable or epileptic flows, particularly those that vary across the day requires automatic control systems to minimize the need for human intervention. A basic control system consist of a level sensor or flow meter and control logic system that generates signals to open and close valves at the turbine inlet. Advanced control subsystem monitors various parameters and safely shut down the turbine and electrical system at any sign of system instability.

2.5 Benefits of Hydropower Generation

2.5.1 Flexibility of operation of hydropower generation

Hydropower is a flexible source of electricity since stations can be ramped up and down very quickly to adapt to changing energy demands. Hydro turbines have a start-up time

of the order of a few minutes (Robert, 2010). It takes around 60 to 90 seconds to bring a unit from cold start-up to full load; this is much shorter than for gas turbines or steam plants (Gracia *et al.*, 2019). Power generation can also be decreased quickly when there is a surplus power (Sorensen, 2004). Hence the limited capacity of hydropower units is not generally used to produce base power except for vacating the flood pool.

2.5.2 Low cost power production

The major advantage of conventional hydroelectric dams with reservoirs is their ability to store water at low cost for dispatch later as high value clean electricity. When used as peak power to meet demand, hydroelectricity possess a higher value than base power and a much higher value compared to intermittent energy sources.

Hydroelectric stations have long economic lives, with some plants still in service after 50–100 years. Operating labour cost is also low, plants are automated with few personnel on site during normal operation.

Where a dam serves multiple purposes, a hydroelectric station may be added with relatively low construction cost, providing a useful revenue stream to offset the costs of dam operation.

2.5.3 Suitability for industrial applications

While many hydroelectric projects supply public electricity needs, some are created to serve specific industries. Dedicated hydroelectric projects are often built to provide the substantial amounts of electricity needed for aluminium electrolytic plants.

2.5.4 Decreased cabondioxide emissions

Since hydroelectric power systems do not use fuel, power generation does not generate carbon dioxide. While carbon dioxide is initially produced during construction of the

project, and some methane is given off annually by reservoirs, hydro normally has the lowest lifecycle greenhouse gas emissions for power generation. Compared to fossil fuels generating an equivalent amount of electricity, hydro displaced three billion tonnes of Co_2 emissions in 2011.

One measurement of greenhouse gas related and other externality comparison between energy sources can be found in the ExternE project by the Paul Scherrer Institute and the University of Stuttgart which was funded by the European Commission (Helston and Farrris, 2016). According to that study, hydroelectricity produces the least amount of greenhouse gases and externality of any energy source. Coming in second place was wind, third was nuclear energy, and fourth was solar photovoltaic **(**Dones *et al*., 2004)

2.5.5 Climate change challenge

Because hydroelectric dams don't burn fossil fuels, they don't emit the emissions that coal and gas plants do, which are responsible for smog and acid rain. They don't produce any smog- and acid rain-related toxins. Carbon emissions from building and operation account for the majority of them. According to research by the Canadian government, hydropower generates 60 times less carbon throughout its lifetime than coal-fired power plants and 18 to 30 times less than natural gas power plants (Helston and Farrris, 2016).

2.5.6 Multipurpose dams application

Dams often provide facilities for water sports, and become tourist attractions. In some countries, aquaculture in reservoirs is common. Multi-use dams installed for irrigation support agriculture with a relatively constant water supply. Large hydro dams are used to control downstream flooding (Atkins, 2003).

2.5.7 Effects on local communities

Most people in the area near waterfalls live on agricultural cultivation. With minimum electricity they can manage their daily life more effectively and comfortably. They can enjoy all the facilities of a city life. In addition, the maintenance of the plant needs a few people for employment. With simple technology using light people have access to good water supply.

2.6 Disadvantages of Hydroelectric Power Plants

2.6.1 Damage to ecosystem

Large reservoirs associated with hydroelectric power stations result in submersion of extensive areas upstream of the dams, sometimes destroying biologically rich and productive lowland and riverine valley forests, and grasslands. Constructing large dams and reservoirs often involves displacing people and wildlife (Worldwatch Institute, 2012). The loss of land is often worsened by habitat fragmentation of surrounding areas caused by the reservoir (Robbins, 2007).

Usually the water world in the waterfall consists of small fishes, prawns and other microorganisms. Their natural surroundings may be hampered by the oil and grease leakage from the mechanical moving parts of the plant.

Water exiting a turbine usually contains very little suspended sediment, which can lead to scouring of river beds and loss of riverbanks. Since turbine gates are often opened intermittently, rapid or even daily fluctuations in river flow are observed.

Though hydroelectric power has traditionally caused some environmental harm, it is not substantial enough to warrant this source of power unusable. Due to changing lifestyles and standards of living worldwide, energy needs are predicted to rise 50% in the nearest future (Spilsbury *et al*., 2008). As the world search for ways to increase the amount of

power accessible without increasing strains on the environment, hydroelectric power could become a major part of the future power generation scenario.

2.7 Hydropower Generation in Nigeria

Nigeria currently has three Hydropower producing Stations, namely Kainji, Jebba and Shiroro hydro power plants. They have installed capacity of 760MW, 570 MW, 600MW respectively (Olaoye *et al*., 2016).

Their available capacity fluctuates according to the availability of water for power generation. In other to make provision for future power demands in Nigeria, the Ministry of Power and Steel has proposed and identified potential hydro power stations nationwide. The Federal Government of Nigeria has initiated action in the construction of hydro power plants in the Mambila Plateau with a capacity of 3050 MW, Zungeru of 700 MW, Gurara of 30 MW, Dadin Kowa of 35 MW (NERC, 2018).

Studies have shown that Nigeria can harness about 964 MW of SHP from 277 sites. There are also indications that about 12,220 MW capacity hydro power sites are exploitable in Nigeria (Olaoye *et al.*, 2016). Hydro power plants produce about 18% of the nation electricity generation output (NERC, 2018).

2.8 Environmental Challenges Associated with Large Hydropower Plants

There are some environmental challenges associated with the generation of power with large hydroelectric power plants. These challenges border largely on flooding of human settlements and interruption of rivers ecosystem, animal habitats and biodervisity.

Large hydro power requires enormous land for the generation of hydroelectric power. The amount of land consume depends on the site, topography of the river and power generation requirement. As a general rule 50 km^2 of land is required for every 100 MW (Tisdal, 2016). This poundage of river water into large artificial lake has serious

consequences for human, birds population, fishes and other animals. In some instances floods covers agricultural land adversely affecting the livelihood of some local communities. Two major cities and about one million people were recently relocated in China to build the Tree Gorge Dam (Helston and Farrris, 2016). The diversion of rivers from their natural path has significant impact on rivers ecosystem. The impoundment area witnessed increased sedimentation due to decreased velocity of flow of water. Fish habitats are covered by sand, clay and silt which impairs the spawning process (Helston and Farrris, 2016). This also adversely affects some fish species that relies on strong moving current of water for movement during migration. Dams act as barrier to adult salmons in their upstream movement for reproduction, although this effects has been minimized by the provision of fish ladders in the dams.. Periodic water releases from the dams generates strong currents that causes erosion and deepening of water flow channels. The low temperature of reservoir water when released causes shock to fishes that live in shallow warm water downstream, coupled with the poor oxygen content of the deep dam water , the fish habitats becomes inhospitable.

The huge quantity of water retained in large dams posses serious risk to humans and animal habitats in the event of dam failure. Powerful fluids can be releases that can cause devastation to human settlements, farm lands and wild habitats. About 26,000 people were killed in the Bangio dam failure in China in 1975 while about 145,000 died from epidemics emanating from the flooding (Tisdal, 2016).

2.9 Current Emphasis on Small Hydropower Generation

The amount of energy needed to support the economies of developing nations is increasing exponentially, placing great strain on the planet's finite resources and leading to increased Co_2 emissions (Mott et al., 2021). Small hydropower has emerged as a

significant source of renewable energy due to the increasing awareness of the need to conserve the environment and the ecology of various species as well as the incentives provided by the relevant authorities. Small hydro power plants have been advocated as the preferred technology for generating electricity in areas with sustainable water supplies as a result of the Co_2 reduction objectives imposed by many nations and accompanying financial incentives to support renewable technology (Tamburrini, 2004).

SHP contributes to sustainable development by being economically feasible, respecting the environment (avoiding greenhouse gas emissions) and allowing decentralized production for the development of dispersed populations. Building SHP plants helps create a more diversified electricity system**,** providing production of electricity in smaller distribution systems when the main grid is disrupted. Furthermore, since SHP is a decentralized energy source located close to the consumers, transmission losses can be reduced.

Small hydropower benefits from different design, planning, and installation methods than those used for bigger hydropower in terms of cost and simplicity. Even in extremely underdeveloped and inaccessible areas, recent developments in small hydro technology have made it a viable source of electricity (Zainudden *et al*., 2009). According to research, small hydroelectric power systems are easier to adapt to their surroundings and have less of an impact on the environment than huge hydropower projects (Hatata *et al*, 2019).

2.10 Challenges in Assessing Data for Hydroelectric Power Development

The flow characteristic of a river can be measures using the area – rainfall method and area – velocity method. The measurement should be based on many years of records (Harvey, 2006). The area - rainfall method is preferable for short duration study in

countries where historical precipitation data is relatively easy to obtain. However, this measurement should be validated with periodic site measurement. The area - rainfall method requires up to 30 years worth of daily rainfall data, accurate drainage basins data, topographical maps, land use pattern and cover map, and impervious surface factors for calculation of runoff (Bailey and Bass, 2009), which are largely not available for many catchment areas in developing countries due to the substantial gap in quality and general data availability for detailed quantitative analysis in water related power generation studies (Larson *et al.,* 2019).

Likewise, for the area – velocity method, the documentation of reliable, long-term and consistent information on river discharges for most basins in developing countries is either lacking or grossly inadequate (Negrel *et al.*, 2011). This is due to the general absence of functional gauging stations along most stream channels in these countries (Ezemonye and Emeribe, 2013).

An assessment of the hydrological services in low and middle income countries to understand their status, performance obstacles, and investment needs by the Global Facility for Disaster Reduction and Recovery (GFDRR) (2018), found institutional constraints in fragmented and myopic policy environments, insufficient budgets, limited and often declining hydrometeorological monitoring networks, insufficient maintenance of hydrological infrastructure, inadequate data management systems, and insufficient integration between hydrological and meteorological services.

Consequently, in the developing world, the design of water retention, regulation and control facilities is carried out with inadequate or sparsely available hydrometreological data. This data when available are either too short and when extended include numerous gaps or discontinuities which render them not useful.

In Nigeria, existing hydrological and meteorological gauge stations fall short of the recommendations of the World Meteorological Organization, The country's lack of data is due to a significant number of established stations being inactive, decommissioned, or discontinued. Lack of funding, technological shortcomings, inadequate institutional capability, and outdated infrastructure have all been mentioned as contributing factors to Nigeria's data shortages (Ngene *et al.,* 2015).

The challenge of long term data availability is address through some data extension and generation techniques in synthetic flow records generation. This is done to extend the scope of available historical flow records from short to long-term using stochastic methods. Chetersingh and Ajaysinh (2014) generated synthetic flow records on Kainji Dam using mean monthly historical records with ARIMA model. The statistical parameter of mean, standard deviation and correlation coefficient of generated data were compared with historical data. The results indicate that the model is capable of generating reliable sequence of flow data with similar statistical parameters with that of the historical data. Tuna (2013) assessed the feasibility of a hydro power plant on the Ulucay River in Nepal, an ungauged river basin. Hydrological data from a nearby gauged river basin were extrapolated with correlation-regression techniques to extend the field data from one year stream discharge to twenty years data. A design flow of 8 m^3/s which corresponds to 22%-time exceedence on the flow duration curve was adopted. The project output was optimized by determining the output from a discharge range of 6.00 - 9.50 m^3/s at an increment of 0.25m^3/s. The installed power and annual power output were worked out in conjunction with the net head for the flow range. Ogunela *et al.* (2019) assessed the economic sustainability of integrated hydro power development of Ero – Omola falls. The rating curve was used to obtain a 12 month data on the stream discharge and hydropower load demand. Stochastic theory using the

Thomas Flearing method was used to extend the data from one year data to long term data using available long term stream data in an adjourning catchment with similar climatic conditions. The potential hydropower of the plant was estimated to be 8.00 MW. Estimation for other associated uses of the dam were also carried out.

Razavi and Coulibay (2020) carried out a review on the regionalization of stream flow data and its advances in the last two decades. Analysis was carried out on developments in continuous stream flow regionalization, optimization processes, uncertainty analysis involved in the regionalization processes and process challenges. Conceptual rainfall-runoff models that have been most utilized in regionalization were identified with the associated physical attributes and meteorological information required.

2.11 Assessment of Metrological Data through Geographical Information System and Remote Sensing

Geographical information systems is a computer base tool for retrieving, storing, analyzing and presenting all forms of geographical data (Teixeira, 2016). It integrates data base operations of query and statistical analysis in conjunction with maps. Global Positioning Systems (GPS) is combined with GIS to provide more complete information of locations on topographic surveys, digital elevation model (DEM), land use and land cover maps

Remote sensing provides effective means of monitoring and identifying numerous hydrological parameters and variables which are required for the estimation of hydrological project reliability. It allows essential hydrological data to be acquired quickly at certain intervals and covering large areas. Satellite imagery has been helpful in the field of meteorology, watershed management and hydrological modeling (Thakur *et al*., 2017).

Ekeu-wei and Blackburn (2018) noted that some of the issues related to the collection of hydrological data in developing countries include poor maintenance of hydrological infrastructure, poor financial commitment, low capacity and institutional gaps, and accidentally collapsing hydrological equipments. The study suggested more effective techniques for gathering and managing hydrological data, including the use of Geographic Information Systems (GIS).

2.12 Rainfall – Runoff Modeling

Surface runoff from rainfall runs across the land without infiltration into streams, rivers and other water reservoirs (Perlman, 2016). Surface runoff is a function of time, physical and geological characteristic of the catchment area. About two – third of the volume of rainfall is infiltrated into the soil and evaporated with about one – third constituting runoff that appears as river discharge. Generated surface runoff flows through land surfaces, discharged into streams and rivers that eventually discharged into the oceans (Sitterson *et al*., 2017). Figure

2.5 indicates the water cycle.

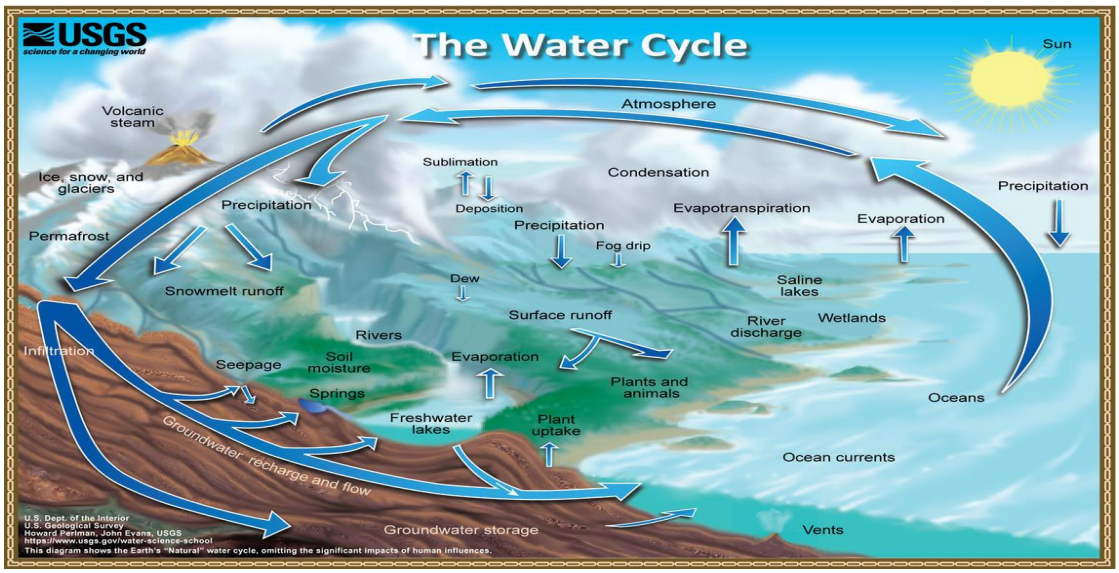

Figure 2.5: The Water Cycle (Sitterson *et al*., 2017)

The water balance equation, as shown by Equation 2.1, controls the hydrological cycle.

$$R = Q_s + E_e + \Delta S_w + \Delta G_w \quad (2.1)$$

Where,

R is rainfall

Q_s is surface discharge

E_e is evaporation

ΔS_w is change in water content

ΔG_w is change in ground water level (Sitterson *et al.*, 2017).

The amount of river discharge in a catchment area is affected by land cover, vegetation, soil properties and volume of rainfall (Sitterson *et al.*, 2017). The volume of runoffs is influenced by the saturation and infiltration excess mechanism (Yang *et al.*, 2015). Figure 2.6 indicates the basic components of runoff hydrograph.

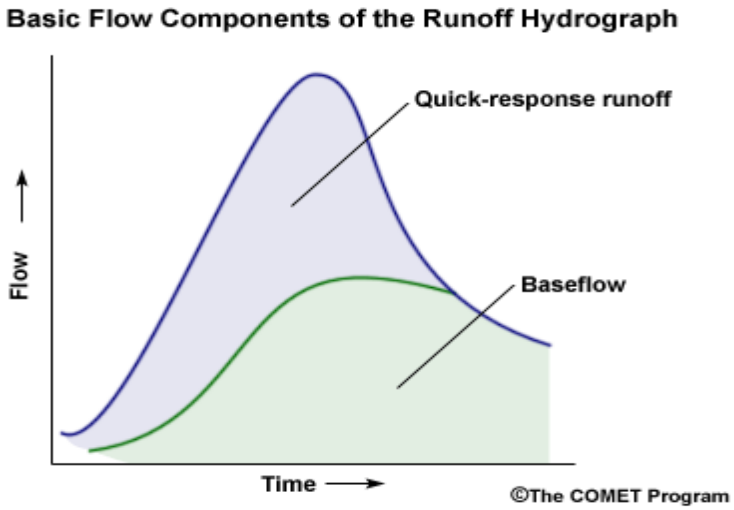

Figure 2.6: Basic Components of a Runoff Hydrograph (Siterson *et al.* 2017)

The total discharge of a river comprise the runoff, the base flow and direct precipitation. The major component of the stream flow being the runoff and base flow. The base flow sustains the river flow in the absence of rainfall and is derived from the undersurface discharge of water across the ground, ground water penetration and soil moisture, which infiltrates into the ground from rainfall.

2.12.1 Runoff modeling

Rainfall – Runoff modeling estimates the volume of runoff generated in a watershed. Runoff modeling assesses the catchment water yields, availability and changes with time (Vaze *et al*., 2012). The components of some models comprise input boundary conditions, governing equations, model processes, output, etc (Sitterson *et al.*, 2017). Surface runoff modeling involves intricate mathematical procedures with many interrelated parameters. (Sitterson *et al.*, 2017).

Numerous methods of classifying models are available, generally models could be classified as empirical, conceptual and physical models. The modeling purpose influence the choice of rainfall – runoffs model used to implement modeling objectives into some of the parameter of the catchment area hydrological process, predicting runoff yield for the purpose of water resources management and assessing the frequency of runoff events (Vaze *et al.,* 2012). Other considerations include limitation of data availability, available time and resources for model implementation.

Some models are easily implemented with some few variables while others require a wide range of intercalated data. Table 2.2 shows the characteristics of the three basic types of models with their strength and weaknesses.

Table 2.2: Comparison of the basic Model structure of Rainfall – Runoff Modeling (Sitterson *et al.*, 2017)

	Empirical	Conceptual	Physical
Technique	Non linear link between inputs and outputs.	Equation that represents the catchment's water storage concisely	Physical laws and equations based on real hydrological processes.
Strength	Fewer parameters needed, more precise, and quick run time.	Simple model construction, simple calibration.	Use extremely fine scale, incorporates both temporal and geographical variability.
Weakness	No connection between physical catchment characteristic, possible input data distortion.	Do not consider spatial variability within catchment	Large numbers of parameters and calibration needed, site specific.
Best use	Ungauged watershed requires simply runoff as an output.	When there is a lack of data or restricted computational time	A modest scale with significant data availability
Examles	Curve number, Artificial neutral network, regression equations	HSPF, TOP MODEL, HBV, STANFORD	MIKE – SHE, KINERDS, VIC, PRMS

2.12.2 Regression base empirical rainfall - runoff models

These are models that use nonlinear statistical relationship between inputs and outputs. They depend on input accuracy and are observational oriented. Historical rainfall and runoff are used as inputs in regression models of rainfall and runoff, while specific location runoffs are the output.

Equation 2.2 shows the general governing relationship for empirical models

$$R = f[X_r, Y_d] \quad (2.2)$$

where,

R is discharge output

X_r is input set of precipitation data

Y is input set of historical river discharge

Empirical model are input and output oriented with little exposure concerning the internal process that controls the evaluation of the results (Granata *et al.,* 2016). They are best suited for ungauged watersheds due to absence of specific data with very few parameters required compared to other models (Pechlivanidis *et al*., 2011). The models have the advantage of faster computation time, cost effectiveness and simplicity of implementation (Sitterson *et al.,* 2017). Empirical models can produce precise simulations under a variety of circumstances, including as extended time steps and reproducing previous runoff values (Vaze *et al.,* 2012). The main source of error is derived from the input data. Regression equations, which identify the functional connection between inputs and outputs, are examples of empirical models. Below is a selection of research articles on regression-based empirical modeling.

Regression analysis and clustering were used in hydrological real-time series by Mishra *et al*. (2018), producing excellent results for data analysis and catchment hydrological runoff predictions. Actual field data, forecasted data, and the validation of the regression yield using the ARIMA model were all compared in the study. It was noted that the created model is better suited for runoff modeling and is very beneficial for allocating and developing water resources. Regression study of runoff volumes and peaks against descriptors of rainfall characteristics and antecedent conditions was performed by Mcintyre *et al.* (2009). Rainfall volume, rainfall peak, rainfall geographic position and variability, and antecedent wetness were shown to be the elements

influencing runoff. The study found that the best predictions and the best prediction confidence bounds were produced by a straightforward linear relationship between rainfall and runoff. According to the report, physical-based models won't produce more accurate forecasts. Tegegne *et al.* (2017) compared two simple conceptual models and one complicated model to investigate daily stream dissipation forecasts for four large gauged watersheds. The model's ability to replicate observed stream flow in the temporal and quantile domains was examined. The results of the study showed that, for recreating observed stream flow in the time domain, the output from simple conceptual models performed better in smaller watersheds, but the complex model performed best for the largest watershed. Zhang *et al.* (2017) used a large data set from 605 catchments throughout Australia to compare the regression tree ensemble approach with the three other widely used techniques of multiple linear regression, multiple log-transformed linear regression, and hydrological modeling to assess the prediction accuracy of thirteen runoff characteristics. All four techniques can accurately anticipate the long-term average and high flow catchment characteristics as well as applications where a particular runoff characteristic is required, according to the study's findings. The strongest forecasts came from regression relationships that directly connected runoff characteristics to catchment parameters. For the Pamela watershed in India's Rangaredy District, Ramana (2014) developed a regression analysis model with three modules for time of concentration, rainfall, and moisture contents. The study came to the conclusion that regression analysis performs similarly to other common models in terms of runoff prediction.

2.13 Uncertainty Analysis in Hydrological Studies

A measured value is only an approximation of the true value of the measurement due to the presence of errors that produces uncertainty in the data correctness. Therefore,

uncertainty exists in the measured quantities of flow data, which may be due to random, and system errors.

Therefore, the uncertainty present in the flow characteristics in the evaluation of the hydro potentials of hydro sites should be evaluated for the determination of the true value of the measurement. The uncertainty is determined by the identification of the defining features and components of errors in the data, evaluation of the quantity of uncertainty and summation of the components of uncertainty applied to the channel flow. The uncertainty is composed into one standard deviation and is expressed stated as a percentage of the measured value (ISO, 2021).

Some related works on the uncertainty studies are presented. Nrzinsinski (2013) investigated the spatial difference in the features of uncertainty in the flow regime of rivers in Europe using the Shannon Information Enthropy theory. The study found a direct link between the volume of flow increasing and the degree of uncertainty in the rivers' flow regime. Nrzinsinski (2013) used the fuzzy set theory to analyze distinct sources of uncertainties in the stage and discharge measurement and their accumulation into combined uncertainty according to ISO 748 regulation. The study indicated that the fuzzy set theory is an effective tool for the analyses of uncertainties in stage discharge measurement with the rating curve on a non-probabilistic basis. For medium-sized rivers and tributaries, Tazioli (2011) presented a comparison of measurements made using various tracers and current meters under various watercourse conditions. The study came to the conclusion that current meters produce accurate readings under typical discharge conditions and advised using artificial tracers during low flow and flood events. In order to reduce overhaul gauging time, Clasing and Munoz (2018) provided an analysis to determine the ideal point velocity measurement time (VMT). The study suggested a minimal VMT of 20s for gauging in shallow rivers. In order to

ascertain the implications of the discharge data used in the calibration of the water level in rivers modeling procedure, Warmink *et al.* (2007) carried out flow error analysis. The conclusions include the fact that extrapolating model roughness introduces uncertainty into model results. A methodology for evaluating and figuring out the degree of uncertainty in river flow data produced from the rating curve approach was created by Baldassare and Moutanari (2009). Uncertainty in the river discharge procedure was found to be significant and to have a major impact on the results' output. Le Coz *et al.* (2012) developed a generalized method for computation of uncertainty in velocity – area discharge flow measurement process using current velocity meters. The paper reported that the new method is more versatile and robust than IS0 748 approach. Harmel *et al.* (2006) engaged the root mean square error propagation to compare accumulated research information on uncertainty in water discharge measurement and determined the cumulative uncertainty in the data. The findings exposed that there is substantial increase in the value of uncertainty with limited quality control measures and shoddy management conditions. Coxon *et al.* (2015) developed a generalize framework for forecasting discharged uncertainty in gauging with errors in stage – discharge relationship with a non – parametric LOWESS regression technique. The developed framework has the capacity to capture place specific uncertainty for some case studies. Hutha and Sloat (2007) used the SonTek® FlowTracker to implement the ISO and the U.S. Geological Survey agency methods to evaluate the uncertainty in wading discharge measurement to extend the impact of these methods from ordinary research and post-processing tools to direct field measurement techniques. The developed algorithms evaluate the components and combined uncertainty of the discharge measurement in real time with immediate feedback to the instrument operator. Comparison was made between a numbers of field measurements.

2.14 Hydroelectric Potentials of Rivers and Power Systems

This section covers reviewed works on the assessment of the hydroelectric potentials of rivers, power generation losses analysis, formulation of model to addressing challenges in hydro power systems and simulation of interacting parameters in hydro power systems.

2.14.1 Assessment of rivers and water systems in the determination of hydroelectric generation features and potentials.

This section review of related literature covers feasibility studies on site assessment and determination of the flow characteristics and suitable head for all categories of hydro power scheme. The design, configuration and operation of retrofit hydro power systems and performance evaluation of selected hydro power sites are also covered.

Hoes *et al.* (2017) provided an assessment of a location's hydropower potential based on the slope and discharge of every river in the globe. According to the study, the theoretical hydropower capacity of the locations is around 52 PWh/year divided by 11.8 million locations, which is equivalent to 33% of the yearly global required energy. However, only 3% of the required energy is now produced by hydropower facilities. Okonkwo and Ezeonu (2012) used the design and installation of a tiny hydropower plant to put the theory of hydropower electric power generation into practice. A storage tank with siphons to boost water pressure served as the model for the dam system, and the penstock was made of plastic pipe. To create the hydroelectric system, the various components were connected.

The feasibility of using rainwater collected by Oregon City's storm water collection system for small-scale electricity generation was investigated by Bailey and Bass (2009). The study explored ways to add micro-hydroelectric turbines to the current

storm water collection system and assessed the advantages and disadvantages of doing so. Two locations were picked for in-depth examination. In light of the present energy rates in Oregon City, the article came to the conclusion that storm water-based hydroelectric energy is not economically viable, but it might be utilized to demonstrate sustainable hydropower producing technology.

In order to provide an alternate source of electrical energy for domestic use, Zainuddin *et al*. (2009) created a pico-hydro generating system that uses drinking water that is distributed to homes. The study showed that using water that is delivered to homes in the town area could be a viable alternative to renewable energy sources. The main pipeline water supply pressure, which serves as the head, the water supply flow rate, the use of adjustable nozzles to vary pressure in accordance with changes in friction loss, and the choice of the type and capacity of the turbine and generator were all noted as essential parameters for optimum system performance.

Dinkar and Morankar (2015) evaluated and ranked the performance of a few Indian Small Hydro Projects (SHPs). The assessment was based on installed capacity, average head, average discharge, cost of energy generation, project cost, labor cost, average power output, capacity utilization factor, and internal rate of return performance indicators. The Analytic Hierarchy Process (AHP), which compares all performance elements pairwise with regard to a certain criterion, was used to conduct the evaluation. AHP deals with the relative priority of relevance of each factor. By dividing them into several tiers, these factors were organized in a hierarchical system. The analysis identified the project's advantages and disadvantages and offered suggestions for further development.

In addition to several case studies, Kapoor (2013) conducted a study on the development of multipurpose pico hydro power projects for raising household living standards in rural areas. The study found that even in some of the world's poorest regions, pico hydro technology is now a flexible and cost-effective source of power. The study came to the conclusion that developing multipurpose pico hydropower projects in rural areas with lots of small water resources, such as rivulets, ponds, small rivers, and springs, as well as high altitude, is feasible. These projects can address the need for adequate and essential power availability at a relatively low cost and with almost no environmental or social impacts. Based on the run-off-river system in Peninsular Malaysia Rivers, Razi *et al.* (2017) conducted a study to forecast the amount of electricity that can be generated by small hydropower. At the intake of the small hydropower system, an ultrasonic level sensor was used to detect the water flow rate. The outcome shows a mean value of 4.25 MW for generated power. The average production value ranged from about 2 MW to about 7 MW. The study offered a framework for developing and choosing possible locations for the development of small hydropower plants.

Pilesjo and Al-Juboori (2016) assessed the potential effects of climate change on hydropower generation in the Dokan region and suggested several measures to maintain the ideal water level necessary to guarantee full capacity of electricity output all year long. Changes in the availability of water resources were converted to changes in hydroelectric generation to influence the analysis. According to the findings, the Dokan power plant's capacity to produce electricity will decline by 20–40 MW by the year 2050. The research suggested enhancing the existing hydropower resources' capacity for water recycling and developing micro dams to store excess water and increase hydroelectric power production.

Dametew (2016) created a cross-flow turbine system-based small hydropower system for generating electricity for rural applications. The turbine and generator efficiencies were chosen and designed using mathematical and numerical (Matlab) approaches, resulting in the theoretical electric power generating potential and capacity for run-of-river systems.

In Bangladesh, the possibility of micro-hydro power plants to supply off-grid electricity to isolated locations not connected to the main grid network was examined by Emeribe *et al*. (2016). The installation of micro hydro power plants can help the nation solve its electricity issue and hasten its economic development, according to a study that supports this claim. Hydrological, topographical, head calculations, and equipment selection and sizing are used to identify the potential of micro-hydro power plants and to establish a strategy for finding new sites. The study offered a fundamental framework for determining the economic viability and fund-raising plan for the construction of the power plants.

Prado Jr. and Berg (2013) conducted an analysis of the capacity factor (CE) of plants by area and plant size in Brazil in relation to the impact of ecological factors on the planning for an increase in hydropower generation. According to the study, it is not viable to build plants with huge reservoirs in light of environmental laws, which would increase reliance on fossil fuel plants and their associated negative environmental effects as well as implications on energy prices. Also offered in the medium term are analytical comparisons with wind power generation. In the future, when considering the expansion of hydropower generation in Brazil, it is crucial to balance the concerns of the populace, the research highlighted.

In order to improve the criteria for future proposals and serve as a foundation for future expansion planning of hydroelectric power stations in Nigeria, Zungeru *et al*. (2012) evaluated the reliability performance of the Kainji hydroelectric power station. They used a frequency and duration approach that quantifies generating unit reliability to compute a set of reliability parameters for each using annual outage durations. The frequency and duration technique was utilized to evaluate the total station reliability by converging the generation and load models. The findings show that the generating units at the Kainji Hydroelectric Power Station have not been appropriately maintained, resulting in frequent and delayed forced outages that impair the power station's performance.

In order to calculate the Gross Hydropower Potential (GHP) of a few selected rivers in Edo State using a run-of-the-river hydropower scheme, Emeribe *et al*. (2016) researched the hydro power potentials of such rivers. The velocity-area approach was used to measure discharges. The rivers Ovia and Ikpoba Edion achieved their best monthly hydropower production in September, and the river Orle experienced its highest monthly hydropower yield in August. The yearly hydroelectric power yield from the River Ovia was 61.619 MW, while the annual yield from the River Ikpoba was 14. 78 MW. The yearly yield of the River Orle was 9.81 MW, whereas the annual yield of the River Edion was 5.49 MW. Despite the findings, the hydrological condition was rated as adequate to average in the paper.

Tazioli (2011) compared measurements made using various tracers and current meters in watercourses with varying conditions for medium-sized rivers and tributaries. In order to confirm how much tracers were absorbed by sediments during floor episodes, experiments were also carried out. According to the results, current meters are not suited for flows that are extremely low or high, non-electrolyte tracers are suitable for

flows that are minimal and medium, and none dye tracers are acceptable for flows that are both medium and high. The study came to the conclusion that current meters produce reliable readings under typical discharge circumstances and suggested using artificial tracers in low flow and flood situations.

The nation's water resources research sector is inextricably linked to the long-term monitoring of hydrologic systems and the archiving of the associated data. The foundation for predictive modeling is data.

Making sure high-quality hydrological measurements are adequate, consistent, and maintained over the long term is the most important problem involved with collecting data on water resources. The persistent and pervasive trend of diminishing networks has been the most well-documented difficulty facing hydrological observations in recent years. The demise of observation centers is typically attributed to inadequate national funding as well as regional and local institutional and political instability. The issue is not unique to underdeveloped or disadvantaged countries. In many wealthy nations, it is a serious problem. Over time, a sizable amount of data has been lost as a result of this (Lins, 2008).

Another difficult task in using hydrological data for study is accounting for uncertainty in methods and networks. In terms of their spatial and temporal fidelity and representativeness, as well as the modeling approach, data are the main source of modeling uncertainty. Decreases in the size and density of data will inevitably raise forecast uncertainty because hydrological forecasting mainly depends on measurements of various hydrological variables taken over extended periods of time (Lins, 2008).

It has been noted that most basins in poor nations lack or have seriously insufficient recording of accurate, ongoing, and consistent information on river outflows (Negrel *et*

al., 2011). This is because most stream courses in these countries generally lack operable gauging stations (Ezemonye and Emeribe, 2013). Along the length of river channels, gauging stations are completely absent, especially in Edo State

2.14.2 Losses profile analysis from the penstock, turbine and turbogenerator in relation to the power output from the system

This review section covers system loss analysis. Rah *et al*. (2012) used the Particle Swarm Optimization (PSO) method to improve the cost-benefit analysis of the production of hydroelectric power. Based on direct expenses and revenue generated, the benefit cost ratio analysis was conducted. The cost ration was found to be greater than unity, establishing the prerequisites for hydroelectric power facilities' economic feasibility.

In order to minimize water consumption in the production of hydroelectric power, Leon (2016) proposed a dimensional analysis for calculating the ideal penstock diameter and discharge for the functioning of impulse and reaction turbine in hydroelectric power systems. The hydraulic and geometric properties of the penstock, the need for power output, and the overall hydraulic head serve as the analysis's fundamental variables. According to the study, the ratio of head loss to gross head shouldn't be higher than 15% in order to reduce water use. The model's applicability in practice was demonstrated.

Wilhelm *et al.* (2016) conducted a prediction analysis in a bulb turbine draft tube at two operating points using Unsteady Reynolds Average Navier Stroke (URANS) Simulations and Large Eddy Simulations (LES). Using a RANS guide vane runner calculation, the draft tube calculation for the inlet boundary condition was exported as a two-dimensional velocity profile. The numerical conclusions were supported by head loss forecasts and experimental data from the flow field. The results show that when

LES at the center draft tube is used instead of URANS output, velocity profile prediction is improved.

In order to investigate methods for enhancing the efficiency of the water flow transformation in the turbine, Zeng *et al*. (2017) analyzed the characteristic characteristics of the inner energy loss of the hydraulic turbine based on the analysis theory of inner energy loss of hydraulic turbine. The Francis-99 turbine start-up test condition was used as a case study to examine the properties of the hydraulic turbine's inner energy under transient and transformation law. The inner mechanical friction loss's analytical process was described. According to the study, the hydraulic turbine's internal mechanical friction loss between the spinning runner and water body constitutes the majority of mechanical friction loss.

2.14.3 Models formulation on evaluation of the hydroelectric power generation characteristic and viability of hydro power projects

The section review discusses the creation of models for hydro power plant systems that address the difficulties and limitations associated with operating a power producing facility.

Using a multilayer perceptron neural network, Abdulkadir *et al*. (2013) created a model for the reservoir variables at the Kainji and Jebba hydropower plants in Nigeria. For the network assessment, monthly historical data for the variables and energy produced by the Kainji and Jebba hydropower reservoirs were gathered from 1970 to 2011 and from 1984 to 2011, respectively. With correlation coefficients of 0.89 and 0.77 for the Kainji and Jebba hydropower, respectively, the results showed a good forecast, showing that multilayer perceptron neutral networks are a trustworthy tool for modeling power production as a function of water storage parameters.

Cook and Walsh (2008) provided an ultimate dispatch cell and power allotting system in a multiple unit power generation system. The conception underlying the optimization strategy is discussed, along with its coverage, and the optimization concept is examined. Comparison of the features of optimization of the plant's operational techniques to those of a real plant was recorded. The system is implemented using a spreadsheet program. The optimum output improved plant performance by more than 2%, and the industry might save up to US $107,000,000 annually as a result. It would reduce the amount of greenhouse gases emitted by fossil power plants while simultaneously boosting industrial profitability

For hydro power facilities, Gupta and Sharma (2016) created a novel calibrated revenue optimization utilizing the Multi-Objective Bat Algorithm (MOBA) to increase income while still meeting time limitations from the hydroelectric flow from the dam. The Bat algorithm-based optimization model could forecast how much water would flow through the turbine in a hydroelectric power plant in order to generate the most income possible in order to pay for the installation costs and future expansion of hydroelectric power plants.

Acakpovi *et al.* (2015) created a platform for reducing energy costs from the consumer's point of view by implementing the ideal mix of first-generation renewable energy plants that can meet the necessary load for a specific period of time. An objective function with a linear form was created by combining an analytical model of a solar, wind, and hydroelectric power plant with cost requirements. Mathlab was used to compute the solution to the objective function. Results show that the dynamism of the hybrid system is consistent and reliable, giving the hydro plant preference due to its cheaper cost. It was revealed that the hybrid system consistently produced a reliable cost estimate that reduced the consumer's bill.

For the purpose of optimizing hydrothermal and nuclear power systems, Rongrong *et al*. (2011) created a model in the power market. The models have two sub models that are used to distribute thermal and hydro loads in the power system. Using a case study, simulation and sensitivity analysis were conducted. The outcomes show that the model is accurate and the approach to finding a solution is successful in optimizing power dispatch for the combined hydro-thermal power systems.

Dozier (2012) created a paradigm for an integrated water and power model that takes into account limits and goals in both the water and power systems. The results demonstrate that hydropower resources can control transmission bottlenecks and energy capacity on other renewable production up to a specific threshold on the penetration level, after which hydropower resources offer no additional value to the system.

A fresh mathematical model based on the actual profit from the production of electricity in pumped storage hydropower plants was presented by (Carnogurskal *et al.*, 2016). By doing a dimensional analysis on the pertinent physical characteristics representing energy generation, the model connection was developed. According to the study, dimensional analysis is an effective method for conveying the technical and financial aspects of PSHP systems.

In order to analyze the cause of some very low frequency oscillations (VLFOs) in the modeling of the dynamic behavior of hydro turbines, Villegas (2011) created a model of a hydro-dominant power system. The study proved that nonlinearities of the dead band type in the controllers and actuators cause limit cycle-type oscillations in the very low frequency range because of phase lag in the closed-loop response in a control system. It also showed that incorrect selection and subpar tuning of control strategies also cause low frequency oscillations similar to those seen in the Colombian power system.

On the basis of the opportunity costs of exports, Bernard and Guertin (2002) created an optimization model for calculating the nodal prices of power generation. It was shown that transmission losses cause significant price discrepancies between the northern and southern regions, but hydro resources and connections with neighbors tend to equalize nodal costs between peak and off-peak hours.

In order to determine the best power supply that satisfies the electricity demand while taking into account the operating conditions of power generating stations, Janicek *et al.* (2008) presented a model for demand and supply planning for hydroelectric power generation in a complex electric power system. Results show that the model is capable of optimizing power generation in a power generation system with a sufficient power supply to satisfy the desired power demand within the given time frame.

In order to accomplish a planned water inflow to the screw to operate hydropower plants using residual flow from a stream or river, Nuernbergk and Rorres (2013) created a new analytical model for the water inflow into the Archimedes spiral and calculated the ideal values of the inflow parameters.

Kahssay and Mishra (2013) used variables including ecology and environment, as well as its impact on income dynamics, to evaluate the effects of the Gilgel Gibe III hydro power project on community development in Ethiopia. The analysis concluded that the project may be a milestone for the growth of the community and that it will help those who live in the area by showing that it has a beneficial impact on community development.

Dynamic duopolistic competition between hydro and thermal generators with unknown demand was examined by Genc and Thille (2008). According to the results, the duopoly conclusion is an effective system when capacities are limited, but the thermal generators

have a tactical reason for choosing to invest in more capacity: they overinvest in the closed-loop equilibrium as opposed to the open-loop equilibrium.

According to their design and operating features, Moreau *et al*. (2011) developed a statistical method to resolve data gaps in life cycle inventories applied to large-scale hydroelectric power plants. According to the suggested results, parameter estimation and model validation can be carried out using cross validation, and the method allows for better estimation without averaging out any of the original data.

Mathematical modeling of a mechanical hydraulic turbine system with constant speed operation was done by Usman and Abdulkadir (2015). The findings show that proper load sharing, consistent speech, and voltage output with a range of load values can all be accomplished with micro-hydro power plants.

2.14.4 Modeling of the influence of interacting parameters in the power profile of hydro power systems

System simulations to capture the operations of hydro power plants under various configurations with the objective of minimizing the power generation system instability and improve system performance are presented.

Manquez *et al*. (2009) presented a modeling of a novel control scheme of a three phase grid connected micro hydro power plant (MAPP). The model control schemes and validation was performed by Matlab Simulink. The simulation studies demonstrated the effectiveness of the multi-level control approaches in the synchronous relating reference frames of the proposed model.

An instructional process for modeling, simulation, and governor adjustment of hydroelectric plants was presented by Naghizadeh *et al*. (2012). The intricate turbine-penstock model's nonlinearity and elasticity are taken into account in the suggested

tuning procedure. The presentation is useful for electrical and power engineering students to simulate, analyze, and tune the governor of a hydroelectric power plant.

A generalized model of simulation of general factors in hydroelectric plants was examined by Sattouf (2012). The electrical generator response to three phase faults at the generator terminals is shown in a window created by the model. It is capable of using and analyzing a wide range of additional defects or operational situations in the electrical systems of generators.

In order to evaluate the dynamic properties of the plant, such as load rejection, and to investigate the worst-case scenario of a complete shutdown of the plant, Magnusdottir and Winkler (2017) developed a simulation of a reference hydro power station. The study came to the conclusion that the model is a useful tool for assessing and forecasting system performance under disruptions.

Ahmed and Abed (2014) developed a simulation model to simulate the regular operation of a Hydropower Plant. The results of the study were used to analyze the power generation capacity versus the quantity of water flow and head height requirement. The developed simulation model was validated.

In order to anticipate short-term power energy based on structural risk management, Gang *et al*. (2014) introduced a novel short-term energy Support Vector Machine (SVM). The model was used to estimate the short-term energy out of SHP in Marguan County. When compared to the traditional approach, the model performed better, demonstrating its effectiveness in forecasting short-term energy output.

2.14.5 Comparative economic and technical review of hydro power status in the power generation industry

This review section is concerned with the characteristics and capacity of hydro power systems to provide solution to rapid national power demands in large hydro power plants and small hydro power application in rural and disperse communities globally to facilitate community development.

Jiakun (2012) examined the importance of the top priority for the development of hydro power energy with a review of the key technological difficulties that China is currently dealing with. The study came to the conclusion that in order to support the all-encompassing and sustainable development of the nation's economy and society, with a focus on eco-environmental conservation, it is required to innovate and establish suitable patterns of hydropower extraction.

Dietrick (2011) conducted a research work into the history and technicalities of hydropower generation and compared hydropower to other types of power, and examined its environmental impacts. Results showed hydropower to be a valuable source of power generation with a history of landscape destruction but the capacity to be the most environmentally friendly power source in the world.

According to Ciocci (2009) analysis of the future prospects for hydroelectric power in the US economy and energy portfolio, the US renewable energy base has the capacity to supply 50% of the nation's electricity needs. It claimed that hydropower offers a tested resource for reasonably priced and appropriate power generation, from renewable portfolio standards to complete energy and climate policies.

With the construction of an affordability evaluation model, Yanlong *et al.* (2015) evaluated the affordability of grid prices for newly constructed hydroelectric power

stations. Alternatives for reducing the mismatch between the hydropower generation cost and the local affordability of the on-grid price were analyzed in light of the results, which showed that the potential affordability of local residents was low. This was done to protect the investment motivation of independent power enterprises.

Using regular environmental surveillance, Bilotta *et al.* (2016) looked into how Run-of-Rivers Hydroelectric Power systems affected local communities. The results revealed that the development and operation of the ROR HEP had an impact on the variety of species that was statistically significant. The other five community composition criteria weren't affected in any statistically meaningful ways, either.

Dametew (2016) created a tiny hydropower plant-based power generation system for rural applications. The chosen turbine and generator efficiencies were used to calculate the theoretical electric power generating capabilities and capacities for run-of-river systems.

2.14.6 General work on hydroelectric power generation

General review work on the electricity industry and efficacy of renewable energy technology in meeting rising energy demands with hydro power in perspective are presented in this section.

Oladipo and Temitayo (2014) did an analysis of the power system contribution to the development of Nigeria. It carried out a critical survey of the past and present conditions of the sector. The paper concluded that for the repositioning of the Nigeria power sector for adequate and efficient power delivery there should be replacement of old and obsolete power system equipments, establishment of more generating stations, embarking on ring transmission network and adequate funding of the sector among other factors.

Mohanta *et al.* (2017) carried out a review on Vibration Condition Monitoring (VCM) of electrical and mechanical equipment used in the hydro power stations along with a brief explanation of vibration related faults considering past literature of about 30 years. Causes of the vibrations on rotating and non-rotating equipment of hydro power station were discussed along with the standards for vibration measurements. Future prospects of VCM were also discussed.

Clack *et al.* (2017) evaluated the assertion by Jacobson *et al.* (2015), on the feasibility of provision of low-cost solution to the grid power reliability with 100% injection of wind, water and solar power across all energy sectors in the continental United States between 2050 and 2055 using electricity and hydrogen only as the base energy carriers. Significant shortcoming were discovered in the analysis as the work used invalid modeling tools with modeling errors, and made implausible and inadequately supported assumptions. The paper concluded that policy maker should cautiously implement any approach of a rapid, reliable and low cost transition to a complete energy system that depends entirely on wind, water solar technology.

Pimentel *et al.* (2002) established that renewable energy technologies techniques have the potential to provide the United States' economy with the alternatives to meet approximately half of its future energy needs. To achieve this objective the United States would have to commit to the development and implementation of non-fossil fuel technologies and energy conservation. The implementation of renewable energy technologies would reduce many of the current environmental problems associated with fossil fuel production and use.

Olaoye *et al.* (2016) reviewed the potentials of Nigeria renewable energy as an additional generation source to meet the energy demand of Nigerian economy. It

focuses on the country's energy crisis and how its natural resources can be harnessed to meet the nation's energy demands while reducing global pollution. The paper presented an analysis of projected energy capacities from the abundant renewable energy resources and how much of these resources are required to be harnessed in the proposed energy mix to achieve over 60,000 MW of power to drive essential components of the economy.

Etukudor *et al.* (2015) analyzed the components of Nigeria electricity supply industry to identify the root-causes of constant power outages in the country which has led to a high unreliability of supply, with a view to proffering workable solutions. The paper established that beside the challenge of insufficient generating capacity, the transmission network which is characterized by high levels of power losses and frequent conductor cuts, is mainly responsible for the incessant power outages experienced across the country.

Gbadamosi *et al.* (2015) carried out an operational efficiency analysis of Shiroro hydro-electric power plant for the reviewed period (2004-2014) with emphasis on plant availability factor, capacity factor and the overall efficiency of the plant. The study reveals low capacity utilization, shortfall of energy generation and poor maintenance culture as factors effecting the effective operation of the plant. Measures to improve the performance indices of the plant were suggested.

Liu *et al.* (2014) assessed the academic landscape in hydroelectric power generation by analyzing the citation network of papers published in academic journals. Utilizing a topological based method, all the papers were categorized into clusters by their own characteristic topics. Results show the existence of 6 principal research clusters: Renewable energy, Optimization of system operation, Environmental issues

(greenhouse-gas emission), Environmental issues (fish management), Environmental issues (sediment) and Pumped hydro storage systems. In-depth subclusters analysis was also conducted to gain better knowledge of those clusters. Combing the analysis results, sub clusters related to pumped-storage and small hydropower are considered to be developing, as indicated by the average publication year of papers and recent increasing trend.

2.15 Environmental Impact Assessment

Environmental Impact Assessment (EIA) is a process that identifies both the positive and negative environmental effects of significant developments prior to planning permission being considered. It aims to prevent, reduce or offset any identified significant adverse environmental effects of proposed projects (Parsons Creek Aggregates, 2008). The EIA process is a method of ensuring that planning decisions are made in the full knowledge of the environmental effects of the project and with full engagement of statutory bodies, local interest groups and members of the public.

Population growth, rising expectations and technological changes have created serious environmental problems (Wood, 2003*).* There is world-wide evidence that the wellbeing of man is governed by the quality of the environment. Thus, environmental issues must be addressed as soon as possible during project planning. Environmental impact assessments measure or estimate the impacts on some environmental components (air, water, soil, land, sound etc.) by human developmental activities. EIA is widely accepted as a tool to ensure sustained development with minimum environmental degradation (Yusuf *et al.,* 2007).

In Nigeria, the environmental and social management system functions under the Environmental Impact Assessment (EIA) Bill by Federal Government of Nigeria

(Office of Environmental Assessment Department, 2017). The regulator for the EIA process in Nigeria are the Federal Ministry of Environment through its Environmental Assessment Department for EIA and the Department of Petroleum Resources (DPR), an arm of the Ministry of Petroleum Resources, which also has a mandate for the regulatory framework for all activities in the Oil and Gas sectors of the economy. By this law, no industrial plan, development activity falling under the Federal Environmental Protection Agency's mandatory list can be executed without prior consideration of the environmental consequences of such a proposed action, in the form of an environmental impact assessment (Ogunba, 2004). The construction of hydro power station falls within this purview.

The physical environment is affected rather significantly by the construction of a hydro power stations (Bobat, 2017). Both the river and ecosystem of the surrounding land area will be altered as soon as dam construction begins. While both Run-off-River (ROR) and reservoir types of hydropower dams may divert water, this is always the case with ROR plants. Often downstream flows are reduced considerably or even completely stopped during certain periods of time with sudden intervals of high flows. Such drastic variability in water flow impacts the structure of aquatic ecosystem. Dams have major impacts on the physical, chemical and geo-morphological properties of a river (Bobat, 2017). Environmental impacts of dams have largely been negative. Large dams with reservoirs significantly alter the timing, amount and pattern of river flow. This changes erosion patterns and the quantity and type of sediments transported by the river. Consequently, hydroelectric power supply has some environmental challenges. It is essential that an Environmental Impact Assessment be carried out for every proposed hydro power project to determine the feasibility of the project from the environmental perspective.

2.16 Measurement of Liquid Flow in Open Channels and Rivers Using Float.

International Standard, ISO 748:2021, specifies the methods to determining the cross-sectional area and velocity of water in rivers and open channels. A float is used to measure the velocity of flow of the river while the cross-section is measured and calculated by distance measuring devices

2.16.1 Methodology of measurement

The methodology involves the measurement of the cross-sectional area of the site and velocity of water flow in the river. The width of the river and the depth is measured at a number of points sufficient to map out the shape of the river bed. The discharge is calculated from the summation of the product of the area and corresponding velocity for a series of observation (ISO 748:2021).

2.16.2 Flow velocity measurement using floats

Measurement of river discharge using floats is particularly recommended over the use of current meters in case of low velocity of flow and shallow depths, excessive velocities and large depths, presence of materials in suspension and access problems (ISO 748:2021).

i. Method of discharge computation

The method is particularly applied to field measurement and discharge computation.

The flow in the shaded segment in Figure 2.7 is evaluated according to Equation (2.1) (ISO 748:2021).

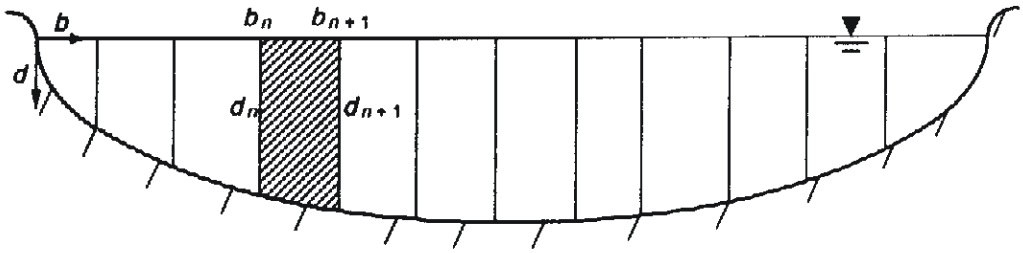

Figure 2.7: Cross Section for Discharge Computation (ISO, 2021)

$$q = (b_{n+1} - b_n)\left[\frac{d_{n*1}+d_n}{2}\right]\left[\frac{\bar{v}_{n+1}+\bar{v}_n}{2}\right] \quad (2.1)$$

Where,

q is the flow rate in nth segment (m^3/s)

b_n is the length of the nth vertical from the bank (m)

d_n is depth of the nth vertical (m)

$\bar{v}$ is the average velocity in each vertical (m/s)

The velocity at the bank is assumed to be zero.

The total flow is a summation of the discharge in each segment (ISO748:2021), therefore,

$$Q = \sum(b_{n+1} - b_n)\left(\frac{d_{n*1}+d_n}{2}\right)\left(\frac{\bar{v}_{n+1}+\bar{v}_n}{2}\right) \quad (2.2)$$

Q is the total flow in the channel (m^3/s) (ISO. 2021)

2.16.3 Flow measurement uncertainties.

Uncertainties are present in the measurement of physical quantities. This uncertainties which constitute the error is the difference between the actual and measured value, and is expressed quantitatively as a parameter. The uncertainty in any measurement is determined by the characterization and identification of all components of errors,

quantification of the corresponding uncertainties and summation of the components uncertainties. Finally, the uncertainty is composed into one standard deviation and is stated as a percentage of the measured values.

2.16.4 Calculation of uncertainty in discharge measurement using floats

The total uncertainty in discharge consist of the following sources;

(a) Uncertainty in width measurement in estimating cross-section area (U_b)

(b) Uncertainty in depth measurement in estimating cross-sectional area (U_d)

(c) Uncertainty in determination of surface float velocities ($U_{v,i}$), which consist;

i. Uncertainty in the coefficient of velocity for the float ($U_{k,f}$)

ii. Uncertainty of the length of travel path ($U_{l,i}$)

iii. Uncertainty of the time taken for the passage of the float ($U_{t,i}$)

where,

$$U_{v,i}^2 = U_{k,f}^2 + U_{L,i}^2 + U_{t,i}^2 \quad (2.3)$$

$U_{v,i}^2$ is the uncertainty of surface float velocity (%)

(d) Uncertainty due to use of limited numbers of segments (U_m) (ISO, 2021)

2.16.5 Combined uncertainty in discharge measurement

The method of calculation of combined uncertainty for floats is indicated in Equation (2.4)

$$U_Q = \sqrt{U_m^2 + \frac{1}{m}(U_b^2 + U_d^2 + U_v^2)} \quad (2.4)$$

Where,

U_Q is combined uncertainty in the discharge measurement (ISO, 2021).

2.17 Correction for sag of tape

The correction for Sag of measuring tape is given as;

$$Ks = \frac{M^3 L^3}{24 F_T^2} \quad (2.5)$$

where,

K_S = Sag correction for length

M = Mass of tape

L = actual length of tape

F_T = Tape tension (ISO, 2021).

2.18 Evaluation of Losses in the Hydroelectric Power Generation System .

2.18.1 Evaluation of losses in the penstock

Losses in the penstock consist of friction losses known as major losses and losses due to bend, fittings and valves known as minor losses.

According to Darcy equation (Nag, 2001), the losses due to pipe friction is given by,

$$h_f = \frac{4fL}{d} . \frac{\bar{V}^2}{2g} \quad (2.6)$$

where,

h_f is head loss due to friction

d is pipe diameter

f is pipe friction coefficient

$\bar{V}$ is average velocity of flow

The losses due to bends, fittings and valves is given by,

$$h_{fl} = k \frac{\bar{V}^2}{2g} \quad (2.7)$$

where,

h_{fl} is losses due to pipe fitting

k is loss coefficient

$\bar{V}$ is average velocity

The effective head (H_e) is gross head (h) less the Friction losses and minor losses. Mathematically,

$$H_e = h - (h_f + h_{fl}) \text{ (Nag, 2001)} \quad (2.8)$$

Gross head is used to determine general feasibility and estimate power availability. The effective head is used to determine actual power supply.

In the minimization of major and minor losses consideration will be given to the following issues (Nag, 2001);

i. Limiting the length of penstock

ii. Carefully selecting an appropriate diameter for the penstock

Select appropriate bends, fittings and valves, and minimize the amount of these components

2.19 Research Gap

The review of related literature in the hydroelectric power generation scenario has the following main points. The work could be categorized into feasibility studies for the assessment of hydroelectric power generation potentials of various sites (Punys and

Jurevicius, 2022), and its capacity to produce adequate electric power to sustain the energy demand of various national economies and local communities. A sizeable numbers of the literatures focus on the environmental impact of various hydroelectric power schemes on humans and water creatures. Research work to enhance the operational efficiency of hydro power machineries, equipment sizing, water control and management for optimal power output are also prevalent. Some studies focused on non-conventional dam operation like pumped hydroelectric, run of the rivers schemes and modification of various water system for hydropower generation (Zainuddin *et al*., 2009). The barriers to the growth of hydropower in various nations were highlighted, and solutions were suggested (Katutsi *et al.*, 2021).

Some works carried out an analysis of the Nigeria electric power generation and supply scenario of the Nigeria economy. Issues of insufficient power generation, low capacity utilization, challenges of power evacuation due to poor transmission and distribution facilities were identified (Emovon *et al*., 2018). The capacity of Nigeria renewable energy base with focus on hydro power development, to augment the power supply to mitigate the energy crisis was established (Olaoye *et al*., 2016).

From the content of the reviewed papers there are established findings that in spite of some concern over the environmental effects of dams, it has been identified as a veritable renewable energy source with capacity to produce adequate magnitude of power to offset the production of greenhouse gases by thermal power plants (DOE, 2004; Pimentel *et al*., 2002). Hydropower as a renewable energy source has some environmental challenges and beneficial effects. Mitigation measures in its applications were identified (Al-Shetwi, 2022). Some studies suggested that the benefits of hydroelectric power as a clean energy source are well worth the environmental costs it may inflict. Development in hydroelectric power generation is now in favor of small

hydro power station because of their minimal environmental impact and pivots for community development (Vasiliev *et al*., 2013).

In this regard it has been strongly advocated that various national governments should facilitate the development of their hydroelectric potentials to increase the percentage of hydro power sources to significantly power the machineries of their economies. It was established that the US renewable energy base, with hydroelectricity constituting more than 75% of the electricity generated from renewable sources (DOE, 2004), as the capacity to provide half the economy electricity consumption in a scenario that is devoid of fuel price shocks, foreign control and worries about climate change but just the availability of clean, abundant, affordable electricity (Ciocci, 2009). The poor generation capacity of the Nigeria electricity industry has further emphasized the need for the rapid development of Nigeria hydroelectric power resources, especially small hydro power, for accelerated community development (Miskat *et al.,* 2020).

Some few works on hydrological assessment of some rivers in Nigeria mostly focused on run of the river scheme with shallow data content without modeling tools to optimize power output (Emeribe *et al.,* 2016; Oyati and Olotu, 2017). The availability of adequate hydrological data base spanning about 30 years for hydroelectric potential assessment in developing countries especially in Nigeria has continued to be a challenge. Government institutions in charge of hydrological data collection and documentation suffer poor maintenance of hydrological infrastructure, poor financial commitment from government, low hydrological data acquisition and management capacity, and obsolete data acquisition facilities (Ngene *et al.,* 2015).

Most development projects in hydroelectric power plants installations are carried out with tedious, extensive time ranging between 20 – 30 years and expensive feasibility

studies requiring large amount of data to ascertain the viability of the projects (Harvey, 2006). In the Nigeria context, the absence of reliable and adequate hydrological data base for the assessment of the hydroelectric power potential continue to pose a serious challenge (Emeribe *et al.*, 2016).

Research technique for hydrological data extension in region with hydrological data shortage includes the use of the rating curve in a standard gauging station, correlation and regression technique of hydrological data from a nearby gauging station with similar climate conditions (Abegunde (2018); Ekeu-wei and Blackburn (2018)).

This study provides a framework to facilitate the evaluation of the hydroelectric potentials of hydro power projects in catchment area with hydrological data shortage for reduced cost, data requirement, improved performance and high accuracy.

CHAPTER THREE

3.0 MATERIALS AND METHODS

3.1 Materials

The following materials shown Table 3.1 were used for the study in line with (ISO, 2021) prescription and requirement for the measurement of hydrological flow characteristic of rivers and open channels flow.

Table 3.1: Study Materials

S/N	Material	Manufacturer	Model	Specification
1	Surface float	Mooring International Inc.		Coefficient: 0.85
2	Double float	Mooring International Inc.		Coefficient: 0.95
	Subsurface float	(Mooring International Inc.		Coefficient: 0.90)
	Graduated vertical rod	Anvil Inc.		accuracy: 0.01
	Dumpy level	Microteknic,	MTSE-03,	Magnification: 24x,
	Measurement tape	Cai Hong Pai	MC 14000005	Length 50 m Accuracy: 0.01
	Stop watches	Lasika Inc.		Electronic Accuracy: 0.01
	Life float	Grand Ocean		Material: Foam Capacity: 16 pax
	Rain boots	Ningbo Jiangbe, China	STTO1	PVC Height: 37 cm
	Microsoft Excel	Microsoft Corporation	2010	
	Mathcad	Parametric Corporation	14.0	
	Solid Works		2021	

3.2 Study Area

The study area is located in Edo North of Nigeria. Rainfall amount in Edo North ranges from 1000mm – 1200mm (Emeribe *et al.,* 2016). Edo North lies between longitude 6.02^0 – 6.69^0 and latitude 6.80^0 – 7.11^0. Figure 3.1 indicates the structure of states Nigeria and Figure 3.2 shows the map of Edo State with the major rivers.

Figure 3.1: Map of Nigeria with 36 States (Edo State watershed Project)

Figure 3.2: Map of Edo North with Major Rivers (Modified from Emeribe *et al.*, (2016))

There are about six to seven months of precipitation in Edo North beginning April/May with cessation in October/November. Over 90% of the rainfall occur between June and October with peak rainfall and run off occurring in September (Emeribe *et al.*, 2016).

The hydrology of Edo North is dependent on the geology. Most of the rivers drains into the river Niger flood plains in the east of Edo North. Major rivers in the area are river Orle, Edion, Ogio, Ojirami and Orbe. The flow characteristics of the rivers are similar with minimum flow occurring in March/April and maximum flow occurring in September/ October annually. Rainfalls in Edo North are of high intensity and with a dry spell usually in August.

The Orle river valley is located at Kilometer three Auchi – Sabogadia Ora road. The valley has vertical height elevation of about 80.56 m, longitudinal width of 2050 m and a length of 5150m (Field measurement). The area consists mostly of forest and sparse cultivated land. There is an abattoir which is the critical structure in the area, some few residential buildings, undeveloped buildings and plots. It is bothered by Oshiomole village in the South-West and East, Warrake in the South and Ayuele village in the East.

The river Edion project site is located at KM 23 along Auchi – Sabogida Ora road. It has a length of about 2150 m, width of about 1155 m and elevation of 64 m. The valley is sparsely populated with farmlands with no evidence of human habitation. It is bothered by Ikpeshi in the north, Ihievbe village in the east, Warrake in the South, Uokha and Afuze in the west.

The Orbe plant site is located at about KM 33 along Auchi – Agenebode road. It has a length of 5450 m width of 2150 m and height elevation of 72 m. The valley is sparsely populated with farmlands. There is no evidence of human habitation. It is bordered by

Iviukwe village to the east, Fugar town by the west, Agiere in the south and Ivianokpodi in the north.

The river basins have similar characteristic and forestry features. Only R. Orle basin witnesses some sparse human habitation.

3.3 Method

3.3.1 Development of a model for flow characteristic measurement and uncertainty determination

A model was developed and validated to integrate the flow characteristic evaluation and uncertainty determination. The model is simple to apply, fast and reliable in its application and avoids the tediousness associated with the IS0 748:2021 models.

The flow characteristics of a river are evaluated in the area-velocity method by measuring the cross section area of a carefully selected channel section as indicated in section 3.4.4, the velocity of flow across the channel was determined according to section 3.4.6 . The product of the area and velocity gives the flow rate.

3.3.2 Model development assumptions

The flow in rivers is open channel flow which is considered turbulent flow (Malverti *et al.,* 2008), with zero velocity at the river banks (ISO 748, 2021). The channel was chosen so that there is no flow in and out of the channel section to fulfill the continuity equation. The following assumptions were made for the modeling process.

i. The channel flow is turbulent

ii. Continuity of flow holds in the channel

iii. The flow velocity at the river banks is zero

iv. No external flow between inlet and exit of the channel

3.3.3 Model development algorithm

The following algorithm was used to develop the model for flow characteristic measurement and uncertainty determination.

i. The average velocity in the channel segments was derived

ii. The cross section of the channel was determined

ii. The average velocity across the channel was determined

iii. The general expression for the area of cross section of the channel was derived

iv. The total discharge across the channel was determined

v. The gross hydroelectric power output from the channel was established

vi. The standard deviation for numbers of repetitive measurement for time of float travel, channel length, channel depth and width were determined

vii. The combined uncertainty of discharge was established

viii. The expanded uncertainty at 95 % confidence interval was established

Consider a channel section divided into a number of segments as shown in Figure 3(a)

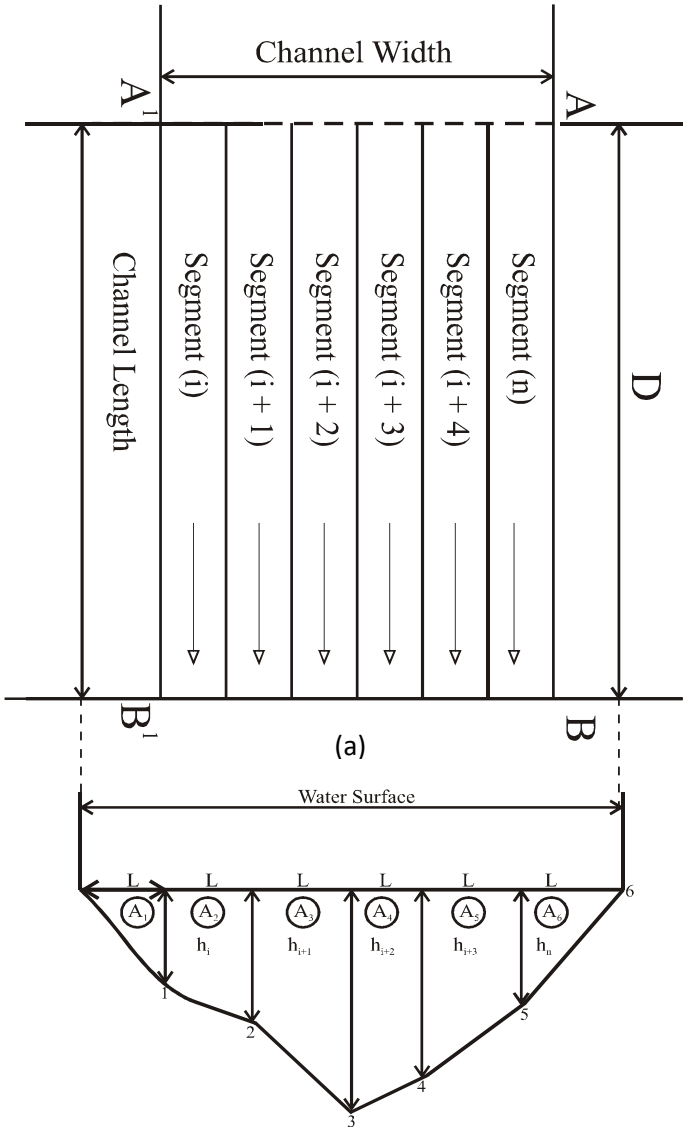

Figure 3.3: Schematic of the river flow model

It is required to determine the velocity in the segments and the average velocity across the channel using the relationship stated as;

$$\text{Velocity} = \frac{\text{Distance float movement}}{\text{Time taken for movement}} \quad (3.1)$$

Imagine the floats to move from section AA' to section BB' covering a distance D in the various segments, in an average time, $t_{i,}$ t_{i+1}, ------ t_n respectively.

where,

n is the number of segments

The average velocity in the segments is given as follows

segment i is given by

$$v_i = \frac{DC_f}{t_i} \quad (3.2)$$

Where,

C_f is correction for float velocity

D is total length of channel (m)

t is time for float to cross the channel (s) from section AA' to section BB'

segment i +1 is given by

$$v_{i+1} = \frac{DC_f}{t_{I+1}} \quad (3.3)$$

Segment n_{th} is given by

$$v_{nth} = \frac{DC_f}{t_{nth}}$$

(3.4)

The average velocity across the channel is given by,

$$V_{av} = \frac{1}{n}(v_i + v_{i+1,} - - - v_n)\, C_f \quad (3.5)$$

$$V_{av} = \frac{DC_f}{n}\left(\frac{1}{t_i} + \frac{1}{t_{i+1}} + - - - + \frac{1}{t_n}\right) \quad (3.6)$$

where,

V_{av} is average velocity (m/s),

Figure 3(b) represents the cross section of the channel with six segments. The area of the cross section is given by,

$$A_T = A_1 + A_2 + A_3 + A_4 + A_5 + A_6 \quad (3.7)$$

where,

$A_T$is total channel area

$$A_T = \frac{1}{2}lh_1 + \frac{1}{2}l(h_1 + h_2) + \frac{1}{2}l(h_2 + h_3) + \frac{1}{2}l(h_3 + h_4) + \frac{1}{2}l(h_4 + h_5) + \frac{1}{2}lh_5 \quad (3.8)$$

$$= \frac{1}{2}l(2h_1) + \frac{1}{2}l(2h_2) + \frac{1}{2}l(2h_3) + \frac{1}{2}l(2h_4) + \frac{1}{2}l(2h_5) \quad (3.9)$$

$$A_T = l(h_1 + h_2 + h_3 + h_4 + h_5) \quad (3.10)$$

Where,

l is the width of segment

h_n is the depth of the nth vertical segment

In general term the area of the cross section of a river as indicated in Figure 3.3 (b) is given by,

$$A_T = l(h_i + h_{i+1} + - - - + h_n) \quad (3.11)$$

The total discharge across the channel is given by,

$$Q = A_T V_{av} \quad (3.12)$$

$$Q = \frac{DlC_f}{n}\left(\frac{1}{t_i} + \frac{1}{t_{i+1}} + - - - + \frac{1}{t_n}\right)(h_i + h_{i+1} + - - - + h_n) \quad (3.13)$$

The power output is given by,

$$P = \rho g h Q \quad (3.14)$$

$$P = \rho gh\left[\frac{DlC_f}{n}\left(\frac{1}{t_i} + \frac{1}{t_{i+1}} + - - - + \frac{1}{t_n}\right)(h_i + h_{i+1} + - - - + h_n)\right] \quad (3.15)$$

3.3.4 Determination of uncertainty in flow characteristics measurement

A complete expression of a measured value is given by Equation 3.16.

$$\text{True value} = \text{Measured value} \pm \text{uncertainty} \quad (3.16)$$

The uncertainty in repeated measurement of the same value measurement is best determined through the average value of the measurement and standard deviation.

The expression for the average value is given by,

$$\text{Average value} = \frac{\text{Sum of measurements}}{\text{Numbers of measurements}} \quad (3.17)$$

$$\text{Average value} = \frac{x_i + x_{i+1} - - - + x_n}{m} \quad (3.18)$$

where,

x is measured value

m is number of measurements

The standard deviation is given by Equation 3.17 (University of North Carolina, 2011),

$$s = \sqrt{\frac{(\delta x_i)^2 + (\delta x_{i+1})^2 --- + (\delta_n)^2}{m-1}} \quad (3.19)$$

where,

s is standard deviation

δx is deviation from average

$$s = \sqrt{\frac{\sum \delta x^2}{m-1}} \quad (3.20)$$

The standard uncertainty (Standard error) is given by Equation 3.19 (University of North Carolina, 2011).

$$\text{Uncertainty(U)} = \text{Standard Error(SE)} = \frac{s}{\sqrt{m}} \quad (3.21)$$

Therefore,

True value = Measured value $\pm$ Uncertainty(U)

3.3.5 Combined uncertainty in discharge

The overhaul uncertainty in discharge is composed of;

(a) Uncertainty in width measurement in estimating cross-section area (U_b)

(b) Uncertainty in depth measurement in estimating cross-sectional area (U_d)

(c) Uncertainty in determination of surface float velocities ($U_{v,i}$), which consist;

i. Uncertainty in the coefficient of velocity for the float ($U_{k,f}$)

ii. Uncertainty of the length of travel path ($U_{D,i}$)

iii. Uncertainty of the time taken for the passage of the float ($U_{t,i}$)

where,

$$U_v = \sqrt{U_{cf}{}^2 + U_D{}^2 + U_t{}^2} \quad (3.22)$$

Where,

U_V is the uncertainty of surface float velocity (%)

U_{cf} is the uncertainty of choice of velocity correction factor (%)

U_t is the uncertainty of the time taken for the passage of the float (%)

(d) Uncertainty due to use of limited numbers of segments (U_g) (%)

The combine uncertainty in discharge is given by Equation 3.23 (ISO, 2021);

$$U_q = \sqrt{U_g{}^2 + \frac{1}{g}\left(U_b{}^2 + U_d{}^2 + U_V{}^2\right)} \quad (3.23)$$

where,

U_q is the standard combined uncertainty of discharge (%)

3.3.6 Expanded uncertainty

To determine the expanded uncertainty at a level of confidence of about U_{95}, a coverage factor of k = 2 is applied) (ISO, 2021).

Therefore,

$$U_{95}(q) = kU_q \quad (3.24)$$

$$U_{95}(q) = 2U_q\ (\%) \quad (3.25)$$

Figure 3.4 shows the flow chart for the programme for the automation of the model to facilitate the evaluation of the hydroelectric power characteristics of the study model, while Figure 3.5 shows the flow chart for uncertainty evaluation.

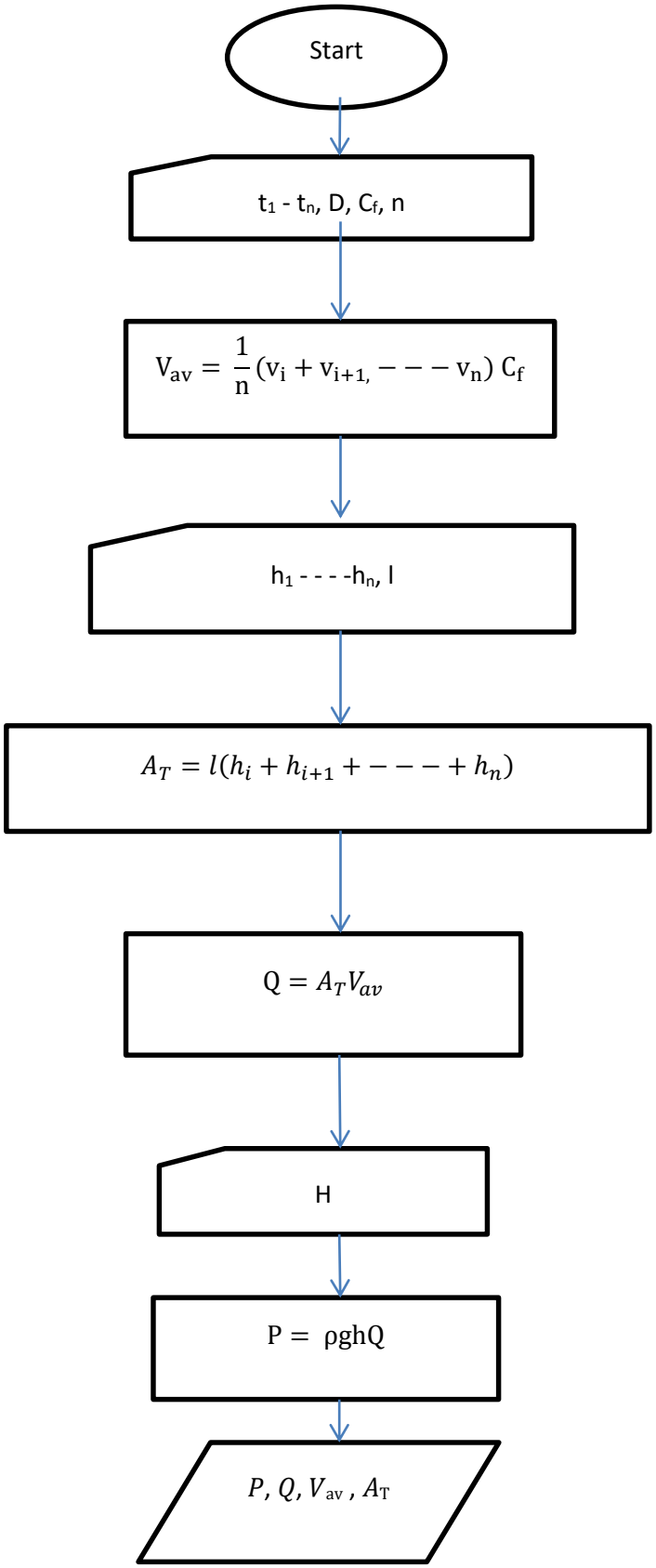

Figure 3.4: Flow Chart of Hydroelectric Power Evaluation Model

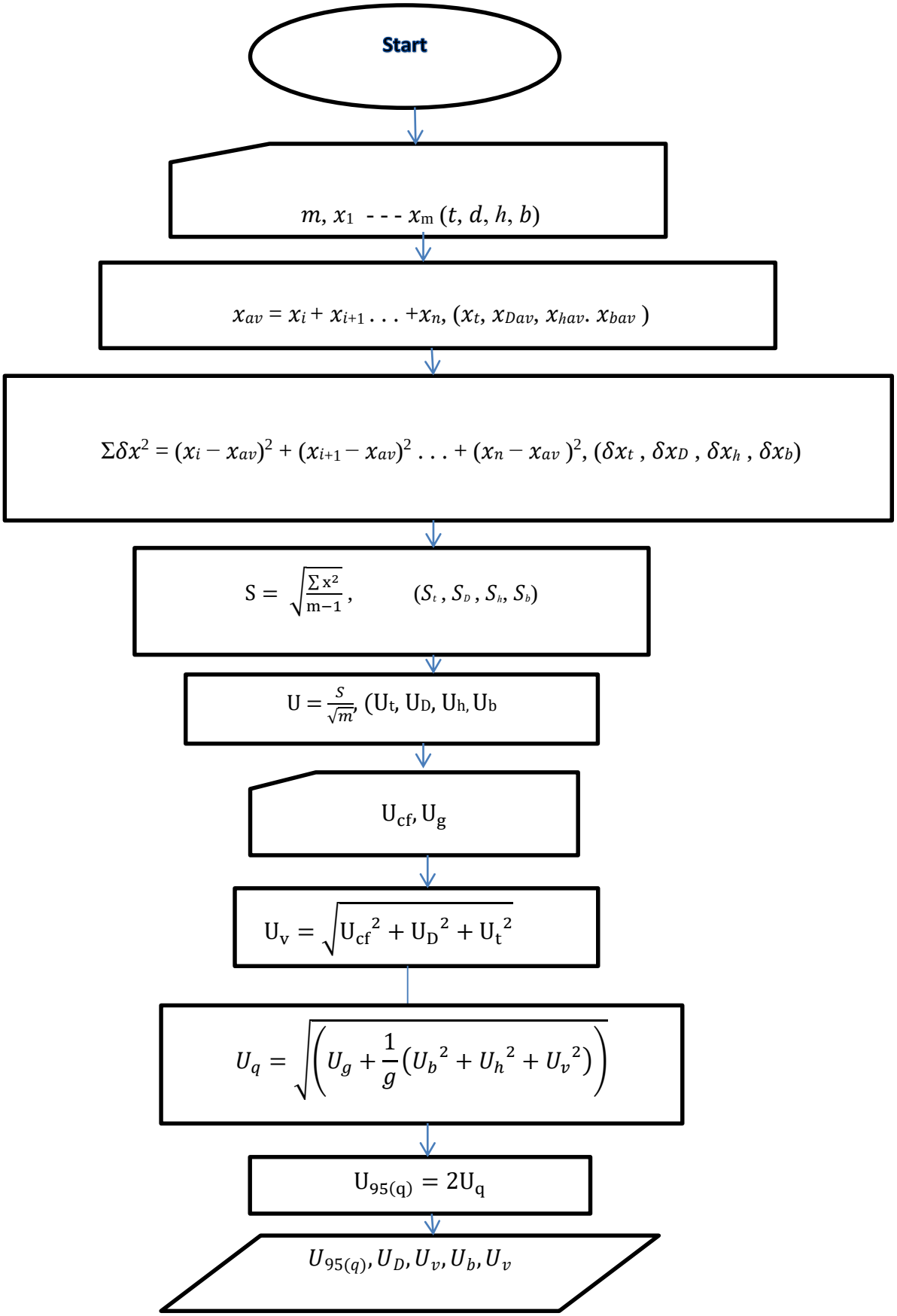

Figure 3.5: Flow Chart of Uncertainty Evaluation

3.4 Experimental Stage Setup and Measurement of Flow Characteristics

3.4.1 Selection and demarcation of site

The following factors were used in the selection of the sites for the measurements as follows;

i. Straight and uniform cross section and slope, with parallel direction of flow at any vertical sections across the width and at right angles to the measurement sections.

ii. Well defined beds of channels and stable flow at all stages to facilitate accurate measurement of the cross section and uniformity of flow conditions

iii. Stable flow conditions at the channel sections and it surroundings

iv. Sufficient depth for float immersion

3.4.2 Measurement of flow characteristic and associated uncertainty

The double and surface floats were used in the flow characteristics measurements in the field experimental evaluation of the hydroelectric generation potentials of the three rivers, while the double, subsurface and surface floats were used for the measurements for the evaluation of the uncertainty associated with the flow characteristics study on River Orle.

Readings were taken every month of year of 2018 and 2019 from the three selected rivers to enable the construction of the flow duration and power output curve. Anova and correlation analysis were performed on the results.

For the uncertainty study, measurements were carried out on river Orle to determine the uncertainty (errors) associated with three different types of floats. Five channels with

different lengths were used. Factors like average velocity, flow rate, power output which are components of the uncertainty were determined. Each channel was divided into ten segments of equal widths.

3.4.3 Floats description

The surface float is a ball of synthetic rubber material with weight regulation by air inflation. The double and subsurface floats are made from reinforced paperboard containers. The double float consists of a surface float connected by a string to a subsurface float. The subsurface float consists of a surface and subsurface float of paper board containers integrated into a unit by strings. The lengths of the floats depend on the depth of the rivers. Figure 3.6 shows the features of the floats.

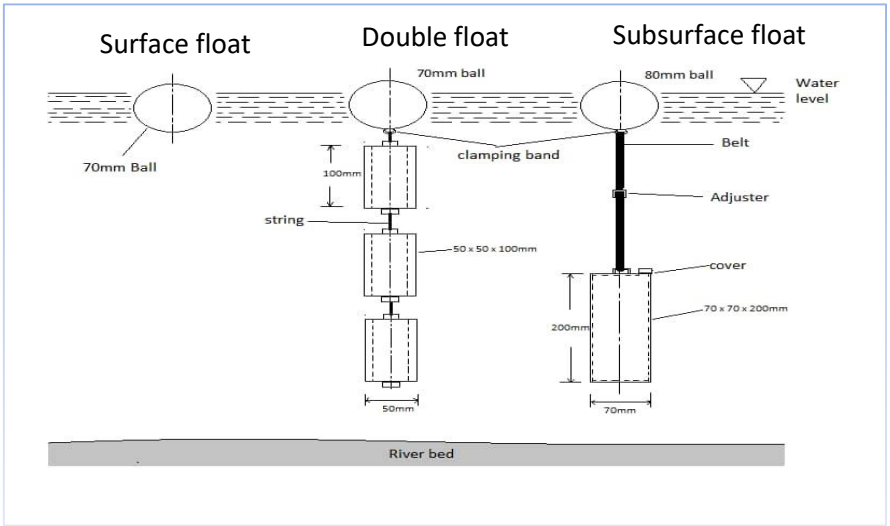

Figure 3.6: Schematic of Floats (Audu *et al.*, 2020)

3.4.4 Cross-sectional area and depth measurement

Ten vertical points were established across the channel bed to establish the cross sectional profile of the river. Horizontal distance across the rivers and between the vertical points were measured by direct means using a graduated tape. The depths of the

vertical points were measured and an average of the measurement obtained. Each measurement was taken three times.

3.4.5 Stage set up

Three types of floats were used in the measurement; Surface float, subsurface float and Double float. The stage setups was guided to minimize random and system errors in dimension taking, length and time of travel of the float. Large material debris and obstruction were filtered from the length and width of the channels. Shallow depths were avoided or eliminated.

Preliminary measurements were made with the floats to observe, identify and minimize system and random errors. It was observed that while winding condition significantly accelerates the movement of the surface float, shallow depths significantly retards the movement of the subsurface float. The double float was not affected by random errors. The sizes of the floats were adjusted to minimize the effects of the above factors. The stage was finally marked out after correction for tape sag effects was established according to Equation 3.26.

3.4.6 Determination of velocity of flow and discharge

The double float was used to measure the velocity of the rivers in stable low wind condition. The surface float was used in flood situation with materials in suspension in the rivers. This condition occurred mostly in the month of September.

The float velocity was determined by dividing the distance travelled by the float with the time taken to move between the channel cross – sections. The float velocity was taken three times and the average of these measurements was then multiplied by a float velocity correction coefficient (C_f) to obtain the mean velocity. Care was taken to

eliminate swirl flow and winding condition that could divert the float from the center of the segments.

The velocity correction factor for the surface, double and subsurface floats are 0.85, 0.95 and 0.90 respectively. This velocity was measured for each segment of the divided section of the river.

3.4.7 Measurement of the Rivers Reynolds Numbers

After an analysis of the flow variability and dynamics of the rivers, the model equation for Reynolds number in open channel flow in the work of Malverti *et al.* (2008) was adopted for the measurement of the rivers Reynolds numbers. The equation is shown in Equation 3.26 (Malverti *et al.*, 2008).

$$\mathrm{Re} = \frac{\mathrm{Uh}}{\nu} \tag{3.26}$$

Where,

U is average velocity

H is flow depth

ν is kinematic viscosity

3.4.8 Uncertainty measurements

A long channel with appropriate features was marked out and demarcated into five section and ten segments each as shown in Figure 3.7.

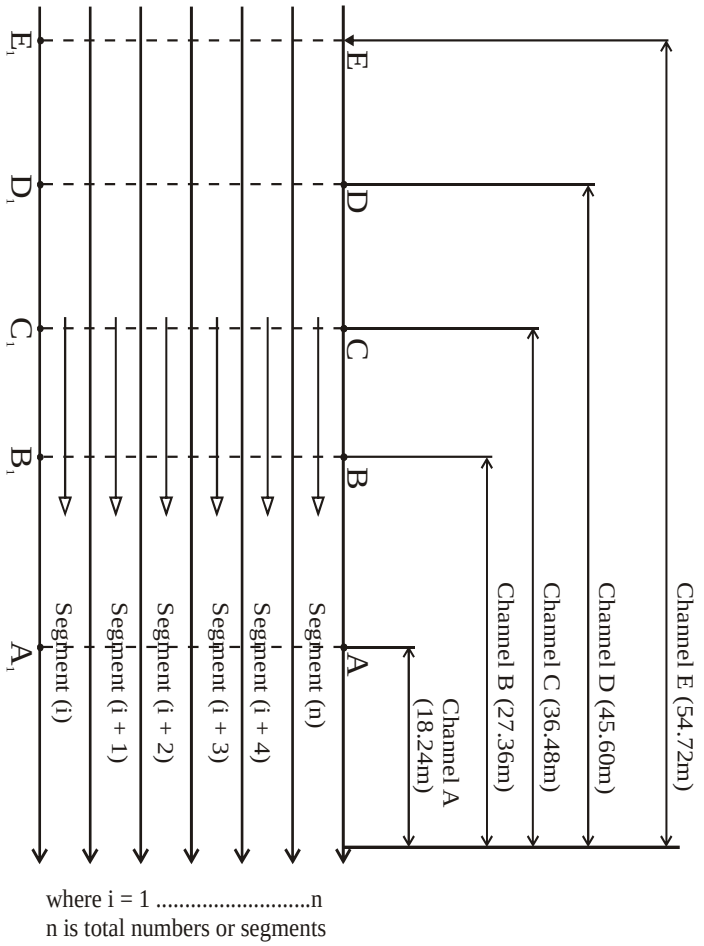

Figure 3.7: River flow channel layout

The details of the demarcation is shown in Table 3.2. The number of segments was 10 and width 25.52 m.

Table 3.2: Channel Characteristics

Channel	Length (m)	Width (m)	Numbers of segments
A	18.24	25.52	10
B	27.36	25.52	10
C	56.48	25.52	10
D	45.6	25.52	10
E	54.72	25.52	10

Three types of floats were used in the measurement; Surface float, subsurface float and Double float to determine the characteristics of the uncertainty associated with each type of float. The different channel lengths were chosen to determine the stability of flow of the floats across the channel and for comparison of the mean velocity of flow across all the channels to access the precision of the readings.

3.4.9 Correction of sag of tape

The correction for Sag of measuring tape was carried out using Equation 3.27 given below;

$$K_s = \frac{M^3 L^3}{24\, F_T^2} \tag{3.27}$$

Where,

K_S = Sag correction for length

M = Mass of tape

L = actual length of tape

F_T = Tape tension

3.4.10 Determination of the gross head

The elevation of the sites was determined by accurate leveling using the surveyor level with reference to an established bench mark close to the sites. The levels of the bench marks were validated by running a leveling from other established adjacent bench marks. Outward and return runs were used to check the accuracy of measurement. The rise and fall methods were used for reduction of the site leveling before instrument pack up to ensure that the leveling was done correctly.

The estimation of an appropriate head for the power project was based on the consideration of minimizing the environmental impact of the dams in the upstream and downstream of the plants. The reservoirs are situated within the respective river basins. This implies that the total reservoir capacity will be within the basins which will assist to minimize any spill over from the dams. The survey measurement of the elevation of the river basins and the estimated heads are shown in Table 3.3.

The gross head was determined by the vertical distance between the head race and tail of the turbine.

Table 3.3: Determination of head

Basin	Vertical elevation (m)	Estimated head (m)
Orle	64	50
Edion	58	50
Orbeh	72	50

3.5 Runoff Modeling and Discharge Data Extension Process

The design of the water control and retention facilities requires the use of meteorological and hydrological data between 20 – 30 years for effective design and specification of the facilities properties. In other to meet this requirement the observed 2 years experimental discharge data were extended to 30 years discharge data using the Guass-Newton non-linear empirical regression algorithm because of its high accuracy and popularity in solving non-linear problem (Siregar *et al.,* 2018). A 30 years historical and predictive discharge data extension was carried out.

The catchment areas of study falls into ungauged channel characterized by limitation of data availability, so the most appropriate discharge data extension tool is the empirical model (Pechlivanidis *et al*., 2011).

3.5.1 Characteristics of regression base empirical rainfall – runoff model structure

The following characteristics of empirical model favored its adoption for rainfall – runoff modeling in ungauaged catchment river basins.

i. Non-linear statistical relationship between inputs and outputs (Siterson *et al.*, 2017).
ii. Depends on input accuracy and observational oriented (Kokkohen *et al*., 2001).
iii. Inputs are historical rainfall and runoff, while outputs are specific location runoff.
iv. Most appropriate for ungauged channel with few parameters required for model execution (Pechlivanidis *et al.*, 2011).
v. Fast computation time, cost effectiveness and simplicity of implementation (Sitterson *et al.*, 2017).

vi. Capable of yielding accurate simulations including long time steps and regeneration of past runoff values (Vaze *et al.*, 2012)

Part of the weakness include no connection between physical catchment characteristics and could be affected by input data distortion.

The general relationship for empirical model is shown in Equation 3.28 (Siterson *et al.*, 2017), shown below,

$$Q = f[X, Y] \tag{3.28}$$

where,

Q is runoff output

X is input dataset of rainfall

Y is input dataset of historical runoff

The empirical models for the catchment areas were implemented with the Minitab Gauss-Newton non-linear regression algorithm.

3.5.2 Gauss-Newton non-linear regression algorithm analysis

The Gauss-Newton regression algorithm analysis is an iterative method to proffer solution to non-linear problems. It is used to find the best fit theoretical model in non-linear regression analysis to generate model output that is in good agreement with available observations. The output of Gauss-Newton method consisted of convergence at simple and multiple roots. It is one of the most popular efficient and simple methods for solving non-linear problems (Siregar *et al.*, 2018). The initial guess must be close to the desired solution point for quick convergence.

3.5.3 Meteorological data source

Historical, predictive and study period meteorological data were obtained from the National Centre for Meteorological Research (CNRM), France. CNRM-CM5 is atmospheric system model designed to run climate simulations. It consists of several models designed and operating independently and connected through the OASIS software developed at CERFACS. ARPEGE-Climate is the particular model for the atmospheric data acquisition (Roehrig *et al*., 2020).

ARPEGE-Climate is able to simulate present climate and its variability on timescales ranging from months to centuries. This model is used to perform experiments in the framework of the Coupled Model Intercomparison Project (CMIP5), which will serve as a base of the next Intergovernmental Panel on Climate Change (IPCC) assessment report. The CNRM-GAME CMIP5 data portal is the entry point to the model output generated by ARPEGE-Climat 6.3.

The CNRM teams employs high-tech facilities of supercomputers and digital models of the Earth system, observation satellites, instrumented airplanes, measurement stations fixed or mobile, instrumented sites in the mountains, wind profiler radar, etc. It cooperates closely with French and international laboratories, universities and research institutions (Roehrig *et al*., 2020).

3.5.4 Description of ARPEGE-Climat 6.3

ARPEGE-Climat 5.1 is the atmospheric component of CNRM-CM5.1. It is based on Cycle 32 of the ARPEGE/IFS code. Its dynamical core and its radiation transfer, orographic gravity wave drag parameterizations marginally evolved in Version 6.3 (Roehrig *et al*., 2020).

As any atmospheric model, ARPEGE-Climat consists of a dry dynamical core and a suite of physical parameterizations for the representation of diabatic processes.

3.5.5 Microphysics of ARPEGE-Climat 6.3

The microphysical scheme used in ARPEGE-Climat 6.3 scheme is represented by the microphysical processes indicated in Figure 3.8 (Roehrig *et al*., 2020).

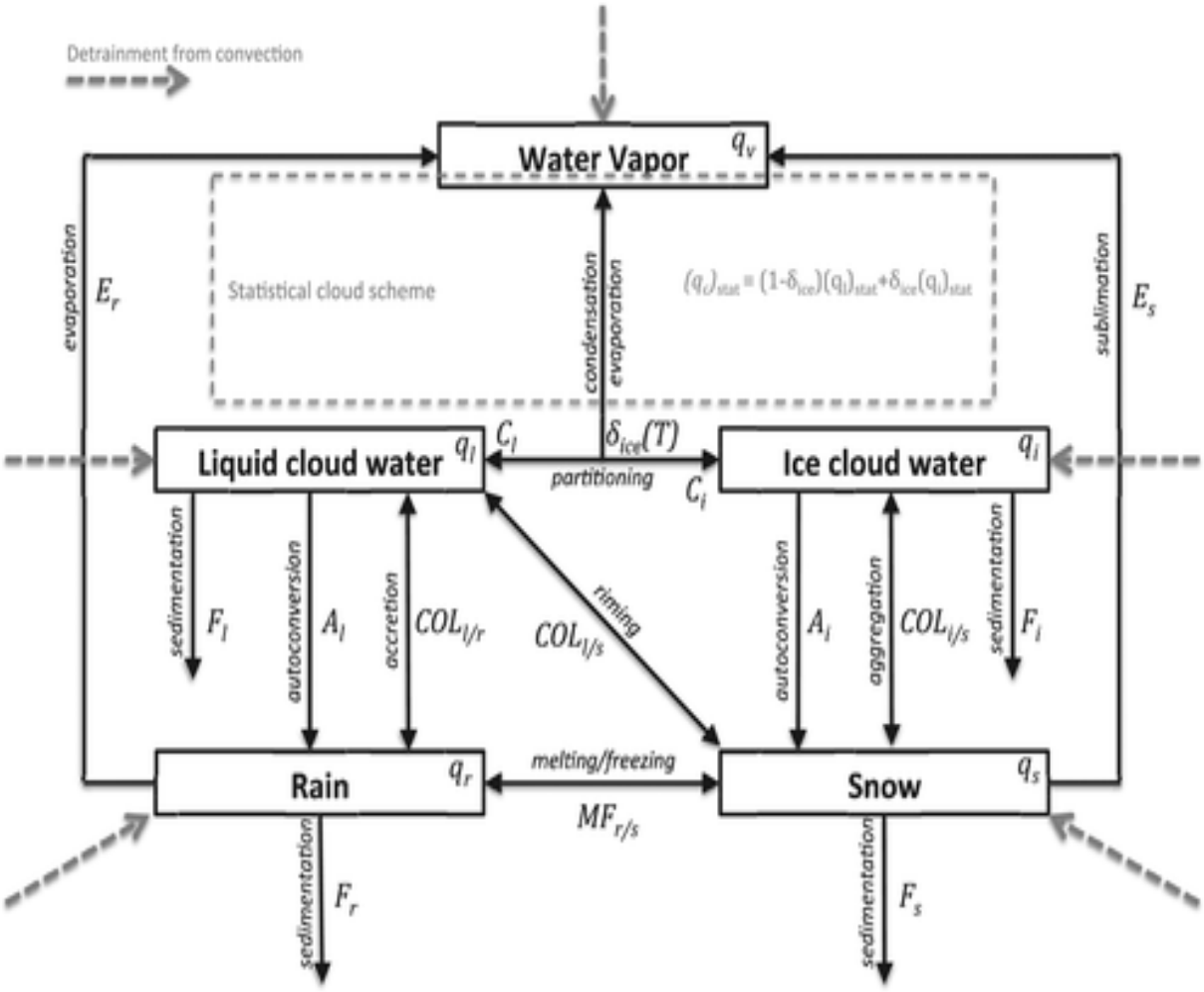

Figure 3.8: Processes accounted for by ARPEGE-Climat 6.3 microphysics scheme (Roehrig *et al*., 2020).

A prognostic treatment of the specific mass of four microphysical species of cloud liquid water, cloud ice, rain, and snow is adopted. It uses two main arguments for using prognostic equations to describe precipitating condensates. It is characterized by a short time step of I5 minutes and spatial resolution of 50 km grid. It provides a finer description of the time evolution of the precipitation vertical distribution and associated processes, and allows a more direct approach for future data assimilation of precipitation data in the ARPEGE version (Roehrig *et al*., 2020).

The integrity and accuracy of CNRM model output is very high. It is the modeling tool for the UN intergovernmental panel on climate change. It is the climate modeling tool used over several region in the world (Nabat *et al.*, 2020 and Mallet *et al.*, 2019). A robust validation of the model on a day to day bases is ongoing and improvement on model structure and performance is rapid (Roehrig *et al.*, 2020). The model output are consistent with various estimates provided in referred literatures (Roehrig *et al.*, 2020).

3.5.6 Rainfall – Runoff model implementation

Implementation of the empirical model Equation 3.28 was carried out with the following algorithm.

i. Metrological data for the study area were obtained from UNRM and Open Weather (Afiliate of UNRM).
ii. Assessment of metrological data quality, statistical relationship and validation
iii. Development of modeling assumptions
iv. Generation of nonlinear regression model equations from the observed discharge and rainfall data for the catchment areas.

v. Generation of the average rivers monthly discharge using the generated regression model equations with the rainfall data from the catchment areas as inputs to the regression models

vi. Validation of the regression model equations.

vii. Generation of historical and predictive discharge data for the three rivers from the 30 years historical and predictive discharge respectively.

viii. Analysis of the results

3.5.7 Rainfall data description

The Metrological data consists of 30 years historical rainfall data from the study area from 1981- 2010 which constitute the base year for the historical data, 30 years of predictive rainfall data from 2026 to 2056 which constitute the base year for the predictive data, monthly rainfall data for the study years of 2018 and 2019 for the catchment areas. All data sources used ensemble system to obtain and validate the meteorological data.

3.5.8 Modeling assumptions

i. The study area is falls into ungauged rivers catchment

ii. Some of the quantity of rainfall is evaporated, infiltrates into the soil to form ground water, captured for consumption and utility purpose and form runoff that appears as rivers discharge

iii. The major component of a river flow is runoff and base flow from ground water

iv. The base flow sustains a river in the absence of rainfall for some time

v. There is a nonlinear relation between rainfall and rivers discharge

3.5.9 Generation of regression model equation from observed river discharged and rainfall data.

Figures 3.9, shows the average rainfall distribution profile for the historical and predictive data which indicates a nonlinear relationship between rainfall amount and monthly time progression annually. Consequently, a nonlinear regression analysis was used to determine the relationship between discharge and rainfall.

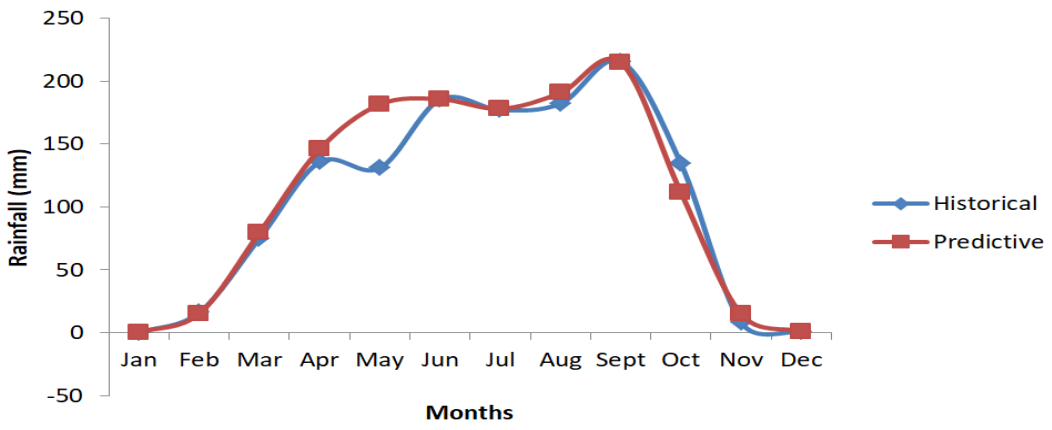

Figure 3.9: Average Historical and Predictive Rainfall Profile for Orle and Edion Catchment Area

3.5.10 Generation of rainfall - discharge regression models equation

The average rainfall for the study period of 2018 and 2019 and the average observed 2 years rivers discharge for the same period were used to generate the regression model equations for each of the river. The 95% confidence and prediction interval of the Minitab regression runs was used to implement the nonlinear regression analysis for the three rivers. Regression model equations were generated with rainfall as predictor variable and discharge as response variable.

3.6. Validation of Gauss –Newton non –linear regression algorithm regression equations

The generated regression equations were used to validate the regression models in the prediction of the river monthly discharge using same rainfall data of 2018 and 2019 for the study period as inputs into the empirical model equations. A comparative analysis was carried out between the models and observed experimental results. A correlation analysis was carried out between the generated discharge results and the observed experimental results.

3.6.1 Generation of historical and predictive discharge data

Historical and predictive discharge data for 30 years were generated using the validated Gauss –Newton non –linear regression analysis model equations for the three rivers. The rainfall data where categorized into average, minimum and maximum monthly rainfall data. These served as input to the Gauss– Newton regression models from which average, minimum and maximum monthly discharge where obtained for the three rivers both for the historical and predictive data.

3.7 Determination of Storage and Discharge Characteristic of the Reservoirs

3.7.1 The mass curve method

The mass curve method was used to determine the storage capacity of the reservoir on the basis of the cumulative inflow to the reservoirs. The net reservoir capacity was adjusted for the rainfall volume on reservoir surface, seepage across reservoir embankment, evaporation of water from reservoir surface and sedimentation at reservoir bottom. Only the storage capacity and discharge requirement design of the reservoir were carried out.

Annual cumulative flow of the rivers were plotted against months in the year as indicated in Table 3.4. The mass curve is one of the most commonly used processes to determine the storage capacity of reservoir (Taka *et al*., 2017).

Table 3.4: Cumulative Inflow into Orle Reservoir

Month	Mean flow (m^3/s)	Inflow volume (m^3)	Cumulative inflow (m^3)
January	6.64	17,210,880	17,210,880
February	9.718	25,189,056.	42,399,936
March	10.5995	27,475,200	69,875,136
April	13.641	35,357,472	105,232,608
May	20.836	54,006,912	159,239,520
June	32.5285	84,315,168	243,554,688
July	27.5135	71,316,288	314,870,976
August	33.2115	86,085,504	400,956,480
September	58.55	151,761,600	552,718,800
October	11.2035	29,040,768	581,758,848
November	8.999	23,328,000	605,086,848
December	6.7945	17,612,640	622,699,488

The mass curves were prepared from the observed inflow of the rivers from the average monthly discharged derived from 60 years rainfall data of the catchment areas. The ordinate of the mass curve corresponding to the months of rainfall were determined and plotted to obtain the mass curve. A uniform rate of flow demand was determined for the river reservoirs by connecting the beginning of the mass curve to the end of it to obtain the uniform demand line of the reservoir.

3.7.2 Analysis of seepage through dams

The model of Fakhari and Gambare (2013) was adopted to determine the rate of seepage through the core materials of the dam due to its ability to predict seepage of dam body with high precision (Fakhari and Gambari, 2013). The dam design consist of a rock filled materials with consist of a central core shown in Figure 3.10.

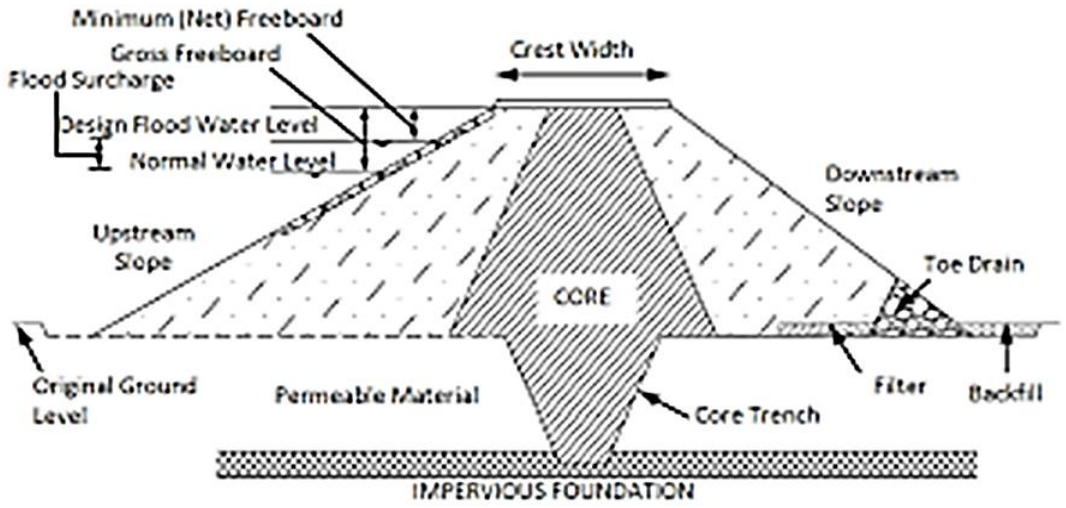

Figure 3.10: Illustration of Rock Filled Dam with Hard Core (Fakhari and Gambare 2013)

The variables that were used in the analysis includes the head of water in the reservoir, width of the dam crest, height of dam, slope of upstream side of the central core. These variables were used in the Fakhari and Gambari (2013) model to calculate the seepage through a multi - parametric analysis to choose the optimum dimensions of the dam to minimize seepage without compromising the structural stability of the dam. The equations for homogenous dam with a vertical core is given in Equation 3.29.

$$Q = f.k.h \tag{3.29}$$

Where,

Q is the seepage (m^3/s)

f is the seepage factor (dimensionless)

k is the permeability (m/sec)

h is the head of water in the upstream side (m)

$$f = (2.27 - 0.006W - 0.004h - 0.38\tan\alpha)H^{(-0.361)}\left(\frac{c}{h}\right)^{(0.3947)\tan\alpha+0.15h-1.3591} \quad (3.29)$$

$$c = b - 0.75\Delta \quad (3.30)$$

Where,

α is the angle of upstream slope (degree)

W is the length of dam core crest (m)

H is the height of the core (m)

Some dams with geometric parameters similar to the projects under study were selected from the study of Fakhari and Gambari (2013) using the gross head as a guide for the implementation of Equation 3.25. Multi – parametric analysis was used to determine the adequate geometry to minimize seepage and enhanced structural stability of the dams using the permeability of the local soil.

3.7.3 Estimation of evapotranspiration rate from the reservoir surface.

The evaporation off the reservoirs surfaces were estimated to determine the volume of water that is lost to evaporation from the reservoir that will constitute evaporation losses. The Linarce's method (Fakhari and Gambare, 2013), was used to determine the evaporation in the reservoirs. It is expressed in Equation 3.31.

$$E_R = (0.15 + 0.000427x10^{-6}h)(0.8R_S - 40 + 2.5Fu - T_d) \quad (3.31)$$

Where,

E_R is reservoir evaporation rate (mmmonth^{-1})

T is mean daily air temperature (^{0}C)

R_S is incident solar radiation on reservoir water surface (wm^{-2})

F is correction factor due to local attitude (dimensionless)

u is wind speed at 2m above surface (m/s)

h is local attitude (m)

T_d is mean monthly due point (^{0}C)

The following data were used in the implementation of Equation 3.31.

Local altitude = 164m

Mean monthly dew point = 10 ^{0}C

Mean daily air temperature = 26.67 ^{0}C

Incident radiation = 655.5310 wm^{-2}

Altitude correction factor = 1 .02

Wind speed = 1.67 m/s

3.8 Design and Simulation of Penstock Characteristics

3.8.1 Design of penstock

The penstock of the hydro power plants consists of a commercial steel materials of HT 570. The material is popular in the construction of small hydro power penstocks. The penstock consist of a sluice gate valve with ultrasonic flow sensor and two 45^0 elbows with flanges. Surge tanks were not provided due to the short length of the penstock. A model of the penstock constructed with Solid Works software is shown in Figure 3.11.

The penstocks of the three rivers project have identical properties which are shown in Table 3.5.

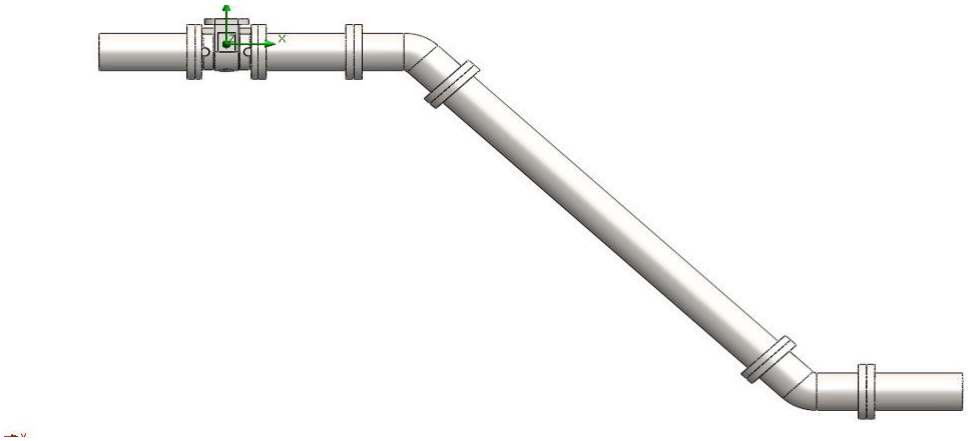

Figure 3.11: Penstock Model

Table 3.5: Properties of the Penstock

Total penstock length (m)	60
Internal diameter (m)	1.6
Outer Diameter (m)	1.98
Type of Valve	Gate Valve
Flange radius (m)	1.92
Height of Penstock (m)	22.25

3.8.2 Design of Penstock Parameters

In the design considerations of the penstock special focus was given to optimal design of the penstock parameters as the most important component of the hydropower plant

which requires a suitable discharge to the turbines and minimization of hydraulic losses in the penstock. The following factors were considered.

i. Configuration of the penstock and selection of fittings to minimize penstock losses
ii. Optimal diameter of the penstock at specified design discharge
iii. The selection of adequate materials for the penstock
iv. The appropriate angle of inclination
v. The type of turbine in association with penstock discharge for power generation.
vi. Minimization of hydraulic losses in the penstock

The identified hydraulic losses in penstock are entrance losses, gate valve losses, friction losses and elbow losses. The loss coefficient for commercial pipes shown in Table 3.6 were used to implement the losses analysis. Careful selection of the penstock fittings was guided by fittings loss coefficient values to minimize the hydraulic losses.

Table 3.6: Loss Coefficient for Commercial Pipes

Fittings	Type	Loss coefficient (k)
Elbow losses	45^0	0.15
Entry losses	Fillet radius entrance (r/d > 0.2)	0.04
Gate valve	Fully opened	0.2
	¾ opened	0.4
	Half opened	5.6

Flow at inlet to the penstock

The entrance losses are due to the liquid acceleration from zero velocity in the reservoir to the velocity corresponding to the flow rate in through the penstock. Appropriate fillet

radius configuration was given to the entrance to the penstock to minimize the entrance losses. The loss is given in Equation 3.32.

$$h_{ent} = k_{ent} \frac{V^2}{2g} \quad (3.32)$$

Where,

h_{ent} is entrance loss

k_{ent} is entrance loss coefficient

V is average velocity

Gate loss

The entrance to the penstock consists of a sluice gate for regulating the discharge of water to the hydro-turbine. The gate is raised or lowered to regulate the flow into the penstock which is made of steel.

The sluice gate is a valve which is used to regulate the flow of water through the penstock. When the sluice gate is open, water flow freely without hindrance into the penstock. When the gate is partially open, some restriction do occur which may led to some minor losses. The loss at the gate is given in Equation 3.33.

$$h_g = k_g \frac{v^2}{2g} \quad (3.33)$$

Where,

h_g = losses at the valve

k_g = loss coefficient

v = average velocity

vii. The appropriate angle of inclination

The model consist of two 45^0 elbows. The 45^0 elbow was used for the low loss coefficient and ease of analysis. The elbow losses were determined through Equation 3.34

$$h_{elb} = k_{elb}\frac{v^2}{2g} \tag{3.34}$$

h_{elb} = losses at the elbow

k_{elb} = loss coefficient at elbow

v = average velocity

viii. Accurate determination of the friction factor for the penstock

The Weisbach – Darcy relation shown in Equation 3.35 was used to evaluate the head loss.

$$h_f = \frac{4fLV^2}{2gD} \tag{3.35}$$

Where,

h_f is head loss due to friction

f is friction factor

L is length of penstock

V is average velocity

D is diameter of penstock

Halland relation shown in Equation 3.36 was used to evaluate the friction factor before iteration in Colebrook friction factor relation indicated in Equation 3.37.

$$\frac{1}{\sqrt{f}} = -1.8\log\left[\frac{6.9}{Re} + \left(\frac{\varepsilon}{3.7D}\right)^{1.11}\right] \quad (3.36)$$

$$\frac{1}{\sqrt{f}} = -1.8\log\left[\frac{\varepsilon}{3.7D} + \frac{2.51}{Re\sqrt{f}}\right] \quad (3.37)$$

$$\frac{1}{\sqrt{f}} + 1.8\log\left[\frac{\varepsilon}{3.7D} + \frac{2.51}{Re\sqrt{f}}\right] = 0 \quad (3.38)$$

The result of the iteration process in the Colebrook equation generated the results in Table 3.7, which indicate the accurate friction factor as 0.01131900. Figure 3.12 indicates that

Equation 3.34 approaches zero at this value.

Table 3.7: Iteration of friction factor in Colebrook Equation

	Friction factor (f)	Value of Eqn. [3.33]
1	0.01131100	3.542e-3
2	0.01131200	3.102e-3
3	0.01131300	2.663e-3
4	0.01131400	2.224e-3
5	0.01131500	1.784e-3
6	0.01131600	1.345e-3
7	0.01131700	9.061e-4
8	0.01131800	4.67e-4
9	0.01131900	2.805e-5
10	0.011320000	-4.109e-4

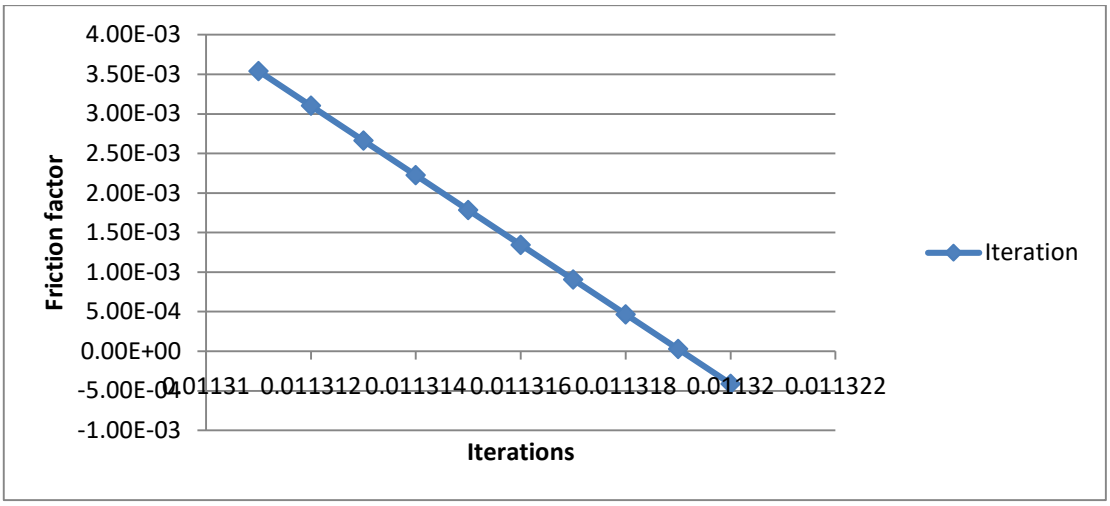

Figure 3.12: Iteration of Friction Factor Value

The total losses in the penstock were determined through the summation of the hydraulic losses shown in Equation 3.39.

Total penstock losses = $h_f + h_g + h_{elb} + h_{ent}$ (3.39)

ix. Selection of turbines

The hydraulic properties of the reservoir were used to select the adequate turbines for power generation. The matching turbine properties are shown in Figure 3.13. From the matching properties, Francis turbine was adopted for the power generation process.

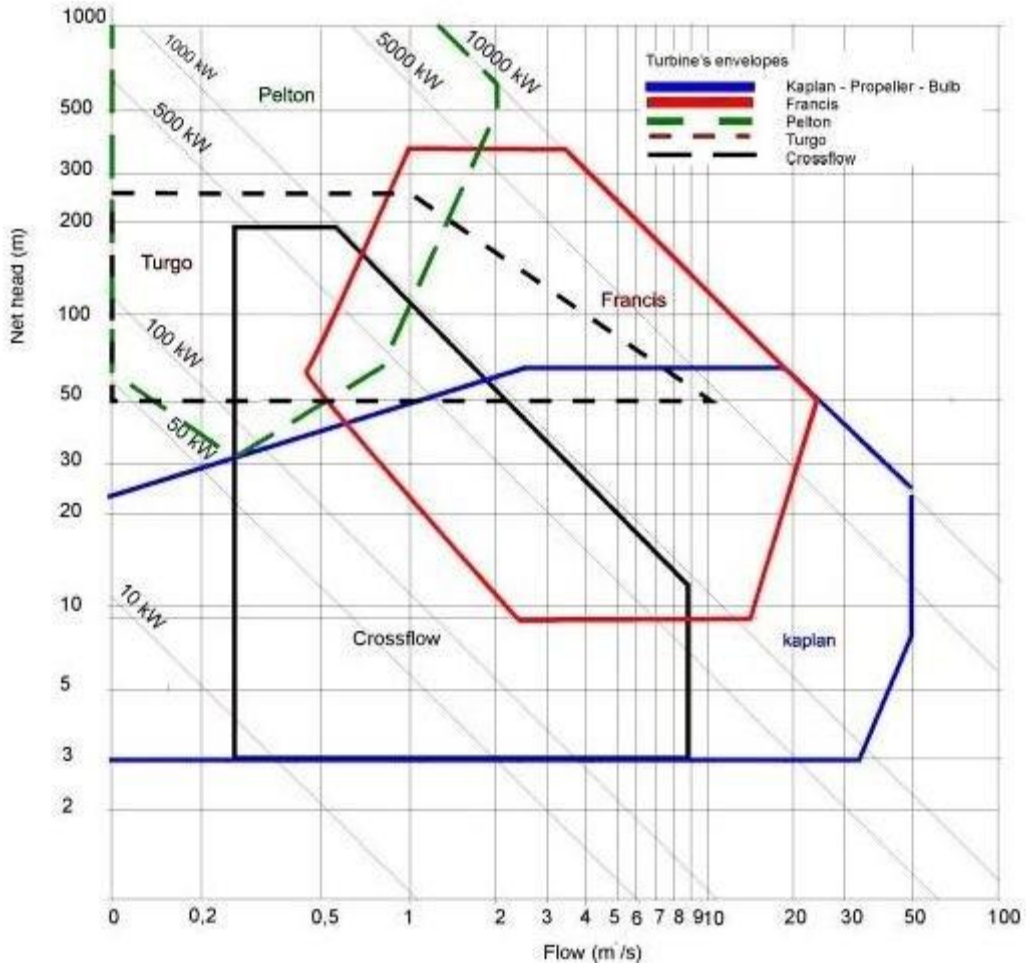

Figure 3.13: Turbine Selection Chart (Sangal *et al.*, 2013)

A power conversion efficiency of 90% was adopted for the Francis turbine.

x. Selection of materials for the penstock

After consideration of factors such as distance, head-loss and cost of materials, a mild steel penstock was adopted for the design (Singhal and Kumar, 2015).

xi. Optimal diameter of the penstock at specified design discharge

The system was selected for multiple penstocks for stability of operation and good system availability. The concept of identical discharge (Bulu, 2021) was used in the design analysis given as follows;

Equation 3.40 was used for the development of identical penstock discharge from the design discharge.

$$Q_n = \frac{Q}{n} \tag{3.40}$$

Where,

Q_n is the flow in identical penstock

Q is design discharge

n is the numbers of penstock

Warmek formula for optimum penstock diameter (Singhal and Kumar, 2015), in Equation 3.41 was used to determine the penstock diameter.

$$D_e = 0.72Q^{0.5} \tag{3.41}$$

Where,

D_e is optimum penstock diameter

The identical velocity in the identical penstocks is given in Equation 3.42.

$$V = \frac{4Q_n}{\pi {D_e}^2} \tag{3.42}$$

Where,

V is velocity of flow

xii. Analysis of water hammer effect on penstock thickness

Water hammer effect due valve closure was determined for the penstocks. The penstock constitutes short length type with the analysis given below;

The penstock thickness is given by Equation 3.43.

$$e = a_2 D_e \tag{3.43}$$

Where,

e is wall thickness

$$a_2 = \frac{P}{2\,\sigma} \tag{3.44}$$

σ is tensile stress of steel

$$P = \text{static} + p_h \tag{3.45}$$

p_h is water hammer pressure

Substituting Equation 3.41 in Equation 3.46,

$$e = \frac{Pr}{\sigma} \tag{3.46}$$

The time (t) to propagate the pressure wave from valve to reservoir and back is given by Equation 3.47.

$$t = \frac{2L}{C_p} \tag{3.47}$$

C_p is the velocity of pressure wave and is given by Equation 3.48 (Singhal and Kumar, 2015)

$$C_p = \sqrt{\frac{K}{\rho_w}} \tag{3.48}$$

Where,

ρ_w is density of water

K is bulk modulus of elasticity of water

For the gradual closure of valve in the penstock,

$t > \frac{2L}{C_p}$ and p_h is given by Equation 3.49

$$P_h = \frac{\rho LV}{t_c} \tag{3.49}$$

t_c is time of closure of the valve

xiii. Weight of Penstock

The penstock weight of the single penstock is

$$G_n = \frac{G}{n} \tag{3.50}$$

G_n is the weight of the penstock

G is weight of the single penstock

3.9 Computational Fluid Dynamics (CFD) for Penstock Design Using Solid Works Flow Simulation 2021

The Analysis of flow of water through Penstock for the rivers was done using Solid Works software Flow Simulation, an add-on of Solid Works Packages. It advantages includes an embedded user-friendly interface that interacts with its user, a fully equipped package to accurately calculate flow through pipes and simulate various flow patterns of velocity, pressure, temperature etc. It assists the system to quickly and efficiently solve its analysis by constantly adjusting the software solver to the computational ability or speed of the system.

Four consecutive flow simulations were carried out with various valve lifts or opening, starting from a fully opened valve, three quarter, half and a quarter valve settings. This was used to predict and simulate the various pressure losses on the penstock with valve opening and to demonstrate the versatility and ease of operation of the Solid Works software flow simulation package. A single simulation configuration was used to achieve the various valves lift and flow simulation through the penstock.

3.9.1 Process design consideration and setup

In other to have an accurate and precise model for the design, the following factors were considered:

i. Mesh Quality.
ii. Computational ability or speed of the computer.
iii. Boundary Conditions.
iv. Process setup goals (output)

3.9.2 The Design Setup

1. Modeling and Assembly of Parts in Solid Works software
2. Activation of Solid Works Flow Simulation.
3. Setting-up Flow Simulation Wizard.
4. Mesh (Discretization).
5. Application of Boundary Conditions.
6. Set up goals
7. Calculation.
8. Results.

3.9.3 Modeling and assembly of parts in Solid Works Software

The Penstock was designed using Solid Works software and then configured to a flow process from a reservoir solved with flow simulation to discharge to a Francis turbine. The flow part consists of a sluice gate valve, commercial mild steel part, two 45^0 elbows. The selection was based on commonly used materials for hydro power penstock, performance and availability of material characteristic data. Associated fitting were minimized to reduce hydraulic losses.

i. Sluice gate valve

A gate valve was adopted for the sluice gate valve. The adopted gate valve has the strength to handle high pressure fluids between 200 psi to 1000 psi. The valve is shown in Figure 3.14. It was configured to be remotely operated through its vertical shaft to adjust valve openings. Using Solid Works software facilities the entire penstock was created according to design specifications. Solid Works system flow simulation requirements necessitated the modification of some penstock parameters for enhanced flow tracking and analysis. The complete penstock assembly is shown in Figure 3.15.

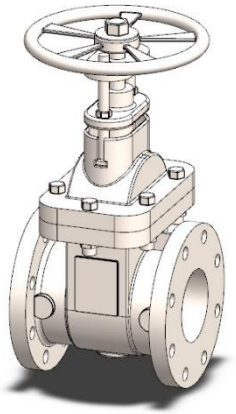

Figure 3.14: Adopted Gate Valve

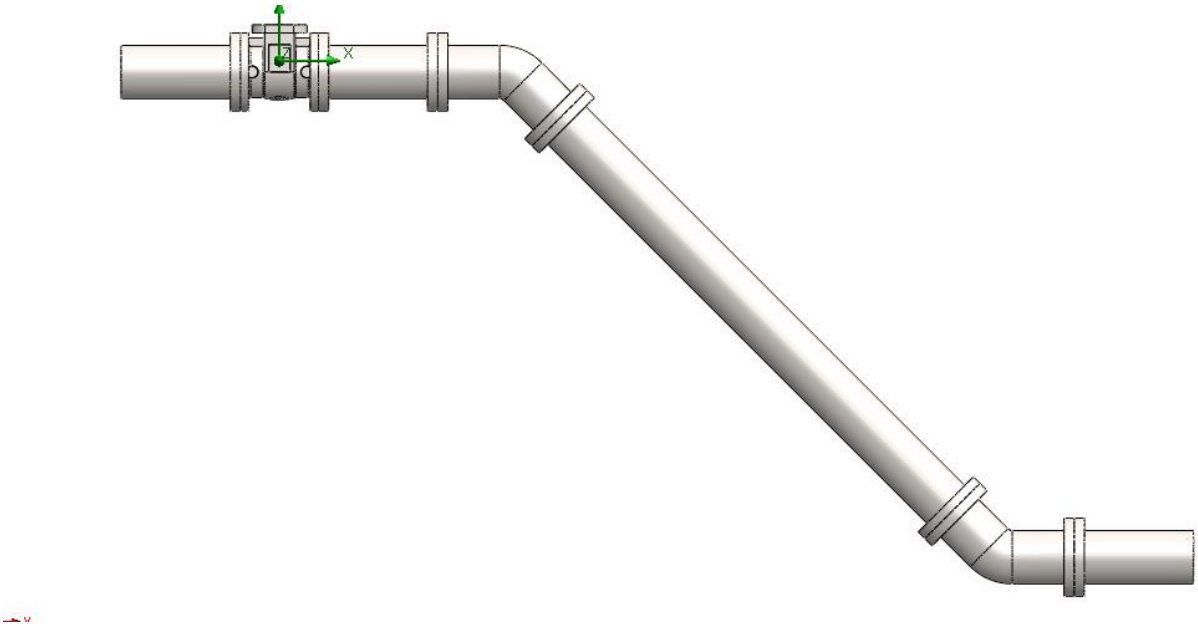

Figure 3.15: Penstock Assembly

3.9.4 Activation of flow simulation

i. Setting-Up Flow Simulation Wizard

The flow simulation wizard was configured and activated with the material and flow properties indicated in Table 3.8. The material flow simulation wizard set up is shown in Figure 3.16, while the set up process is shown in Figure 3.17.

Table 3.8: Materials and Flow Properties of Penstock

Type of Analysis	Internal flow
Project Fluid	Water
Flow Characteristics	Turbulent Flow
Wall Conditions	Real wall
Roughness	45 micrometers
Parameters	Pressure, volume and velocity

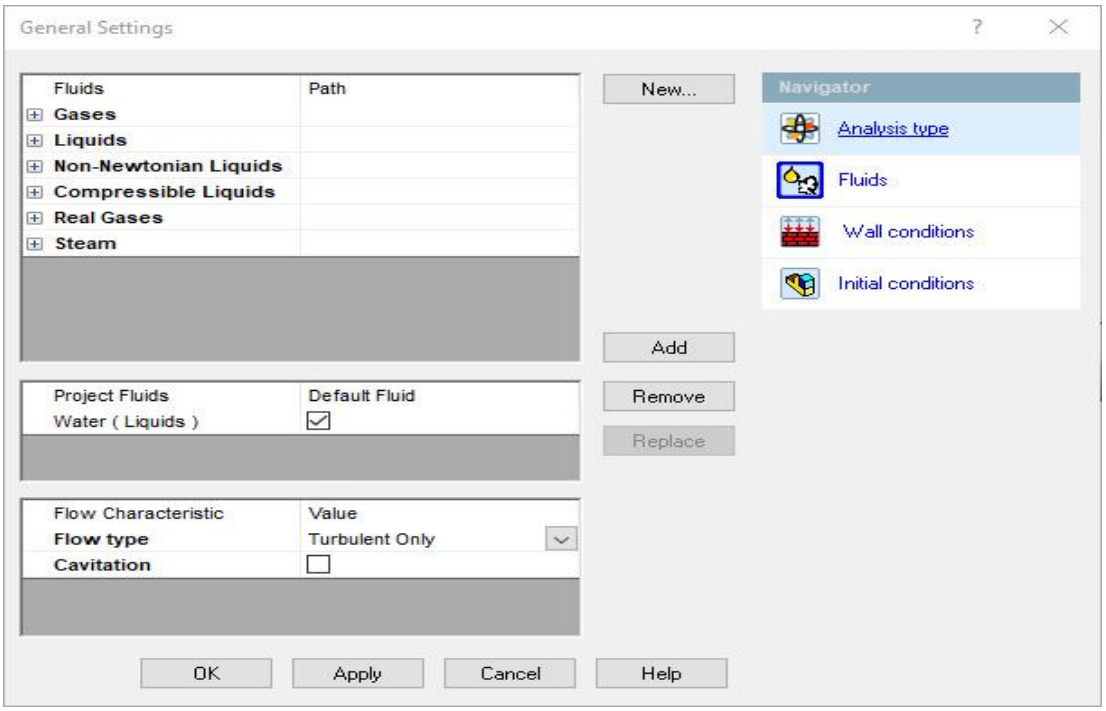

Figure 3.16: Solid Works Materials Flow Simulation Wizard Set up

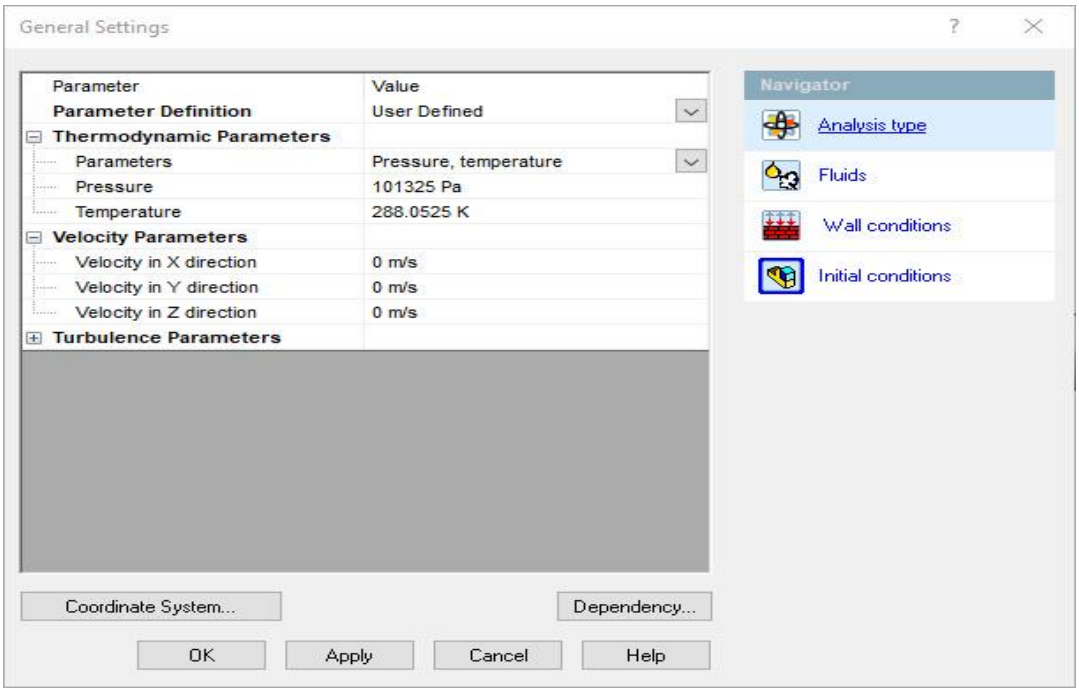

Figure 3.17: Solid Works Parameters Flow Simulation Wizard Set up

3.9.5 Computational Flow Domain

The computational domain was automatically generated on acceptance of the wizard setup. The computational domain is an enclosed fluid region that makes the model a water tight entity by creating a rectangular box or enclosure around the part as indicated in Figure 3.18. This was set to hidden by activating hide command to assist better visualization. A section through the computational fluid domain is shown in Figure 3.19.

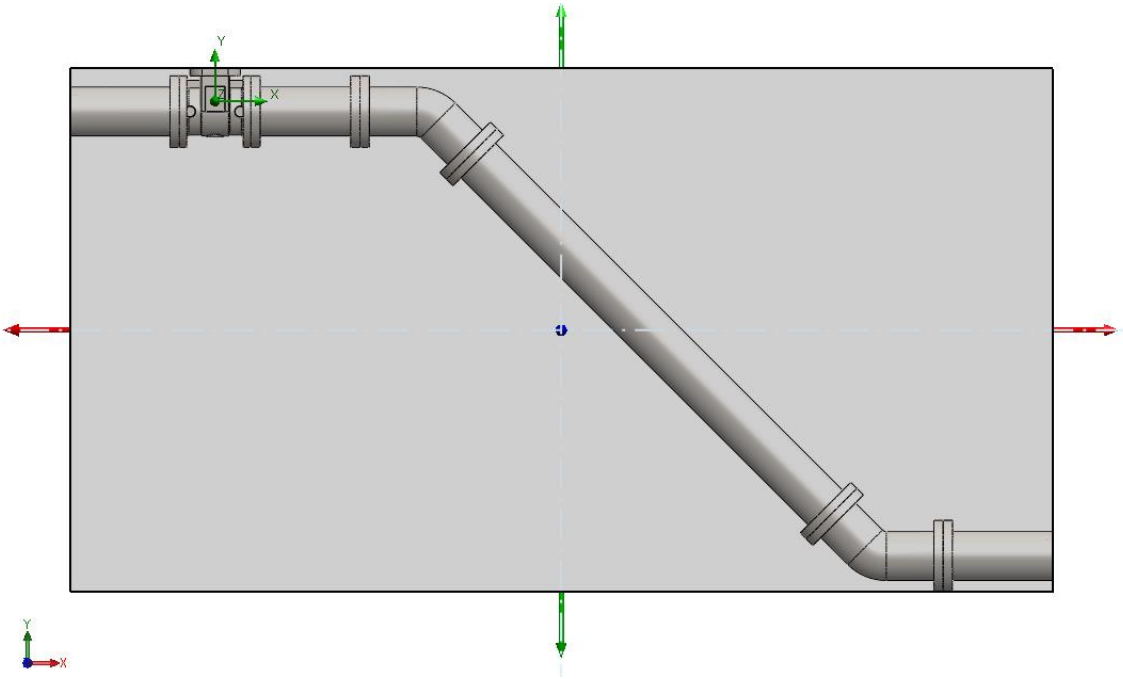

Figure 3.18: Computational Fluid Domain

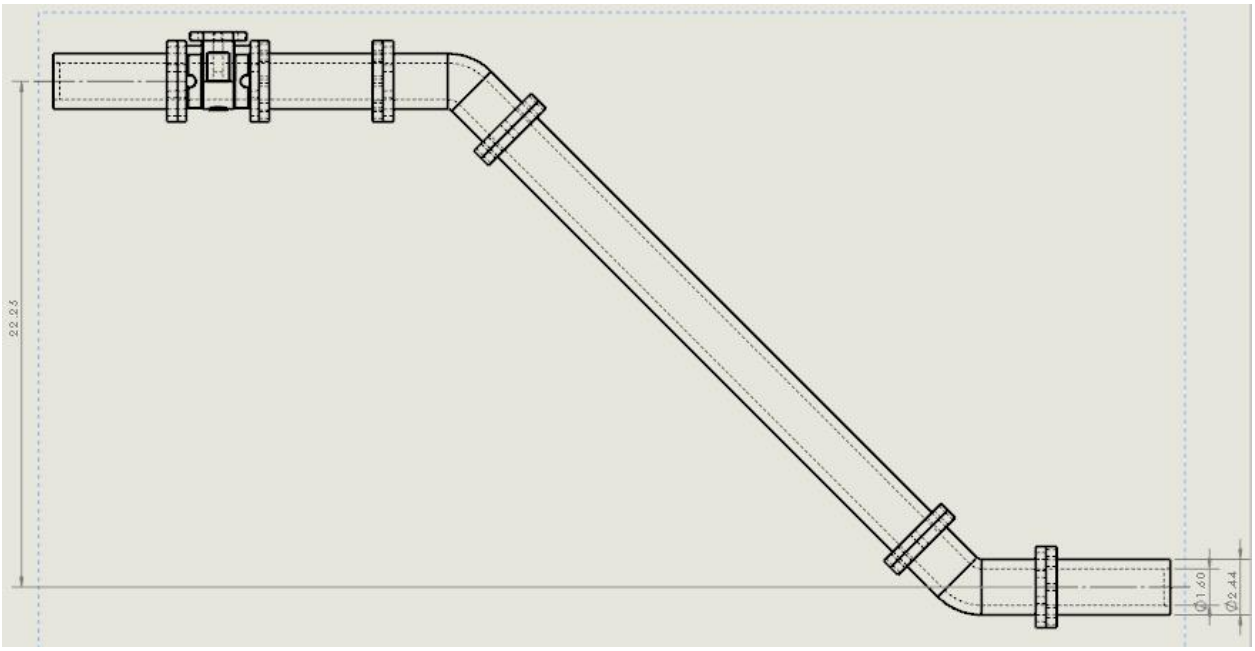

Figure 3.19: Penstock Model in Solid Works software Computational Domain

3.9.6 Setting-Up boundary conditions

The applied boundary conditions are indicated in Table 3.9 for the inlet and outlet interface. They represent the pressure at inlet to the penstock, the wall roughness and flow at outlet of the penstock.

Table 3.9: Applied Boundary Conditions

Outlet Volume Flow	4.811 m^3/s
Real Wall (Roughness)	45 micrometers
Static Pressure	343350 Pa

3.9.7 Setting-up simulation goals

The goals specified the output from the flow simulation process. In this setup, various goals were set-up to determine and cross-check the output data to that of the analytical data. The set goals include the pressure at inlet and outlet of the penstock, the average

velocity, mass and volumetric flow rate across the penstock. The set-up goals are configured manually.

3.9.8 Mesh refinement

Flow Simulation automatically breaks down the mesh sizes by adjusting the software solver to the computational speed of the computer. Figure 3.20 indicates the mesh generation configuration in the fluid computational domain while Figure 3.21 indicates the mesh generation process report with convergence of goals at 134 iterations.

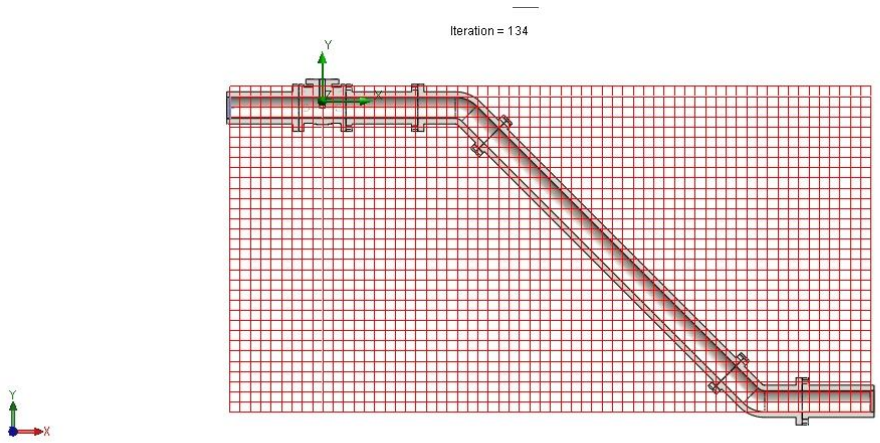

Figure 3.20: Mesh Generation in the Fluid Computational Domain

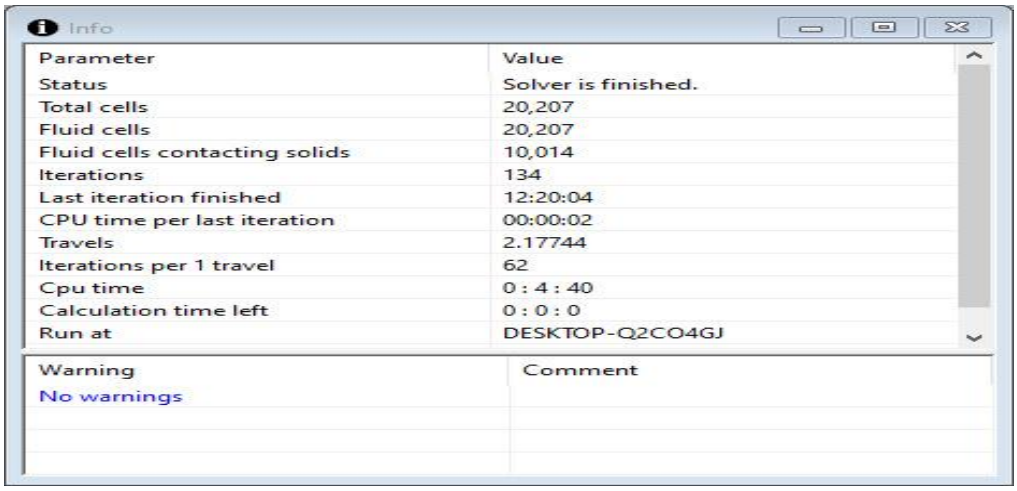

Figure 3.21: Mesh Generation Process Report

Five levels of mesh refinement were carried out in accordance with the solid works resolution levels. The levels span from 1 – 7. After initial test runs, mesh refinement were carried out from level 4 to 7.

3.9.9 Calculation of head losses

The hydraulic losses were calculated through the average pressure difference and average velocity across the penstock using Equation 3.51 (Solid Work Software),

$$h_l = \frac{\Delta P}{\rho \frac{v^2}{2}} \tag{3.51}$$

Where,

h_l is head loss

ρ is density

V is average velocity

3.10 Environmental Impact Assessment of Mounting of Small Hydropower Plants in the Rivers Basins

3.10.1 Methodology of environmental impact assessment of construction of small hydropower plant in the rivers basins

The EIA was carried out in line with the basic requirements of the Environmental Impact Assessment (EIA) Bill of 2017 by Federal Government of Nigeria (Office of Environmental Assessment Department, 2017). A summary of the basic processes is given below.

i. Determine the scope of the environmental impact assessment (EIA) through a process of screening.

ii. Identify the key issues to be examined in more detail during the assessment including the impacts to be assessed.

iii. Provide an Environmental Statement on the EIA describing the proposed development

iv. Consider the alternatives to the proposed development that may be more environmentally acceptable.

v. Study the state of the potentially affected environment in the absence of the project to provide a baseline against which the possible effects of the project can be measured.

vi. Predict the likely significant environmental effects of the proposed development depending on the type of industry

xiv. Describe the measures designed to avoid, reduce and if possible, remedy significant environmental effects of the project

3.10.2 Project sites description

i. River Orle plant

The study area is the Orle river valley basin located at Kilometer three Auchi – Sabogadia Ora road. The valley has vertical height elevation of about 80.56 m, longitudinal width of about 2050 m and a length of 4150 m (Field measurement). The area consist mostly of forest and sparse cultivated land. There is an abattoir which is the critical structure in the area, some few residential buildings, undeveloped buildings and plots. It is bothered by Oshiomole village in the South-West and East, Warrake in the South and Aviele village in the East.

ii. River Edion plant

The river Edion project sites is located at KM 23 along Auchi – Sabogida Ora road. It has a length of about 2150 m, width of about 1155 m and elevation of 64 m. The valley is sparsely populated with farmlands with no evidence of human habitation. It is bothered by Ikpeshi in the north, Ihievbe village in the east, Warrake in the South, Uokha and Afuze in the west.

iii. River Orbe plant

The Orbe plant site is located at about KM 33 along Auchi – Agenebode road. It has a length of 5450 m width of 2150 m and height elevation of 72 m. The valley is sparsely populated with farmlands. There is no evidence of human habitation. It is bordered by Iviukwe village to the east, Fugar town by the west, Agiere in the south and Ivianokpodi in the north.

The river basins have similar characteristic and forestry features. Only R. Orle basin witnesses some sparse human habitation.

3.10.3 Projects design and description

A feasibility assessment of the hydrological and hydroelectric properties of the Rivers are shown in Table 3.9 to 3.11. The values were derived from the experimental measurement of the flow characteristics of the rivers.

The hydrological and hydroelectric characteristics of River Orle are shown in Table 3.10.

Table 3.10: Hydrological and Hydro Power Characteristic of River Orle

Parameters	Minimum	Maximum	Average
Velocity (m/s)	0.462	0.564	0.513
Flow rate (m^3/s)	6.64	58.550	19.243
Power (MW)	4.00	28.718	10.00
Head (m)	-	50	-

The project consist of a small reservoir with an area 4,392,000 m^2 integrated into the Orle valley. Effective head of the dam is 50 m, average power production is 10 MW, peak power production is 28.718 MW (Audu *et al.*, 2020). The project consists of 4 units Francis turbines.

The hydrological and hydroelectric characteristics of River Edion are shown in Table 3.11.

Table 3.11: Hydrological and Hydro Power Characteristic of River Edion

Parameters	Minimum	Maximum	Average
Velocity (m/s)	0.477	0.565	0.508
Flow rate (m^3/s)	5.200	15.931	9.805
Power (MW)	3.0	7.814	4.5
Head (m)	-	50	-

The project consist of a small reservoir with an area of 1,216,500 m^2 integrated into the Edion basin. Effective head of the dam is 50 m, average power production is 4.457

MW, peak power production is 7.814 MW. The project consists of 2 units Francis turbines.

The hydrological and hydroelectric characteristics of River Orbe are shown in Table 3.12.

Table 3.12: Hydrological and Hydro Power Characteristic of River Orbe

Parameters	Minimum	Maximum	Average
Velocity (m/s)	0.486	0.563	0.512
Flow rate (m^3/s)	6.878	19.665	10.925
Power (MW)	3.00	8.00	5.00
Head (m)	-	50	-

The project consist of a small reservoir with an area 1,297,600 m^2 and capacity integrated into the Orbe basin. Effective head of the dam is 50 m, minimum power output is 3.00 MW average power production is 5.00 MW, peak power production is 8.00 MW. The project consists of 2 units Francis turbines.

The dams are equipped with spill ways to evacuate excess flood. A water level sensor is provided to monitor the water level rise in case of excessive discharge. The sensor is automated to control the spillway gates to initiate the evacuation of fluid in volumes commensurate with the rate of rise of water above a bench mark level. The design is to avoid the accumulation of water in the reservoir to a level that will cause downstream flooding and excessive erosion.

3.10.4 Determination of the scope of the environmental impact assessment (EIA) through a process of screening.

i. Scope of assessment

The scope of the Projects for the purposes of the EIA involves the impact of site preparation, construction and operation. These include material movement, access roads, water and electricity provision.

ii. Site clearing and civil works construction

The clearing and construction-related impacts such as equipment emission, vibration and noise impacts are short-term in duration, their impact is not significant (Huawei Technologies Nigeria Limited**)**. Also there is no significant human habitation in the project areas The quality of surface water will largely be affected during the construction stage in the project areas (Zelanakova *et al*. 2018), but the effects is largely mitigated by the diversion of the rivers before major construction work.

iii. Access road

The project sites are accessed by functional standard roads. There is no need to construct access roads through difficult terrain for personnel, material and equipment movement.

v. **Construction, equipment and material site**

Construction, equipment and material storage space location at the sites is adequate along the main access roads. A space of 300 m by 300 m by the main roads passing through the basins is sufficient for materials, equipments, and construction materials storage. This does not pose any hindrance or threat of any kind since the basins have sparse farmlands and very low level human habitations.

vi. Excavation work and waste

Excavation work for the reservoirs will produce earth materials for disposal without risk to the environment. Since the reservoirs are located in the rivers basins basin, minimum excavation will be required. Material excavated from the basins could be sold for the filling numerous gullies within the surrounding towns and villages ravaged by gulley erosion. Filling sand for building construction and repair of road ravaged by gulley erosion are in high demand within Edo North.

vii. Electricity and water access

The project sites are accessed directly by high tension cables from the National Power Grid (NPG) from which power could be derived for equipment and utilities consumption.

3.11 Power Plants Cost Modeling

The cost of the hydropower plants was evaluated using the International Renewable Energy Association (IRENA) and the modified CAPEX model (Atchike *et al.*, 2020). The modeling parameters are power rating, cost and head of the power plants. The modeling cost components are indicated in Table 3.13. The levelized cost of energy (LCOE), the net current cost of hydropower generation over the life time of the plants was generated. The cost was evaluated in the United State dollars.

Table 3.13: Cost Components of Hydropower Systems

Cost item	Description
Investment cost	Project development
	Site preparation
	Electro-mechanical equipments
	Working capital
	Auxiliary equipments
	Non-convectional costs
Operation and maintenance cost	Taken as a percentage of the investment cost per kWh/year. Taken as 4% for SHP (IRENA, 2021)
Capacity factor and other associated cost	The cost of not running the plants below the installed capacity
	Cost of finance
	Resource quality
	Contingencies
LCOE	The net current cost of hydropower generation over the lifetime of the plants. The life span of SHP plants was taken as 50 years (IRENA,2021)

The CAPEX model for West and Sub-Saharan Africa was also used because hydro plants could be site-specific. Most hydropower plants constructed in this region are built and financed by China.

3.11.1 Cost modeling assumptions

i. The analysis is undertaken as an investment plan

ii. The cost consideration is for SHP

iii. The assessment targeted the average generated SHP generation cost

iv. The cost analysis is to guide policy makers in decision making on the plants construction

3.11.2 Sources of data

The primary data for the cost modeling were obtained from IRENA (2021), and the work of Atchike *et al*. (2020). Table 3.14 shows the cost parameters for various renewable technology while Figure 3.22 indicates the profile of global installed hydropower cost.

Table 3.14: Cost parameters Value of Renewable Energy Technology (Atchike *et al.,* 2020)

	Total installed costs (2021 USD/kW)			Capacity factor (%)			Levelised cost of electricity (2021 USD/kWh)		
	2010	2021	Percent change	2010	2021	Percent change	2010	2021	Percent change
Bioenergy	2 714	2 353	-13%	72	68	-6%	0.078	0.067	-14%
Geothermal	2 714	3 991	47%	87	77	-11%	0.050	0.068	34%
Hydropower	1 315	2 135	62%	44	45	2%	0.039	0.048	24%
Solar PV	4 808	857	-82%	14	17	25%	0.417	0.048	-88%
CSP	9 422	9 091	-4%	30	80	167%	0.358	0.114	-68%
Onshore wind	2 042	1 325	-35%	27	39	44%	0.102	0.033	-68%
Offshore wind	4 876	2 858	-41%	38	39	3%	0.188	0.075	-60%

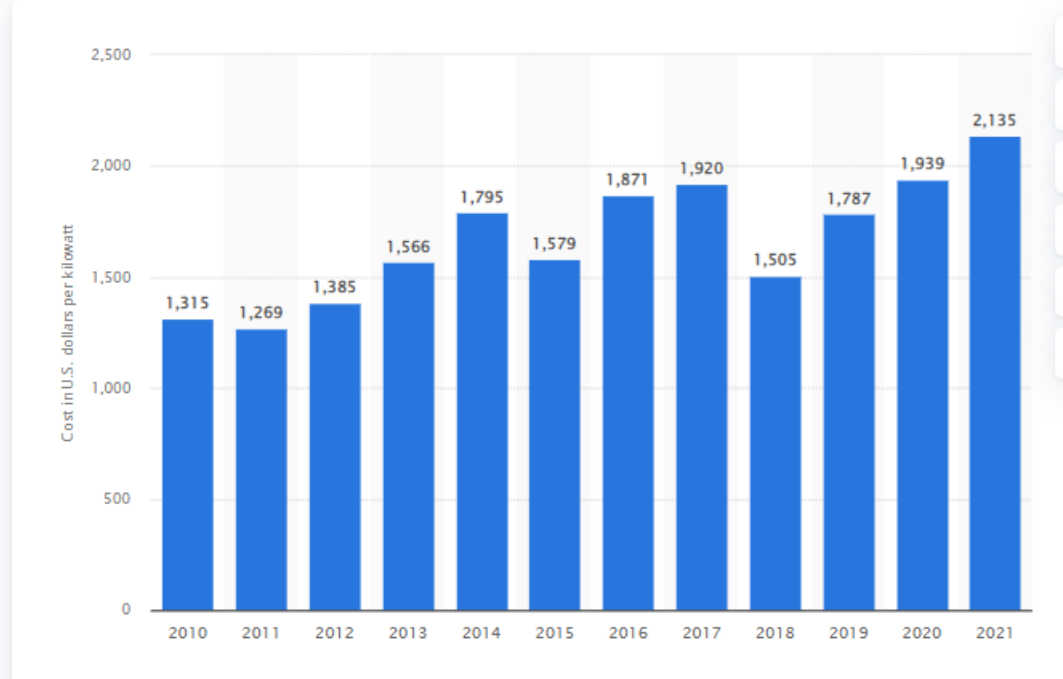

Figure 3.22 : Profile of Average Global Installed Hydropower Cost Per kWh (Statista, 2022)

3.11.3 Modeling equations

i. Cost of escalation

The obtained costs of the parameters were escalated to the present year by the use of Equation 3.52

$$CST_f = CST_i(1 + i)^t \quad (3.52)$$

Where,

CST_f is the escalated cost in 2022

CST_i is the initial investment cost in the reference year

i is the escalation rate

t is the difference between the reference year and the current year

ii. Levelized cost of energy (LCOE)

The relationship for evaluating the LCOE is indicated by Equation 3.53

$$\mathrm{LCOE} = \frac{\sum_{t=1}^{n} \frac{\mathrm{I_N + M_n + F_n}}{(1+\mathrm{r})^{\mathrm{n}}}}{\sum_{\mathrm{t=1}}^{\mathrm{n}} \frac{\mathrm{E_n}}{(1+\mathrm{r})^{\mathrm{n}}}} \tag{3.53}$$

Where,

LCOE is the average lifetime levelized cost of hydropower generation

I_n is the investment expenditure in the year n

$\mathrm{M_n}$ is the Operation and Maintenance cost in the year n

$\mathrm{F_n}$ is the fuel cost in year n

$\mathrm{E_n}$ is electricity generation in year n

n is the economic life of the plant

iii. Modified CAPEX model

The modified CAPEX cost model for hydropower generation in Sub-Saharan Africa is given in Equation 3.54

$$\mathrm{CAPEX} = 8533755\mathrm{P}^{0.843}\mathrm{H}^{0.00645} \tag{3.54}$$

CHAPTER FOUR

4.0 RESULTS AND DISCUSSION

4.1 Model Validation

Figure 4.1 indicates the close proximity between the model results and analytical method for area of channel measurement. It indicates that there is strong agreement in the variation of the area of channels from the first to the last segments. The model accuracy of measurements is 99.99% for area of cross section measurement.

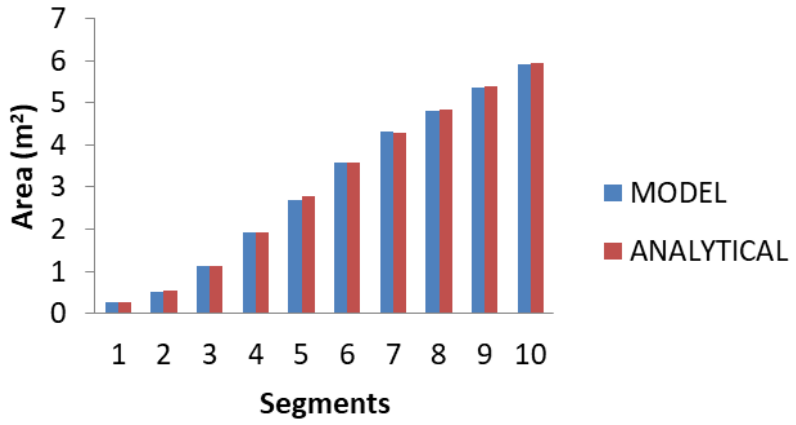

Figure 4.1: Study model and direct computational method results comparison for area of cross section of channel measurement

Figure 4.2 indicates the variation of velocity of the river in segments across the channel. The velocity at the ends of the channel is zero and increases to a maximum at the center of the channel. The study model output indicates it has a precision and accuracy of 99.54% in comparison with the direct manual computation for velocity measurements.

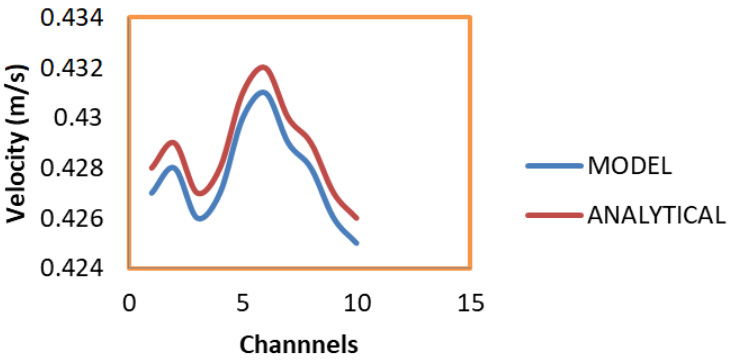

Figure 4.2: Variation of Velocity across the River Channel

The cumulative measurement of the flow rate in segments across the channels by the model, analytical method and ISO 748:2021 model is depicted in Figure 4.3. It indicate the close and high agreement between the three models. The model has a precision and accuracy of 99.98% in comparison with the analytical method for flow rate measurement. The ISO 748:2021 model has a precision and accuracy of 99.82% for flow rate evaluation with the analytical method. The study model has a correlation coefficient of 1 and p – value of 0.000 with the direct manual computation and ISO 748:2021 model respectively.

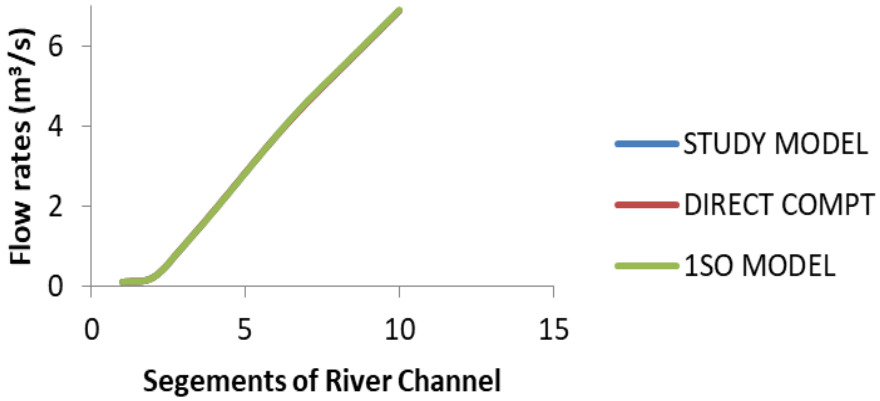

Figure 4.3: Cumulative Measurement of Flow Rates across the River Channel

The ISO 748:2007 model does not capture the average velocity and area of cross section of channel output. In contrast, the model is fast and simple to apply avoiding tedious calculation associated with ISO 748:2021 evaluations. It has other advantages of capturing area of cross section and average velocity evaluation and output.

4.2 Flow Characteristics Assessment

Figure 4.4 indicates the variation of velocity of the rivers annually from January to December. It indicates that the average velocity increases in line with the rainfall pattern of the region.

Analysis of Figure 4.4 indicates that River Orle has a minimum velocity of 0.462 m/s in March and a maximum velocity of 0.564 m/s in September. The average velocity of the river is 0.513 m/s. The minimum velocity for River Edion of 0.486 m/s occurred in February and the maximum velocity of 0.563 m/s occurred in September, while the annual average velocity is 0.512 m/s. It is also indicated that the minimum velocity for River Orbeh is 0.486 m/s which occurred in February, while the maximum velocity of 0.563 m/s occurred in September. The annual average velocity is 0.514 m/s.

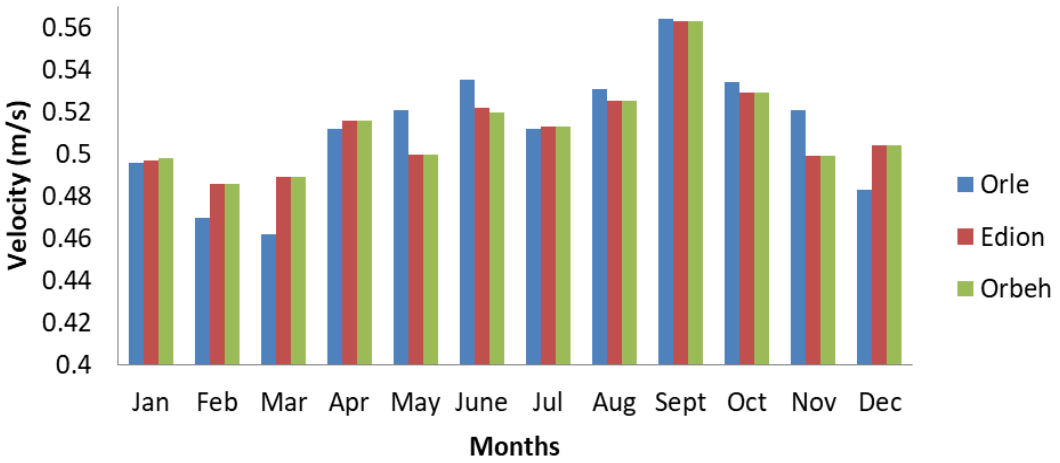

Figure 4.4: Mean Velocity Column Plot

The assessment of the velocity values of the river indicates they have the same flow pattern, the minimum velocity of the rivers occurred in February/March while the maximum velocity occurred in September. This is in line with the rainfall pattern in Edo North, since the rivers flow is nourished by run off from rainfall. The average annual average velocity fall within the same range of 0.512 m/s. The maximum velocity as occurred in the three rivers is also within the same range as indicated in Figure 4.4.

4.2.1 Flow rate and power analysis

The variation of the flow rates of the rivers from January to December is indicated in Figure 4.5. The minimum flow rate of the River Orle is 8.067 m^3/s which occurred in the month of February producing a power output of 3.957 MW at a head of 50 m. The maximum average flow rate is 68.035 m^3/s in the month of September producing a power output of 33.74 MW in the month of September for the same head. The annual average flow rate is 19.283 m^3/s producing a power of 9.349 MW.

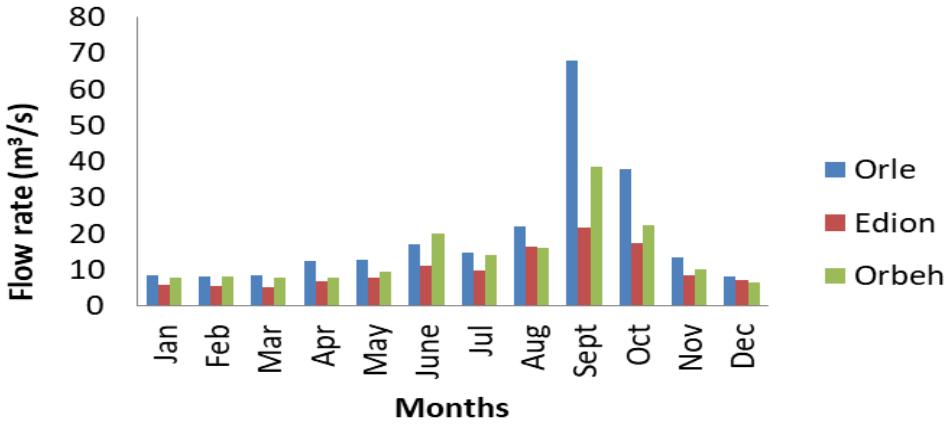

Figure 4.5: Mean Flow Rate Column Plot

Figure 4.6 further emphasize the characteristics of flow rate variation and similarity of the flow pattern for the rivers. The rivers generally have low flow rate between January and May which then rises to a peak in September and decreases sharply to December.

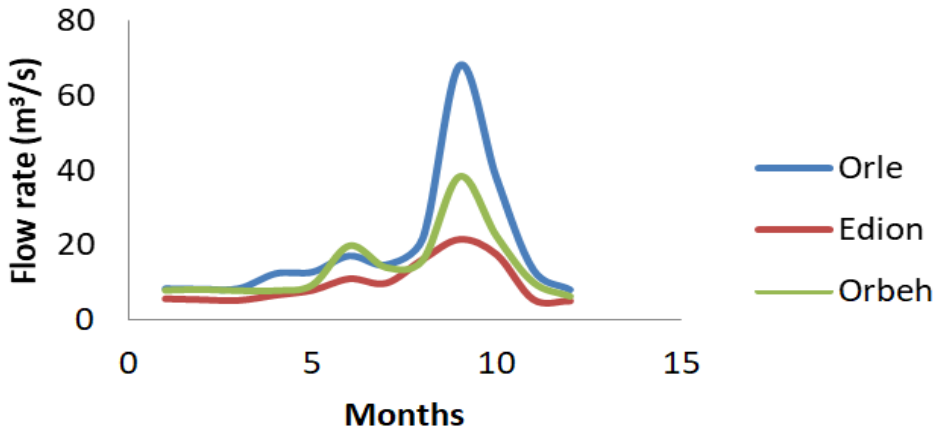

Figure 4.6: Mean Flow Rate Profile of the Three Rivers

The minimum flow rate of river Edion is 5.084 m^3/s producing a power of 2.494 MW in the month of December. The maximum flow rate is 21.549 m^3/s producing a power output of 11.493 MW in the month of September. The average flow rate is 9.827 m^3/s producing a power output of 4.887 MW throughout the year as indicated in Figure 4.6. Figure 4.7 indicates the relation and variation of the magnitude of hydropower that could be generated from the three rivers. It is indicated that River Orle has the maximum power output 33.74 MW in the months of September for the period of study.

The maximum average flow rate of River Orbeh is 34.685 m^3/s producing a power of 17.013MW in the month of September. The minimum average flow rate of 6.242 m^3/s is in the month of December, producing a power output of 3.128 mw. The annual average flow rate is 13.484 m^3/s producing a power output of 6.500 mw throughout the year.

Figure: 4.7 indicates that River Orle produces the highest power output, followed by River Orbeh and Edion with highest output taken place in September. The lowest output took place between February and March in a year. The three rivers are capable of yielding power through the year.

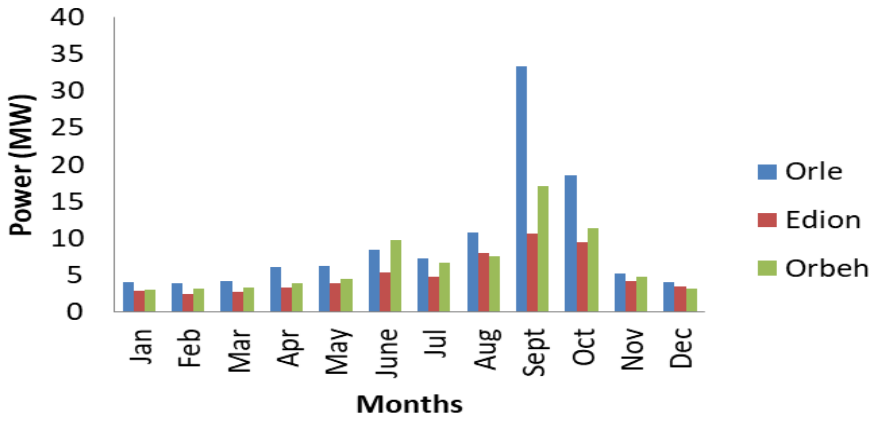

Figure 4.7: Mean Power Column Plot

Figure: 4.8 further indicate the mean power output variation of the three rivers which also indicates that the rivers have similar flow rate and power output pattern in line with the rainfall pattern in Edo North.

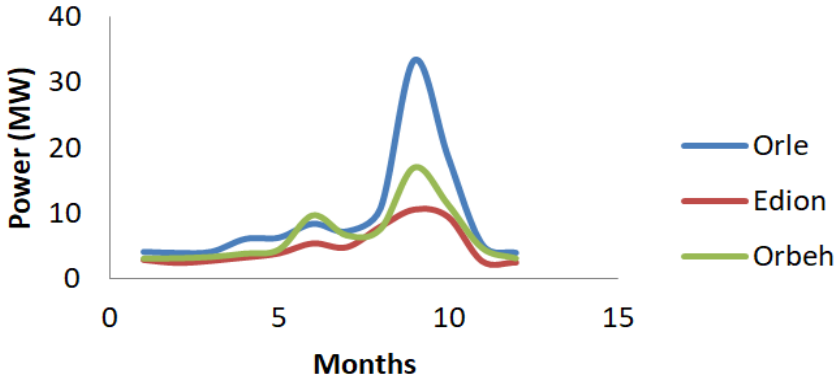

Figure 4.8: Mean Power Profile of the Rivers

4.3 Analysis of Measurement of Reynolds Number

The results of the implementation of Equation 3.26 are indicated in Table 4.1

Table 4.1: Reynolds Number of the Rivers

Parameter	Orle	Edion	Orbe
Average flow rate	19.283	9.827	13.484
Kinematic viscosity	$1.0035x10^{6}$	$1.0035x10^{6}$	$1.0035x10^{6}$
Reynolds number	$1.922x10^{7}$	$9.793x10^{6}$	$1.344x10^{7}$

The Reynolds number for River Orle, Edion and Orbe are $1.922x10^{7}$, $9.793x10^{6}$, and $1.344x10^{7}$ respectively. The range of value of the Reynold numbers is in agreement with the value quoted in Malverti *et al.* (2008) for natural rivers Reynolds numbers $Re \geq 10^{6}$. This established that the flow of the rivers is really turbulent and validates the assumption in the modeling process.

4.4. Statistical Analysis of Data

4.4.1 Anova and correlation analysis of results

The Anova analysis of the mean velocity, flow rate and hydropower potentials of the three rivers are shown in Table 4.2. The p-values of 0.911, 0.171 and 0.214 for mean velocity, flow rate and power output respectively of the three rivers indicate that the three rivers Orle, Edion and Orbeh are not significantly different with respect to Velocity, Flow Rate and Power output, which indicate that the similarity of the result and a pointer to the precision and accuracy of the results. This strongly supports the reliability of the results of the study.

Table 4.2: Anova of the Mean velocity, Flow Rate and Hydropower Potentials of the three Rivers

	Sum of Squares	df	Mean Square	F	Sig.
Mean velocity (m/s)	0.000	2	0.000	0.094	0.911
Between Groups	0.023	33	0.001		
Within Groups	0.023	35			
Total					
Mean flow rate (m^3/s)	505.335	2	252.667	1.867	0.171
Between Groups	4466.426	33	135.346		
Within Groups	4971.761	35			
Total					
Mean power (mw)	109.450	2	54.725	1.618	0.214
Between Groups	1116.328	33	33.828		
Within Groups	1225.779	35			
Total					

The correlation analysis for the mean velocity, flow rate and power potentials of the three rivers are shown in Table 4.3. The velocity correlation indicates that River Orle has a Pearson correlation factor of 0.613 with River Edion and a correlation value of 0.863 with River Orbeh, while River Edion has a correlation factor of 0.856 with River Orbeh. The flow rate correlation indicates that River Orle has a correlation value of 0.915 with River Edion and 0.951 with River Orbeh. River Edion has a correlation of 0.925 with River Orbeh. The power correlation analysis indicates that River Orle has a correlation of 0.932 with River Edion and 0.950 with River Orbeh. The correlation between Orbeh and Edion is 0.944.

Table 4.3: Correlation Analysis of Results

Rivers		Velocity	
	Orle	Edion	Orbeh
Orle	1		
Edion	0.613	1	
Orbeh	0.863	0.856	1
		Flow rate	
	Orle	Edion	Orbeh
Orle	1		
Edion	0.915	1	
Orbeh	0.951	0.925	1
		Power	
	Orle	Edion	Orbeh
Orle	1		
Edion	0.932	1	
Orbeh	0.950	0.944	1

The analysis indicates that three rivers under study; Orle, Edion and Orbeh exhibit strong correlation with respect to Velocity, Flow Rate and Power, reinforcing the accuracy and reliability of the results.

4.4.2 Regression analysis for power versus discharge of three rivers

Table 4.4 shows the results of the preliminary statistical test carried out on the data set in order to determine the data fulfilment of the assumptions of regression of linearity of data, absence of outliers, and independence of observations and normality of residuals.

Table 4.4: Results for the Test of Assumptions of Regression of Linearity of Data

	R. Orle	R. Edion	R. Orbeh	Assumption fulfilled
Regression factor				
Standardized residuals (-3.29 - +3.29)	-1.293 - + 2.072	-2.039 - + 1.259	-1.548 + 1.517	No outliers in the data
Durbin Watson (1 < d >3)	2.441	1.952	1.711	Independence of observation
Anova	0.000	0.000	0.000	Effectiveness of regression model
Normality (p –p plots of standardized residuals with dots line up on 45^0 line)	Dots generally lined up on the 45^0 line	Dots generally lined up on the 45^0 line	Dots generally lined up on the 45^0 line	Assumption of normality
Linearity	Indicated in Figure 3.14	Indicated in Figure 3.15	Indicated in Figure 3.16	Linear distribution of data

It indicates that all four assumptions of regression were fulfilled. The Durbin Watson and standardized residual are within the allowable range, while the p – p plots of standardize residuals and scatter plot data points generally lie on the 45^0 and fit to total line.

4.4.3 Regression analysis for River Orle

The scatter plot for power versus discharge for River Orle data is shown in Figure 4.9. The plot indicates a positive relationship between power and discharge with a good linear fit. This indicates the linearity of the data

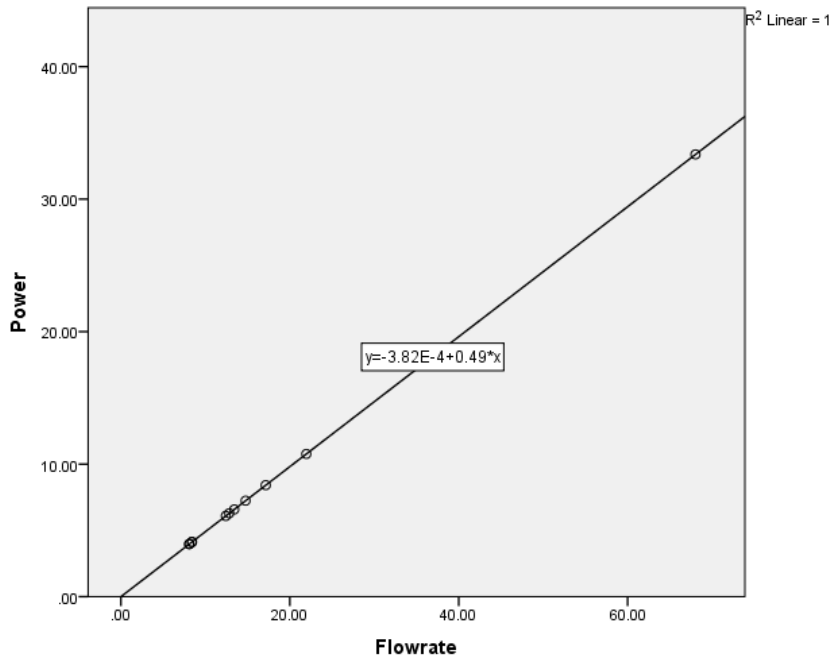

Figure 4.9: Regression Plot of Power versus Discharge for River Orle

The generated regression equation is given in Equation 4.1 from the coefficient shown in Table 4.4.

Power (MW) = - 0.0004 + 0.491Q (4.1)

Where,

Q is mean discharge (m^3/s)

Equation 3.24 indicates that there is 0.491 MW increase in power output with a unit increase in discharge (m^3/s). From Table 4.5, the p value of 0.000 suggest that changes in power output are significantly associated with changes in discharge which is further strongly supported by R value of 1, R^2 value of 1 and R^2 (adj) of 1.

Table 4.5: Summary of Regression Analysis for Power versus Discharge (Orle)

Model Summary

Model	R	R Square	Adjusted R Square	Std. Error of the Estimate
1	1[a]	1	1	.39658

Anova Output

Model		Sum of Squares	df	Mean Square	F	Sig.
1	Regression	809.563	1	809.563	3389608507	0.000
	Residual	0.000	10	0.000		
Total		809.563	11			

Coefficient

		Unstandardized Coefficients		Standardized Coefficients	T	
Model		B	Std. Error	Beta		Sig.
1	(Constant)	0.000	0.000		1.777	0.106
	Flow rate	0.491	0.000	1.000	58220.344	0.000

4.4.4 Regression analysis for River Edion and Orbe

The linear plot for River Edion is shown in Figure 4.10, while the generated regression equation is shown in Equation 4.2. The plot indicates a good linear fit and positive relation between discharge and power output.

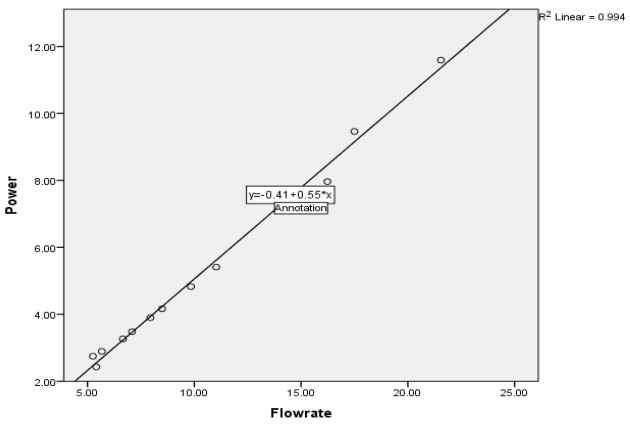

Figure 4.10: Regression Plot of Power versus Discharge for River Edion

Power (MW) = -0.406 + 0.546Q (4.2)

Table 4.5 depicts the summary of regression analysis for power versus discharge for river Edion. Equation 4.2 indicates that there is 0.546 MW increase in power output with a unit increase in discharge (m^3/s). The p value of 0.000 suggests that changes in power output are significantly associated with changes in discharge. The R value of 0.997, R^2 value of 0.994 and R^2 (adj) of 0.993 shown in Table 4.5, indicates high correlation and significant response of power output to changes in the value of discharge of the river.

Table 4.6: Summary of Regression Analysis for Power versus Discharge (Edion)

Model Summary

Model	R	R Square	Adjusted R Square	Std. Error of the Estimate
1	0.997[a]	0.994	0.993	0.23698

Anova Output

Model		Sum of Squares	df	Mean Square	F	Sig.
1	Regression	94.746	1	94.746	1572.721	0.000
	Residual	0.602	10	0.060		
	Total	95.348	11			

Coefficient

Model		Unstandardized Coefficients		Standardized Coefficients	T	Sig.
		B	Std. Error	Beta		
2	(Constant)	-0.406	0.158		-2.576	0.028
	Flow rate	0.546	0.014	0.997	39.658	0.000

Figure 4.11 represents the linear regression plot of River Orbe for power versus discharge. It indicates a good linear fit with all the data points falling on the linear line. The generated regression equation for River Orbeh is given in Equation 4.3.

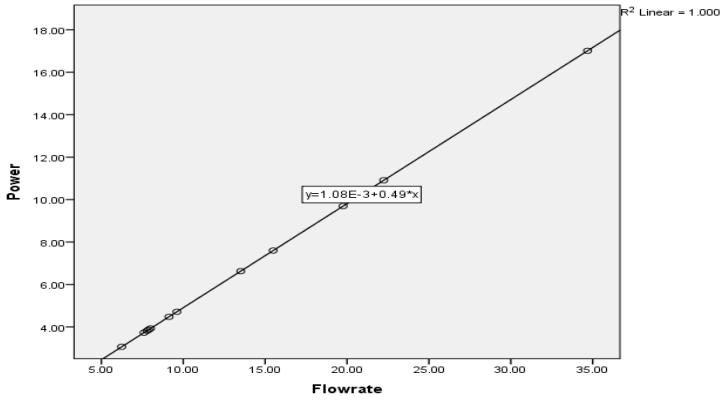

Figure 4.11: Regression Plot of Power versus Discharge for River Orbe

Equation 4.3 indicates that there is 0.490 MW increase in power output with a unit increase in discharge (m^3/s).

Power = - 0.001 + 0.490Q (m^3/s) (4.3)

The changes in discharge are strongly related to corresponding changes in power output with p – value of 0.000, R – value of 1, R^2 value of 1 and R^2 (adj) of 1 as shown in Table 4.7.

Table 4.7: Summary of Regression Analysis for Power versus Discharge (Orbe)

Model Summary

Model	R	R Square	Adjusted R Square	Std. Error of the Estimate
1	1[a]	1	1	0.00169

Anova Output

Model		Sum of Squares	df	Mean Square	F	Sig.
1	Regression	188.742	1	188.742	66249253.28	0.000[b]
	Residual	0.000	10	0.000		
Total		188.742	11			

Coefficient

Model		Unstandardized Coefficients		Standardized Coefficients	t	Sig.
		B	Std. Error	Beta		
1	(Constant)	-0.001	0.001		-1.139	0.281
	Flow rate	0.490	0.000	1.000	8139.364	0.000

4.4.5 Validation of generated regression equations

Table 4.8 shows the results of the correlation analysis between the experimental and regression model results for River Orle. The results indicates a very strong correlation of 1 and significant value of 0.000 which indicate high accuracy and precision of the model in predicting the power output characteristic of River Orle from discharge data.

Table 4.8: Correlation Analysis Output for Experimental versus Model Results for R. Orle

Correlations

		Experimental	Model
Experimental	Pearson Correlation	1	1.000**
	Sig. (2-tailed)		.000
	Sum of Squares and Cross-products	809.563	810.343
	Covariance	73.597	73.668
	N	12	12
Model	Pearson Correlation	1.000**	1
	Sig. (2-tailed)	0.000	
	Sum of Squares and Cross-products	810.343	811.125
	Covariance	73.668	73.739
	N	12	12

**. Correlation is significant at the 0.01 level (2-tailed).

The accuracy and precision is further emphasized by the column plot of the experiment and regression model results as shown in Figure 4.12. The plot indicates very close unison of agreement and power profile for the experimental and model results.

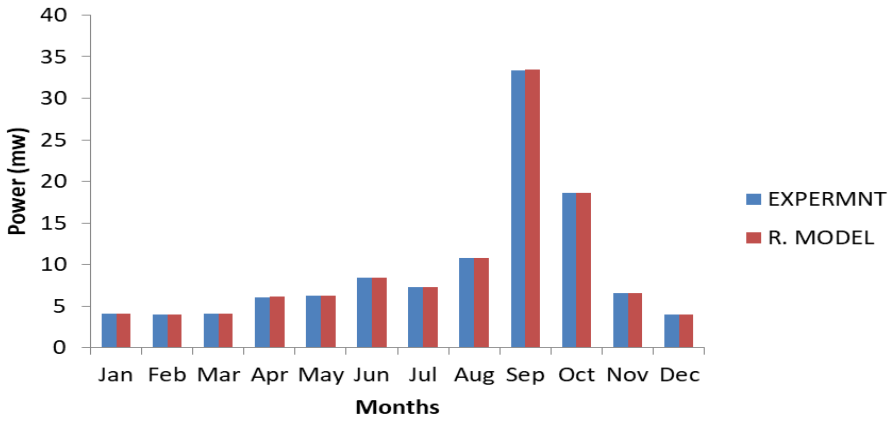

Figure 4.12: Column Plot of Experimental and Regression Model Results for River Orle

A very strong correlation value of 0.997 and significant value of 0.000 were obtained for the correlation analysis of experimental and model results for River Edion as indicated in Table 4.9. This gives justification to the accuracy and precision of the model equation in predicting the power output from the discharge in harmony with the experimental results.

Table 4.9: Correlation Analysis Output for Experimental versus Model Results for River Edion.

Correlations

		Experimental	Model
Experimental	Pearson Correlation	1	.997**
	Sig. (2-tailed)		.000
	Sum of Squares and Cross-products	94.163	94.069
	Covariance	8.560	8.552
	N	12	12
Model	Pearson Correlation	.997**	1
	Sig. (2-tailed)	.000	
	Sum of Squares and Cross-products	94.069	94.570
	Covariance	8.552	8.597
	N	12	12

**. Correlation is significant at the 0.01 level (2-tailed).

Figure 4.13 presents the column plot for the experimental and regression model prediction of power from corresponding discharge from January to December for River Edion. The plot indicates 99.7% accuracy, precision and harmony of the model in line with experimental data. The model could be sufficiently used to predict accurate power output data for River Edion from discharge values.

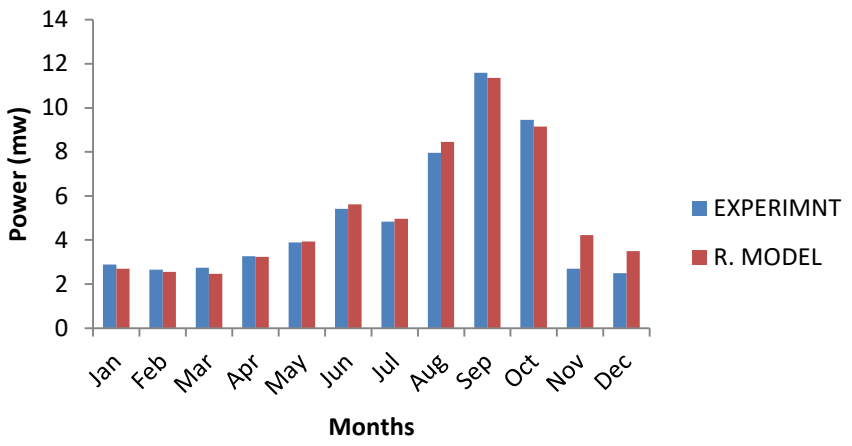

Figure 4.13: Column Plot of Experimental and Regression Model Results for River Edion

A very strong correlation value of 1 and significant value of 0.000 was obtained from the correlation analysis of the experimental and regression model for River Orbeh as indicated in Table 4.10. This represent 100 % accuracy, precision and harmony in predicting power from corresponding discharge.

Table 4.10: Correlation Analysis Output for Experimental versus Model Results for River Orbeh.

Correlations

		Experimental	Model
Experimental	Pearson Correlation	1	1.000**
	Sig. (2-tailed)		.000
	Sum of Squares and Cross-products	188.742	188.591
	Covariance	17.158	17.145
	N	12	12
Model	Pearson Correlation	1.000**	1
	Sig. (2-tailed)	.000	
	Sum of Squares and Cross-products	188.591	188.441
	Covariance	17.145	17.131
	N	12	12

**. Correlation is significant at the 0.01 level (2-tailed).

This close agreement and relationship between the experiment and model results is further indicated in Figure 4.14, which indicates the flow rate and corresponding power output.

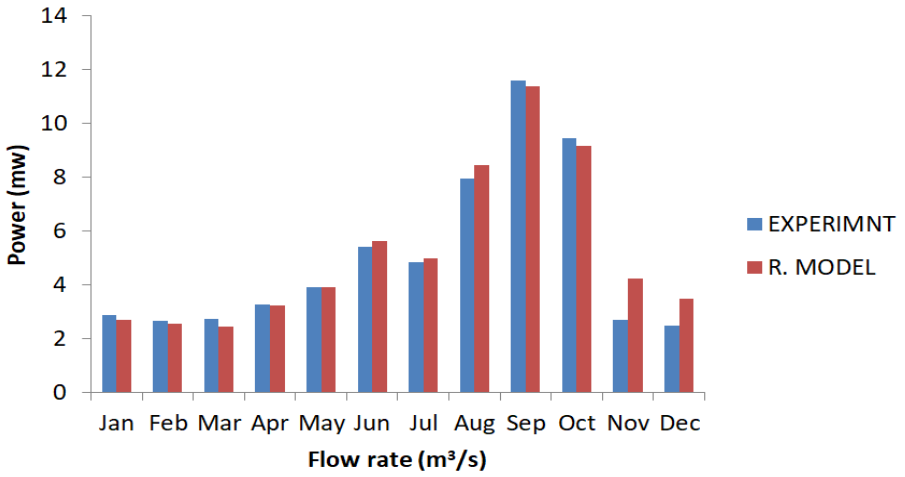

Figure 4.14: Column Plot of Experimental and Regression Model Results for River Orbeh

From the statistical analysis all the results for the three rivers have very strong positive relationship between power and discharge. R. Orle has the strongest relationship followed by R. Orbeh and R. Edion.

4.5 Uncertainty Study Analysis

Three types of floats were used in the measurement to be able to fully categorize the uncertainty characteristics. The aggregate combined and expanded uncertainty value for surface float are 4.962% and 9.923%, the double float are 5.0% and 10.00% and the subsurface float are 4.992 and 9.983% respectively as indicated in Figure 4.15. This indicates that under local flow condition, the accuracy of the measurement process with good stage set is about 95% for all the floats with insignificant variations between the floats. Thus, the measured value is about ±5 % of the true value of the measurement.

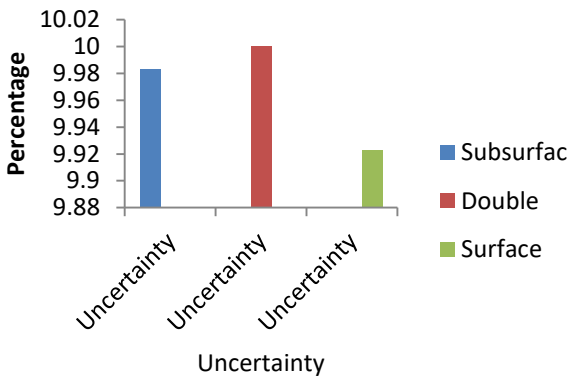

Figure 4.15: Comparison of Results of Expanded Uncertainty of the three Floats

Figure 4.16 presents the expanded uncertainty of the flow regime of the river measured in March, June, September and December 2018. It is indicated that the lowest uncertainty value occurred in the month of March while the highest occurred in September. The high September value is due to the high volumetric flow rate due to high run off from high intensity rainfall generating high flow in the river with some turbulence, materials in suspension and swirl.

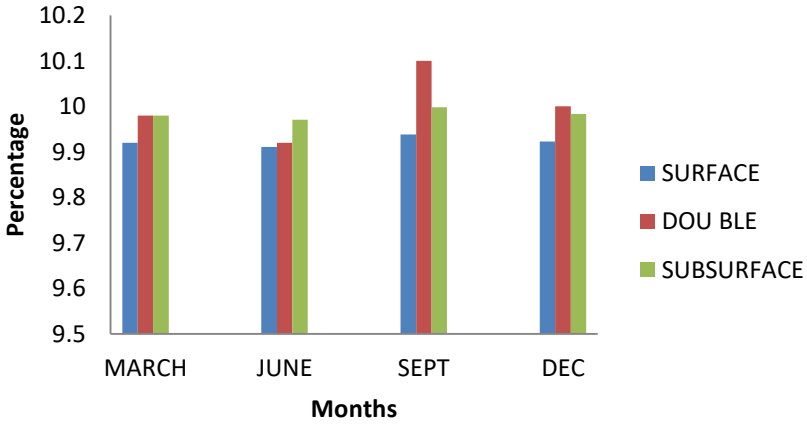

Figure 4.16: Uncertainty of the three floats according to the annual flow regime of river Orle

Figure 4.17, represents the plot of the average velocity in each segment across the channel. It indicates the proximity and close fit of the results for the average velocity

measurement with maximum fit between the surface and subsurface float while the profile of the plot is of the same pattern. This is also a pointer to the accuracy and precision of the measurement process.

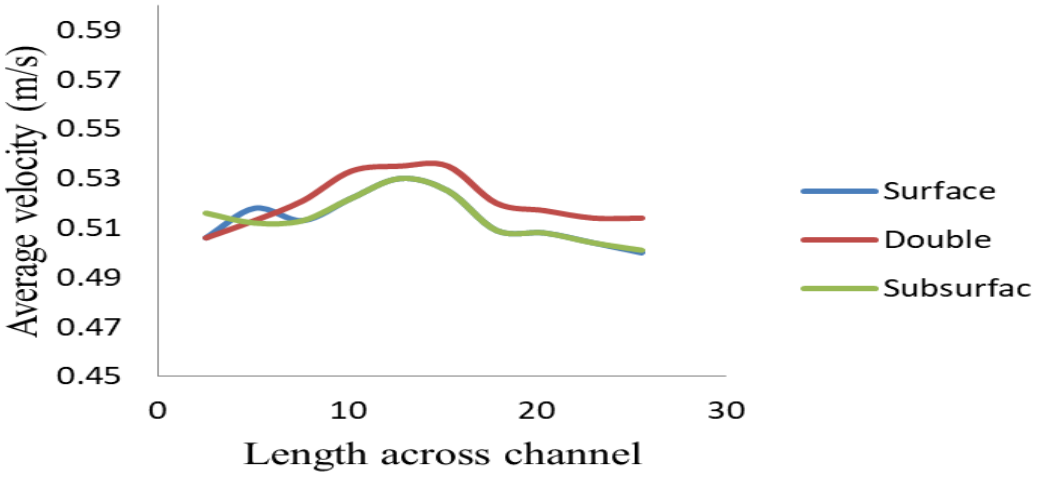

Figure 4.17: Average velocity profile for the three floats across the channel

Figure 4.18 compares the values of the of the average velocity of flow in segments across the channels for the three types of floats, there is complete harmony in the measured value for channel B, C and D, there is some variation of results in channel A and D in respect of the surface and subsurface floats. Measurement by the double float is stable across the channels indicating a higher level of precision.

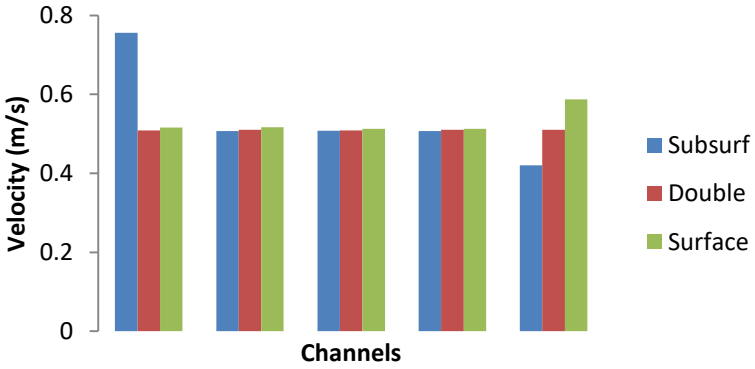

Figure 4.18: Comparison of results of average velocity in channels

Figure 4.19 represents a comparison between the flow rates of the three types of floats with complete harmony of results for the floats in channel A, B and C with variation of results in channel D and E with surface and subsurface floats. Highest precision of results was observed for the double float in all channels.

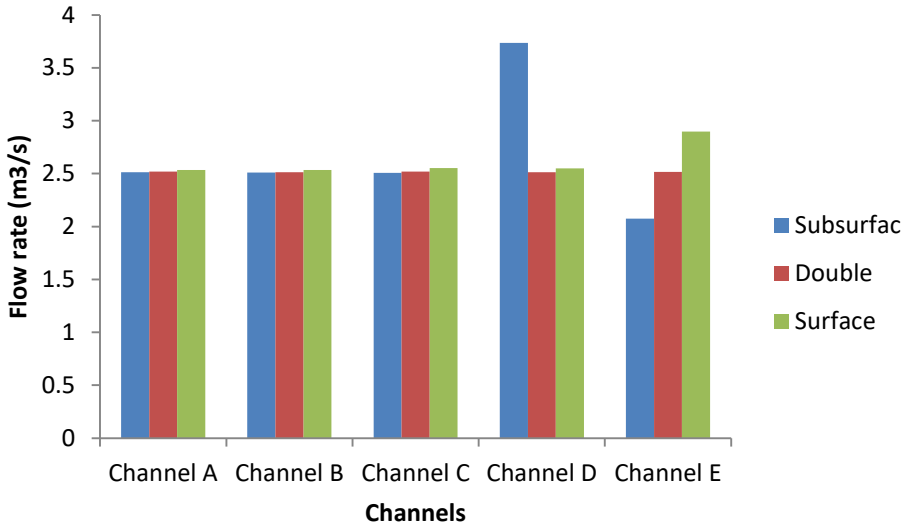

Figure 4.19: Comparison of results of flow rate in channels

The analysis of the velocity and flow data indicates that the double float has the highest level of accuracy and precision. For the double float there is only a variation of 1.57% in the average velocity and 0.28% in flow rate values of its measurement across all channels. The surface floats has a variation of 11.34% of average velocity and 12.59% in flow rate measurement of its measurement across all channels, while the subsurface float has a variation of 44.44% of average velocity and 32.74% of flow rate measurement of its measurement across the channels. Therefore, the double float is recommended for use in the flow characteristics measurement in rivers in Edo North except in flood situation or constrained by shallow depth.

4.5.1 Anova analysis of uncertainty results

Table 4.11 gives the analysis of variance results. It is indicated that all *p*-values are greater than 0.05 indicating that there exists no significant difference between the average velocity and flow rate across the three floats respectively. This further enhances the accuracies, precision and reliability of the results.

Table 4.11: Anova Output for Measured Parameters of the three Floats

	Sum of Squares	Mean Square	F	Sig.
Average velocity (m/s)			0.209	0.815
Between Groups	0.002	0.001		
Within Groups	0.068	0.006		
Total	0.071			
Flow rate (m^3/s)			0.212	0.812
Between Groups	0.059	0.029		
Within Groups	1.668	0.139		
Total	1.727			

Base on the establishment of the uncertainty associated with the flow characteristics measurement, the application of the uncertainty values to the results of the flow characteristic results is shown in Table 4.12.

Table 4.12: Real Values of Hydro Power Output from the Selected Rivers

S/N	Hydro project	Peak power output (MW)	Base power output (MW)	Low power output (MW)
1	Orle	18.000 ± 5%	12.000 ± 5%	5.000 ± 5%
2	Edion	9.000 ± 5%	6.000 ± 5%	3.000 ± 5%
3	Orbeh	11.000 ± 5%	7.000 ± 5%	3.000 ± 5%

4.6 Comparative Analysis of Results with Other Related Study

4.6.1 Comparison with the the work of Emeribe *et al.* (2016)

A comparison of the results of the present study and Emeribe *et al.* (2016) is shown in Figure 4.20. The Emeribe work studied the hydrological characteristics of River Orle between January to December of 2013 using the United Nation Industrial Development Organization (UNIDO) model.

In the present study, the total mean annual discharge for River Orle is 231.394 m^3/s with a mean monthly discharge of 19.282 m^3/s. The total mean annual flow rate for Emeribe's work is 352.330 m^3/s with a mean monthly discharge of 29.360 m^3/s. The maximum mean monthly discharge of 68.035 m^3/s of the present study occurred in September while the minimum mean monthly discharge of 8.067 m^3/s occurred in March. The maximum monthly discharge of Emeribe's work is 102.10 m^3/s in the month of August while the lowest monthly discharge is 2.13 m^3/s in the month of March.

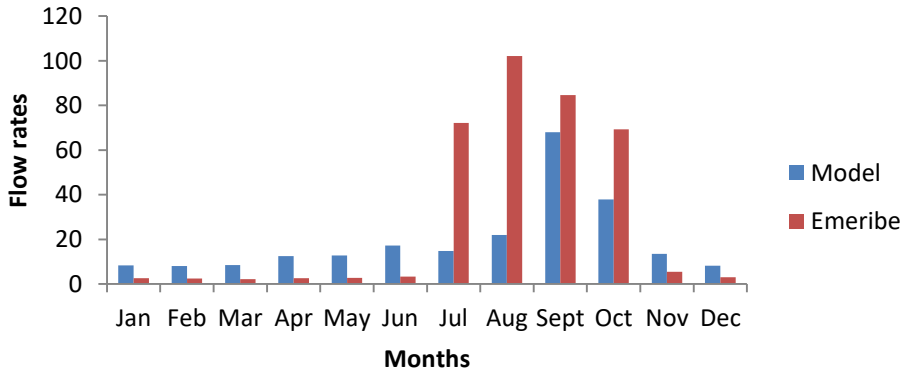

Figure 4.20: Comparison of the Discharge of River Orleh

The Emeribe's work recorded an excess of 34.32 % of total annual discharge over the present study, the excess discharge were recorded between July to October of 2013. The present study recorded higher and more consistent discharge over Emeribe's work between November to June.

The Emeribe's work recorded the highest monthly discharge of 102.100 m^3/s in August. This rainfall pattern that will produce the highest August discharge in any year is very rare in Edo North as the region is used to maximum rainfall in mostly in September with spill over to October (Emeribe *et al.* (2016).

Figure: 4.21 indicates that the total mean annual power output for the present study is 108.207 MW for a net head of 50 m. The maximum mean monthly power output is 33.374 MW which occurred in September, the minimum mean power output is 3.957 MW which occurred in February.

The total annual power output for Emeribe's work for 2013 is 9.189 MW with the highest power output for August of 3.296 MW and minimum power output in the month of March of 0.04 MW for ROR hydro power scheme. This indicates the effectiveness of the study approach of the present study in harnessing an excess of 99.018 MW using a small dam over Emeribe's study of ROR.

The overall differences in the results are due to the difference in rainfall pattern for the different years and the hydro power scheme used. The head of 50 against a Run-Off-River scheme. Emeribe's work relied on one year measurement data of 2013 for its analysis, while the present study utilized average value of result for two years of 2018 and 2019 respectively.

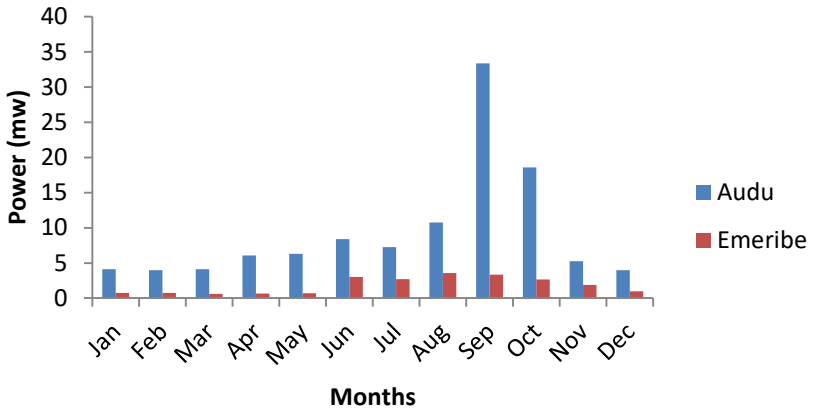

Figure 4.21: Comparison of the Hydro Power Potentials of River Orleh Between Two Studies

4.6.2 Benin – Owena River Basin Study of River Owan

Figure 4.22 Shows the Benin - Owena River Basin Development Authority discharge results for 1999 of River Owan close to River Edion in Owan East Local Area. River Owan is about 10 km from river Edion. The total annual discharge for the river is 99.86 m^3/s with a maximum discharge of 22.53 m^3/s in October and a minimum discharge of 3.18 m^3/s in March. The mean discharge is 8.322 m^3/s. In the present study, the total annual discharge for Edion is 122.654 m^3/s. The maximum discharge is 21.549 m^3/s which occurred in September and minimum discharge 5.253 m^3/s which occurred in the month of March. The mean discharge for Edion is 10.221 m^3/s. The results indicate the same pattern of flow in attaining maximum and minimum discharge in line with the rainfall pattern and volume for the years. The mean discharge of the two rivers is almost the same in spite of the difference in years, the minimum discharge occurred in the same month of March. The difference in total annual discharge is due to the different volume of rainfall for the different years. The discharge profile is in the same pattern which authenticates the accuracy of the present study.

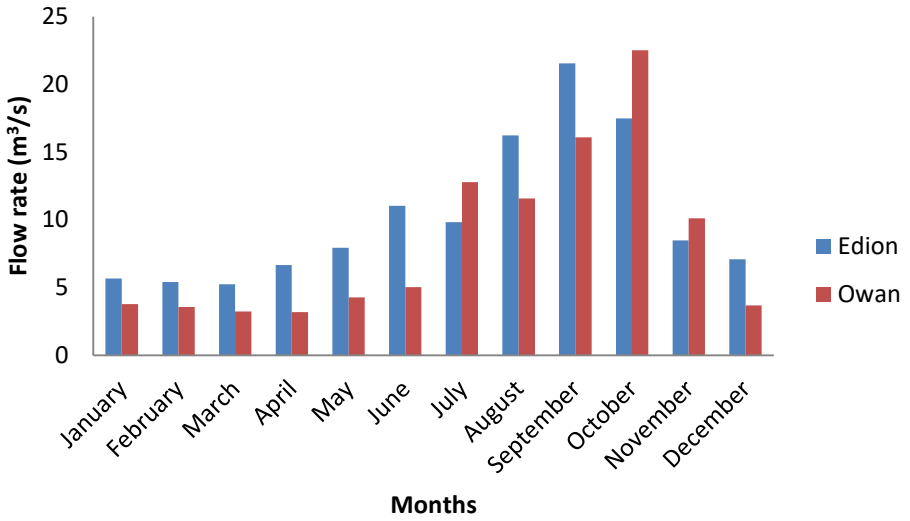

Figure 4.22: Comparison of the Discharge of River Owan and River Edion

4.7 Data Extension Process Analysis

4.7.1 Rainfall Data Analysis

For the R. Orle and Edion catchment area, the annual average CNRM rainfall data range is between 1157 mm – 1574 mm and with mean value of 1310.4 mm. The annual historical rainfall range for the Edo North is reported to be within 1000 – 1200 mm with mean values of 1,100 mm (Emeribe *et al*., 2016).The CNRM rainfall data agreement with the documented rainfall data for Edo North is 83.94% which is a strong agreement.

Further analysis of the data indicates that there is agreement in the data with rainfall pattern of months of April to October and with the two rainfall peaks of June and September annually for the historical, predictive and study period rainfall data. This is in line with research reviews on rainfall pattern in the study areas (Emeribe *et al*., 2016).

Figures 4.23 indicates that both the historical and predictive rainfall data maintains the same rainfall pattern, magnitude and range over the years.

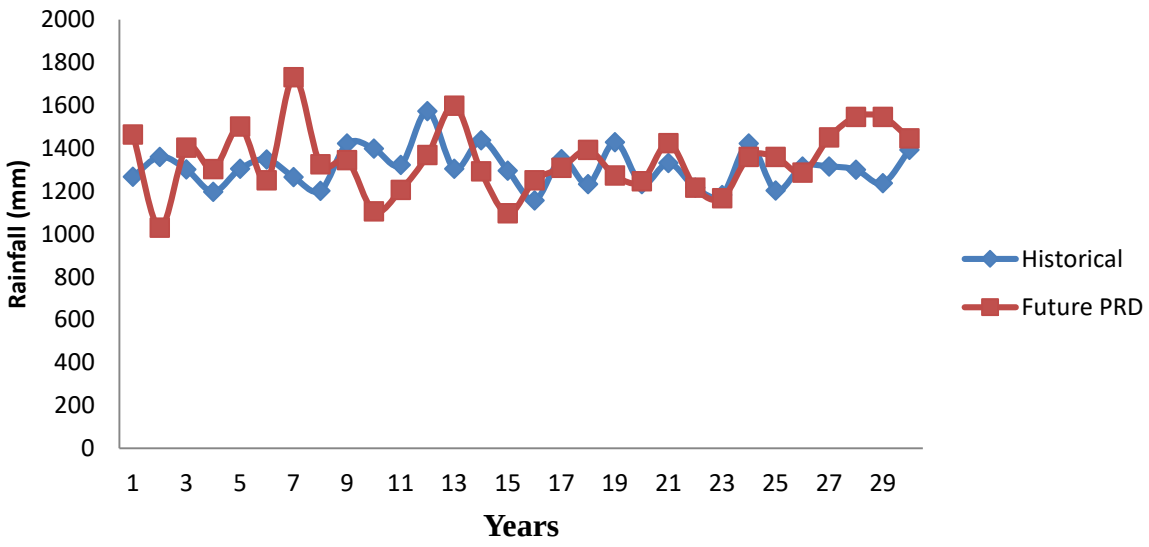

Figure 4.23: Historical and Predictive 30 Years Rainfall data Comparison for Orle and Edion Catchment Area

The minimum annual historical rainfall is 1157 mm while the maximum is 1574 mm.The maximum predictive rainfall value is 1732 mm while the minimum is 1029 mm. This indicates the rainfall pattern and magnitude is maintained from the historical to the future as indicated in Figure 4.23.

The same relationship exists for the historical and predictive rainfall data for the Orbe catchment area as indicated in the Figure 4.24. This further confirmed that there is no significant variation in the magnitude and pattern of rainfall from the historical to the future.

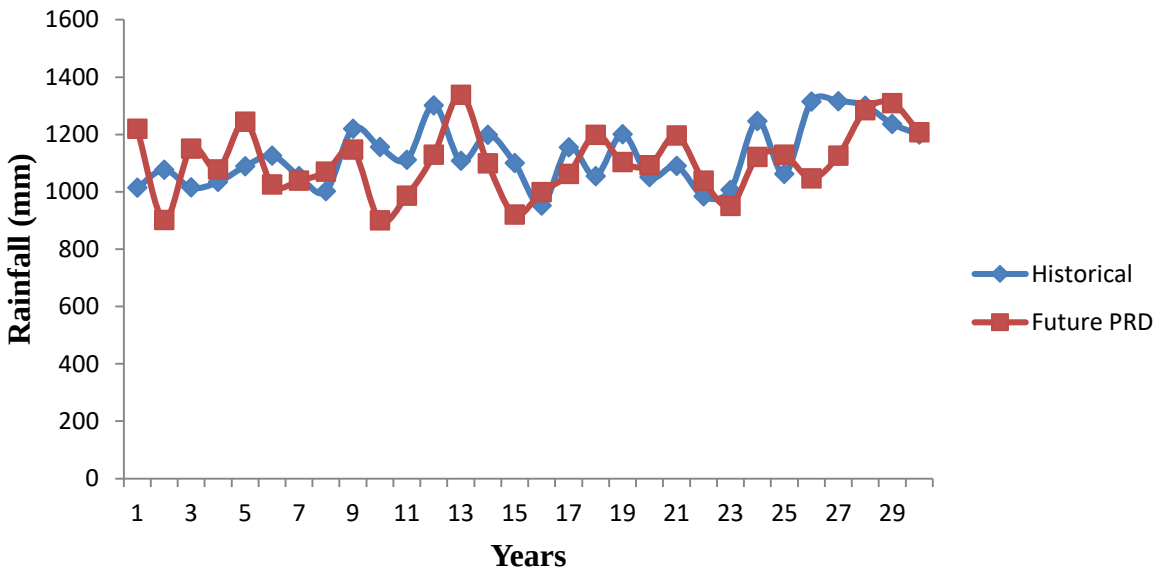

Figure 4.24: Historical and Predictive 30 Years Rainfall data Comparison for Orbe Catchment Area

4.7.2 T- Text Analysis

In order to statistically determine the similarity of the rainfall pattern and trend between the historical and predictive rainfall data, a 2 sample T-text analysis was conducted, The output from the T-text is shown in the Table 4.13.

Table 4.13: T – Test Analysis Output for Historical and Predictive Rainfall data for Orle and Edion Catchment Area.

	N	Mean	Se mean
Historical	18	1318.7	23
Future	18	1332	41
P - value			0.783

From Table 4.12, the p = 0.783 and is higher than 0.05, this indicate there is no significant difference between the predictive and historical discharge rainfall data. This established that the rainfall distribution and magnitude both for the historical and

predictive period will be the same with the implication that the rivers discharge over the two period which maintain the same profile.

4.7.3 Regression model output

i. **River Orle Rainfall – Discharge Regression Output**

The R. Orle Rainfall – Discharge output is shown in Figure 4.25. It indicates a good fit with the data point clustering very close to the regression fitted line plot. This indicate low values of residuals which equally indicate the agreement between the models and experimental results.

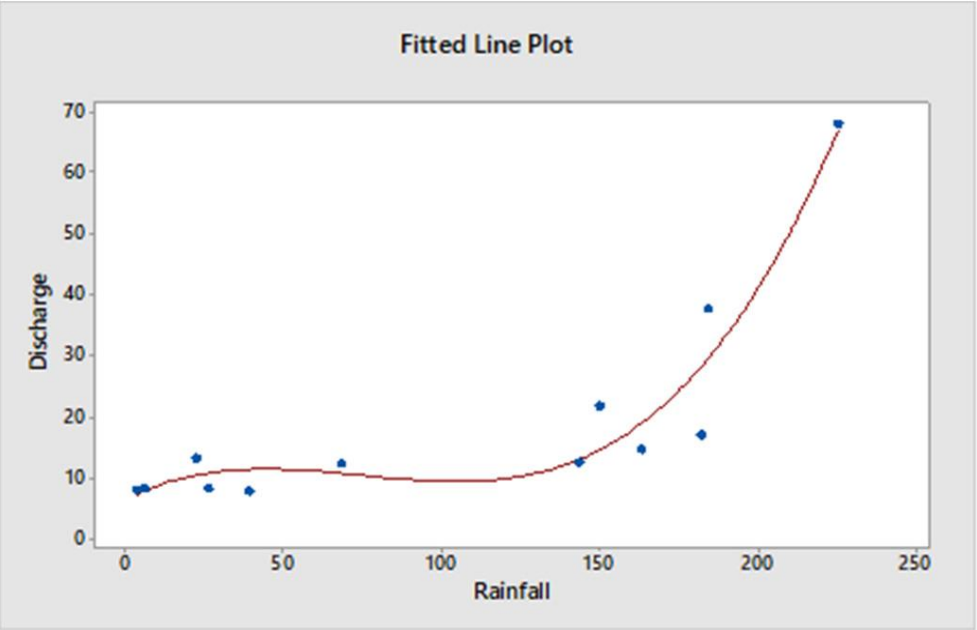

Figure 4.25: Fitted Rainfall – Discharge Line Plot for River Orle

The generated regression model equations for the rainfall – Discharge modeling is given in Equation 4.4.

$$D = 6.5870 + 0.2614F - 0.0042F^2 + 0.000019F^3 \quad (4.4)$$

Where,

D is Discharge (m^3/s)

F is rainfall (mm)

iv. River Edion Rainfall – Discharge regression output

The R. Edion Rainfall – Discharge output is shown in Figure 4.26, which indicates a good fit with the data point clustering very close to the regression fitted line plot. The low values of residuals indicates the agreement between the models and experimental results.

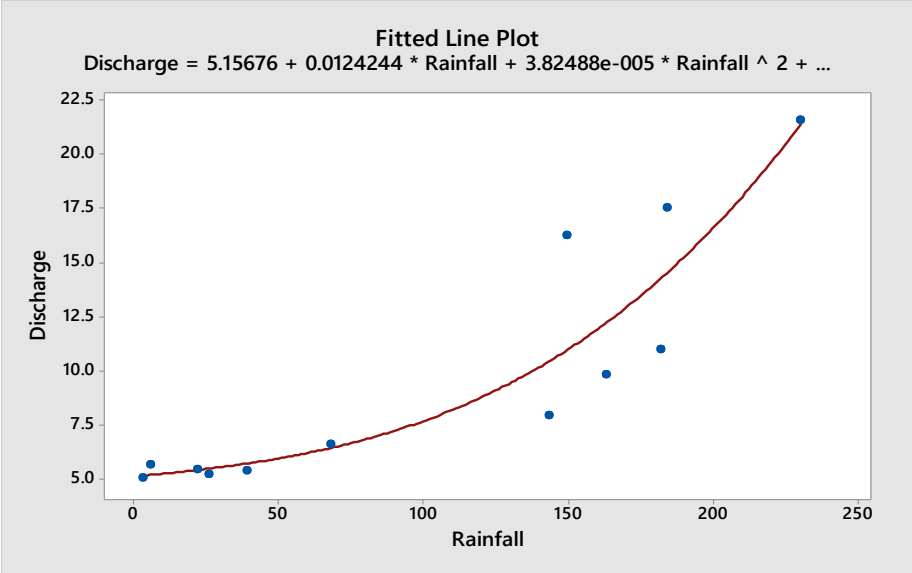

Figure 4.26: Fitted Rainfall – Discharge Line Plot for River Edion

The generated regression model equations for the rainfall – Discharge modeling is given in Equation 4.5.

$$D = 5.157 + 0.0124F - 0.3824F^2 + 0.00000125F^3 \quad (4.5)$$

v. River Orbe Rainfall –Discharge regression output

The R. Orbe Rainfall – Discharge output is shown in Figure 4.27, which indicates a good fit with the data point clustering very close to the regression fitted line plot. The

low values of residuals indicates the agreement between the models and experimental results.

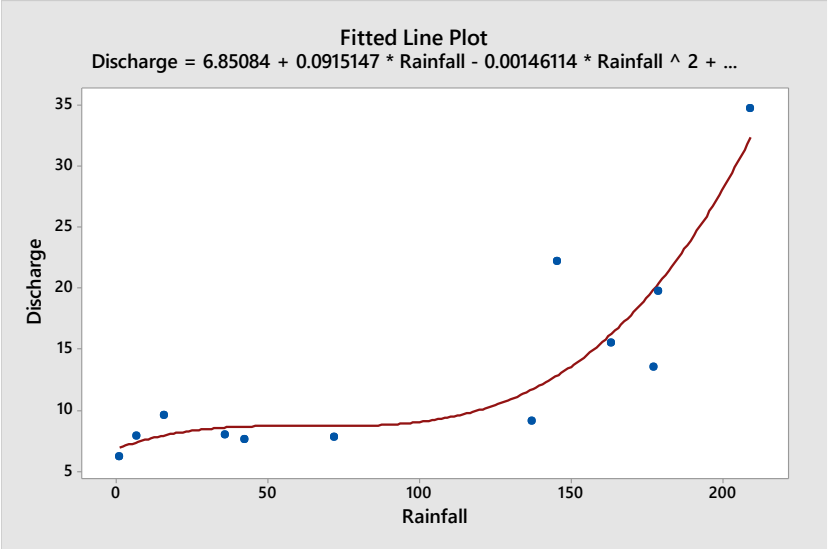

Figure 4.27: Regression Output of Discharge versus Rainfall for River Orbe

The generated regression model equations for the rainfall – Discharge modeling is given in Equation 4.6.

$$D = 6.851 + 0.0915F - 0.0015F^2 + 0.00000767F^2 \quad (4.6)$$

4.8 Model Validation Analysis

Figures: 4.28 – 4.30, represent the plot of the observed experimental results and the regression model output for the three rivers. The experimental results were used to validate the model output in line with the established practice of Chatenet *et al*. (2016).

There is agreement in the peak discharge period of September and the low discharge period from December to March annually for the three rivers.

4.8.1 River Orle Output

From the nonlinear regression analysis output of R. Orle indicated in Figure 4.28, the mean annual discharge for the experimental and model results are 19.282 m^3/s and 19.937 m^3/s respectively, while the total average discharges are 231.393 m^3/s and 239.252 m^3/s respectively. This indicates a model discharge predictive accuracy of 96.71 % compare to the experimental results.

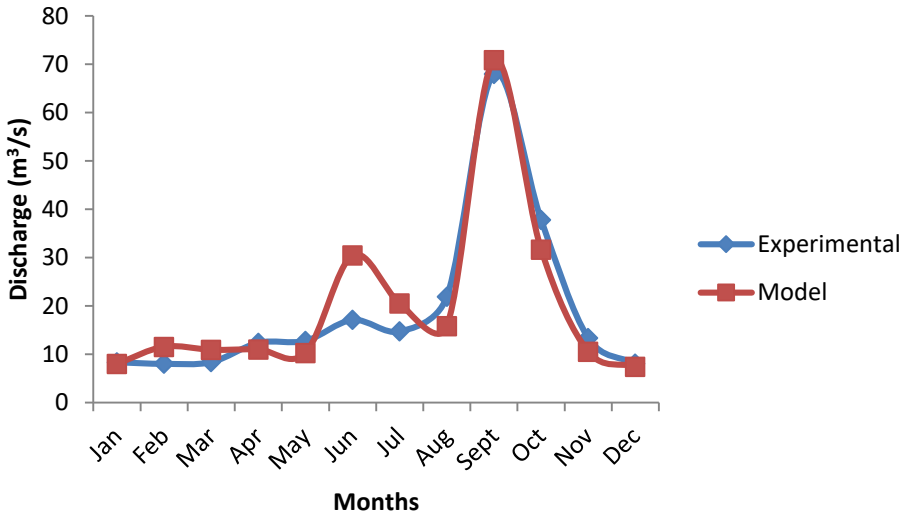

Figure 4.28; Profile of Experimental and Model Plot for River Orle

There is good harmony between the model and experimental plot. Some minor disparity existed from May to June. However, since it is an isolated position. The model accuracy and precision is upheld.

4.8.2 River Edion Output

Figure 4.29 indicate the variation in the model and experimental output for R. Edion. The total annual discharge for experiment and model output are 117.654 m^3/s and 104.84 m^3/s while the average outputs are 9.0845 MW and 8.737 MW respectively, representing a model accuracy of 89.12 %.

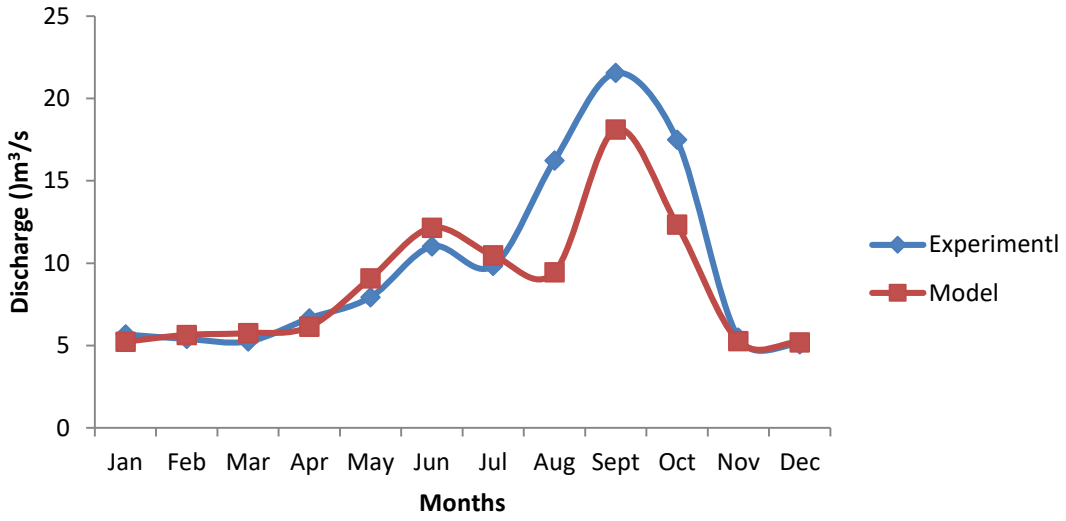

Figure 4.29: Variation of Experimental and Model Output for River Edion

Figure 4.29 indicate a high degree of harmony between experiment and model results throughout the annual profile of R. Edion discharge. The model predicted a slightly lower value of discharge between August, September and October. The disparity is minimal as indicated in Figure 4.29, which upheld the model accuracy and integrity.

4.8.3 River Orbe output

Figure 4.30 shows the variation of experimental and model regression analysis output for R. Orbe. It indicates that the total annual output for the experimental to model output are 161.933m3/s and 154.639 respectively, representing a model accuracy of 95.47 percentage. There is very good discharge agreement between January to June and minor deviations between June to August and September to November as indicated in Figure 4.30. The total average deviation is 4.51 % which is insignificant. The model accuracy and integrity is thus upheld.

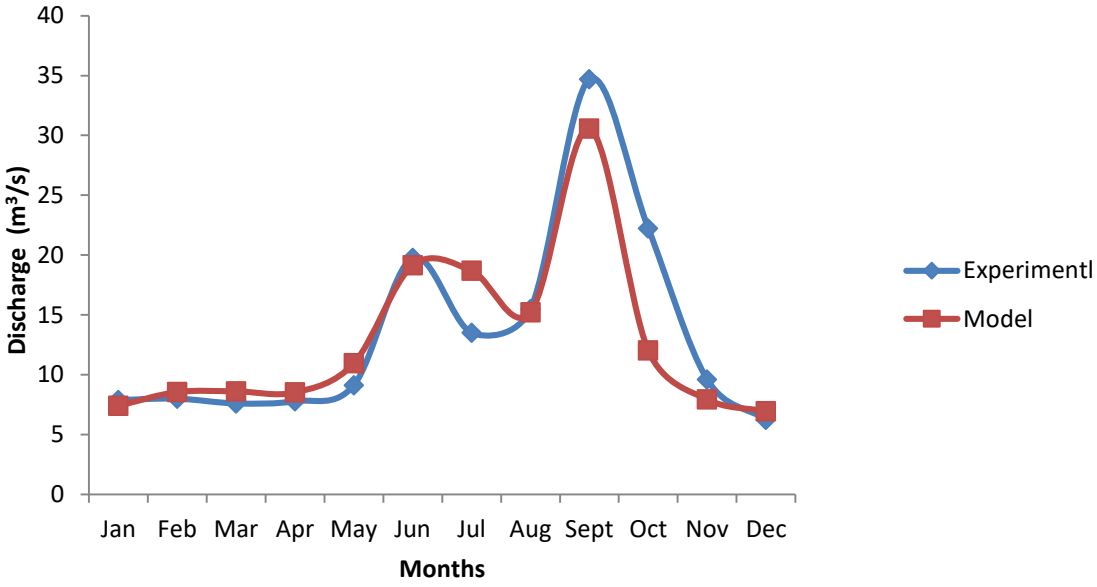

Figure 4.30: Variation of Experimental and Model Output for River Orbe

The high level model agreement and performance in comparison with experiment results justified model integrity to produce accurate discharge results from the catchment area rainfall data for the rivers when the annual average monthly historical discharge values of the rivers are known.

4.9 Experimental, Historical and Predictive Discharge Analysis

Figures 4.31 – 4.33, represent the plot of experimental, historical and predictive discharge of the rivers. The summary of the analysis of results is shown in Table 4.14.

Table 4.14: Summary of Experimental, Historical and Predictive Discharge of three Rivers

	Experimental Discharge		Historical Discharge		Predictive Discharge	
Orle	Average	Sum	Average	Sum	Average	Sum
	19.283	231.394	18.997	227.965	21.042	252.505
Edion	Average	Sum	Average	Sum	Average	Sum
	9.805	117.84	9.045	105.55	9.27	109.526
Orbe	Average	Sum	Average	Sum	Average	Sum
	12.866	154.639	11.940	134.335	10.835	130.022

Figure 4.31 indicates the variation of Experimental, Historical and Predictive Plots for R. Orle. The plots indicate a high level of agreement in the months and period of high discharge and low discharge for the river. The plots also have the same discharge profile with slightly higher harmony between the historical and predictive discharge .This observation is due to the longer period of 30 years covered by these discharge compare to two years of the experimental discharge. It indicates that the average rainfall for the period of study of two years is slightly higher in the period of September to November compared to the historical and predictive periods of 30 years each.

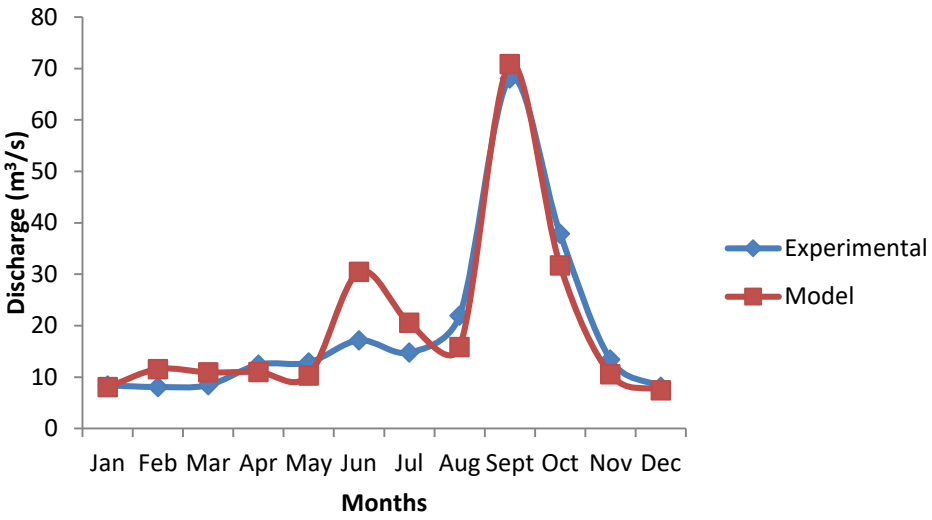

Figure 4.31: Profile of Experimental, Historical and Predictive Plots for River Orle

Figure 4.32 indicates the relation between the Experimental, Historical and Predictive Plots for R. Edion. The proximity in the discharge profiles indicates that the average monthly annual discharge of the river falls within the same range which is in agreement with the rainfall analysis for the catchment areas both for the historical and predictive discharge which demonstrates the accuracy and precision of the models. A stronger agreement exists between the historical and predictive data plots. The experimental discharge values are slightly lower from February to July and higher from July to November. This is due to the volume of rainfall in the years of coverage. The pattern of the three data plots is in strong agreement.

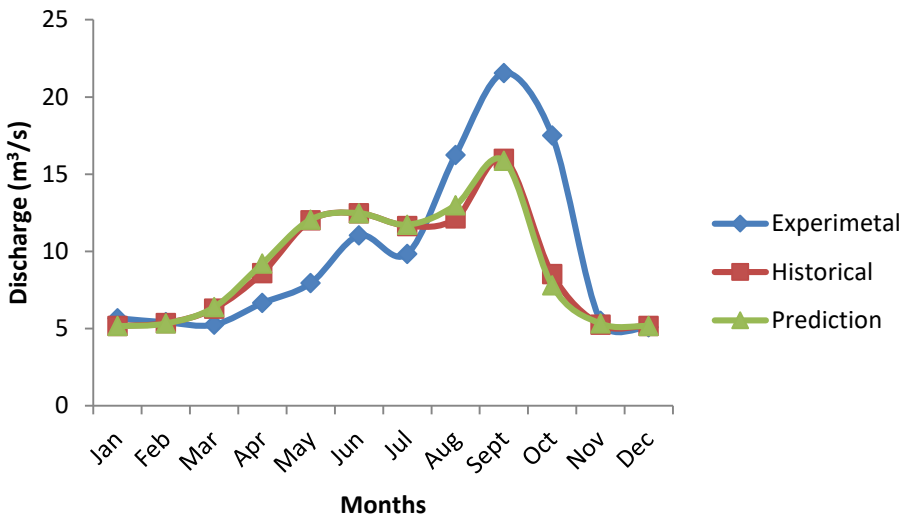

Figure 4.32: Profile of Experimental, Historical and Predictive Plots for River Edion

Figure 4.33 indicates the monthly output of the Experimental, Historical and Predictive Plots for R. Orbe. The harmony was maintained as in the case of R. Orle and Edion. The pattern and peak of discharge are the same from January to December.

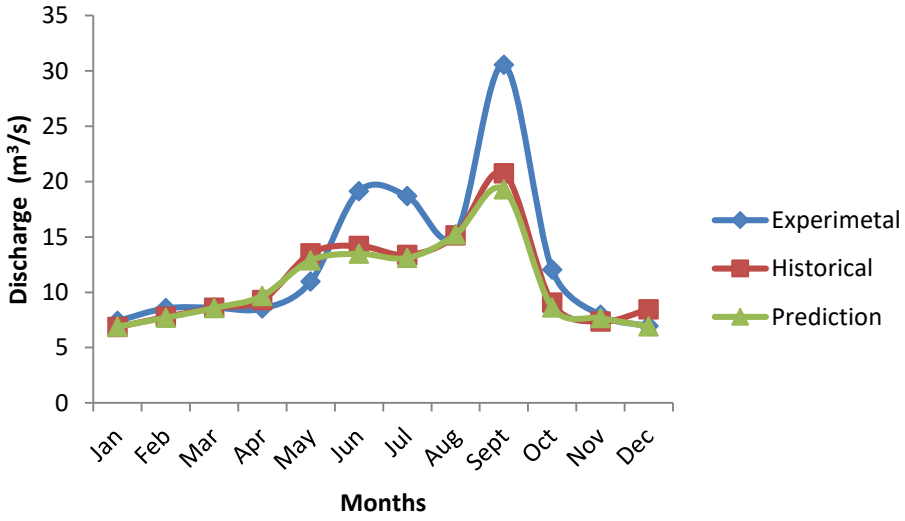

Figure 4.33: Profile of Experimental, Historical and Predictive Plots for River Orbe

Table 4.15 indicate that the agreement between the average experimental and historical discharge is 98.517%, while that of the experimental to the predictive discharge is 91.640% for River Orle.

Table 4.15: Summary of the Discharge Characteristics of the Rivers

	Experimental Discharge (m^3/s)		Historical Discharge (m^3/s)		Predictive Discharge (m^3/s)	
Orle	Average	Sum	Average	Sum	Average	Sum
	19.283	231.394	18.997	227.965	21.042	252.505
Edion	Average	Sum	Average	Sum	Average	Sum
	9.805	117.84	9.045	105.55	9.27	109.526
Orbe	Average	Sum	Average	Sum	Average	Sum
	12.866	154.639	11.940	134.335	10.835	130.022

For River Edion, the harmony between the experimental average and historical discharge is 92.24% percentage, while that of the experimental to the predictive discharge is 93.085.%, while for River Orbe the harmony between the experimental average and historical discharge is 87%, that of the experimental to the predictive discharge is 84.214% %. These strong correlations established the accuracy of the data extension empirical – runoff model. The correlation are strong as indicated in Table 4.14.

4.10 Historical and Predictive Discharge Analysis

In other to get the full historical and future discharge range of the rivers the maximum monthly and the minimum monthly discharge in each year were determined for the historical and predictive discharge. The maximum monthly discharge for a month is the maximum discharge obtainable in that particular month in 30 years period while the

minimum discharge is the lowest discharge obtained in the month for the 30 years period.

Table 4.16 shows a summary of the discharge characteristics of the rivers. It indicates that the magnitude of the historical and predictive discharges have close proximity for all categories of classification of the flows rate measurement. The maximum disparity in the figures is always less than 5 units of the flow measurement.

Table 4.16: Summary of the Profile of Historical and Predictive Discharge

	Mean Max Monthly Flow (m^3/s)		Total Average annual flow (m^3/s)		Average annual flow (m^3/s)		Mean annual minimum flow (m^3/s)	
	Historical	Predictive	Historical	Predictive	Historical	Predictive	Historical	Predictive
Orle	42.401	45.496	227.965	252.505	18.997	21.042	10.907	10.273
Edion	14.186	14.346	108.555	109.526	9.045	9.127	5.895	5.770
Orbe	17.098	18.685	134.345	130.022	10.738	10.835	8.296	8.835

Table 4.17 shows the relationship between the historical and predictive discharge from the rivers. It indicates a very strong positive correlation between the discharges. This established the fact that the magnitude and profile of the historical and predictive discharge are closely related.

Table 4.17: Comparative Historical and Predictive Discharge Analysis

		Mean Max Monthly Flow (%)	Total Average annual flow (%)	Average annual flow (%)	Mean annual minimum flow (%)
Orle		Historical	Historical	Historical	Historical
	Predictive	93.197%	90.281%	90.281%	106.171%
Edion	Predictive	98.885%	99.113%	99.102%	102.166%
Orbe	Predictive	91.506%	99.101%	99.104%	93.899%

Figure 4.34 represent the historical and predictive average, minimum and maximum discharge of the River Orle. An assessment of the plot indicates that they have the same profile and pattern. For the historical, the minimum recorded historical flow is 6.587 m^3/s between November to February while the peak historical flow is 126.210 m^3/s which occurred in the month of September, 1994. The peak of the maximum, average and the minimum flow all occurred in the month of September. The mean maximum, average and minimum discharge are 47.402 m^3/s, 18.997 m^3/s and 10.907 m^3/s respectively.

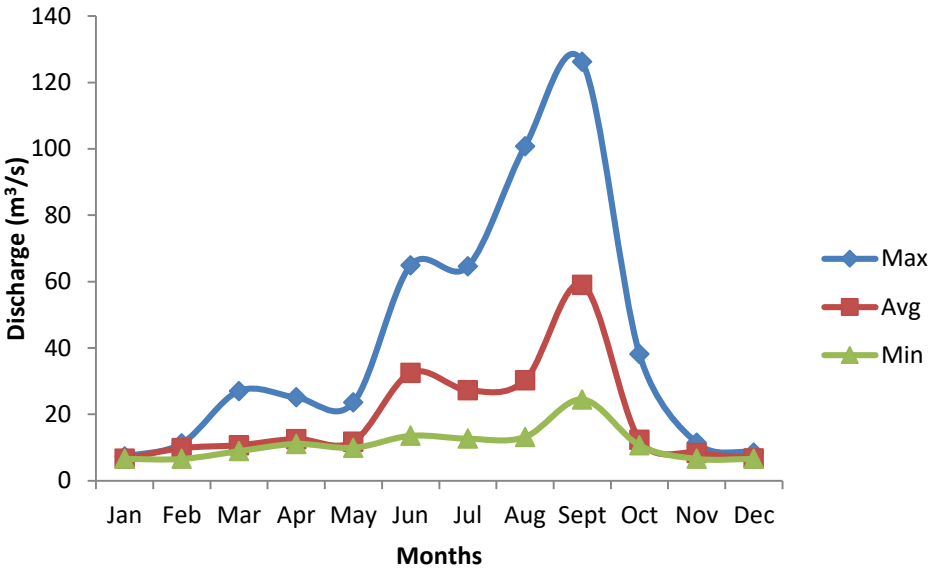

Figure 4.34: Average, Minimum and Maximum Historical Discharge for River Orle

Figure 4.35 depicts the average, minimum and maximum predictive discharge for River Orle. In the predictive R. Orle discharge, the profile and pattern of historical discharge was replicated with higher harmony between the average and maximum flow. The low discharge period extend from January to August with a peak in September for the minimum predictive flow. The mean maximum, average and minimum discharge are 45.946 m^3/s, 21.042 m^3/s and 10.273 m^3/s respectively. This is consonance with the observation of Emeribe *et al.* (2016).

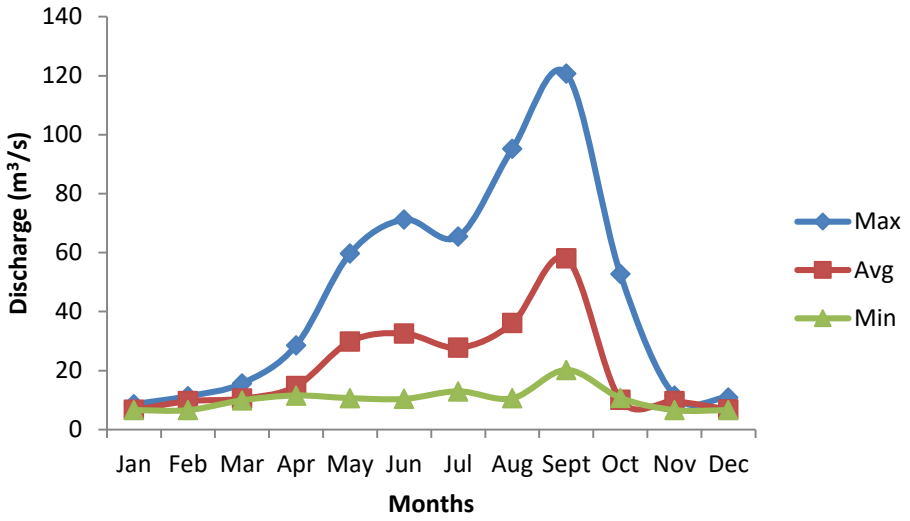

Figure 4.35: Average, Minimum and Maximum Predictive Discharge for River Orle

The River Edion maximum, average and minimum monthly historical discharges are indicated in Figure 4.36.

The minimum historical flow is 5.157 m^3/s and the maximum discharge of 23.272 m^3/s occurred in September 1994. All peak flow occurred in September and minimum discharge period occurred between November to March. This represent period of scarce rainfall. The mean maximum, average and minimum discharge are 14.186 m^3/s, 9.046 m^3/s and 5.896 m^3/s respectively. There is higher harmony between the average and minimum discharge profile. The maximum discharge plot indicates a very high discharge between May and June in the past. The indication is that there could be occasional high monthly discharge in this period, the level and magnitude as indicated in the plot. The knowledge of this high discharge gives insight to flood control and management.

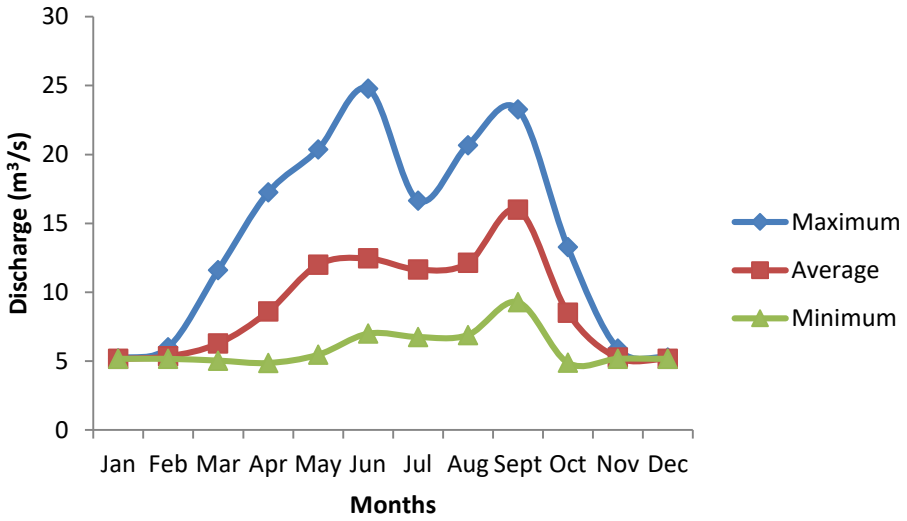

Figure 4.36: Average, Minimum and Maximum Historical Discharge for River Edion

Figure 4.37 indicates the average, minimum and maximum predictive discharge of R. Edion

The predictive discharge of Edion has similar characteristics with the historical discharges with heavy discharge between March and June. The maximum discharge 22.733 m^3/s in 30 years occurred in September and the minimum discharge 5.157 m^3/s spanned from December to August. The mean maximum, average and minimum monthly discharge are 14.346 m^3/s, 9.127 m^3/s and 5.770 m^3/s.

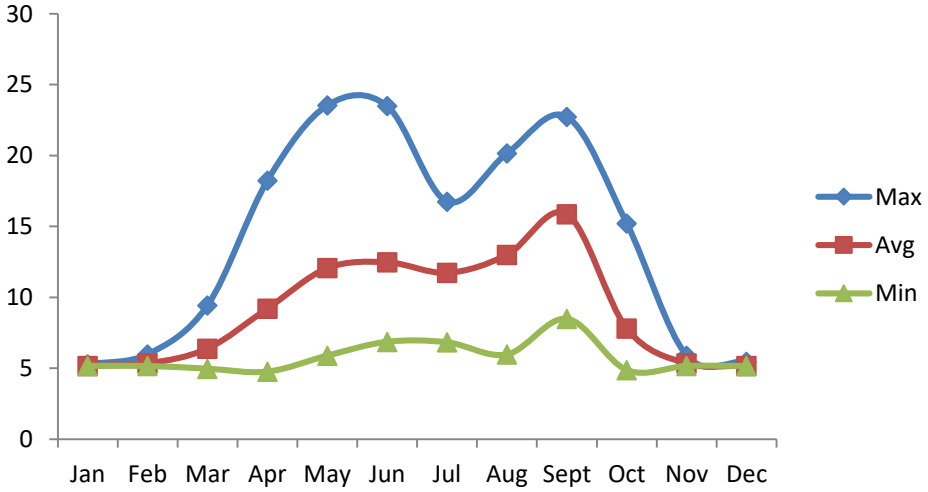

Figure 4.37: Average, Minimum and Maximum Predictive Discharge for River Edion

Figure 4.38 represents the average, minimum and maximum historical discharge for R.Orbe

The maximum Orbe discharge 33.479 m^3/s occurred in September 2008, while the minimum discharge is 6.851 m^3/s occurred usually between November to February. The mean annual maximum, average and minimum discharges are 17.098 m^3/s, 11.195 m^3/s and 8.286 m^3/s respectively.

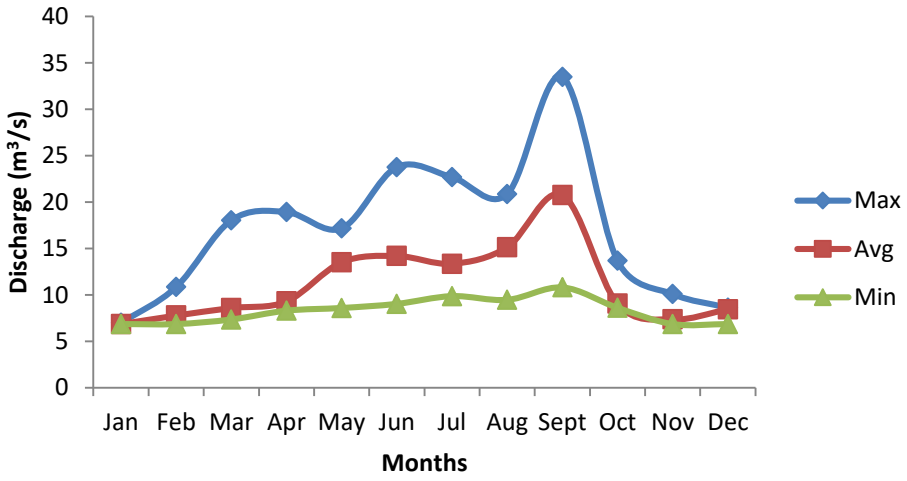

Figure 4.38: Average, Minimum and Maximum Historical Discharge for River Orbe

Figure 4.39 indicate the average, minimum and maximum predictive discharge for River Orbe. In the Orbe predictive, the maximum discharge of 32.009 m^3/s occurred in September and the minimum discharge of 6.851 m^3/s spanned from November to February. The mean annual maximum, average and minimum predictive discharge is 18.685 m^3/s, 10.835 m^3/s and 8.835 m^3/s respectively.

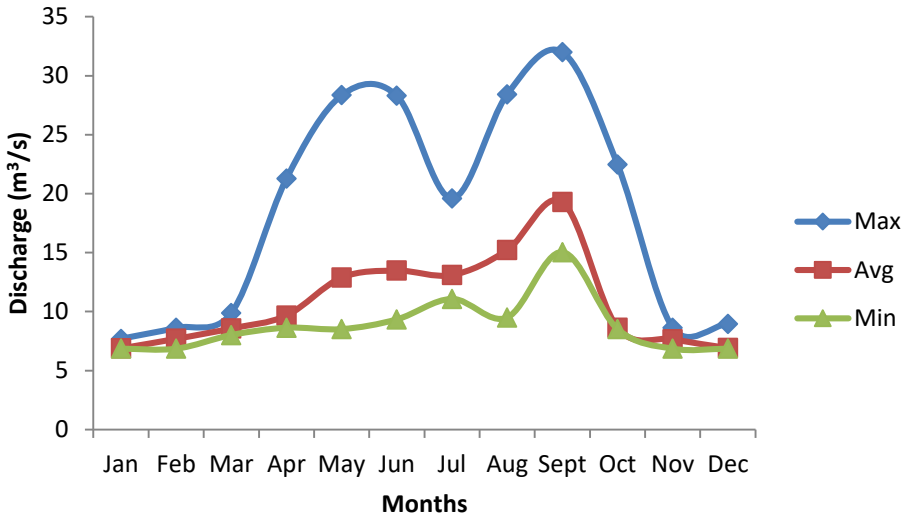

Figure 4.39: Average, Minimum and Maximum Predictive Discharge for River Orbe

The maximum, average and minimum discharge gives insight into the discharge profile of the rivers over the years. The average is fundamental to actual power generation output from the river channels.

The maximum discharge is instrumental to flood control and management. The predictive monthly maximum discharge enables the prediction of eventual excess flooding of the river channels and enables appropriate containment measures to be put in place, The minimum average monthly indicates the minimum eventual discharge that can occur in any month in a year and also give insight into the water management process.

4.11 Summary of Historical and Predictive Discharge Analysis

The study indicates that the predictive and the historical discharges have nearly the same magnitude in line with the rainfall pattern and profile. There is no significant variation in the discharge of the three rivers from the historical to the future. Further analysis indicate that the discharge stability have been maintained by the rivers over the

years. Thus, there is a good prospect for the power generation characteristics of the three rivers as the power output will be stable with time.

4.12 Statistical Analysis of the Strength and Direction of the Relationship between Model Input and Output Data

A correlation coefficient was determined between the observed experimental discharge and the model discharge output using the same rainfall data. The result of the correlation analysis is shown in Table 4.18.

Table 4.18: Summary of Coefficient Analysis

	Discharge: Experimental output vs Model output		Discharge: Model output vs Extension output		Rainfall data: Model input vs Extension input	
	r	*p*	r	*p*	r	*p*
Orle	0.954	0.000	0.840	0.001	0.878	0.000
Edion	0.909	0.000	0.855	0.000	0.878	0.000
Orbe	0.900	0.000	0.919	0.000	0.945	0.000

The correlation coefficient between the observed experimental discharge and model output discharge for R. Orle is 0.954, Edion is 0.909 and Orbe is 0.900. All the *p* values are 0.000. Theses represents a very strong correlation which indicate a close relationship in the direction and strength of the experimental and model discharges. The *p* values also indicate the model and experimental discharge are not significantly different in

their statistical relationship. These analyses established the accuracy and reliability of the model output.

The model accuracy and reliability was further highlighted by the use of Pearson Correlation analysis to establish the strength and direction of relationship between the rainfall data input to the model validation process and long term data extension process, and the discharge output from the model validation process and data extension process respectively.

For R. Orle the correlation coefficient between the rainfall data to the model in the validation process and the data extension process is 0.878, while the correlation coefficient between the model discharge output and data extension output process is 0.840. This represent the model accuracy of 95.67%

For River Orle the model correlation coefficient between the model rainfall data input for the validation process and rainfall data to the data extension study is 0.878, while the correlation coefficient between the model discharge output (validation) and average discharge data (extension process) is 0.840. For River Edion is 0.878 and 0.855, while Orbe is 0.945 and 0.919 for the same processes.

The results indicates the model maintain same relation and trend in the input data and the output results. For River Orle, the degree of sustenance is 95.67%, while Edion and Orbe are 97.38% and 97.24% respectively. This further enhanced and supports the models accuracy and reliability.

4.13 Hydrographs and Flow Duration Curves

4.13.1 Hydrographs

Figure 4.40 – 4.455, indicate the historical and predictive hydrograph of the three rivers that indicates the variation in the mean monthly flow rates of the rivers. The hydrograph

is used in the planning of the design of the power projects. From the hydrograph of the rivers maximum power yield from the projects is obtained in the month of September in the year. Figure 4.40 – 4.45, also indicate that the power generation profile increases from May through June and peaks in September and then decreases to December. The low power generation region spans from November to April annually. The design of the capacity of the dams of the hydropower plants should accommodate this flow regime for the three power plants.

Figure 4.40 and Figure 4.41, represent the historical and predictive hydrograph of River Orle. They indicate that R. Orle is capable of a peak average discharge of 1.518 x 10^8 m^3/month in September, annual average of 5.095 x 10^7 m^3/ year and total discharge of 6.114 x 10^8 m^3/ year.

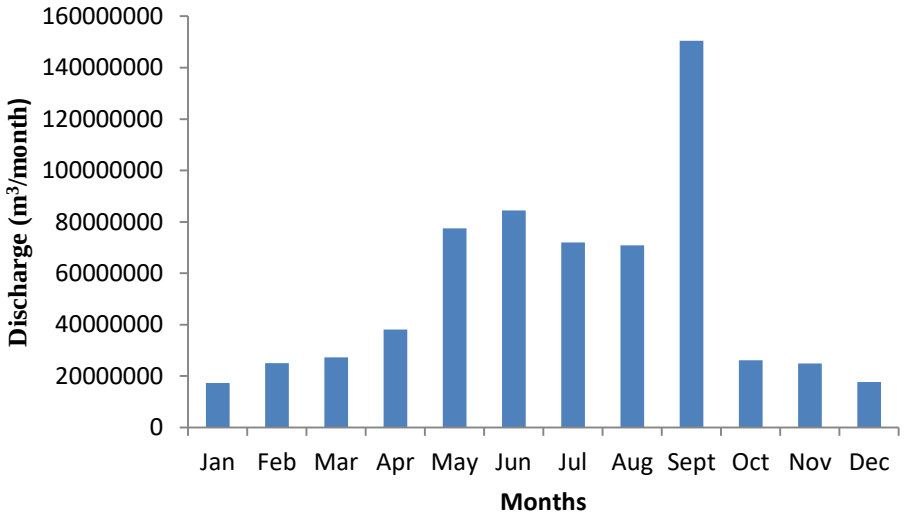

Figure 4.40: Historical Monthly Hydrograph of River Orle

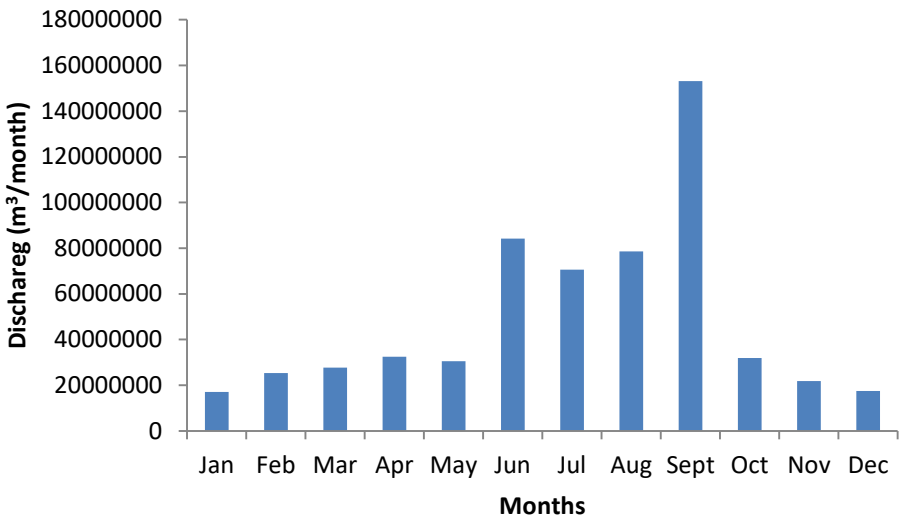

Figure 4.41: Predictive Monthly Hydrograph of River Orle

The historical and predictive hydrographs of R. Edion are shown in Figure 4.42 and Figure 4.43. From the hydrographs R. Edion is capable of a peak average discharge of 4.760 x 10^7 m^3/month in September, annual average of 2.355 x 10^7 m^3/ year and total discharge of 2.826 x 10^8 m^3/ year.

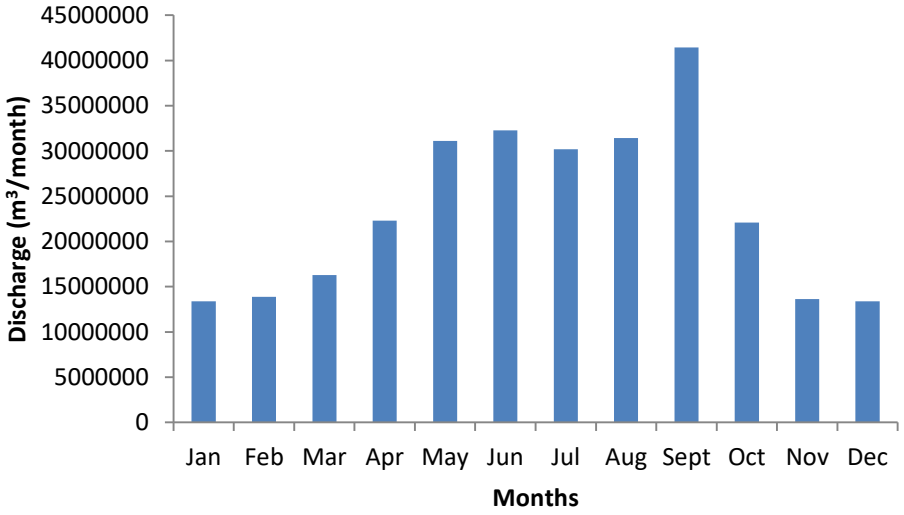

Figure 4.42: Historical Hydrograph of River Edion

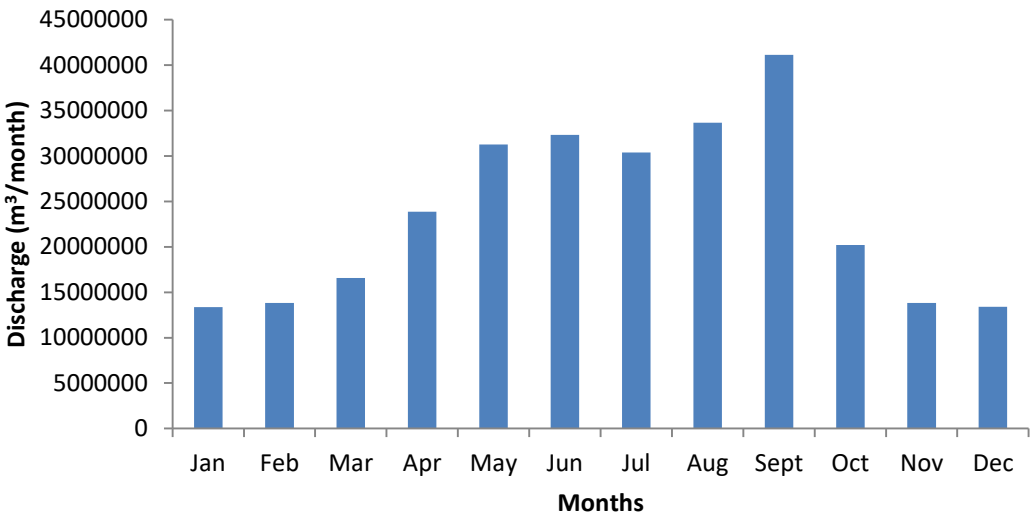

Figure 4.43: Predictive Monthly Hydrograph of River Edion

Figure 4.44 and Figure 4.45 represent the historical and predictive hydrograph of R. Orbe. They indicate that R. Orbe is capable of a peak average discharge of 5.192 x 10^7 m^3/month in September, annual average of 2.849 x 10^7 m^3/ year and total discharge of 3.418 x 10^8 m^3/ year.

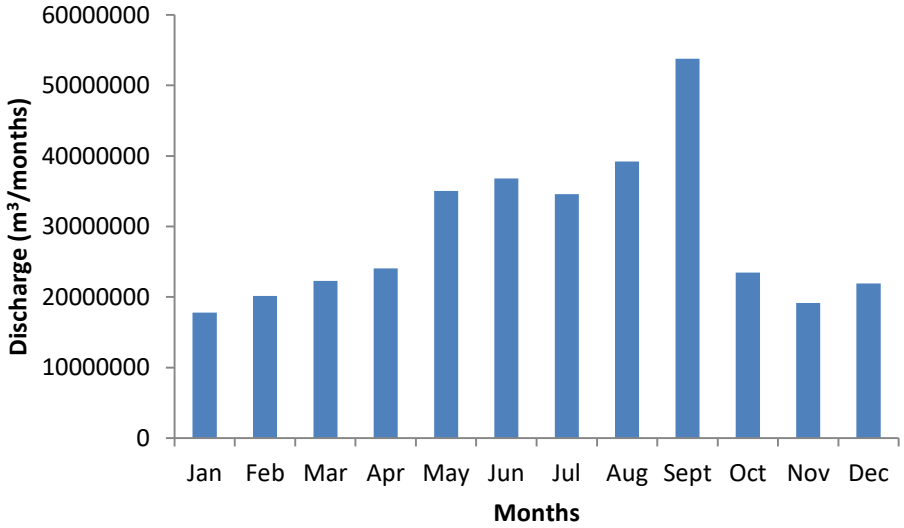

Figure 4.44: Historical Hydrograph of River Orbe

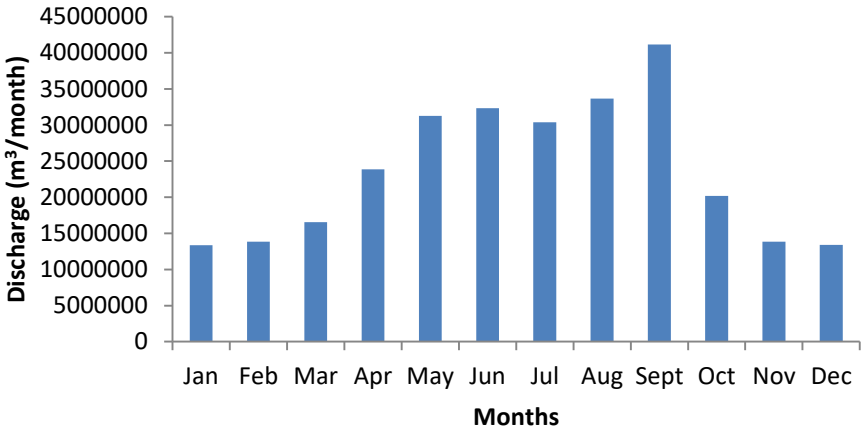

Figure 4.45: Predictive Monthly Hydrograph of River Orbe

4.14 Flow Duration Curves

The flow duration curve provides fundamental information for the design of the hydroelectric power project. It characterizes the capability of the stream to supply flows of various magnitudes, stream flow characteristics, type of flood flow regime and the ability of the stream basin to sustain continuous low discharge during the dry season. It indicates when the river discharge is equal or exceeded in a particular time.

4.14.1 Output base on power exceedence (Mega – Watt)

Figure 4.46 – 4.48, show the integrated flow and power duration curves for average monthly discharge (m^3/s) and power output (MW). The plots represent the average values of the historical and predictive discharge.

The plots indicate that the rivers have high flow regimes which are sustained throughout the month of September with spill over partly to October. This corresponds to Q_0 to Q_{10} on the flow duration curve. The hydropower system should be design to accommodate such high plows. In that regime the flow rate of River Orle is 58.550 m^3/s with a power output of 28.718 MW at ahead of 50 m as indicated in Figure: 4.46. River Edion has a flow rate of 15.931 m^3/s and a power output of 7.844 MW for a head of 50 m as

indicated in Figure: 4.47 River Orbeh has a flow rate of 20.03m^3/s and a power output of 9.825 MW at a head of 50 m as indicated in Figure 4.48.

Figure 4.46 also indicates that R. Orle has a primary (base) of 6.640 m^3/s and 3.25 MW respectively at 100% exceedence (365 days) in a year at a head of 50 m. 4.767 MW will be available at 75% (274 days) in a year, 6.581 MW at 50% (197 days), 15.966 MW at 25% exceedence (91 days). 28.965 MW will be available at 8.33 % exceedence (30 days). The average and total power output are 9.814 MW and 127.576 MW respectively.

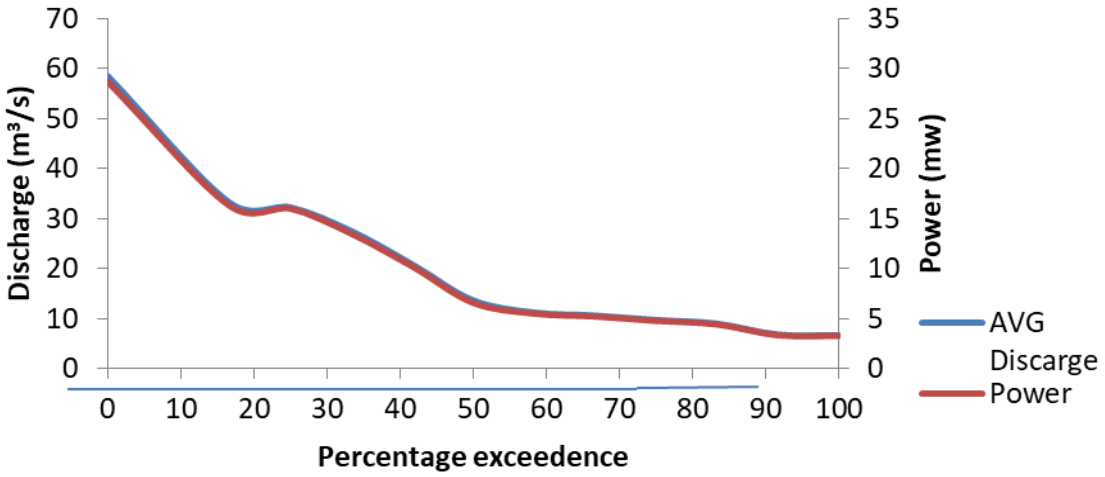

Figure 4.46: Integrated Flow and Power Duration Curve for River Orle

River Edion has a primary discharge and power output of 5.158 m^3/s and 2,53 MW at a head of 50 m as indicated in Figure 4.47. Also 4.179 MW will be available for 53.85% (197 days), 5.888 MW will be available for 25% (91 days), while 7.884 MW will be available for 8.33% (30 days) in a year. The average and total power output are 4.437 MW and 57.678 MW respectively.

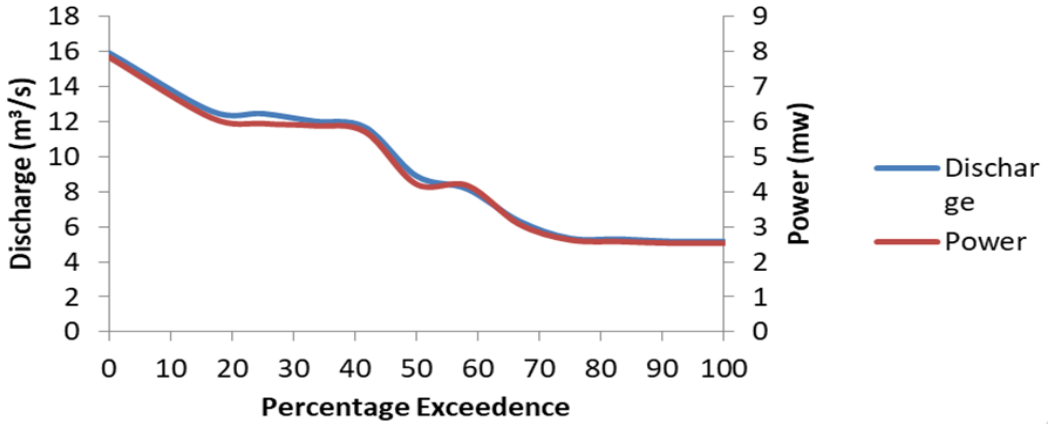

Figure 4.47: Integrated Flow and Power Duration Curve for River Edion

With a head of 50 m and primary discharge of 6.858 m^3/s, R. Orbe has a primary power output of 3.377 MW for 365 days as indicated in Figure 4.48, 4.439 MW will be available for 58.33% (223 days), 6.552 MW will be available for 25% (91 days), while 10.182 MW will be available for 8.33% (30 days) in a year. The average and total power output are 5.413 MW and 70.360 MW respectively.

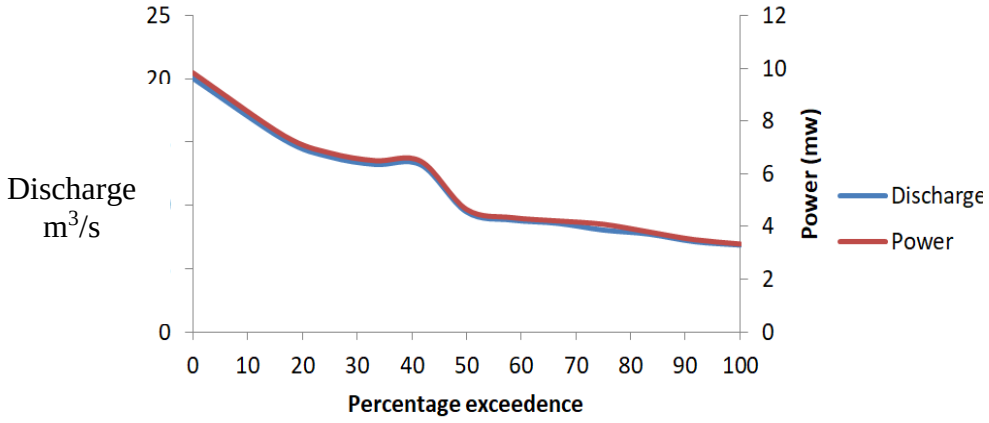

Figure 4.48: Integrated Flow and Power Duration Curve for River Orbe

4.14.2 Output base on power exceedence (Kilo – Watt Hour)

Figure 4.49 – 4.51, indicate the output of the rivers in kilowatt - hour. This is to enable the analysis of the output of the rivers in relations to the energy consumption by

households, commercial and industrial establishment in the actual feasibility assessment. The Kilowatt - hour is also the unit for electricity billing.

Figure 4.49 indicates that River Orle has a total and average annual generation capacity 9.19 x 10^4 kWh and 7.07 x 10^3 kWh respectively. The base output is 2,345 kWh at 100% exceedence, 3432.12 kWh at 75% exceedence, 4695.12 kWh at 50%, 11,106 kWh at 25% exceedence and 20700 kWh at 8.33% exceedence.

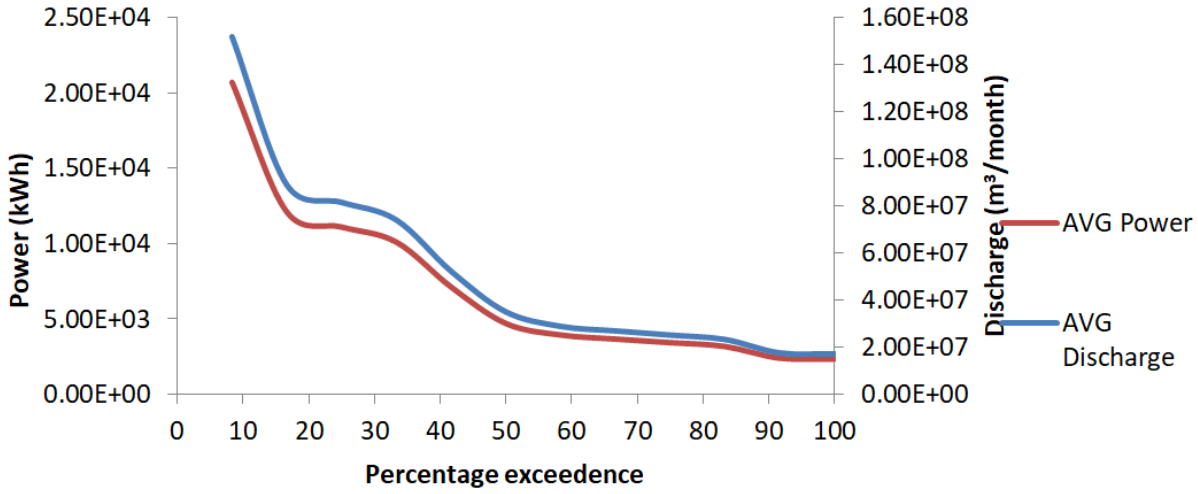

Figure 4.49: Integrated Flow (m^3/month) and Power (kWh) Duration Curve for Orle

For River Edion the total and average annual generation capacity are 4.17 x 10^4 kWh and 3.21 x 10^3 kWh respectively as indicated in Figure 4.50. The base output is 1821.50 kWh at 100% exceedence, 1887.84 kWh at 75% exceedence, 3,145.32 kWh at 50%, 4,343.76 kWh at 25% exceedence and 5626.08 at 8.33% exceedence.

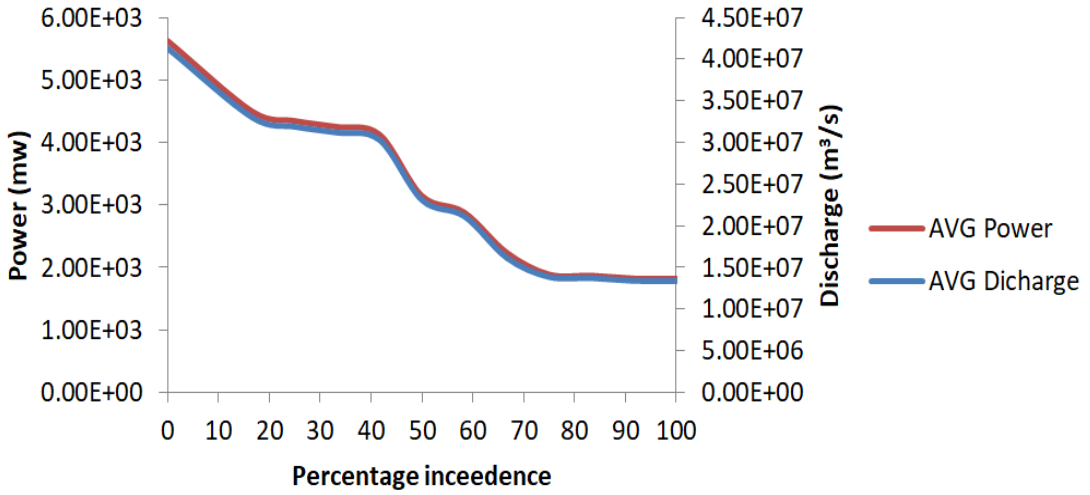

Figure 4.50: Integrated Flow (m^3/month) and Power (kWh) Duration Curve for River Edion

River Orbe has a total and average annual generation capacity of 5.06 x 10^4 kWh and 3.89 x 10^3 kWh respectively. The base output is 2,43.44 x10^3 kWh at 100% exceedence, 2,851.19 at 75% exceedence, 3,349.34 kWh at 50%, 4,886.62 kWh at 25% exceedence and 7.073.64 kWh at 8.33% exceedence indicated in Figure 4.51.

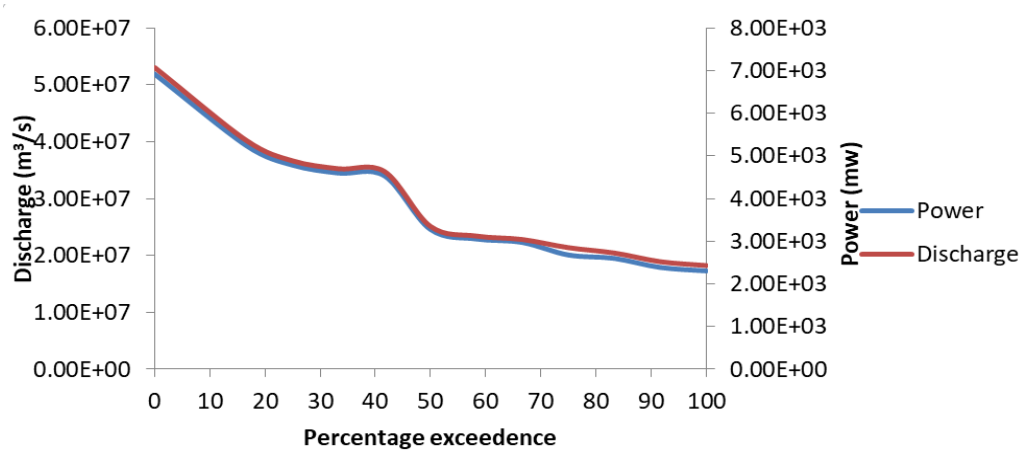

Figure 4.51: Integrated Flow (m^3/month) and Power (kWh) Duration Curve for River Orbe

A summary of the Discharge (m^3/Month) and (kWh) power output for the three rivers is shown in Table 4.19.

Table 4.19: Time of Exceedence with Associated Discharge (m^3/Month) and Power Output (kWh)

Time of Exceedence	R. Orle		Edion		Orbe	
	Discharge (m^3/month)	Power (kWh)	Discharge (m^3/month)	Power (kWh)	Discharge (m^3/month)	Power (kWh)
8.33	1.52E+08	2.07E+04	4.13E+07	5.63E+03	5.19E+07	7.07E+03
16.67	8.89E+07	1.21E+04	3.30E+07	4.49E+03	3.93E+07	5.36E+03
25	8.15E+07	1.11E+04	3.19E+07	4.34E+03	3.59E+07	4.89E+03
33.33	7.41E+07	1.01E+04	3.12E+07	4.25E+03	3.45E+07	4.70E+03
41.67	5.23E+07	7.12E+03	3.03E+07	4.13E+03	3.40E+07	4.63E+03
50	3.50E+07	4.70E+03	2.31E+07	3.15E+03	2.46E+07	3.35E+03
58.33	2.89E+07	3.94E+03	2.11E+07	2.88E+03	2.29E+07	3.12E+03
66.67	2.69E+07	3.67E+03	1.62E+07	2.24E+03	2.23E+07	3.04E+03
75	2.52E+07	3.43E+03	1.39E+07	1.89E+03	2.01E+07	2.85E+03
83.33	2.33E+07	3.18E+03	1.37E+07	1.87E+03	1.95E+07	2.73E+03
91.67	1.76E+07	2.40E+03	1.34E+07	1.82E+03	1.79E+07	2.52E+03
100	1.72E+07	2.35E+03	1.34E+07	1.82E+03	1.73E+07	2.43E+03
Average	5.19E+07	7.06E+03	2.35E+07	3.21E+03	2.83E+07	3.89E+03
Total	6.75E+08	9.18E+04	3.06E+08	4.17E+04	3.68E+08	5.06E+04

4.15 Secondary Power Generation

Secondary power represents power that can be generated with the provision of a reservoir across the river. The amount of storage is derivable from the integrated Flow/power duration Curve.

Figure 4.52 indicates the storage requirement of the River Orle for specified power generation.

For river Orle to produce an average power of 9.318 MW (approximately 10 MW) throughout the year. The quantity of storage required for this level of output is represented by section ABCD. For a higher power output flow demand could actually be targeted to produce a mean flow rate of 40m^3/s to produce a power output of 19.62 MW (approximately 20 MW) throughout the year. The quantity of storage required as indicated by the flow demand line is equivalent to section ABGH. The additional quantity of storage required is area CKN.

.However, hydropower systems are designed to operate more efficiently between the medium range of flow which is between the Q_{10} to $Q_{70.}$ The medium flow range of River Orle is between 49 m^3/s – 10 m^3/s which corresponds to about 24 MW - 5 MW power output as indicated in Figure 4.52. The additional storage requirement is area CGM.

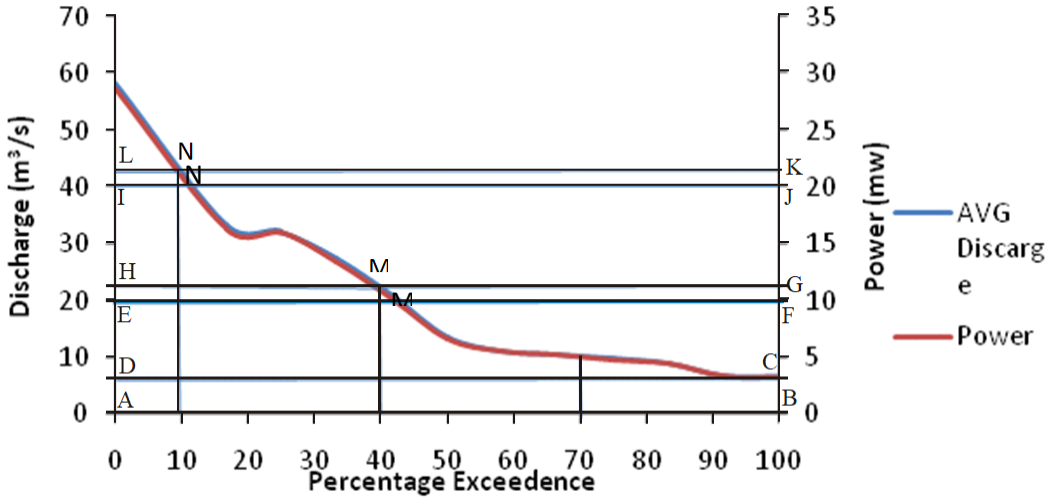

Figure 4.52: Integrated Power output and Reservoir Storage Requirement for River Orle

Figure 4.53 indicate the storage requirement of the R. Edion for specified power generation.

For River Edion the medium flow range is between 14.500 m^3/s – 5.800 m^3/s which correspond to about 7.112 MW – 2.845 MW as indicated in Figure 4.53, which correspond to area ABGH, and additional storage requirement is area CGI.

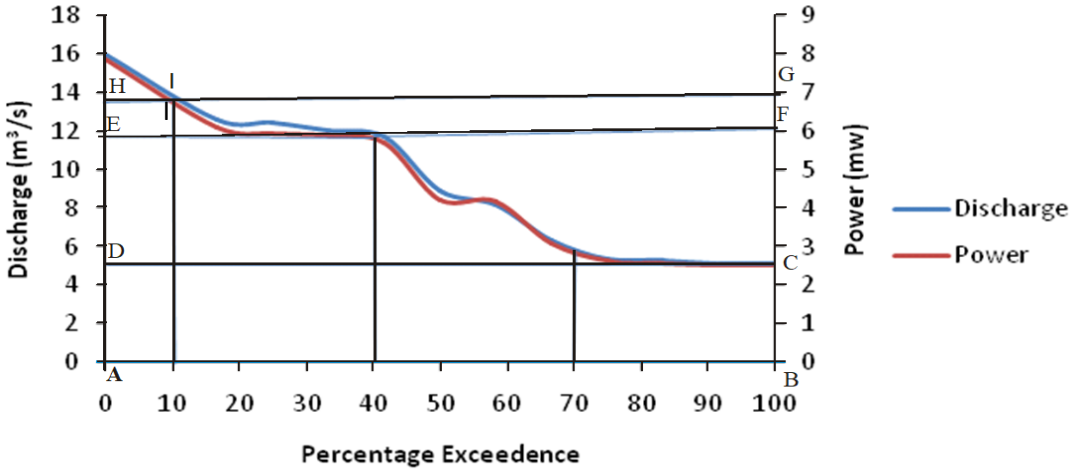

Figure 4.53: Power output and Reservoir Storage Requirement for River Edion

Figure 4.54 indicates the discharge, storage requirement and corresponding power output for R. Orbeh. It has a medium flow range between 18.000 m^3/s – 6.400 m^3/s with a power range of about 8.300 MW – 3.000 MW indicated in Figure 4.54. This corresponds to area ABGH, and additional storage requirement is area CGI.

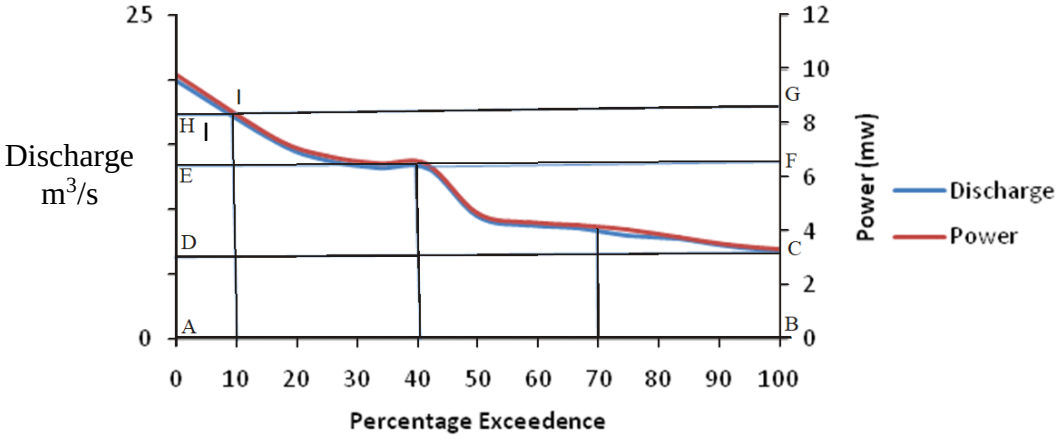

Figure 4.54: Power output and Reservoir Storage Requirement for River Orbe

Table 4.20 shows the hydroelectric power production phase of the three rivers under the medium flow range (Q_{70} – Q_{10}) of the three rivers. River Orle has peak power production potentials of 22 MW, base power of 12 MW and low power of 5 MW.

River Edion has peak power production potentials of 7 MW, base power of 6 MW and low power of 3 MW. River Orbe has peak power production potentials of 8.300 MW, base power of 6.500 MW and low power of 3 MW. Reservoir design, determination of equipment specification and characteristics for the rivers hydro power systems should be carried out in line with power production phase.

Table 4.20: Summary of the Power Production Phase of the three Rivers

S/N	Hydro project	Peak power output (MW)	Base power output (MW)	Low power output (MW)
1	Orle	22.000	12.000	5.000
2	Edion	7.000	6.500	3.000
3	Orbe	8.000	7.000	3.000

4.16 Reservoir Design Analysis

4.16.1 Determination of reservoir discharge

The annual reservoir inflow derived from 60 years of average monthly discharge is shown in Figure 4.55 for River Orle. It represents the profile of the inflow across the year. The reservoir capacity and discharge are derivable from the curve. The mass curve is represented by line AJGIB. The slope of the uniform demand line represent the uniform discharge rate that can be maintained by the reservoir throughout the years. The slope of the uniform demand is 19.243 m^3/s.

This uniform demand from the reservoir is discharged across the year to produce all-round the year mean power of 9.703 MW. The flow above the uniform demand line constitute excess flow that serves as storage used for power generation in times of low inflow.

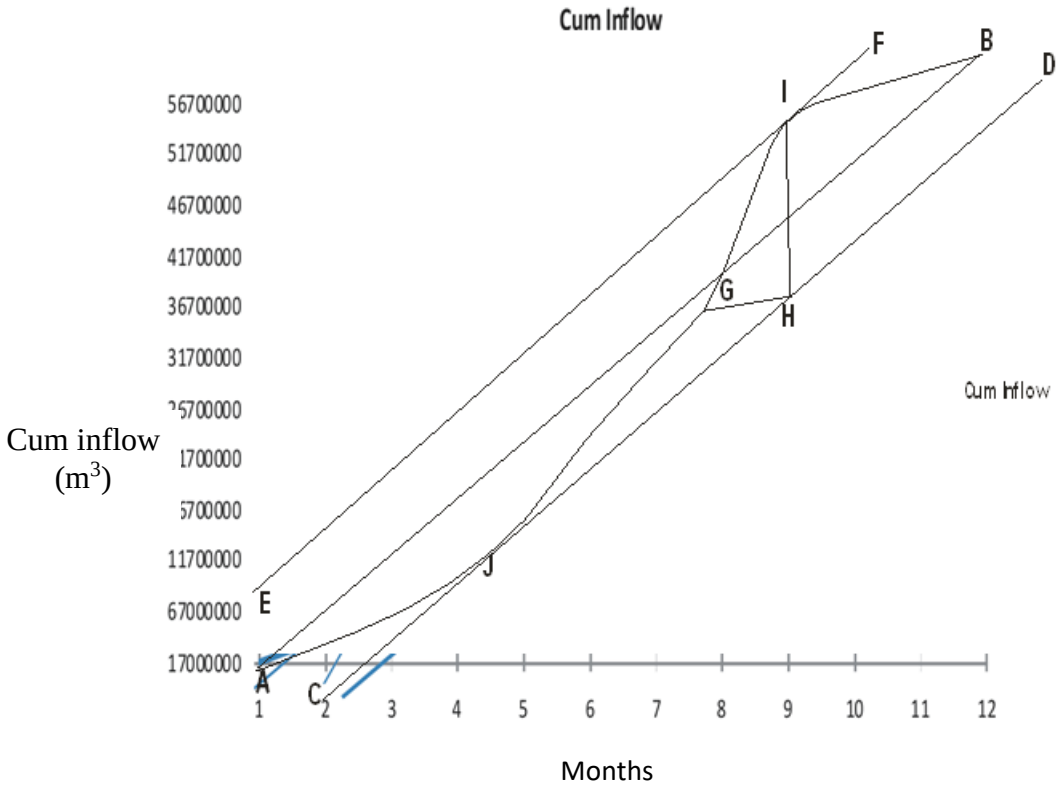

Figure 4.55: Mass Curve of River Orle

A uniform demand rate is effective in mitigating the effects of shortage of water for the downstream activities of the reservoir. The reservoir minimum storage capacity is the vertical intercept between the tangential lines drawn parallel to the uniform demand line at the crest and bottom of the mass curve.

For a constant demand line indicated in Figure 4.55 as AB the discharge from the reservoir will produce a gross power of 9.703 MW which is approximately 10 MW. In

this flow regime at point A the inflow rate equals the demand rate, but the demand rate exceeds the inflow rate from A - G and water is drawn from the reservoir storage. The storage requirements to meet the uniform power demand rate at point J is 80 x 10^6 m^3. At point G - I inflow exceed demand rate and the reservoir is filling. At point I, the reservoir is at full capacity. The capacity of the reservoir at full capacitor is 162,500,000 m^3. From I – B inflow still exceeds demand rate but the reservoir storage depletes to B. The cycle of storage is similar to the operation of the reservoirs of Edion and Orbe as indicated in Figure 4.56 and Figure 4.57.

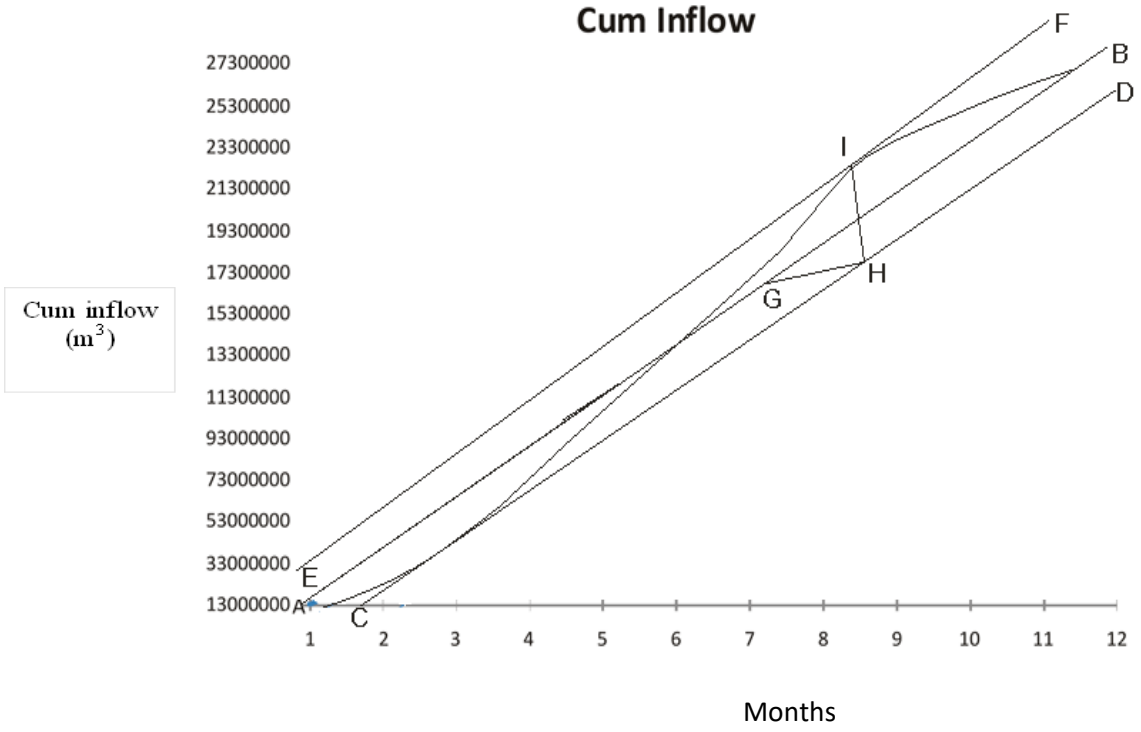

Figure 4.56: Mass Curve of River Edion

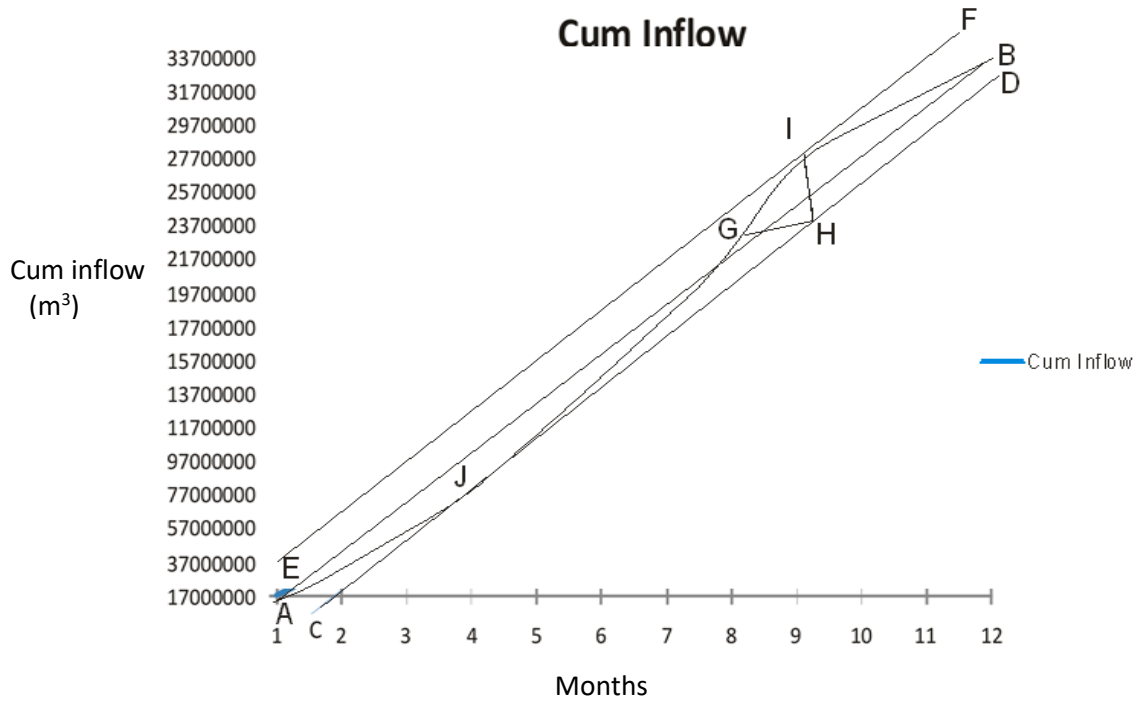

Figure4.57: Mass Curve of River Orbe

A Summary of the output and characteristics of the reservoirs is shown in Table 4.21. It indicates the storage, discharge, power characteristics, and surface area of the reservoir.

Table 4.21: Summary of Reservoirs Output and Power Characteristics

Reservoir	Inflow capacity (m^3)	Uniform discharge (m^3/s)	Uniform power output (MW)	Area of Reservoir surface (m^2)
Orle	162,500,000	19.243	9.703	4,392,000
Edion	42,500,00	9.087	4.5	1,216,500
Orbe	48,000,000	10.95	5.382	1,297,600

The reservoir capacity assessment did not capture flash flood that accompanies heavy rainfall as the river were too turbulent for any form of measurement to be carried out in

the flow course. However allowance was made to accommodate the water volume associated with such high discharge.

The design of the reservoir made it an effective flood retention and control structure (Tisdall 2016). The flash floods that most of the times overflow the river bank devastating farm lands could be retained in the reservoir and release in control measures to generate power. The flood used to damage farmland forming swamps that make the farmlands inaccessible.

The discharge of about 19.243 m^3/s at a uniform rate will stabilize the flow in the river course as against the variable flow of very low flow of 6.64 m^3/s around January to very high flow of about 58.55 m^3/s in around September.

4.16.2 Analysis of rate of seepage

The output from the multi – parametric analysis is shown in Table 4.22. The process enabled the simulation of the reservoir characteristics for the selection of the most appropriate dimensions of the reservoir.

Table 4.22: Output from the Multi- Parametric Analysis

Base length (b, m)	Width of Dam Crest (W, m)	Height of dam (H, m)	Seepage factor	Seepage (m^3/s)	Annual seepage (m^3/s)
105	5	50	0.376	1.881×10^{-5}	585.108
111	7	52	0.362	1.809×10^{-5}	562.703
118	10	54	0.346	1.732×10^{-5}	538.752
124	12	56	0.334	1.672×10^{-5}	519.971
131	15	58	0.321	1.606×10^{-5}	499.538
140	20	60	0.305	1.527×10^{-5}	474.995

The geometric factors selected from the multi – parametric analysis for the dams are shown in Table 4.23.

Table 4.23: Selected Geometric Parameters from the Multi – Parametric Analysis

Dam crest (m)	Dam height (m)	Seepage factor (dimensionless)	Seepage (m^3/s)	Annual seepage (m^3/s)
10	60	0.324	1.62×10^{-5}	503.844

The selected dam geometry represents the minimum seepage value commensurate with the hydraulic properties of the dam. The size of the embankment was also minimized with the conservation of materials for the dam construction without compromise to the structural integrity of the reservoir.

4.16.3 Precipitation into the Reservoir

The volume of inflow through the reservoir surface due to rainfall was evaluated. The mean annual rainfall for the catchment area was used in the analysis. The result is shown in Table 4.24.

Table 4.24: Annual Rainfall Inflow through the Reservoirs surface.

	Area of reservoir (m^2)	Mean annual rainfall (mm)	Annual water inflow (m^3)
Orle	4,392,000	1251.683	3,392.2
Edion	1,216,500	1251.683	1,252
Orbe	1,297,600	1223.199	1,223

4.16.4 Reservoir evaporation assessment

Table 4.25 shows the annual evaporation of water from the water surface of the reservoirs with a monthly evaporation rate of 5.099 mm/month.

Table 4.25: Annual Evaporation of Water Volume from the Reservoirs

Reservoir	Area (m^2)	Annual evaporation volume (m^3)
Orle	4,392,000	498,900
Edion	1,216,500	184,100
Orbe	1,297,600	184,100

The net reservoir capacity for the three rivers is shown in Table 4.26. Dead storage capacity for sediment trapping was allocated 10% of the total reservoir storage.

Table 4.26: Net Reservoirs Capacity

	Reservoir river Inflow volume (+,m^3)	Evaporation volume (-,m^3)	Rainfall Volume (+,m^3)	Seepage Volume (-,m^3)	Net reservoir capacity (m^3)
Orle	162,500,000	498.900	3,392	503.840	162,502,389
Edion	42,500,500	184.100	1,252	503.844	42,000,564
Orbe	48,000,000	184.100	1,223	503.844	48,000,543

4.17 Analysis of Penstock Characteristic

Table 4.27 – 4.29 show the summary of the results of the analyses of the characteristics of the penstock. Th

ey contain the evaluated characteristics of the various rivers penstocks at different flow conditions. The three rivers hydro project has the same penstock characteristics.

Table 4.27: Analytical Penstock Characteristics for River Orle

Parameter	100% flow	75% flow	50% flow	25% flow
Flow volume (m^3/s	4.811	3.608	2.406	1.203
Velocity (m/s)	2.293	1.810	1.196	0.598
Reynolds number	3.815×10^6	2.886×10^6	1.908×10^6	9.540×10^5
Friction factor	0.01131600	0.01131600	0.01131600	0.01232178
Total head loss (m)	0.653	0.899	1.963	5.019
Hydraulic efficiency	0.989	0.985	0.967	0.916

Table 4.28: Analytical Penstock Characteristics for River Edion

Parameter	100% flow	75% flow	50% flow	25% flow
Flow volume (m^3/s)	4.453	3.407	2.272	1.113
Velocity (m/s)	2.26	1.695	1.13	0.565
Reynolds number	3.603×10^6	2.702×10^6	1.801×10^6	2.253×10^5
Friction factor	0.010657998	0.010657998	0.010888998	0.0155227
Total head loss (m)	0.557	0.833	1.939	4.474
Penstock efficiency	0.991	0.986	0.968	0.926

Table 4.29: Analytical Penstock Characteristics for River Orbe

Parameter	100% flow	75% flow	50% flow	25% flow
Flow volume (m^3/s	5.475	4.106	2.737	1.369
Velocity (m/s)	2.723	2.042	1.362	0.681
Reynolds number	4.342×10^6	3.256×10^6	2.171×10^6	1.08×10^5
Friction factor	0.010506205	0.010506205	0.010506205	0.01210000
Total head loss (m)	0.800	0.987	2.01	6.470
Penstock efficiency	0.987	0.984	0.967	0.892

4.18 Transient Flow Analysis

Transient flow occurs in the penstock with the closure of the gate valve that generates high pressure waves that travel across the penstock. The generated pressure waves have a water hammer effect on the penstock pipe. The analysis was done for the gradual closure of the gate valve with the critical time of closure evaluated. The total pressure in the penstock is calculated for a valve closure time of 25 s.

Table 4.30 indicates the transient flow outcome of the closure of the gate valve for the three rivers penstocks. The results show that as the value of the valve closure time increases, the total pressure in the penstock decreases. This observation is in agreement with the conclusion in the work of Yuce and Omer (2019).

Table 4.30: Transient Flow Outcome of the Penstocks

Penstock	Critical time of closure (t_c) (s)	Water hammer pressure (P_h) (Pa)	Pressure at closure time of 25s (P_{25}) (Pa)	$P_{static} + P_h$ (Pa)	$P_{static} + P_{25}$ (Pa)
Orle	0.083	$3.478x10^6$	$1.155x10^4$	$3.792x10^6$	$3.255x10^5$
Edion	0.083	$1.634x10^6$	$5.424x10^3$	$1.948x10^6$	3.193x10^5
Orbe	0.083	$4.03x10^6$	$1.338x10^4$	$4.344x10^6$	3.273x10^5

There is significant reduction in the water hammer effects with increase in valve closure time. For River Orle, Edion and Orbe the reduction is 11.650, 6.100 and 13.272 times respectively. These analyses give essential insights into the management of valve closure time in penstocks.

4.19 Solid Works Software Penstock Characteristics Simulation Analysis

The Solid Works 2021 was used to simulate the flow through the penstock to determine the penstock flow characteristics. The Solid Works capability to achieve one configuration set up on various openings of the sluice gate and flow through the penstock was used in the simulation configuration set up.

Careful selection of the penstock parameters and fittings was done to simplify and facilitate the model analysis and flow simulation to enhance accuracy of results and precision of measurement. The set up goals of the simulation process were targeted at establishing the average velocity across the penstock, the pressure at inlet and outlet, mass and volume flow rate. The specific goals of average velocity across the penstock,

the pressure at inlet and outlet of the penstock are important parameters that were used to determine the head losses.

The flow analysis was carried out on three conditions of full (100%), three-quarter (75%) and half (50%) flow respectively. The head losses and penstock hydraulic efficiencies were evaluated. These approach provided insight into the dynamics of the flow process and enabled the configuration of the operation of the hydropower plant and determination of the power generation profile subject to the availability of water at any time of the year.

4.19.1 Set goals output

The set goals output from the flow simulation are shown in Table 4.31. It indicates the values of various parameters at various location of the penstock.

Table 4.31: Goals Plots Output

Goal Name	Unit	Value	Averaged Value	Minimum Value	Maximum Value
Inlet Pressure	Pa	340428.96	340428.96	340428.96	340428.96
Outlet Pressure	Pa	338436.62	338418.81	338399.89	338443.59
Average Velocity	m/s	2.424	2.424	2.424	2.424
Mass Flow Rate	kg/s	4805.0188	4805.0189	4805.0189	4805.0188
Volume Flow Rate	m^3/s	4.8110	4.8110	4.8110	4.8110

4.19.2 Pressure losses in penstock

The pressure characteristics across the domain and the various losses are shown in Table 4.32 - 4.43 for the various flow configurations. The various mesh volumes corresponding to the levels of mesh refinement and resolutions are also indicated. The results consist of output for various mesh refinement from resolution 4 to resolution 7 (highest level) of the solid works simulation process.

Analysis of the results indicates that the head loss is inversely proportion to the mesh volume due to higher level of mesh refinement. For River Orle full flow, the mesh volume for the initial flow at resolution four was 20,199 which built up to 531,142 volume at resolution seven. The head loss progressively fell with higher mesh refinement. It was observed that the simulation results gradually converge on the analytical solution. The higher mesh refinement progressive convergence on the analytical solution indicates that configuration of the computational domain was in order and a pointer to the accuracy of the process.

4.19.3 River Orle penstock head losses

Table 4.32: 100% Flow Head Losses

Head loss (m)	Total pressure At entrance (Pa)	Total Pressure At exit (Pa)	Density (kg/m^3)	Average Velocity (m/s)	Mesh Volume
0.790	340428.957	338428.1816	998.1934	2.428	20199
0.758	340476.226	338680.351	998.1934	2.413	24,166
0.732	340428.957	338665.99	998.1934	2.418	90,993.
0.694	340480.542	338780.7	998.1934	2.408	185,573
0.680	340488.019	338382.844	998.1934	2.401	531,942

Table 4.33: 75% Flow Head Losses

Head loss (m)	Total pressure At entrance (Pa)	Total Pressure At exit (Pa)	Density (kg/m^3)	Average Velocity (m/s)	Mesh Volume
1.017	341706.65	340044.359	998.1934	1.81	16,015
0.975	341709.935	340116.161	998.1934	1.81	21,048
0.964	341735.177	340257.237	998.1934	1.81	90,745
0.916	341735.623	340303.396	998.1934	1.81	159,924
0.904	341740.13	340357.75	998.1934	1.81	540,823

Table 4.34: 50% Flow Head Losses

Head loss (m)	Total pressure At entrance (Pa)	Total Pressure At exit (Pa)	Density (kg/m^3)	Average Velocity (m/s)	Mesh Volume
2.982	342619.162	340940.712	998.1934	1.205	15,408
2.743	342631.595	340941.72	998.1934	1.205	21,186
2.337	342621.873	340927.893	998.1934	1.205	90,245
2.332	342632.423	340644.275	998.1934	1.205	187,036
2.316	342634.378	340473.362	998.1934	1.205	548,469

Table 4.35: 25% Flow Head Losses

Head loss (m)	Total pressure At entrance (Pa)	Total Pressure At exit (Pa)	Density (kg/m^3)	Average Velocity (m/s)	Mesh Volume
9.200	343619	341962	998.1934	0.601	14,251
8.645	343620	342155	998.1934	0.601	19456
8.311	342630	342141	998.1934	0.601	80194
7.240	342241		998.1934	0.601	178654
6.40	343646	342491	998.1934	0.601	521789

4.19.4 River Edion penstock head losses

Table 4.36: 100% Head Losses

Head loss (m)	Total pressure At entrance (Pa)	Total Pressure At exit (Pa)	Density (kg/m^3)	Average Velocity (m/s)	Mesh Volume
0.727	315096.634	313244.624	998.1934	2.26	19067
0.652	315140.226	313477.872	998.1934	2.26	22818.
0.614	315095.798	313464.905	998.1934	2.26	85897
0.617	315143.928	313570.430	998.1934	2,26	175185
0.583	315151.333	313664.840	998.1934	2.26	502158

Table 4.37: 75% Flow Head Losses

Head loss (m)	Total pressure At entrance (Pa)	Total Pressure At exit (Pa)	Density (kg/m^3)	Average Velocity (m/s)	Mesh Volume
1.094	322669.718	321100.308	998.1934	1.697	14990
1.048	322672.551	321168.296	998.1934	1.697	19700
0.968	322697.102	321320.324	998.1934	1.697	84937
0.944	322697.102	321344.878	998.1934	1.697	149695
0.907	322701.823	321395.87	998.1934	1.697	506338

Table 4.38: 50% Head Losses

Head loss (m)	Total pressure At entrance (Pa)	Total Pressure At exit (Pa)	Density (kg/m^3)	Average Velocity (m/s)	Mesh Volume
3.034	323537.144	321951.654	998.1934	1.140	14280
2.458	323548.475	321952.599	998.1934	1.183	19921
2.439	323539.032	321939.378	998.1934	1.142	85644.77
2.298	323549.420	321672.140	998.1934	1.161	151308
2.285	323551.308	321510.663	998.1934	1.161	511627

Table 4.39: 25% Head Losses

Head loss (m)	Total pressure At entrance (Pa)	Total Pressure At exit (Pa)	Density (kg/m^3)	Average Velocity (m/s)	Mesh Volume
7.610	324367.978	323155.235	998.1934	0.565	13871
6.376	324371.119	323355.235	998.1934	0.565	18931
5.879	324385.426	323445.374	998.1934	0.566	78844.77
5.072	324396.227	323585.244	998.1934	0.565	1159311
4.989	324406.117	323611.214	998.1934	0.565	506533

4.19.5 River Orbe penstock head losses

Table 4.40: 100% Head Losses

Head loss (m)	Total pressure At entrance (Pa)	Total Pressure At exit (Pa)	Density (kg/m^3)	Average Velocity (m/s)	Mesh Volume
0.973	387412.866	383817.044	998.1934	2.680	22978
0.906	387467.748	384,107.011	998.1934	2.720	27450
0.895	387413.955	384207.669	998.1934	2.721	105558
0.875	387472.660	384238.211	998.1934	2.721	211178
0.846	387481.109	384354.452	998.1934	2.722	604493

Table 4.41: 75% Flow Head Losses

Head loss (m)	Total pressure At entrance (Pa)	Total Pressure At exit (Pa)	Density (kg/m^3)	Average Velocity (m/s)	Mesh Volume
1.126	411813.802	409509.844	998.1934	2.025	17944
1.087	411817.139	409596.377	998.1934	2.023	23538
1.007	411847.560	409790.560	998.1934	2.023	101435
0.998	411848.097	409822.026	998.1934	2.023	178346
0.992	411853.529	409887.532	998.1934	2.023	606362

Table 4.42: 50% Flow Head Losses

Head loss (m)	Total pressure At entrance (Pa)	Total Pressure At exit (Pa)	Density (kg/m^3)	Average Velocity (m/s)	Mesh Volume
2.184	412741.481	410719.511	998.1934	1.362	20906
2.202	412756.459	410720.725	998.1934	1.361	27459
2.425	412744.747	410704.068	998.1934	1.360	117515
2.363	412757.457	410362.403	998.1934	1.364	243560
2.265	412759.811	410156.510	998.1934	1.364	714008

Table 4.43: 25% Flow Head Losses

Head loss (m)	Total pressure At entrance (Pa)	Total Pressure At exit (Pa)	Density (kg/m^3)	Average Velocity (m/s)	Mesh Volume
8.762	412762.481	410734.600	998.1934	0.681	19786
8.801	412768.113	410897.624	998.1934	0.681	26792
7.343	412774.113	411074.568	998.1934	0.681	99675
7.236	412773.284	411098.505	998.1934	0.681	223561
6.851	412784.335	411198.432	998.1934	0.681	687234

4.19.6 Pressure and velocity flow analysis

The pressure and velocity profile of the various flow configurations for R. Orle are indicated in the pressure and velocity contours in Figure 4.58 to Figure 4.65. Figure 4.48 indicates the velocity contours for full flow for R. Orle penstock analysis. The colour legend indicates a dominant yellow colour which represents an average velocity 2.428 m/s. A flash of higher velocities of magnitude of 2.986 m/s – 3.484 m/s are indicated at the inner corner of the 45^0 elbows, while lower velocities of between 1.244 m/s – 1.981 m/s are indicated in the outer corners of the elbows. This is in line with the observation of Gajbhiye *et al.* (2020)

The highest velocities are concentrated around the sluice gate and elbow region. The flow was more uniform at the entrance to the penstock which conforms to a fillet radius pipe entrance with minimum disturbance and low flow loss coefficient. The flow across the fittings and elbow regions indicated some minor degree of variation which indicates the flow profile in a real flow condition (Gajbhiye *et al.,* 2020). This also indicates the

accuracy of the solid works simulation process and an indication of the content validity of the simulation process.

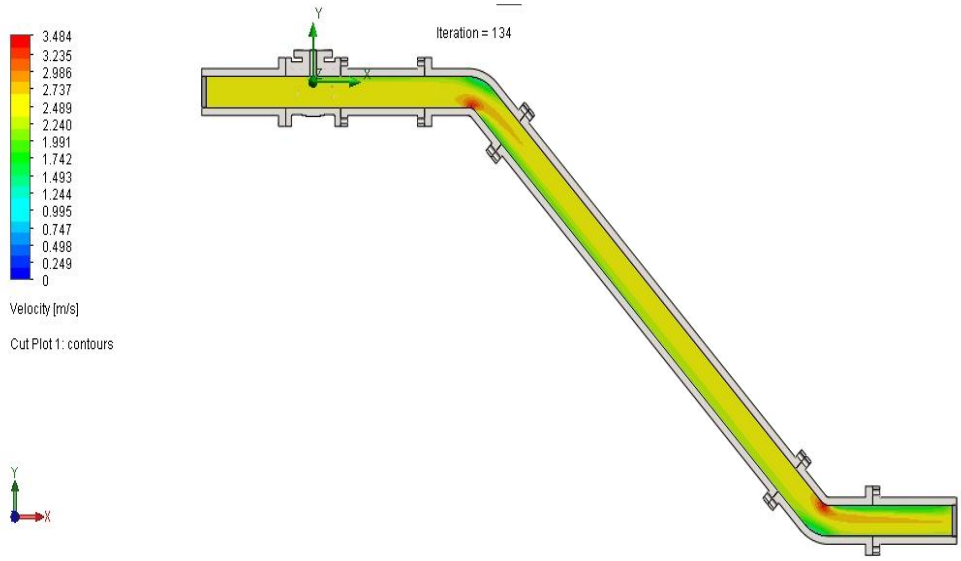

Figure 4.58: Velocity Contours for R. Orle flow analysis (Full Flow)

The pressure colour legend in Figure 4.59, indicates a higher pressure at the penstock inlet and a decrease in pressure afterwards. The decrease in pressure uniformly prevailed from the inlet to the outlet. The pressure distribution in line with the observation of Al-Waily *et al*. (2017). This is naturally due to the pipe wall roughness and the fittings which consists of the sluice gate and elbows.

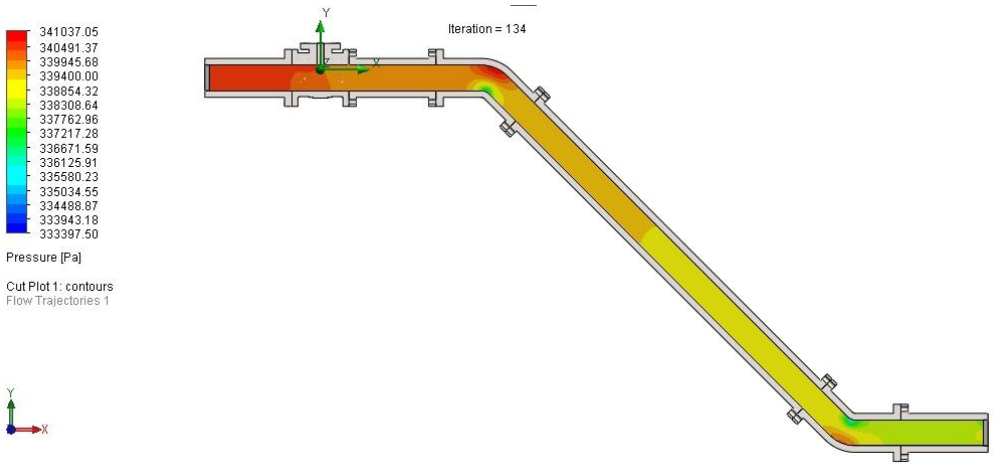

Figure 4.59: Pressure Contours for R. Orle flow analysis (Full Flow)

The pressure and velocity contours for other conditions of valve openings indicate similarity with the flow pattern for the full flow (100%) conditions of flow as descried above in Figure 4.58 to Figure 4.65, for the three quarter and half flow. However, the magnitude of velocity and pressure across the flow domain differs. The flow pattern for River Edion and Orbe for the four valves opening conditions are observed to have similar flow pattern.

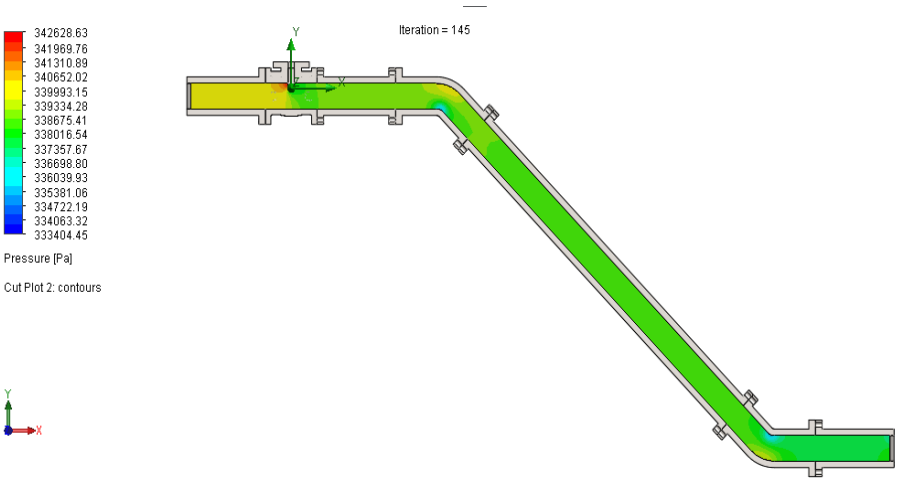

Figure 4.60: Pressure Contours for Three – quarter Valve opening

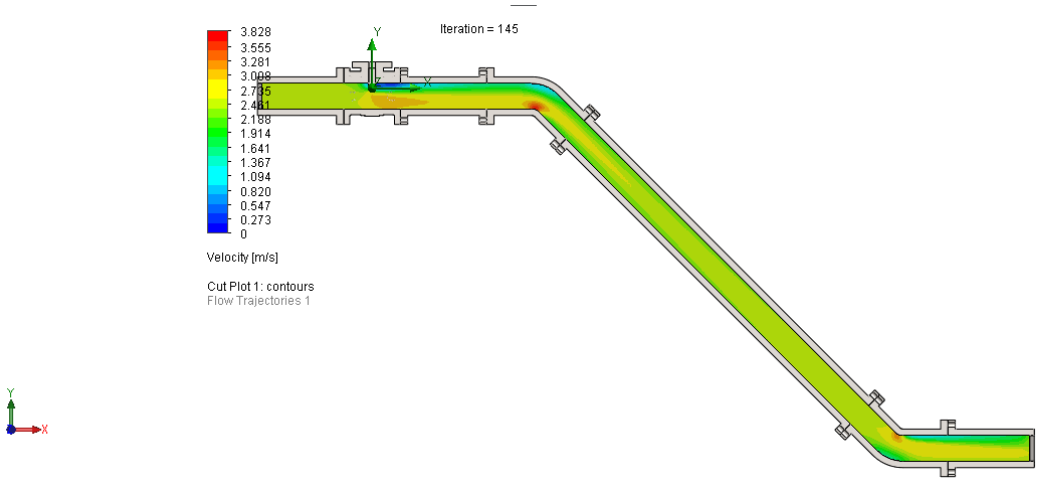

Figure 4.61: Velocity Contours for Three – quarter Valve Opening

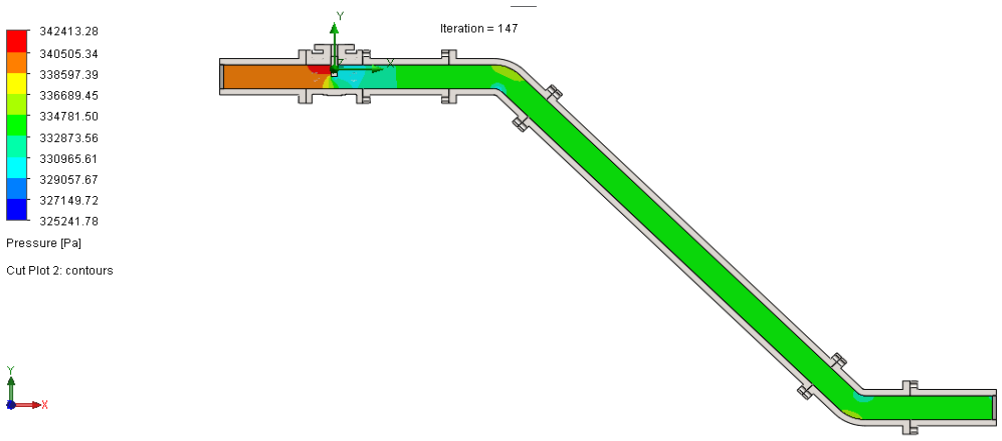

Figure 4.62: Pressure Contours for Half Valve Opening

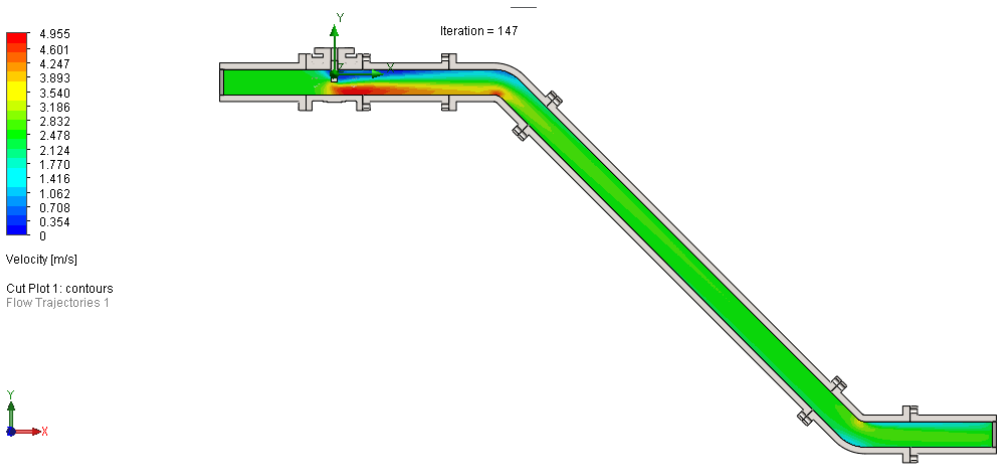

Figure 4.63: Velocity Contours for Half Valve Opening

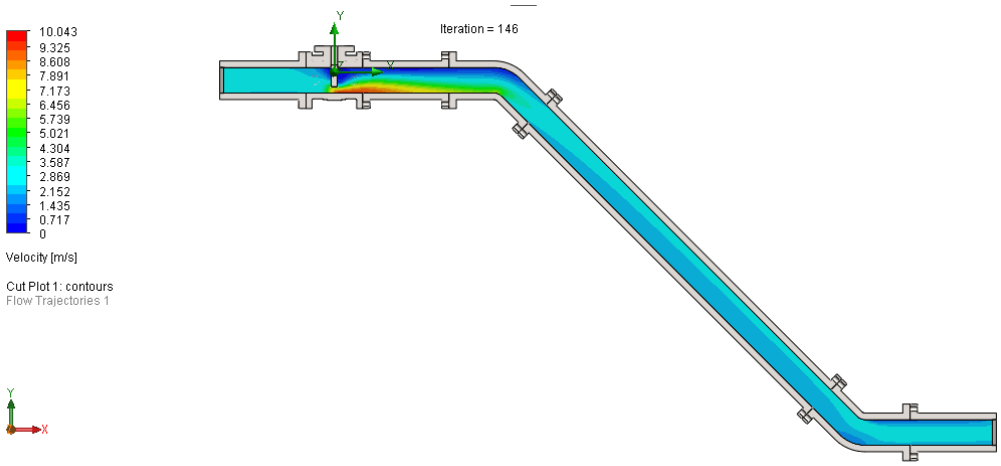

Figure 4.64: Velocity Contours for 25% Flow

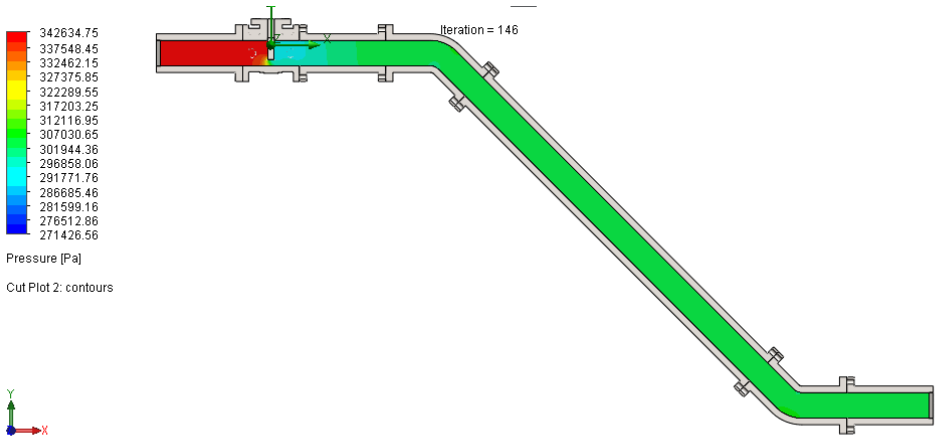

Figure 4.65: Pressure Contours for 25% Flow

4.19.7 Validation of simulation data

A two stage validation process was carried out for the penstock simulation process by a comparative analysis of the simulation process with an accurately packaged analytical penstock characteristic and flow analysis, and the determination of the correlation coefficient between the simulation process output and the analytical results.

The comparison of the analytical and simulation results for the rivers is shown in Table 4.44 to Table 4.47.

This characteristic of progressive convergence on the analytical solution is common to all other simulation run for the other flow condition and the other rivers penstock simulation process as indicated in Table 4.44 to 4.47. These indicate uniformity of flow assessment, which indicate the precision and accuracy of the solid works flow simulation process.

Table 4.44 indicates that the convergence accuracy of the solid works simulation is very high. The convergence accuracy of River Orle flow simulation is 99.90%, 99.89%, 99.27% and 96.88% at full, three-quarter, half and one-quarter flow respectively. The convergence accuracy decreases with decrease in valve openings.

Table 4.44: Comparative Penstock Characteristic for River Orle

Parameter	100% flow		75% flow		50% flow		25% flow	
	Simulat n	Analytic al	Simula tn	Analytic al	Simula tn	Analytic al	Simula tn	Analttical
Vol (m^3/s)	4.811	4.811	3.608	3.608	2.406	2.406	1.203	1.203
Vel (m/s)	2.428	2.393	1.810	1.810	1.196	1.205	0.601	0.598
head loss (m)	0.680	0.653	0.904	0.899	2.316	1.963	6.40	5.019
Penstock efficiency	0.986	0.987	0.981	0.982	0.954	0.961	0.872	0.900
Converge nce Accuracy (%)	99.90		99.89		99.27		96.88	

Table 4.45 indicates that the convergence accuracy of R. Edion is 99.90%, 99.89%, 99.27% and 98.68 for full, three-quarter, half flow, and one-quarter flow respectively. It indicates that the convergence accuracy decreases progressively with restriction of water flow.

Table 4.45: Comparative Penstock Characteristic for River Edion

Parameter	100% flow		75% flow		50% flow		25% flow	
	Simulat n	Analyti cl	Simulat n	Analyti cl	Simulat n	Analyti cl	Simulat n	Analytc al
Vol (m^3/s)	4.453	4.453	3.407	3.407	2.272	2.272	1.113	1.113
Vel (m/s)	2.26	2.26	1.697	1.695	1.40	1.130	0.565	0.565
head loss (m)	0.583	0.557	0.907	0.833	2.285	1.939	4.989	4.474
Penstock efficiency	0.988	0.989	0.981	0.983	0.954	0.961	0.900	0.912
Convergen ce accuracy (%)	99.90		99.89		99.27		98.68	

River Orbe has convergence accuracy of 99.90%, 99.90% and 99.47% and 99.08% for full, three-quarter, half flow and one-quarter flow respectively as indicated in Table 4.46. The high convergence accuracy indicates the validity of the Solid Works 2021 penstock simulation process.

Table 4.46: Comparative Penstock Characteristic for River Orbe

Parament	100% flow		75% flow		50% flow		25% flow	
	Simulatn	Analyticl	Simulatn	Analyticl	Simulatn	Analyticl	Simulatn	Analyticl
Vol (m^3/s)	5.475	5.475	4.106	4.106	2.737	2.737	1.369	1.369
Vel (m/s)	2.722	2.723	2.203	2.042	1.364	1.362	0.681	0.681
head loss (m)	0.846	0.800	0.992	0.987	2.265	2.010	6.851	6.47
Penstock efficiency	0.983	0.984	0.980	0.981	0.955	0.960	0.863	0.871
	99.90		99.90		99.47		99.08	

The average convergence accuracy at full flow is 99.90%, 99.89 at three – quarter flow, 99.34% at half flow and 98.21% at one-quarter flow.

The convergence accuracy is observed to be slightly lower at half flow (50%) and below consistently for the three rivers simulation results as indicated in Figure 4.64 to 4.66, which represent the comparative penstock head loss plots for the various flow conditions for the three rivers. The close convergence between the simulation and analytical results profile demonstrates the precision and accuracy of the simulation process.

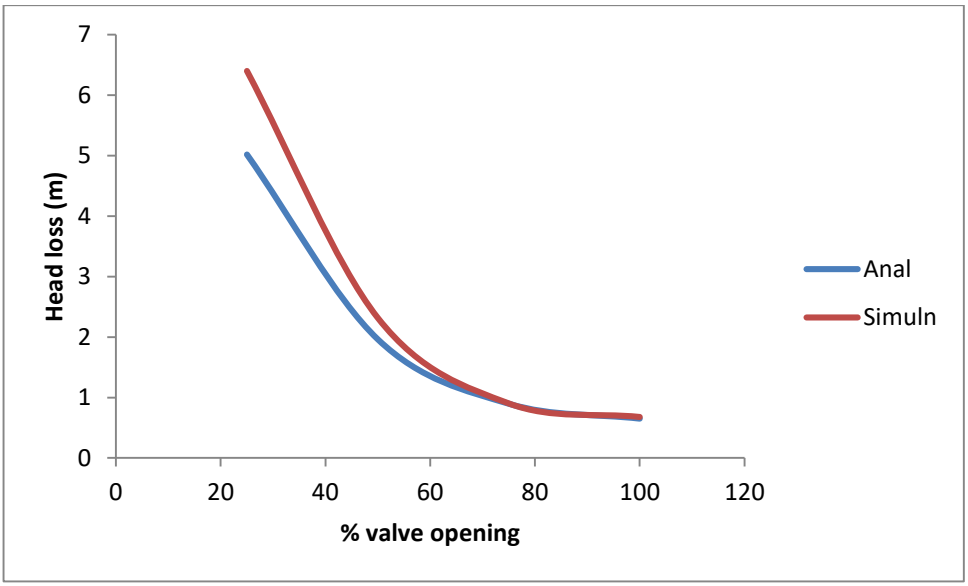

Figure 4.66: Comparative Penstock Plot for River Orle

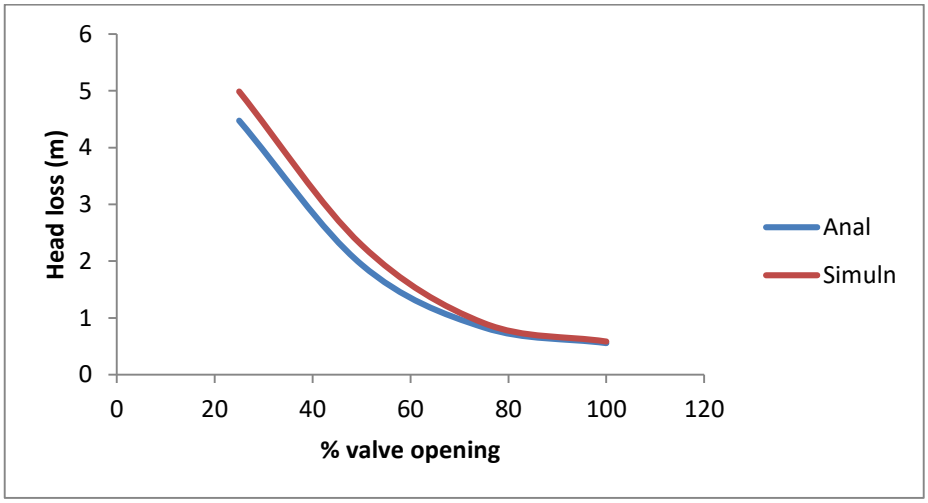

Figure 4.67: Comparative Penstock Plot for River Edion

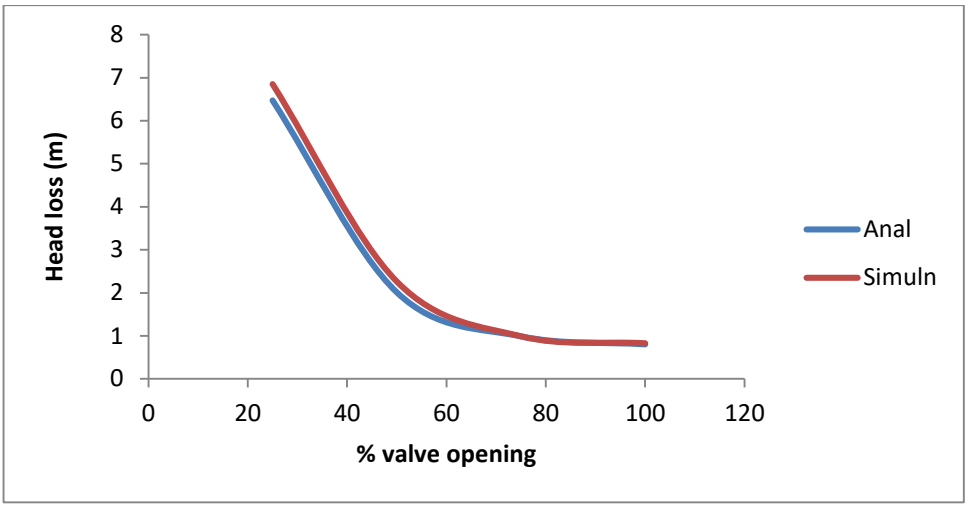

Figure 4.68: Comparative Penstock Plot for River Orbe

Table 4.47 to 4.49 show the characteristics of the power plants for full (100%), three – quarter (75%), half (50%) and one- quarter (25%) flow of the penstock. For each of the river the head loss is minimum at full flow, followed by three – quarter and half flow. The highest head loss occurs at 25% flow. The power generation also follows the same pattern. This implies that the plant operation should be concentrated on full penstock flow. In case of shortage of water for full flow, some of the penstocks should shut down to achieve full flow of plants operation.

Table 4.47: Net Power Generation Profile of River Orle

	Orle			
Volume of flow	100% Flow	75% Flow	50% Flow	25% Flow
Gross head	50	50	50	50
Head loss (m)	0.680	0.904	2.316	6.660
Net Head (m)	49.32	49.096	47.684	43.34
Flow rate (m^3/s)	4.811	3.608	2.406	1.203
Turbine Eff.	0.900	0.900	0.900	0.90
Net Power per penstock (MW)	2.140	1.594	1.033	0.511
Nos of penstocks	4	4	4	4
Total net power (MW)	8.560 ± 5%	6.376 ± 5%	4.132 ± 5%	2.046 ± 5%

Table 4.48: Net Power Generation Profile of River Edion

	Edion			
Volume of flow	100% Flow	75% Flow	50% Flow	25% Flow
Gross head	50	50	50	50
Head loss (m)	0.583	0.907	2.285	4.989
Net Head (m)	49.417	49.093	47.715	45.011
Flow rate (m^3/s)	4.453	3.407	2.272	1.113
Turbine Eff.	0.900	0.900	0.900	0.90
Net Power per penstock (MW)	1.981	1.505	0.98	0.442
Nos of penstocks	2	2	2	2
Total net power (MW)	3.962 ± 5%	3.01 ± 5%	1.96 ± 5%	0.885± 5%

Table 4.49: Net Power Generation Profile of River Orbe

	Orbe			
Volume of flow	100% Flow	75% Flow	50% Flow	25% Flow
Gross head	50	50	50	50
Head loss (m)	0.846	0.992	2.265	6.851
Net Head (m)	49.154	49.008	47.735	43.149
Flow rate (m3/s)	5.475	4.106	2.737	1.369
Turbine Eff.	0.900	0.900	0.900	0.900
Net Power per penstock (MW)	2.422	1.811	1.176	0.522
Nos of penstocks	2	2	2	2
Total net power (MW)	4.844 ± 5%	3.622 ± 5%	2.352 ± 5%	1.044± 5%

4.19.8 Correlation Analysis of Head Losses Results

The results of the Pearson correlation coefficient to determine the degree of statistical relation between the two pairs of results is shown in Table 4.48.

Table 4.50: Correlation Process Analysis

Correlation: analytical Versus simulation	R. Orle	R. Edion	R. Orbe
r	0.999	1.000	0.999
p - value	0.032	0.006	0.026

The correlation analysis indicates a very strong correlation between the analytical and simulation for the various flow conditions and a good statistical relationship within the two pairs of data with the various p – values which are generally lower than 0.065. This indicate a very strong agreement between the two set of results as they follow the same profile, a pointer to the accuracy of the process. Thus the solid works 2021 simulation configuration was well captured and the penstock flow characteristics adequately determined.

4.20 Summary of Hydro Project Characteristics

The power generation from River Orle is 10.00 MW, 7.50 MW and 5.00 MW at full 100%, 75% and 50% flow respectively. R.iverEdion power generation profile is 4.477 MW, 3.556 MW and 2.316 MW at full 100%, 75% and 50% flow respectively. The profile of River Orbe is 5.718 MW,, 4.278 and 2.79 MW at full 100%, 75% and 50% flow respectively.

From the power generation profile of the plants with its associated characteristics, it is more feasible to run the plant at full flow due to minimum penstock friction losses in this condition. The reservoir design is to generate an average discharge that will be available throughout the year from the 60 years data extension analysis. This indicate

constant power output from the plants base on the rainfall characteristic of the regions except there is maintenance challenges in the management of the plants. Base on the design the constant output from the rivers will be a minimum of 10.00 MW from River Orle, 4.477 MW for river Edion and 5.718 MW for River Orbe respectively. The flash flood accompanying torrential rainfall could not be captured in the measurement but allowance was made to accommodate the flood storage in the reservoir design. The implication is that higher power generation from the established power profile is feasible.

4.21 Small Hydro Project Impact Assessment Analysis

4.21.1 Analysis of the environmental impact assessment of SHP in the river basins

The study accessed the environmental impact and determine mitigation measures in the construction of a small hydropower project reservoirs for hydroelectric power generation and transmission to the Nigeria National Power Grid (NPG). The contribution and justification of Environmental Impact Assessment (EIA) were established. The analysis of the EIA is given below.

4.21.2 Identification of key issues examined in more detail during the assessment including the assesses impacts and alternatives considered.

The following issues are fundamental in the assessment of the effects of hydroelectric power systems on the environment.

i. Impact of Size, Type and Operation of Small Hydropower Plant

Generally plants with smaller dams are considered less environmentally damaging than those with larger dams (Zelanakova *et al*., 2018). The hydro plant reservoir size was determined from the average annual flow rate determined by the present study.

The proposed reservoirs are a small. Some safety measures were undertaken in the design of the configuration of the reservoirs. The locations of the plants are situated at the formation of the rivers basins to create a storage to accommodate the total reservoir volume within the depth of the valley. The gross heads were determined from the longitudinal height elevation of the basins. In conjunction with other safety design features the reservoirs are safe from spillage over the edges.

ii. Impact of River Diversion

An open channel of 6000 m by 10 m will be constructed to divert the rivers round the project sites. The construction activity is initiated in the dry periods around December when the rivers have very low flow volume. The diversion is done to avoid the disruption of the flow of the river during the construction phase to minimize the impact on water use in the downstream, the river ecosystem and biodiversity.

iii. Impact of the Reservoir

The impact of the physical, chemical and geomorphological properties of the project dams were considered. The land behind the dams is unusable and unavailable immediately the barrier for the reservoir is put in place. The area of the river basins are largely nonresidential. Farmlands are not common in the vicinity of the project sites because of the flooding characteristics of rivers between September and October annually. The same flooding plane is to contain the reservoirs. The major difference is that while the annual flooding water recedes as from mid-October the reservoir storage remains.

iv. **Sedimentation of Hydro Projects**

Large dams with reservoirs significantly alter the timing, amount and pattern of river flow. (Marcinkowski and Grygoruk, 2017),. This changes erosion patterns and the quantity and type of sediments transported by the river.

The sedimentation in the reservoirs will affect the amount and pattern of rivers flow and change the erosion pattern in the area. Mud and other sediments are deposited in the flooded area and may alter the area ecosystem.

Since removal of sediments is a normal practice in hydro dam operation, this effect is going to be minimized. The creation of the reservoir is likely to boost the area ecosystem diversity and water used which will include a boost in irrigation activities.

v. Downstream Erosion

Trapping of sediments at the dams has downstream impacts by reducing the flux of sediments downstream which can lead to the gradual loss of soil fertility in flood plain soils. Clean water stripped of its sediment load flows faster downstream of dams (Tullos *et al*., 2021). This clean water has more force and velocity than water carrying high sediment load and thus erosion of the riverbed and banks becomes problematic (Marcinkowski and Grygoruk, 2017). Since this is unnatural and a form of forced flow, it occurs at a much faster rate than natural river process erosion to which the local ecosystem would have to adapt.

There will be moderate to severe erosion of the river courses as a result of the faster water velocity downstream, which has more force than the natural river water. Thus, the erosion of the river bed and banks may be more severe. Also, regulated release of high volume of water due to heavy rains could lead to severe erosion downstream. In reality

this effect will persist for some distance downstream before the river will normalize its flow by picking up sediments.

vi. Impact on Fisheries

Dams and river diversion can impact fresh water, as well as marine Fisheries. Migratory fish are especially vulnerable to the impacts of dam construction. Dams can prevent migrating fish such as salmon and eel to reach their spawn grounds.

The area of coverage of the reservoirs is a small covering only some few kilometers compared to large dams of length close to a hundred kilometers long. There will be no significant impact on fisheries in the reservoir and downstream of it. Large population of fish has not been observed according to interview with people around the rivers. The creation of the dam will create a large volume of water for the breeding of fishes which were not available with the normal flow of the river. The fishes in the river can easily migrate away from the short length of the dam.

vii. **Use of natural resources**

The operation of the reservoir has no direct impact on the use of natural resources in the area. The working fluid is water which will flow naturally downstream of the dam. The water does not carry any major contaminant.

viii. Production of waste

There is no direct production of any waste material, pollution and nuisance by the plant. There is also no associated pollution activity of the reservoir. Only a small amount waste lubricant may leak of the plants, but the quantity is insignificant compare to the volume of river flow.

ix. **Impact of Dam Failure**

The impact of dam failure will release large floods of water downstream that will affect the communities downstream. Farmlands in the above communities may be washed away. There are no direct human settlements on the part of the course of the rivers. The geography of the area indicates that there are no communities situated on the path of the rivers flow downstream. Farmlands may be submerged in floods. The safety design features of the dam enhanced its structural stability and spill control mechanism to avoid dam failure and release of excessive floods.

x. Loss of Lives

The assessment indicates that the loss of lives will be low because the flood is likely to occupy mostly farmland far from villages from the observed navigational course of the river and its proximity to human settlements. The loss of lives will however be circumstantial concerning people trapped in moving fluids.

4.21.3 Study the state of the potentially affected environment

Out of the three projects areas only the Orle catchment contain some elements of sparse human habitation. It contains the following infrastructure as indicated in Table 4.48.

Table 4.51: Enumeration of facilities in Orle Valley

Structure/Facilities	Quantity	Purpose	Remark
Public utility building	5	Assembly for religious and social functions	Most are not fully operational
Residential buildings	12	Low density area residential areas	Situated at the outskirt of the project site
Abattoir	1	Slathering of animals for sale to the Auchi Community	Fully operational but can be relocated
Farmlands	Sparse	Cultivation of crops	The flooding of the river limited farming activities in the valley

4.21.4 Consideration of alternatives to the proposed development that may be more environmentally acceptable.

The alternatives to the projects are solar photovoltaic (PV) modules and thermal power plants. The solar PV modules occupy large space with low level power output and high capital cost. Solar systems are suited for small power appliances. They are also affected by low solar insolation and variation of weather.

Thermal power plants have problems of inadequate gas supply, low level maintenance and vandalism of gas supply lines. Gas is piped from locations in the Niger Delta Region which is about 300 km from Edo North. The cost of installation of the lines that

is further prone to supply disruption is enormous. Thermal plants also contribute largely to the production of greenhouse gases responsible for global warming.

4.21.5 Technological enhancement of reservoirs to mitigate failure

The following design features have been integrated into the design of the reservoirs to prevent the dam failure.;

i. Spillway over top.

ii. Maximum water level sensor.

iii. Twin side spillways

iv. Enhanced structural stabilization.

i. Spill over top

The dams are incorporated with a spillway over the top. This is to ensure that when the maximum water level in the dam is reached, water is released through the spillway instead of accumulating in the reservoir. In this way, the hydraulic pressure of the water is regulated. Large spill ways are also designed for at the sides of the dam for the emergency evacuation of floods.

ii. Maximum water level sensor

This sensor sounds an alarm when the maximum water level of the dam is approached. This alarm will automatically activate the spillways openings corresponding to the surge in the volume of water.

iii. Twin side spillways

The twin spillways are incorporated in the reservoirs design. The spillway which is sensored to the maximum water level will be activated to gradually spill the contents of the dams at regulated volumes to avoid flooding in the downstream of the reservoirs.

iv. Enhanced structural Stabilization:

Enhanced structural stabilization for the dam is targeted at containing the maximum lateral hydraulic stress from the reservoirs. Stabilization was implemented with concrete and boulder material well positioned around the poundage area. Adequate reinforcement was provided through appropriate design approach.

4.21.6 Anticipated level of damage to assets in the project areas

The anticipated level of damage to assets in the project areas is indicated in Table 4.52 and 4.50. The analysis indicates the risk assessment of assets in the area base on the possible damage to the properties from the operation and failure of the power plants.

The anticipated level of damage to assets in the Orle project area from the EIA is shown in Table 4.52. it indicates high risk factor to two assets which can easily be moved out of the project area. The risk assessments for other assets indicate low risk of damage to the assets.

Table 4.52: Anticipated level of Damage for River Orle Basin

Assets	Location of Address	Approximate Distance (m)	Anticipated level of damage for scenario (High, Medium and Low)
Abattoir	Close to the river	500	High
Family homes	No family home in the dam area. Habited houses are far beyond the valley	2500	Low
Business (Club house)	Close to the river	200	High
Industry	No established industry in the area	Nil	Low
Fishing site	No form of fishing activity	Nil	Low
Farm land	Sparse around the area	Sparse	Low

The project area of River Edion and Orbe have the same features in common with low human presence and activities. Fishing activity is not undertaken in the rivers. A summary of the assessments is given in Table 4.53.

Table 4.53: Summary of Anticipate level of Damage for River Orbe and Edion Project Area

Assets	Location of Address	Approximate Distance (m)	Anticipated level of damage for scenario (High, Medium and Low)
Family homes	No family home in the dam area. Habited houses are far beyond the valley	2500	Low
Business	Not available	Not available	low
Industry	Not available	Nil	Low
Fishing site	No form of fishing activity	Nil	Low
Farm land	Sparse farmland around the area	Sparsely distributed Around the project area	Low

4.21.7 Assessments of the impact on the social and economic lives of the communities

Assessment of the social and economic lives of the communities close to the project areas revealed the effects summarized in Table 4.54 to 4.55. Table 4.54 indicates the inundation of assets in the Orle project area. Only some family home may witness inundation in case of any flooding with the number of displaced person about 50. The

family homes are located at the peak of Orle valley. The business premises which is close to the river is a night club.

Table 4.54: Occupancy of Inundation Area for Orle River Basin

Asset	Anticipated level of flood severity	Typical occupancy	Estimated occupancy for dam failure scenario
Abatoir	High	0	0
Family home	Low	300	50
Business premises	High	5	Nil
Industry	Low	Nil	Nil
Farmland	Low	10	Nil
Fishing sites	Low	Nil	Nil

Table 4.55 indicates the typical inundation of facilities in the Orbe and Edion project areas. The general absence of family homes and sparse farmlands made the level of occupancy to flooding or failure from the dam to be very low.

Table 4.55: Occupancy of Inundation Area for Edion and Orbe Basin

Asset	Anticipated level of flood severity	Typical occupancy	Estimated occupancy for dam failure scenario
Family home	Low	Nil	Nil
Business premises	low	Nil	Nil
Industry	Low	Nil	Nil
Farmland	Low	10	Nil
Fishing sites	Low	Nil	Nil

4.21.8 Environmental impact on use of resources in the study area

The assessment of the anticipated level of damage is shown in Table 4.45 and 4.46. It is indicated that the anticipated level of damage to the infrastructures in the hydropower project areas is generally low, except for the Orle project with an abattoir and a night club. However, this assets can easily be relocated to other side beyond the Orle Valley.

4.21.9 Impact on the consequence of the dam failure

The probability of the dams failure is very low based on the modern safety by design features that were considered in the dam design. The safety by design features incorporates sensors into the dam system that will activate the opening of the spill gates to allow the passage of excess water downstream. The function is supplemented by the spill over top of the dam complemented by automated side spillways. Dams with these features have high level safety against failure.

Adequate reinforcement coupled with the use of sound construction materials will retain the hydraulic pressure of the water of the dam to minimize the occurrence of failure. Modern engineering has made dams safer irrespective of their size

4.21.10 Impact on the ecosystem and biodiversity

The Orle valley witness low existence of other animal habitats due to the activity of human around the area which also affected the biodiversity around the valley. The persistent flooding of the valley by the river is also a strong factor why the valley witness low animal presence. Other animals have migrated from the vicinity with the exceptions of those associated with water. More availability of water in the reservoir will enhance the lives and activity of other animals and water related animals in the area. The presence of the dam will enhance the ecosystem and multiply the biodiversity in the area.

4.21.11 Impact on the use of economic resources in the area and downstream

The dams are small with uniform discharge not too far above the natural flow of rivers. Water retained in the period of surplus rain between June and October will be used to power the dam during the dry season. Consequently, there is no significant effect of the dam downstream in the retention of water. The dam will bring about increased regulated flow that will enhance both fishing and irrigation activities downstream (World Bank, 2020).

The constant design discharge will stabilize the river flow throughout the year downstream avoiding variability of flow across the year. The variation in the river flow in case of river Orle from about 8 m^3/s in around January to 60 m^3/s in September/October will be eliminated. The large variation of flow do frequently lead to the overflowing of the river's bank leading to flooding of farmlands along its course.

These floods occupy these farmlands at essential time of the year between August to October before receding with the loss of large amount of harvest.

4.21.12 Impact on economic activities on the study area

The reservoirs construction and operation will significantly boost economic activities in the areas. There will be the production of electricity that will enhance economic activities in the area, water will be available for irrigation purpose and processing for pipe borne water supply (World Bank, 2020).

Commercial fishing activities will commence and serve as a major boost in economic earnings in the communities.

4.21.13 Summary of the environmental impacts assessment

The Environmental Impact Assessment of the Construction of a hydro power Plant on Orle, Edion and Orbe river basins was carried out. The major findings indicate that with good safety by design features the probability of the dams failure is low. The dams are equipped with sensor enhanced spillways that can regulate rise in coming flood level and release water in time to avoid dangerous level of accumulation of flood in the reservoir. Mondern design practice of appropriate consideration of geological factors and use of sound materials for construction will enhance the stabilization of the dams structure against failure (Adamo *et al.*, 2020).

The impact of the disruption of economic and social activities by the construction of the dam is still low because of the low level of economic activities in the area, The main facilities of inundation with reservoir water are vegetation and farmlands.

The hydroelectric power plants will boost economic activity in the area by bringing stable power supply to the area; enhance farming, fishing and irrigation activities. It will

also multiply the biodiversity and bring about stable water related ecosystems in the area. The economic benefits of the dam will largely offset the aggregate cost of assets that will be consumed by the dam construction.

4.22 Hydropower Generation Cost Modeling

The evaluated installation cost of the hydropower projects are Orle $22,033,600 and $46,333,381 for the IRENA (2021) and CAPEX (2020) respectively, Edion are $11,016,600 and $25,794,294 while the cost of Orbe are $13,219,920 and $30,090665 respectively. The IRENA installation cost for Orle , Edion and Orbe represent 47.55%, 42.71% and 43.93% of respectively of the CAPEX model. The disparity may be due to the fact that the IRENA cost factors are based on Western technology and economic indices while the CAPEX is base on China finance and technology. The CAPEX is influenced by local site conditions while the IRENA cost factor is a general global average.

Table 4.56 and 4.57 indicates that the LCOE for Orle, Edion and Orbe is $0.044/kWh for the IRENA cost factors while the LCOE for the three plants for the CAPEX cost factors is $0.097/kWh.The LCOE of $0.044/kWh indicates the break-even point for the 50 years of plant operation for the IRENA cost factors. The local electricity tariffs in Nigeria vary between $0.074/kWh - $0.134/kWh depending on the consumer electricity band for naira to the dollar exchange rate of N443.76 official CBN rate. The profit margin of operation of the plants will be between $0.03 – $0.09/kWh. This indicates the high economic viability of the operation of the plants from the global hydropower price trend analysis.

Table 4.56: Results of the Implementation of CAPEX (2020) Model

Project	Rating (kW)	Investment cost ($/kW)	O &M Cost ($/kW))	Capacity factor ($/kW))	LCOE ($/kWh)
Orle	10,000	22033600	44066400	12118260	0.044
Edion	5000	11,016600	22030000	6039000	0.044
Orbe	6000	13,219,920	26440000	7271000	0.044

Table 4.57: Results of the Implementation of the Modified CAPEX (2020) Model

Project	Rating (kW)	Investment cost ($/kW)	O &M Cost ($/kW))	Capacity factor ($/kW))	LCOE ($/kWh)
Orle	10,000	46,333381	92670000	25480000	0.092
Edion	5000	25,794294	51590000	14190000	0.102
Orbe	6000	30,090665	60180000	16550000	0.099

The IRENA cost factors represents the global average, actual operational cost may be higher as indicated by the CAPEX cost factors. The CAPEX average value of $0.097 falls between the local electricity tariffs range of $0.074 – $0.134 which validates the economic competitiveness of the plants. Actual electricity tariffs are expected to rise in the future which indicates that both under IRENA and CAPEX cost factors the operation of the plants is economically competitive.

CHAPTER FIVE

5.0 CONCLUSION AND RECOMMENDATIONS

5.1 Conclusion

A model was developed for the evaluation of the hydroelectric power generation potentials of River Orle, Edion, and Orbe in ungauged river channels using the double and surface floats after the characterization of uncertainty associated with flow characteristic measurement.

The mean annual flow rates of River Orle, Edion, and Orbe are 19.283 m^3/s, 9.827 m^3/s, and 13.484 m^3/s respectively. A head of 50 m was determined for the hydropower plants. The hydropower potentials of River Orle, Edion, and Orbe are 10.00 MW, 4.477 MW, and 5.718 MW respectively. The model that has an accuracy of 99.99%, 99.54%, and 99.98% for area of cross section, velocity and flow rate measurements respectively compare to analytical process. The ISO 748, 2021 has an accuracy of 99.82% compare to the analytical process. The model has the advantage of high accuracy and simplicity with capability to determine the area of cross section of flow channels, average velocity, discharge, power potentials, and associated uncertainty in an automated process in comparison with the ISO 748:2021 models. The study model established a precise and accurate method for the determination of uncertainty of ungauged channels using floats. The statistical analysis of the results indicated that the rivers has similar flow pattern.

The aggregate combined and expanded uncertainty values for surface float are ±4.962% and ±9.923%, the double float are ±5.00% and ±10.00% and the subsurface float are ±4.962% and ±9.983% respectively. The analysis of the flow data indicates that the double float has the highest level of accuracy and precision and is recommended for use in the flow characteristics measurement in rivers in Edo North.

A 30 years historical and predictive discharge data extension was carried out using the Guass-Newton non-linear empirical regression algorithm from the observed 2 years experimental discharge data in order to meet the requirement for the design of water control and retention facilities. Model discharge predictive accuracy of 96.71% and correlation coefficient 0.954 were established between the model and experimental results.

The mass curve method was used to determine the storage capacity of the reservoir on the basis of the cumulative inflow to the reservoirs. The net reservoir capacity was adjusted for the rainfall volume on reservoir surface, seepage across reservoir embankment, evaporation of water from reservoir surface and sedimentation at reservoir bottom. Only the storage capacity and discharge requirement design of the reservoir were carried out. The capacity of the reservoir of R. Orle is 162,500,000 m^3, R. Edion is 42,500,000 m^3 while R. Orbe is 48,000,000 m^3 respectively. The Solid Works 2021 was used to simulate the flow through the penstock to determine penstock flow dynamics and characteristics due to its capability to achieve one configuration set up on various openings of the sluice gate and flow through the penstock. The convergence accuracy of R. Orle, Edion and Orbe are on the analytical process results are 95.90%, 95.30% and 94.20% respectively. The power generation profile for R. Orle is 10.00 MW, 7.50 MW and 5.00 MW at full 100%, 75% and 50% flow respectively. R. Edion power generation profile is 4.477 MW, 3.556 MW and 2.316 MW at full 100%, 75% and 50% flow respectively. The profile of Orbe is 5.718 MW, 4.278 MW and 2.79 MW at full 100%, 75% and 50% flow respectively. From the power generation profile of the plants with its associated characteristics, it is more feasible to run the plant at full flow due to minimum penstock friction losses.

The Environmental Impact Assessment of the Construction of a hydropower Plants indicates that with good safety by design features the probability of the dams failure is low. The hydroelectric power plants will boost economic activity in the area by bringing stable power supply to the area; enhance farming, fishing and irrigation activities. It will also multiply the biodiversity and bring about stable water related ecosystems in the area. The economic benefits of the dam will largely offset the aggregate cost of assets that will be consumed by the dam construction.

The economic cost analysis indicates that the projects are economically viable and competitive with an LCOE of $0.044/kWh for the IRENA cost factor which is in tandem with global average LCOE value of $0.048/kWh for SHP. The CARPEX model value of $0.097/kWh is between the range of $0.074kWh – $0.134/kWh for the actual local electricity tariffs in Nigeria.

The study established a model that facilities the feasibility assessment of hydropower sites in ungauged river basins and provide essential insight into reservoir design, equipment specification and characteristics for rivers hydropower systems. The implementation of the model will assist in the exploration of Nigeria hydro power resources that will provide the required electrical power generation to sustain the Nigeria economy.

5.2 Recommendations

Following are some recommendations based on the findings of the research process:

i. The study model should be used to evaluate the hydroelectric power potential of rivers across the nation in order to provide the data needed to direct policymakers on the construction of hydropower projects across the nation.

ii. To integrate hydropower development in mini- and micro-hydropower generation and to promote development and wealth creation in rural areas, the Nigerian framework for rural area development should use the template developed in the study.
iii. For the purpose of providing accurate hydrological data and insight into the management of national water resources, additional research should be conducted on the development and management of a national hydrological data bank, water reservoir management, and reservoir maintenance.
iv. Further research should be done on the creation and application of smart reservoir management technologies to reduce flooding downstream of reservoirs brought on by high water release rates.

5.3 Contribution to Knowledge

The study developed a mathematical model to overcome the challenge of the conservative design of facilities in hydropower generation. The model utilized minimum hydrological data of two years in the prediction of the hydropower potentials of rivers. It has the unique advantage of determining the area of cross-section, average velocity, flow rate, hydropower of river channels, and associated uncertainty in comparison with the ISO 748, 2021 models. The prediction accuracy for the area of cross-section, velocity, and flow rate measurements are 99.99%, 99.54%, and 99.98% respectively.

Characterization of combined uncertainty of flow characteristics measurement by floats in ungauged river channels with an aggregate value of ±5 %.

Development of a template with 96.71% accuracy for discharge data extension in hydrological data scarce regions. The template established the incorporation of historical and predictive precipitation data in discharge data extension process.

Development of the integrated flow and power duration curves for enhanced visualization of the flow exceedence, secondary water storage, and corresponding hydropower potentials of rivers.

REFERENCES

Abdulkadir, T. S., Salami, A. W., Anwar, A. R. & Kareem, A. G. (2013). Modelling of hydropower reservoir variables for energy generation: neural network approach. ethiopian *Journal of Environmental Studies and Management*, 6(3), 125 -129.

Abegunde, L. A. (2018). Use of limited hydrological data and mathematical parameters for catchment regionalization of Ogun Drainage Basin, Southwest, Masters Thesis in Hydrology and Climate Change programme, *Federal University of Agriculture, Abeokuta.*

Acakpovi, A., Hagan, E. B. & Fifatin E. X. (2015). Cost optimization of an electrical energy supply from a hybrid solar, wind and hydropower plant. *International Journal of Computer Applications*, 114(19). 44 – 51.

Adamo, N., Al-Ansari, N., Sissakian, V., Jan Laue, J. & Knutsson, S. (2020). Dams safety and geology, *Journal of Earth Sciences and Geotechnical Engineering*, 10 (6). 1792 - 1799.

Ahmed, M. I. & Abed, S. Y. (2014). A simulation model for Stage –IV Koyna hydropower plant. *International Journal of Advances in Engineering & Technology*, 6(6), 2373 - 2381.

Akinlo, A. E. (2009). Electricity consumption and economic growth in nigeria: evidence from cointegration and co-feature analysis. *Journal of Policy Modeling*, 31 (5), 681 – 692.

Al-Waily, M., Al-Baghdadi, M. and Resan, K. K. (2017). CFD investigation of the erosion severity in 3d flow elbow during crude oil contaminated sand transportation, *Engineering and Technology Journal*, 35(9), 87 – 95.

Al-Shetwi, A. Q. (2022). Sustainable development of renewable energy integrated power sector: Trends, environmental impacts, and recent challenges. *Science of The Total Environment, 822,* 1 – 10.

Atchike, D. W., Zhen-Yu, Z., & Bao, G. (2020). Bootstrapping the cost modeling of hydropower projects in sub-Saharan Africa: Case of Chinese financed projects. *International Journal of Energy Economics and Policy*, 2020, 10(3), 136 - 146.

Audu, M. L. Musa, A. N. & Nasir, A. (2020). Determination of power profile of hydro resources in ungauged channels, *International Journal of Research in Engineering and Applied Sciences*, 5(3), 79 – 85.

Atkins, W. (2003). Hydroelectric Power. *Water: Science and Issue*, 2 (1), 187 – 191.

Bailey, T., & Bass, R. (2009). *Hydroelectric feasibility study: An assessment of the feasibility of generating electric power using urban storm water in Oregon City*.

Baldassare G. & Montaneri A. (2009). Uncertainty in rivers discharge observation: A quantitative analysis. *Journal of Hydrological Earth System Science*, 13(1), 913 - 921.

Bernard, J. & Guertin, C. (2002). Nodal pricing and transmission losses: An application to a hydroelectric power system. *Resources and Energy,* 7(4), 353 – 375.

Bilotta, G. S., Burnside, N. G., Gray J. C. & Orr H. G. (2016). The effects of run-of-river hydroelectric power schemes on fish community composition in temperate streams and rivers. 11(5): 115 – 123.

Bobat A. (2017). Environmental impact assessment of hydropower projects in Turkey: applications and problems, *Fresenius Environmental Bulletin*, 26(2), 1192 - 1200.

Bulu, A. (2021). Hydroelectric power plants

Carnogurskal, M., Prihoda M., Zelenakova M. Lazarl M. & Brestovicl T. (2016). Modeling the profit from hydropower plant energy generation using dimensional analysis. *Policy Journal of Environmental. Studies,* 25 (1), 73-81.

Cepin, M. (2011). Distribution and transmission system reliability measures: assessment of power system reliability, *London: Springer-Verlag*.

Chatenet, Q. , Tahan , A.. Gagnon, M. & Chamberland-Lauzon, J. (2016). Numerical model validation using experimental data: Application of the area metric on a Francis runner, *Earth and Environmental Science*, 49, 116 – 122.

Chetansinh R. V. & Ajaysinh R. V. (2014). Synthetic flow generation, *International Journal of Engineering Research and Application*s, 4(1), 66 - 71.

Ciocci, C. L. (2009). Time to think hydropower, *Journal of Water Science*, 4(1), 23 – 31.

Clack, A. E., Adams, J. and Murick, Z. (2017). Evaluation of a proposal for a reliable low-cost grid power with 100% wind, water end Soloar. *Proceedings National Academy of Science.* 114 (26), 6722 – 6727.

Clasing, R. & Munoz E. (2018). Estimating the optimal velocity time in rivers flow measurement: an uncertainty approach. *Journal of Hydrology,* 10(7), 147 – 158.

Cook, J. & Walsh, J. (2008). Optimization of hydropower plants for generation. *Journal of Hyropower Technology, 4(3), 227 – 241*.

Coxon, G., Freer, J., Westerberg, I. K., Wagner, T., Woods, R. & Smith, P. J. (2015). A novel framework for discharge uncertainty quantification applied to 500 UK gauging station. *Water Resource. Resources*, 51, 5531–5546, doi:10.1002/2014WR016532

Crettenand, N. (2012).The facilitation of mini and small hydropower in Switzerland: shaping the institutional framework. With a particular focus on storage and pumped-storage schemes. *Ecole Polytechnique Fédérale de Lausanne* (EPFL). PhD Thesis.

Dametew, W. A. (2016). Design and analysis of small hydro power for rural electrification. *Global Journal of Researches in Engineering*, 16(6), 234 – 241.

Dai, L., Jia, R. and Wang, X. (2022). Relationship between economic growth and energy consumption from the perspective of sustainable development, *Journal of Environmental and Public Health*, 44(3), 271 – 282.

Dietrick, B. (2011) H_2O: The Effects of Hydroelectric Power Production on the Environment in the Western US.

Dinkar, P. S. & Morankar, D. V. (2015). Performance evaluation of small hydropower projects in Maharashtra. *International Journal of Advances In Engineering and Technology*. 8(4), 551-558.

Directorate of Energy (2018). *Types of Hydropower Plants.* Retrieved from www.energy.gov/eere/water/types-hydropower-plants

Directorate of Energy (2004). *Hydropower: Setting a Course for Our Energy Future*.

Dones, R., Heck T. & Hirschberg, S. (2004). Greenhouse gas emissions from energy systems, comparison and overview., In Encyclopaedia of Energy, 3, 77-95, San Diego: Academic Press

Dozier, A. (2012). Integrated water and power modeling framework for renewable energy integration. Degree of Master of Science Thesis, Department of Civil and Environmental Engineering, Colorado State University Fort Collins, Colorado.

Ekeu-wei, I. T. & Blackburn, A. G. (2018). Applications of open-access remotely sensed data for flood modelling and mapping in developing regions, *Journal of Hydrology*, 5(39), 567 – 578.

Emeribe, C. N., Ogbomodia E. T., Fasipe O. A., Biose O. Aganmwonyi, I. Isiekwe, M. & Fasipe O. A. Biose O. Aganmwonyi I. Isiekwe, M. and Fasipe I. P. (2016). Hydrological assessments of some rivers in edo state, nigeria for small – scale hydropower developments Nigeria, *Journal of Technology*, 35 (3), 656 – 668.

Emovon, K., Samuel, D. O., Mgbemena, C. O. & Adeyeri, K. M. (2018). Electric power generation crisis in Nigeria: A Review of causes and solutions, *International Journal of Integrated Engineering*, 10(1), 47 – 56.

Energy Storage Association (2018). Pumped hydroelectric storage.

Etukudor, C., Ademola A., & Olayinka, A. (2015). The daunting challenges of the Nigerian electricity supply industry. *Journal of Energy Technologies and Policy*, 5 (9), 25 – 32.

Ezemonye M. N & Emeribe C. N (2013). Appraisal of the hydrological potential of ungauged basin using morphometric parameters, *Ethiopian Journal of Environmental Studies and Management*, 6(4), 34 – 41.

Fakhari, A. & Ghanbari, A. (2013). A simple method of calculating the seepage from earth dams with clay core. *Journal of Geoengineering*, 8(1), 27 – 32.

Gajbhiye, B, D., Kulkarni, A. H., Tiwari, S. S. and Mathpati, S. C. (2020). Teaching turbulent flow through pipe fittings using computational fluid dynamics approach, *Engineering Reports*. 7(8), 45 – 60.

Gang, L., Yongjun, S., Yong, H., Xiufeng, L. & Qiyu, T. (2014). Short-term power generation energy forecasting model for small hydropower stations using GA - SVM, *Journal Mathematical Problems in Engineering*, 3(4), 112 – 123.

Gbadamosi, S. L.; Adedayo, O. O. & Nnaa L. (2015). Evaluation of operational efficiency of Shiroro hydro-electric plant in Nigeria. *International Journal of Science and Engineering Investigations*, 4(42), 12 – 17.

Genc, T. S. & Thille H. (2008). Dynamic competition in electricity markets: hydropower and thermal generation.

Global Facility for Disaster Reduction & Recovery (GFDRR). (2018). Assessment of the State of Hydrological Services in Developing Countries, Retrieved from International Bank for Reconstruction and Development

Granata, F., Gargano, R. & Demarinis, G. (2016). Support vector regression for rainfall-runoff modeling in urban drainage: A comparison with the EPA's storm water management model. *Journal of Water, 8*(3), 13(1). 456 – 462.

Gupta, S. & Sharma K. (2016). Optimization of revenue generated by hydro power plant by Bat Algorithm (BA). *Journal of Engineering, Environmental Science, Physics*, 5(7), 3576 – 3580.

Harmel, R. D., Copper R. J., Slade R. M., Haney R. L. & Harnod J. G. (2006). Cumulative uncertainty in stream flow and water quality data for small watershed. *Journal of America Society of Agricultural and Biological Engineers*, 40(3), 689 – 701.

Harvey, A (2006). *Micro-Hydro Design Manual*. Warwickshire: Technology Publications Ltd.

Hatata, A. Y., El-Saadawi. M. M. M. & Saad, S. (2019). A feasibility study of small hydro power for selected locations in Egypt, *Energy Strategy Reviews*, 24 (1), 300 – 313.

Helston, C. & Farrris, A. (2016). Large Hydro, British Columbia Energy, Retrieved from http://www.energybc.ca/largehydro.html

Hoes, O. A. C., Lourens J. J. Meijer , L. J. J. Ruud J. E., & Nick C. G. (2017). *Systematic high-resolution assessment of global hydropower potential.*

Hutha, C. and Sloat, J. (2007). *Discharge Uncertainty calculations using a SonTek FlowTracker*.

International Hydropower Association (2018). 2018 *Hydro status report*.

International Organization for Standardization. (2021). *Hydrometry: measurement of liquid flow in open channels using current meters or floats*.

International Renewable Energy Association (2021). *Rewable power generation cost*.

Izura, C. (2022, August 9). *Nigeria requires 30,000 MW of electricity generation to meet current demand.*

Jacobson, M. Z., Delucchi, M. A., Cameron, M. A. & Frew, B. A. (2015). Low-cost solution to the grid reliability problem with 100% penetration of intermittent wind, water, and solar for all purposes. *Proceedings of National Academy of Science*, USA, 112, 15060–15065.

Janicek, F. Causevski, A. & Minovski, D. (2008). Operation of hydro and thermal power plants in a complex power system. journal of power system operation and control, 1(1), 29 -33.

Jiakun, L. (2012). Research on Prospect and Problem for Hydropower development of China *Procedia Engineering*, 28(1), 677 - 682.

Kahssay, A. & Mishra, S. (2013). Community development through hydroelectric project: A case study of Gilgel Gibe III Hydroelectric power project in Ethiopia. *International Journal of Community Developmen*t, 1(1), 19 - 34.

Kapoor, R. (2013). Pico power: a boon for rural electrification. *Advance in Electronic and Electric Engineering*. 3(7). 865 - 872.

Katutsi, V., Kaddu, M., Migisha, A. G., Rubanda, E. M. & Adaramola, S. M. (2021). Overview of hydropower resources and development in Uganda, *AIMS Energy*, 9(6), 1299 – 1320.

Kokkohen, T., Koivusalo, H., & Karvonen, T. (2001). A semi-distributed approach to rainfall-runoff modeling—A case study in a snow affected catchment. *Journal of Environmental Modeling and Software,* 16(5), 481 - 493.

Ladokun, L. L., Sule, F. B., Ajao, R. K. & Adeogun, G. A. (2018). Resource assessment and feasibility study for the generation of hydrokinetic power in the tailwaters of selected hydropower stations in Nigeria, *Journal of Water Science*, 32(2). 338 – 354.

Larson, M. A. D., Petrovica, S. Engstrom, R. E., Drews, M., Liesch, S., Karisson, K. B. & Howells, M. (2019).Challenges of data availability: Analyzing the water-energy nexus in electricity generation, *Energy Strategy Reviews*, 26(1), 45 – 62.

Leon, S. A (2016). Determining optimal discharge and optimal penstocle diameter in water turbines. *Hydraulic Structures and Water System Management,* 8(3*)*, 271 – 283, doi: 10. 151421 T 390628160853

Le Coz, J., Camenen, B., Peyrard, X. & Dramais, G. (2012). Uncertainty in open-channel discharges measured with the velocity-area method. flow measurement and instrumentation, *Journal of Applied Science*, 26(1), 18 – 29.

Lins, H. F. (2008). *Challenges to hydrological observations*. Retrieved from World Metrological Observation.

Liu, Z., Sasaki, H. & Sakata, I. (2014). Study on the academic landscape of hydropower: A citation-analysis based method and its application. *Journal of Management of Engineering nad Technology*. 8(3), 345 – 352.

Magnusdottir, A. & Winkler, D. (2017). Modeling of a hydro power station in an island operation. Proceedings of the 12th International Modelica Conference, May 15-17, 2017, *Prague, Czech Republic.*

Mallet, M., Nabat, P., Zuidema, P., Redemann, J., Sayer, A. M. & Stengel, M. (2019). Simulation of the transport, vertical distribution, optical properties and radiative impact of smoke aerosols with the ALADIN regional climate model during the ORACLES-2016 and LASIC experiments. *Journal of Atmospheric Chemistry and Physics*, 19(7), 4963–4990.

Malverti, L. Lajeunesse, E. & Metivier, F. (2008). Small is beautiful: Upscaling from microscale laminar to natural turbulent rivers, *Journal of Geophysical Research*: *Earth Surface*, 113(2), 654 – 678.

Manquez, J. L., Molina M. G. & Pascas J. M. (2009). Modeling and simulation of a Micro Hydro power plant for application in distributed generations, *Journal of Water Engineering*, 13(04). 404 – 411.

Marcinkowski P. N. & Grygoruk M. (2017). Long-term downstream effects of a dam on a lowland river flow regime: Case study of the Upper Narew, *Journal of Water*, 9, 1 -19.

Mbakaa J. G. & Mwanikibi M. W. (2016). Small hydro-power plants in kenya: a review of status, challenges and future prospects. *Journal of Renewable Energy and Environment*. 4(3), 159 – 168.

Mcintyre, N., Al-Qurashi, A. & Wheater, H. (2009). Regression analysis of rainfall–runoff data from an arid catchment in Oman, *Hydrological Sciences–Journal*, 52(6), 1103 – 1118.

Mishra, S., Saravanan, C. & Shukla J. P. (2018). Rainfall- runoff modeling k-agglometive hiriachy using clustering and regression analysis for the River Brahmapatra Basin. *Journal of the Geological Society of India*, 92, 305 - 312.

Miskat, M. I., Ahmed, A., Rahman, S. M., Chowdhury, H. Chowdhury, T,. Chowdhury, P. Sait, M. S. & Park, K. Y. (2020). An overview of the hydropower production potential in Bangladesh to meet the energy requirements, *Environmental Engineering Research* 26(6), 78 – 93.

Mohanta, K. R. Allamsetty S. & Ghosh, A. A. (2017). Sources of vibration and their treatment in hydro power stations: A review, 20(2), 637 - 648.

Moreau, V., Bage G., Marcotte D. & Samson R. (2011). *Modeling the inventory of hydropower plants.*

Mott, G. Razo, C. and Hamwe, R. (2021). *Emissions anywhere threaten development everywhere*, Retrieved from United Nation Conference on Trade and Development.

Nabat, P., Somot, S., Cassou, C., Mallet, M., Michou, M. & Bouniol, D. (2020). Modulation of radiative aerosols effects by atmosphericcirculation over the Euro-Mediterranean region. *Journal of Atmospheric Chemistry and Physics*, 3(2), 144 – 157,

Nag, P. K. (2001). Power plant engineering (2nd ed.). *New Delhi: Tata McGrawhil*.

Naghizadeh, A. R., Jazebi S. & Vahidi B. (2012). Modeling hydro power plants and tuning hydro governors as an educational guideline. *International Review on Modeling and Simulations*, 5(4), 1780-1790.

Negrel, J. Kosuth, P. & Bercher N. (2011). Estimating river discharge from earth observation measurements of river surface hydraulic variables. *Journal of Hydrological Earth System. Science*, 15(1), 2049–2058.

Ngene, B. U., Agunwamba, J. C., Nwachukwu, B. A. & Okoro, B. C. (2015). The challenges to nigerian raingauge network improvement. *Research Journal of Environmental and Earth Sciences* , 7(1), 68–74.

Nigeria Electricity Regulatory Commission. (2018). *Power generation in Nigeria.*

Nrzesinski D. (2013). Uncertainty in flow regime characterirtic of Europe. *Quaestiones Geograhucare,* 32(1), 43 -53.

Nuernbergk, D. M. & Rorres, C. (2013). Analytical model for water inflow of an archimedes screw used in hydropower generation. *Journal of Hydraulic Engineering* , 139(2), 102 – 110.

Office of Enviromental Assessment Department (2017). Guidelines *and standards for enviromental impact assessment.*

Ogunba, A. O. (2004). EIA systems in Nigeria: Evolution, current practice and shortcomings, *Environmental Impact Assessment Review*, 24(6), 643 - 660.

Ogunlela, A. O., Salami, A. W. Lawal K. M. & Sule, B. F. (2019). Synthetic stream flow generation of ungauged stations using rating equation, *Journal Natural Hazard and Earth System Science*, 21(3), 1519 – 1526.

Okonkwo G. N & Ezeonu S. O. (2012). Design and installation of a mini hydroelectric power plant. *Scholarly Journal of Engineering Research*, 1(1), 11 – 15.

Oladipo, F. & Temitiyo, O. (2014). The Nigerian *power system till date*: A review. *International Journal of Advance Foundation and Research in Science and Engineering*, 1(1), 20 – 23.

Olaoye, T., Ajilore, T. , Akinluwade, K. , Omole, F. & Adetunji, A. (2016). energy crisis in nigeria: need for renewable energy mix. *American Journal of Electrical and Electronic Engineering*, 4(1), 1 - 8.

Oyati, E. N. & Olotu, Y. (2017). Interpolation of rainfall-river orle discharge for developing 1.032 MW of hydropower in Estako-West, Nigeria. *Applied Science Reports*, 8(1), 211 – 221, doi:10.15192/PSCP.ASR.2017.18.1.16

Parsons Creek Aggregates (2008). Environmental Impact Assessment (EIA) Methodology.

Pechlivanidis, I. G., Jackson, B. M., Mcintyre, N. R., & Wheater, H. S. (2011). Catchment scale hydrological modeling: A review of model types, calibration approaches and uncertainty analysis methods in the context of recent developments in technology and applications. *Global Network of Environmental Science and Technology Journal*, *13*(3), 193 - 214.

Perlman, H. (2016). *The water cycle*, Retrieved from USGS Water Science School.

Pilesjo, P. & Al-Juboori, S. S.. (2016). Modelling the Effects of Climate Change on Hydroelectric Power in Dokan, Iraq. *International Journal of Energy and Power Engineering. Special Issue: Modeling and Simulation of Electric Power Systems and Smart Grids*. 5(1-2), 7 – 12.

Pimentel, D., Herz, M., Glickstein, M., Zimmerman, M., Allen, R., Becker, K ., Evans, J., Hussain, B. & Sarsfeld, R. (2002). Renewable energy: Current and potential issues. *American Journal of Electrical and Electronic Engineering*. 4(1), 1 - 8.

Prado Jr, F. A. & Berg V. S. (2013). Capacity Factor of Brazil Hydro Electric Power Plants; Implication for Cost Effectiveness. *Journal of Environmental Science.*

Punys, P. and Jurevicius (2022). Assessment of hydropower potential in wastewater systems and application in a lowland country, *Lithuania of Energies*, 15(1), 5173 – 5184.

Rah, O. P. Chande, A. K. & Sham, M. G. (2012). Optimization of hydro power plant design by particle swarm optimization (PSO). *Procedia Engineering*, 30(1), 418 - 425.

Ramana, V. G. (2014). Regression analysis of rainfall and runoff process of a typical watershed, *International Journal of Science and Applied Information Technology*, 3(1), 16 - 26.

Razi M., Yusuff M. A., Tee B. T. & Zakaria K. A. (2017). Prediction of available power being generated in small hydropower system at Sungai Perting Bentong Pahang. The 2nd International Conference on Automotive Innovation and Green Vehicle (AiGEV 2016).

Razavi, T. & Coulibay, P. (2020). Streamflow prediction in ungauged basins: review of regionalization methods, *Journal of Hydrologic Engineering*, 18(8), pp. 958 – 975, doi: 10.1061/(ASCE)HE.1943-5584.0000690

Roehrig, R., Beau, I., Saint-Martin, D., Alias, A., Decharme, B., & Guérémy, J. (2020). The CNRM globalatmosphere model ARPEGE-Climat6.3: Description and evaluation. *Journalof Advances in Modeling Earth Systems*, 12(1), 1 – 10.

Robbins, P. (2007). *Hydropower*. Retrieved from Encyclopedia of Environment and Society website: www. us.sagepub.com/.../encyclopedia-of-environment-and-society/bo

Robert A. H. (2010). *Energy storage*. New York: Springer.

Rongrong, Z.. Jing B. & Zhiping Y. (2011). The optimization of power dispatch for hydro-thermal power systems. *Procedia Environmental Sciences*, 11(6) 624 – 630.

Sangal, S., Garg, A. & Kumar, D. (2013). Review of optimal selection of turbines for hydroelectric projects. *Emerging Technology and Advanced Engineering*, 3(3), 424-430.

Sattouf, M. (2012). Simulation model of hydro power plant using matlab/simulink. *International Journal of Engineering Research and Applications*. 4(1), 295 – 301.

Singhal M. K. & Kumar, A. (2015). Optimum design of penstock for hydro projects, energy and power engineering, *International Journal of Energy and Power Engineering*, 4(4), 216 – 226.

Siregar, R. W., Ramli, T. & Ramli, M. (2018) Analysis of local convergence of Gauss-Newton Method, IOP Conference. Series: *Material Science and Engineering, Medan, Indonesia*, 21 -23.

Sitterson, I. J. Knightes, C. Pamar, R. & Wolfe, K. (2017). An overview of rainfall-runoff model types, Retrieved from United States Environmental Protection Agency.

Solid Works (2021). *an introduction to flow analysis applications with solid works flow simulation, student guide.*

Sørensen, B. (2004). Renewable energy: its physics, engineering, use, environmental impacts, economy, and planning aspects. *London: Academic Press.*

Spilsbury, L., Richard, S. & Louise Spilsbury T. (2008). *The pros and cons of water power.* New York: Rosen Central.

Statista (2022). *Average installation cost for hydropower worldwide from 2010 to 2021*.

Takal, M. K., Sorgul, R. A. & Balarakarzi (2 017). Estimation of reservoir storage capacity and maximum potential head for hydro-power generation of proposed Gizab Reservoir, Afghanistan, using mass curve method, *International Journal of Advanced Engineering Research and Science*, 4(11), 1 – 12.

Tamburrini, M. (2004). A feasibility study for a micro-hydro installation for the strangford lough wildfowlers & conservation association, Master Thesis, Department of Mechanical Engineering, University of Strathclyde, Glasgow, UK.

Tazioli A. (2011) Experimental Methods for river discharge measurement: Comparison among tracers and Current Meters. *Hydrological Science Journal*, 56(7), 1314 – 1324.

Tegegne, G., Park, K. D. & Ohkim, Y. (2017). Comparison of hydrological models for the assessment of water resources in a data-scarce region, the Upper Blue Nile River Basin, *Journal of Hydrology: Regional Studies*, 14, 49 – 66.

Teixeira, S. (2016). Qualitative geographic information systems (GIS): An Untapped research approach for social work, *Sage Journals*, 17(1), 9 – 23.

Thakur, P. K., Nikam, R. B. Garg, V., Agarwal, P. S., Chouksey, A., Dhote, P. R. & Ghosh, S. (2017). Hydrological parameters estimation using remote sensing and GIS for Indian Region: A Review, Proceedings of the National Academy of Sciences, India - Section A Physical Science 87(4), 641–659.

Tisdall, S. (2016, March 3). *A creaky dam in mosul is the latest weapon in US anti-ISIS propaganda.* Retrieved from the The Guardian.

Tullos, D., Nelson, P. A. Hotchkiss, R. H. & Wegne, D. (2021). Sedimentation mismanagement put reservoirs and ecosystem at risk, Retrieved from United Nation Office of Disaster Risk Reduction.

Tuna M. C. (2013). Feasibility assessment of hydroelectric power plant in ungauged river basin: A case study, *Arab Journal of Science and Engineering*, 38(1), 1359 – 1367, doi 10.1007/s13369-013-0590-5

University of North Carolina (2011). Measurement and Error Analysis.

Usman, A. A. & Abdulkadir R. A. (2015). Modeling and simulation of micro hydro power plant using mathab simulinle. *International Journal or Advanced in Engineering Technology and science*, 3 (1), 260 – 277.

Vasiliev I. E., Klyuev R. V. & Dolgano A. A. (2013). The development of the scientific and technical bases for calculating the operation and management of small hydro. Sustainable *Journal of Development of Mountain Territories*, 3(17), 5 – 9.

Vaze, J., Jordan, P., Beecham, R., Frost, A. & Summerell, G. (2012). Guidelines for rainfall-runoff modelling: Towards Best practice model application, *Journal of Fresh Water Ecology*, 1(3), 1 – 12.

Villegas, H. N. (2011). Electromechanical oscillations in hydro-dominant power systems: an application to the Colombian Power System. Master of Science Graduate Thesis, Electrical and Electronic Engineering, Department, IOWA State University.

Warmink, J. J., Booij M. J., Van der Klis, H., and Hulscher, S. J. (2007). Uncertainty in water level predictions due to various calibrations. Paper presented at 1st International Conference on Adaptive and Integrated Water Management (CAIWA), Basel, Switzerland.

Wilhelm S., Balarac G., Metais O. & Segoufin C. (2016). Head losses prediction and analysis in a bulb turbine draft tube under different operating conditions using unsteady simulation. *Journal of Earth and Environmental Science*, 49(1), 1-1 0.

Wood C. (2003). Environmental impact assessment in developing countries: an overview. Conference on New Directions in Impact Assessment for Development: Methods and Practice, 24–25 November 2003. United Kingdom, EIA Centre, University of Manchester.

World Bank (2020). *Kandadji Niger Basin Water Resources Program*. Retrieved from https://www.worldbank.org/en/country/niger/brief/kandadji-project

Worldwatch Institute (2012). *Use and Capacity of Global Hydropower Increases*.

Yang, W. Y., Li, D., Sun, T., & Ni, G. H. (2015). Saturation-excess and infiltration-excess runoff on green roofs. *Journal of Ecological Engineering, 74*, 327 - 336.

Yanlong, H., Weibin H. Shijun C., Jinlong W., & Yue L. (2015). Analysis of the hydropower generation cost and the affordability of the hydropower on-grid price in Tibet. *Journal of Renewable and Sustainable Energy*, 7(1), 123 – 142.

Yuce, M. I., Omer, A. F. (2019). Hydraulic transients in pipelines due to various valve closure schemes. *Journal of Application of Science.* 1(1), 1- 10.

Yusuf, R. O., Agarry S. E. & Durojaiye A. O. (2007). Environmental impact assessment challenge in Nigeria, *Journal of Environmental Science and Technology*, 2(2), 75 – 82.

Zainuddin, H. Yahaya, M. S Lazi, J. M Basar, M. F. M. & Ibrahim, Z. (2009). Design and development of pico-hydro generation system for energy storage using consuming water distributed to houses. *International Journal of Electrical, Computer, Energetic, Electronic and Communication Engineering,* , 3(11), 1928 – 1933.

Zelanakova,M., Fijko, R., Diaconu, C. D. & Remanokova I. (2018). Environmental *Impact of Small Hydro PowerPlan*t - A case study. *Journal of Environment,* 5(12), 1 – 10. doi:10.3390/environments5010012

Zeng, Y., Zhang, L., X., Guo, J. P., Guo Y. k., Pan Q. L. & Qian J. (2017). Efficiency limits factor analysis for the Francis-99 turbine. Journal of Physics, 1(1), 1 – 10.

Zhang, Y., Chiew, S. H. F., Li, M. & Post D. (2017). Predicting runoff signatures using regression and hydrological modeling approaches, *Journal of Water Resources*, 54(10), 7859 - 7878, https://doi.org/10.1029/2018WR023325

Zungeru A. M., Anaoye A. B., Garegy B. B. Garba A.J. & Tola O.,J. (2012). Reliability evaluation of Kainji Hydro Electric Power Station in Nigeria. *Journal of Energy Technologies and Policy*, 2(2), 15 – 21.

APPENDICES

Appendix A: Journal Publications and Conference Proceedings

i. Environmental Impact Assessment of a Small Hydropower Plant: A Case Study of Orle River Auchi. Nigeria Journal of Engineering Science Research, 5(2), 28 – 29. 2022.

ii. Determination of Power Profile of Hydro Resources in Ungauged Channels. International Journal of Research in Engineering and Applied Sciences, 5(3), 79 – 86, 2020.

iii. Model Development for Discharge Data Extension for Ungauged Rivers Channels: A Case Study of Proposed River Orle Hydropower Plant, International Conference on Advances in Mechanical Engineering, Capital University of Science and Technology, Islamabad, Pakistan August 25 2022.

APPENDIX B: River Measurement Photos

Appendix B 1: Pre-Measurement Talk

Appendix B 2: Channel Width Measurement

Appendix B 3: Channel Segments Mapping

Appendix B 4: Channel Length Measurement

Appendix B 5: Floating Time Measurement

Appendix B 6: Channel Depth Measurement